# Notes on Defects in Materials

**Ju Li, MIT, September 6, 2023**

# Chapter 1

# Overview

Defects are **long-lived aberrations** to a reference atomic structure (perfect crystal in most contexts). For each aberration, it is more efficient to talk about **excess quantities**, contrasting the present with the reference configuration (similar to the "diff" command in Unix,or the "marginal cost" in economy). Thus a defect will have excess masses (different chemical elements $n_c^{\text{excess}}$, $c = 1..C$, aka **segregation**), excess charge $Q^{\text{excess}}$, excess enthalpy $H^{\text{excess}}$, excess volume $V^{\text{excess}}$, excess entropy $S^{\text{excess}}$, excess dipole, quadrupole moments, etc. that "belong" to the defect when it is well isolated from other defects. The detailed spatial distribution of these aberrations / excesses, for example difference in charge density

$$\rho^{\text{excess}}(\mathbf{x}) \equiv \rho_{\text{present}}(\mathbf{x}) - \rho_{\text{reference}}(\mathbf{x}), \quad Q^{\text{excess}} = \int_{\text{some proper cutoff}} d\mathbf{x}\rho^{\text{excess}}(\mathbf{x}) \tag{1.1}$$

tend to have quite intense amplitude in the **defect core**, like a delta function when viewed at lengthscale much larger than the lattice spacing $a_0$. These also become **source terms** in continuum electrostatic/elastostatic/magentostatic... equations of the surrounding medium, for example

$$\nabla^2\phi^{\text{excess}} = -\frac{\rho^{\text{excess}}}{\varepsilon_0}, \quad \mathbf{E} \equiv -\nabla\phi, \quad \varepsilon_0 : \text{vacuum permittivity.} \tag{1.2}$$

In the case of a monopolar excess charge $Q^{\text{excess}}$, the leading order asymptotic solution of (1.2) is

$$\phi^{\text{excess}} = \frac{Q^{\text{excess}}}{4\pi\varepsilon\varepsilon_0 r} + \mathcal{O}(r^{-2}) + \mathcal{O}(r^{-3}) \tag{1.3}$$

where $\varepsilon$ is the dielectric constant of the medium, and influence the medium surrounding the defect **perturbatively in ampltiude**, but at distances much larger than the spatial extent of the defect core itself. These are called **long-range fields**, and usually has a power-law decay as a function of distance $\propto r^{-\alpha}$. It is customary therefore to divide up the material into "defect core" region ($r_0$, usually a few $a_0$) where the atomic structure and bonding topology are significantly different (as viewed, for example, by the atomic coordination number $Z_i$) and needs full atomistic treatment, and "continuum" region ($r \gg r_0$) where the crystal structure is perturbed but the **atomic bonding topology** is intact, and continuum equations like (1.3) apply.

When the defects are well separated ($d \gg r_0$), they "communicate" with each other and **interact** via these long-range electric/stress/magnetic.. fields in the continuum medium. In reality, there can also be a ring region where the **atomic nearest-neighbor (NN)** bonding topology maintains, but continuum treatment is not warranted. We can use $R_0$ to denote that. Because of such **nominally divergent** behavior $\propto r^{-\alpha}$ when $r > R_0$, defects are considered to be **singularities** in the continuum mechanics.

By long-lived aberrations, we are contrasting with band phonons and other small-amplitude transient excitations (e.g. fleeting band holes or electrons or magnons) in the solid. The defects we deal with in this course do not disperse away if left alone (namely at low temperature and no other defects coming into its neighborhood). So defects are **metastable** configurations of the atoms.

Many defects like vacancies, dislocations and grain boundaries **can also move** around without losing their essential characteristics (e.g. those "charges", or "genomes"). In biology analogue, they have "strongly conserved traits", and so they are called defect **species**.

We need to study defects because they influence a lot of the material properties very sensitively - in other words they are the reasons for the difference between "real material properties" and "ideal properties". A perfect crystal without any defect should be able to sustain the **ideal shear strength**, on the order of $G/10$ (take copper $G = 45$GPa, this would be 4.5GPa shear strength). With **just a few** initial glissile dislocations in an infinite crystal, this value drops to **essentially zero** ($\sim$MPa), and would still be on the order of $10^{-3}G$ (45 MPa) when the dislocation population grows significantly as the macroscopic plastic strain reaches tens of percent. Pure silicon, with band gap of 1.1eV, is pretty much **useless** as an electronic material - they only become useful and more valuable than gold when doped properly, by Boron (p-type), Phosphorus (n-type), etc. that substitute silicon in the lattice, that

are either chemically diffused in or ion implanted. There is a famous quote by Sir Charles Frank, the discoverer of the Frank–Read dislocation source: "**crystals are like people: it's the defects that make them interesting**" (and in some important cases, **useful**).

Because the defects can move, can interact in the long-range, as well as react in the short-range by "atomic coordination interactions" ("collision of the singularities" seen by continuum mechanicians who cannot or do not care to resolve the cores' details), the microstructure, which often consists of multiple defect species, "evolve". For example, excess amount of vacancies could be generated by radiation or cold work. Then if we heat up the crystal a bit, so the vacancies can move around, the vacancies may find grain boundaries to annihilate at. Since the vacancies scatter electrons, what one sees would be an reduction of the electrical resistivity of the material. This is a simple example of the material science mantra "**microstructure controls properties**".

Now onto classification of defect structures. The biggest classification is 0D/1D/2D defects:

- 0D defects: vacancies, interstitials, solutes (in random solid solution), antisites (in compound), stacking fault tetrahedra, bubble/void/cavity ...
- 1D defects: edge dislocations, screw dislocations, mixed dislocations, disclinations, ...
- 2D defects: surfaces, grain boundaries, stacking fault, phase boundaries, ferroelectric/ferromagnetic domain walls, antiphase boundaries...

among which 1D/2D defects are also called **extended defects**. Extended means "almost arbitrarily extendable in a certain dimension". For example, a dislocation loop is generally considered 1D, because it is straightforward to envision the loop growing and the circumference $L$ growing to arbitrarily large sizes, where **one** dimensional size has the ability to diverge. In this sense, the bubble/void/cavity may also be considered "3D defects" if they can/are expected to grow readily in all three directions, for example under heavy radiation. And so would be the precipitates ($\rightarrow$new phases), which can be considered 0D obstacles in alloys if they are not growing, but can also be considered new 3D phases if they are expected to grow.

In the list above, a crack should probably be classified as 1D/2D defects. While the crack core is 1D line singularity (stress $\sigma$ nominally diverging as $r^{1/2}$), it also leaves behind two open surfaces which are 2D. These open surfaces have two 2D arrays of atoms with lower coordination numbers $Z_i$ (loss of coordination), a free surface excess energy $\gamma$ per area. This

should be contrasted with the **full-dislocation singularity** which leaves **no damages** behind.

The word "damage" is important, but still-vague concept in materials science and mechanics. It generally corresponds to some kind of "**total coordination deficiency**" (voids, open surfaces) in the atomic structure, and more often than not, **softening** of the elastic modulus. The vaguess and difficulty in quantifying damage as a single variable stems from the great variety of different sized voids/openings. (In this view, a vacancy is the smallest unit of damage). Because of the softening and load shedding, there tends to be autocatalyic growth and **localization** of damage, and it tends to accelerates greatly when reaching some kind of critical lengthscale, and leading to eventual fracture of the material into topologically separated pieces. The "extreme-value statistics" nature of this process makes the mathematical treatment of damage evolution difficult.[1, 2, 3, 4, 5, 6, 7]

Localization is a key concept in physics and materials. A defect is just localized-in-extent, intense-in-amplitude nonlinear **ionic disorder**, i.e. a soliton, in contrast to phonons, which are diffuse in extent, but perturbational in amplitude. Similarly, a band-hole wavefunction in silicon is diffuse in extent (the idealized representation is a Bloch wavefunction $\psi_{n\mathbf{k}}(\mathbf{x}) = \phi_{n\mathbf{k}}(\mathbf{x})\rangle e^{i\mathbf{k}\cdot\mathbf{x}}/\sqrt{V}$, a less idealized representation is a Bloch wavefunction multiplied by a diffuse Gaussian envelope, a "wavepack"), whereas a localized electronic state residing on Boron or Phosphorus with energy in the band gap is exponentially localized. Generally speaking, the more delocalized, the higher the mobility, whether electronic or ionic excitations. Thus band-hole or band-electron states have "band transport" (because of in-resonance condition with many many atoms), whereas the localized states must undergo thermally activated "hopping transport". The delocalized and localized can inter-convert under appropriate conditions. For example the localized electron on neutral Phosphorus atom can be "ionized" can turned into a band-electron state, which is much more mobile. This takes energy, and thus won't happen at zero temperature. However, at finite temperature, there is entropy and as band-electron wavepack can sample many many silcon, there is an energy-entropy tradeoff, and so a finite fraction (even a dominant fraction) of the Phosphorus substitutional atoms will be auto-ionized, and the doped silicon gains electronic conductivity. In reverse, delocalized phonons can also turn into a defect[8], or drive defect to move. A basic view of transition-state theory (TST) of how a defect migrate, is that this defect is hit by tens of phonons (which is of course very rare, and described by the probability $\propto \exp(-Q/k_{\mathrm{B}}T)$) simultaneously, throwing it over the requisite energy barrier $Q$. Such dualistic view of "waves" and "particles" is a key philosophy in physics.

# Chapter 2

# Atomistic Energy Landscape

Atomistics (and electronic structure) is the most microscopic view of this world for most applications. Given that continuum mechanicians and thermodynamicists can do amazing work without ever talking about atoms or electrons, it is important to acknowledge that this is not the ONLY way, or the most efficient or elegant way, to look at this world (and go ask economists and linguists and behavioral artists also). However, it is one way to look at what happens in the world.

The amazing intuition of the ancient Greek philosopher Democritus (c.460—370 BC) is that the world is made of atoms, represented by **discrete** variables $\{\mathbf{x}_i\}$, $i = 1..N$. $\mathbf{x}_i$ is a 3D vector (the position of each nucleus) if we consider a monatomic material ($C = 1$), but we can also tag extra integer variables onto $\mathbf{x}_i$ to denote the chemical species (and charge state, e.g. $Ti^{3+/4+}$, $Fe^{2+/3+}$, $Mn^{3+/4+}$, $Ni^{2+/3+/4+}$, $Co^{3+/4+}$, $O^{2-/1-}$, roughly in rising voltage sequence in transition metal-oxide Li-ion battery electrodes[9]) of the atom/ion for chemically complex materials.

Isolated atoms have valence electrons (outer shells) that are more loosely bound to the nuclei than the core electrons. When we assemble atoms into condensed matter by bringing them into close proximity, these valence electrons start to move around more diffusely. In metallically bonded system, some electrons become truly delocalized, being able to propagate around ("itinerant") and shared between many ions, and do not "belong" to a particular ion. In contrast, covalent bonding is some electrons shared between 2,3,... atoms, like the shared property of a small family or kibbutz (think covalent as "collaboration"). Ionic bonding is one atom having conspicuously more/less electrons than neutral, like a selfish member of

a family (givers and takers), which causes long-range interactions of the form (simplified version):

$$U^{\text{ionic}}(\mathbf{x}^{3N}) \;=\; \sum_{i<j}^{N} \frac{q_i q_j}{4\pi\varepsilon\varepsilon_0 |\mathbf{x}_j - \mathbf{x}_i|} \tag{2.1}$$

where we use $\mathbf{x}^{3N}$ to denote the concatenated $\{\mathbf{x}_i\}$, and $3N$ is to remind us that this is usually a very very huge vector (consider typically $N \sim 10^{24} = 10^8 \times 10^8 \times 10^8$).

Even in ionically bonded systems, there can be a degree of covalency (sharing and selfishness co-exist). The exact meaning of **bonding** is that bringing the atoms together likely reduce the total potential energy compared to the individual isolated atomic states:

$$U(\mathbf{x}^{3N}) \;\equiv\; E_{\text{together}}(N) - N e_{\text{isolated}} \;<\; 0 \tag{2.2}$$

Before discussing defects, we start with the infinite perfect crystal reference. We define

$$E_{\text{b}}(N) \;\equiv\; U(\mathbf{x}^{3N}_{\text{crystalline}}) \tag{2.3}$$

We can define binding energy or cohesive enery per particle:

$$e_{\text{b}} \;\equiv\; \lim_{N\to\infty} \frac{E_{\text{b}}(N)}{N} \tag{2.4}$$

where the surface contribution is filtered out by the **large-number limit**. $e_{\text{b}}$ of course is **crystal structure** and **lattice constant** $a$ **(elastic strain)** dependent. In FCC Cu, $e_{\text{b}} = -3.54$ eV/atom and $a_0 = 3.615$Å ($\Omega = 11.81$Å$^3$).

A typical way people described metallic bonding is the embedded-atom model [10]:

$$U(\{\mathbf{x}_i\}) \;=\; \sum_i \frac{\sum_{j\neq i} u(r_{ij})}{2} + F_i(\sum_{j\neq i} \rho(r_{ij})), \tag{2.5}$$

where $\rho(r_{ij})$ is the electron "glue projection" function, and $F_i$ is the "ion embedding" function. $U(\mathbf{x}^{3N})$ is called the interatomic potential or the atomistic **potential energy landscape (PEL)**. The $u(r_{ij})$ is the pair and additive contributions like the simplest Lennard-Jones potentials, but the second term makes the many-body nature of bonding manifest. The embedding function, $F_i(\cdot)$, is often chosen to be $-\sqrt{\cdot}$ in the so-called Finnis-Sinclair forms.[11] This provides a bonding energy benefit that scales as $-\sqrt{Z}$, where $Z$ is the coordination number. This $-\sqrt{Z}$ form has a coordinate-saturation effect that stablizes lower-coordination

crystal lattices such as BCC, relative to the FCC and HCP close-packed lattices.

With a many-body potential form like (2.5), we can sum over lattice sites to obtain $e_{\rm b}$ for a given lattice structure geometry at $T = 0$. The plot of $e_{\rm b}(\Omega)$, where $\Omega$ is the atomic volume, is called the **cohesive energy curve**. This would allow us to compare the stability of different crystal structures at zero pressure, as well as at finite pressures (after adding the $+P\Omega$ term). For example, when we cross-plot $e_{\rm b}^{\rm FCC}(\Omega)$ ($Z = 12$), $e_{\rm b}^{\rm HCP}(\Omega)$ ($Z = 12$), $e_{\rm b}^{\rm BCC}(\Omega)$ ($Z = 8$), $e_{\rm b}^{\rm Diamond}(\Omega)$ ($Z = 4$), $e_{\rm b}^{\rm Graphite}(\Omega)$ ($Z = 3$), $e_{\rm b}^{\rm LinearChain}(\Omega)$ ($Z = 2$) on one plot, we can get the convex-hull, which tells us when we compress a material inside a diamond anvil cell with a fixed total volume, whether it should be 1-phase, or 2-phase mixture (their volume fraction and coexisting pressure).

With $U(\mathbf{x}^{3N})$, we can also calculate the total potential for an assmebly of **non-perfectly arranged** atoms (imagine thermal fluctuations of ion positions, aka phonons, and/or defects - a defect is defined by a set of atoms having atomic-neighbor relations or **bond topologies significantly different** from those in the perfect reference lattice - defects tend to have higher energy and sit in PEL's **metastable** energy basins), and run molecular dynamics (MD) simulations with it

$$m_i \frac{d^2\mathbf{x}_i}{dt^2} \;=\; m_i \ddot{\mathbf{x}}_i \;=\; -\frac{\partial U(\{\mathbf{x}_i\})}{\partial \mathbf{x}_i} \tag{2.6}$$

From a pure theorist point of view, (2.6) creates a complete "world", in the sense that all crystal and defect structures, their time evolutions and therefore thermomechanical properties can in principle be obtained by integrating (2.6) forward in time.[1]

## 2.1 Elastic deformation and modulus

The lattice at mechanical equilibrium at $T = 0$ is the result of

$$a_0(c_0, ...) \;\equiv\; \arg \min_{\text{structure}} e_{\rm b}. \tag{2.7}$$

Elastic deformation is defined as "**small**", **reversible**, but **diffuse/delocalized** change to the Bravais lattice vectors $\{\mathbf{a}_i(\mathbf{x})\}$ of a perfect crystal, where $\mathbf{x}$ is a coarse-grained posi-

[1] The practical computability is another matter. In this course, even though we do not teach how to implement (2.6) in the computer, we do want to ask people to think from the "atomistic world" perspective, which is one of the important perspectives in thinking about materials.

tion inside the material.[12] By definition, elastic deformation **excludes highly localized changes** in atomic geometry, which samples the **nonlinear nonconvex** part of the atomistic potential energy landscape (PEL).[13, 8] The elastic response can be probed by applying an external stress $\boldsymbol{\sigma}_{\rm ext}$:

$$\min_{\boldsymbol{\varepsilon}} e_{\rm b}(\boldsymbol{\varepsilon}) - \Omega {\rm Tr}(\boldsymbol{\sigma}_{\rm ext}\boldsymbol{\varepsilon}) \;\; \rightarrow \;\; \boldsymbol{\sigma}_{\rm int} \equiv \frac{1}{\Omega}\frac{\partial e_{\rm b}(\boldsymbol{\varepsilon})}{\partial \boldsymbol{\varepsilon}} = \boldsymbol{\sigma}_{\rm ext}. \tag{2.8}$$

We could define shear modulus $G$ by

$$G \;\equiv\; \left.\frac{\partial \sigma_{\rm int}^{\rm shear}}{\partial \varepsilon_{\rm shear}}\right|_{\boldsymbol{\varepsilon}=0} = \frac{1}{\Omega}\frac{\partial^2 e_{\rm b}}{\partial \varepsilon_{\rm shear}^2} \tag{2.9}$$

and the bulk modulus $B$ by

$$B \;\equiv\; \left.\frac{\partial \sigma_{\rm int}^{\rm hydro}}{\partial \varepsilon_{\rm hydro}}\right|_{\boldsymbol{\varepsilon}=0} = \frac{1}{\Omega}\frac{\partial^2 e_{\rm b}}{\partial \varepsilon_{\rm hydro}^2} \tag{2.10}$$

where $\varepsilon_{\rm shear}$ is the shear elastic strain. Generally, we will use the engineering shear strain, for example

$$\varepsilon_{\rm shear} \equiv \gamma_{xz} = \partial_x u_z + \partial_z u_x = 2\varepsilon_{xz} \tag{2.11}$$

and

$$\varepsilon_{\rm hydro} \;\equiv\; \varepsilon_{xx} + \varepsilon_{yy} + \varepsilon_{zz} \tag{2.12}$$

is the hydrostatic strain invariant. For pedagogical simplicity, we could imagine a prototypical elastic deformation that looks like

$$\boldsymbol{\varepsilon} \;=\; \begin{pmatrix} \frac{\varepsilon_{\rm hydro}}{3} & 0 & \frac{\varepsilon_{\rm shear}}{2} \\ 0 & \frac{\varepsilon_{\rm hydro}}{3} & 0 \\ \frac{\varepsilon_{\rm shear}}{2} & 0 & \frac{\varepsilon_{\rm hydro}}{3} \end{pmatrix}. \tag{2.13}$$

In a crude sense, the elastic constants $G$ and $B$ (generally, $C_{ijkl}$ tensor) characterize the **curvature** of the energy landscape with respect to **small, diffuse** changes to $\{\mathbf{a}_i(\mathbf{x})\}$ (the *elastic* strains):

$$e_{\rm b}(\varepsilon_{\rm hydro}, \varepsilon_{\rm shear}) \;=\; e_{\rm b}(0,0) + \frac{\Omega}{2}(G\varepsilon_{\rm shear}^2 + B\varepsilon_{\rm hydro}^2) + O(\varepsilon^3) \tag{2.14}$$

At finite $T$, we just need to add $-Ts$ term to $e_{\rm b}$, and use $f_{\rm b} = e_{\rm b} - Ts = -N^{-1}k_{\rm B}T\ln Z$, the Helmholtz free energy of binding per particle, instead of $e_{\rm b}$. This is so-called thermoelasticity

formalism. $Z$ is the partition function of the $\mathbf{x}^{3N}$-system in statistical mechanics.

## 2.2 Non-Convexity and Barrier Hopping

The potential energy landscape $U(\mathbf{x}^{3N})$ is generally a highly nonlinear and often nonconvex function, and can have multiple local minima (metastable states) as shown in Fig. 2.1, denoted by $\alpha$. At each minima, the force is zero:

$$-\nabla U|_{\mathbf{x}_\alpha^{3N}} \;=\; 0 \tag{2.15}$$

and the $3N \times 3N$ Hessian matrix

$$(\mathbf{A})_{mn} \;\equiv\; \frac{\partial^2 U}{\partial \mathbf{x}_m^{3N} \mathbf{x}_n^{3N}} \tag{2.16}$$

is postive definite (if one ignore the zero modes of 3 rigid-body translations and 3 rigid-body rotations, which can be done by fixing six degrees of freedom in the particle-system and not counting them toward the $3N$ DOF). These minima are denoted by $\{\mathbf{x}_\alpha^{3N}, U_\alpha\}$.

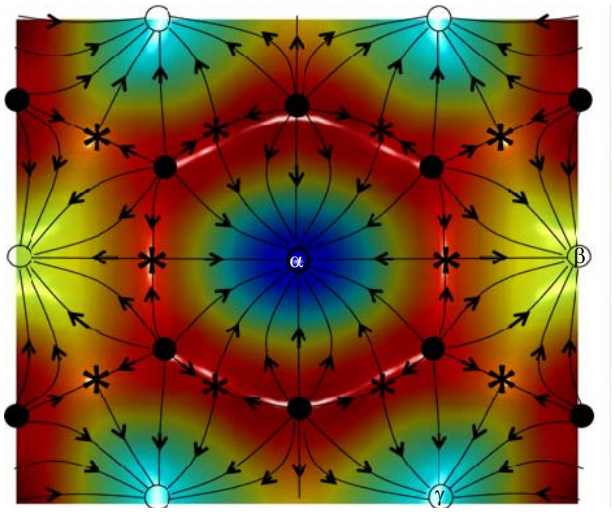


Figure 2.1: 2D illustration of potential energy landscape $U(\mathbf{x}^{3N})$.

The entire configuration space is thus divided into basins. To know which configuration $\mathbf{x}^{3N}$

is in which basin, one just runs a steepest descent algorithm:

$$\frac{d\mathbf{x}^{3N}}{d\lambda} = -\nabla U(d\mathbf{x}^{3N}(\lambda)) \tag{2.17}$$

Two adjacent potential energy **basins** are separated by the **dividing surface**, a $3N-1$ dimensional surface. There exists at least one saddle point $\mathbf{x}_{\alpha\beta}^{3N*}$ that connects the two basins. There exists so-called *minimum energy path* (MEP) that connects $\mathbf{x}_{\alpha}^{3N} \leftrightarrow \mathbf{x}_{\alpha\beta}^{3N*} \leftrightarrow \mathbf{x}_{\beta}^{3N}$.

According to classical harmonic transition-state theory, the rate of forward transition is

$$R_{\alpha\to\beta} = \frac{\prod_{m=1..3N}\nu_m^{\alpha}}{\prod_{m=1..3N-1}\nu_m^{*}} \exp\left(-\frac{U(\mathbf{x}_{\alpha\beta}^{3N*}) - U(\mathbf{x}_{\alpha}^{3N})}{k_{\mathrm{B}}T}\right) \tag{2.18}$$

whereas the rate of back transition is

$$R_{\beta\to\alpha} = \frac{\prod_{m=1..3N}\nu_m^{\beta}}{\prod_{m=1..3N-1}\nu_m^{*}} \exp\left(-\frac{U(\mathbf{x}_{\alpha\beta}^{3N*}) - U(\mathbf{x}_{\beta}^{3N})}{k_{\mathrm{B}}T}\right) \tag{2.19}$$

with so-called detailed balance

$$\frac{R_{\alpha\to\beta}}{R_{\beta\to\alpha}} = \frac{\prod_{m=1..3N}\nu_m^{\alpha}}{\prod_{m=1..3N}\nu_m^{\beta}} \exp\left(-\frac{U(\mathbf{x}_{\beta}^{3N}) - U(\mathbf{x}_{\alpha}^{3N})}{k_{\mathrm{B}}T}\right) \tag{2.20}$$

where the saddle-point information gets cancelled out. It can be understood that what really matters is the vibrational free-energy $U(\mathbf{x}_{\beta}^{3N}) + k_{\mathrm{B}}T \ln \prod_{m=1..3N}\nu_m^{\beta}$ around the minimum, or the constrained free-energy of the saddle-point. In this expression, we see that the softer the mode is, the larger the vibrational entropy of that mode. Note that this expression is only valid in the classical limit, i.e. when the atomic mass is not too light and the temperature is quite high so the classical thermodynamics can be used. When light atoms such as hydrogen or helium is involved, quantum tunneling and zero-point vibration makes the expression more complicated.

Pondering on any actual photographs of **geographic landscapes** should convince one that real landscapes tend to be complex and even fractalline [14]. What we perceive to be main barriers and features of the landscape depends on the lengthscale of our "elevation": at 10 um, we see what we see as a bacteria; at 1mm, we see what we see as an ant; at 50cm, we see what we see as a child; at 1.7m, we see what we see as an adult; at 100m, we see what we see on a helicopter; at 10000m, we get the jet pilot's view; at 384,000 km, we see a smooth sphere. In PEL, the flight "elevation" can be the energy scale. An activation energy barrier

$Q$ (say 0.4eV) that can get one stuck at 30K may no longer be a problem at 300K.

The disconnectivity graph is a way to visualize the adjacency relationship between energy basins. We know the $\mathbf{x}^{3N}$-space is partitioned into basins and dividing lines. Imagine a playboy having a helicopter which has an absolute elevation limit (e.g. cannot fly above 900m above sea level). Starting from a leaf-node basin (labeled by solid circle), a natural question any helicopter playboy would ask oneself is: in this mountainous terrain, where can this helicopter get me to? Town A? B? C? Rio de Janeiro? The answer is that there might be a handful of sibling basins one can get to with the 900m-elevation helicopter. We can group these sibling basins as one **metabasin**, e.g. a family of basins, controlled by a parameter 900m. Let us label this metabasin by an open circle symbol at elevation 900m ($z$) around the $x, y$ of this family of basins. There might be other 900m metabasins (e.g. if you give this helicopter to another playboy in another corner of the Earth), but this 900m-metabasin (open circle) and that 900m-metabasin (open circle) is not connected, because they are separated by mountain passes taller than 900m. But now imagine the playboy uprated his helicpoter to 1000m capable. Now the old metabasin might be able to join other metabasins through the 1000m-elevation rated helicopter.

In the disconnectivity tree graph, one starts from the global ground state (say FCC crystal) and call this elevation (altitude) 0. One then choose integer-multiple elevations, 100meV, 200meV, 300meV, ... For each elevation, one determine the metabasins (open circle symbol), which can have other metabasins (open circle symbol) or basins (closed circle symbol) as children. Sometimes, a metabasin can have just one metabasin children, like a 400-meV metabasin having a single 300-meV metabasin children having a single 200-meV children, in which case we may delete the open circles in the middle, and just draw a vertical line. This will form a tree, like Fig.1 of [15].

The disconnectivity tree graph shows what it takes (which kind of helicopter) to go from one place to another. The main drawback is that it does not give the exact saddle-point energy, but only bounds (say between 700meV and 800meV, minus the basin energy one is at now). The open circle relays some inexact information about saddle-points (there could be multiple pathways, all with saddle-point between 700meV and 800meV, the disconnectivity graph cannot tell that), whereas the closed symbol reflects local minimum information.

# Chapter 3

# Point Defects

Point defect is the reason that some transparent ceramics becomes colored (so-called color centers). The nitrogen-vacancy (NV) defect in diamond is now heavily investigated for quantum computing and quantum sensing. Even though they are the smallest defects possible, they can have striking macroscopic consequences. For example, diffusion drives a lot of the phase transformations, and diffusion is often supported by lattice vacancy exchange mechanism (random walk) within certain temperature range. For these reasons and more, we need to understand the basic mechanics and properties of point defects.

We use a monatomic crystal $C = 1$ to start our discussions. A "**Frenkel disorder**" is removing an atom from the lattice and inserting it elsewhere in the crystal, creating a vacancy (V) and a self-interestial (I). Self-interstitial tends to have a very large formation energy, for example $e_{\mathrm{i}}^{\mathrm{f}} = 3\mathrm{eV}$ [16], versus $e_{\mathrm{V}}^{\mathrm{f}} = 1.27\mathrm{eV}$ in FCC Cu [16]). Self-interstitials are so "expensive" that they are often **only** considered under radiation or other far-from-equilibrium situations like dynamic plastic deformation, since thermal fluctuations are unlikely to generate them. Because self-interstitials are so expensive, alternatively one can have just vacancies. It may look as if we are breaking some kind of balance, but it actually does not. Consider creating "**Schottky disorder**", a two-step process where one (a) extracts an atom from the lattice and put it to infinity, and (b) stick it onto a surface ledge. This "puffs" up the solid a bit. If you don't believe it, consider repeating the process multiple times: eventually a new row of atoms would plate on the surface, growing the crystal, but also with internal "**atomic porosities**" distributed inside the crystal. The energy cost of this "Schottky

vacancy creation process" is called the vacancy formation energy

$$e_{\rm V}^{\rm f} \equiv E(N_1, N_{\rm V}+1) - E(N_1, N_{\rm V}) \tag{3.1}$$

where $N_1$ is the number of real atoms, and $N_{\rm V}$ is the number of vacancies. The total number of **sites** occupied by the crystal is

$$N = N_1 + N_{\rm V} \tag{3.2}$$

and we see $N \to N+1$ before and after the "Schottky vacancy creation process". This is what the "Schottky disorder" (vacancy creation) does, creating porosity inside the solid, simultaneously making the solid appear **larger in volume** than the fully dense state (social analogy would be "hype" or "foam").

Here I would like to make a distinction between atomic *sites* and *atoms* in a crystal. This distinction is similar to the difference between US government structure (white house, senate, supreme court etc.) with who are occupying the offices now. The government structure (site lattice) tends to be **more permanent** than the office holders, in crystalline solids; although sites can also be created and destroyed as well. The sites can also be moved, which is the essence of **deformation** (when we feel or see some object is deformed, we are not really registering which labelled atom goes where, only the shifting of atomic site which are occupied by *some* atom - in other word our hand canot tell tracer or self diffusion). Adding/removing/moving the sites traditionally falls into the realm of MechE, while chemical diffusion, e.g. swapping different atoms on sites, traditionally falls into the realm of DMSE, even though there can be strong coupling between the two.

When one performs X-ray diffraction to measure the lattice constant, the position of diffraction peaks represents the average spacing between *sites* [17]. Again here it is hard to tell the individuality of atoms. Indeed, in quantum mechanics and quantum statistical mechanics, particle indistinguishability is a big deal and requires involved mathematical and philosophical treatment. In this course, we take the classical mechanics and statistical mechanics view, and still assign labels on identical particles and track particle trajectories (which to a large degree, is supported by quantum mechanics), but just keep in mind that labeling atom is a mental accounting "trick", and for all actual measurables a materials scientist can do, we don't need to keep labels.

While (3.1) is the definition, the algorithm to calculate it is usually the following:

$$E(N_1, N_\mathrm{V}+1) - E(N_1, N_\mathrm{V}) \;=\; \Delta_\mathrm{a}E + \Delta_\mathrm{b}E \tag{3.3}$$

$\Delta_\mathrm{b}E$ is just $e_\mathrm{b}$, because we can build a perfect crystal by such sequential addition onto surface ledges (save some small change of creating the ledges in the limit of large $N$). $\Delta_\mathrm{a}E$ can be very easily calculated (in approximation) by an atomistic simulation under periodic boundary condition (PBC), where we contrast $E_{\mathrm{b,PBC}}(n-1,1)$ with $E_{\mathrm{b,PBC}}(n,0)$, where $n \ll N$:

$$\Delta_\mathrm{a}E \;\approx\; E_{\mathrm{b,PBC}}(n-1,1) - E_{\mathrm{b,PBC}}(n,0) = E_{\mathrm{b,PBC}}(n-1,1) - ne_\mathrm{b} \tag{3.4}$$

Thus the vacancy formation energy can be computed as

$$e_\mathrm{V}^\mathrm{f} \;=\; E_{\mathrm{b,PBC}}(n-1,1) - \frac{n-1}{n}E_{\mathrm{b,PBC}}(n,0). \tag{3.5}$$

At finite temperature, this vacancy formation energy $e_\mathrm{V}^\mathrm{f}$ would be modified by vibrational contribution, so $e_\mathrm{V}^\mathrm{f} \to f_\mathrm{V}^\mathrm{f}$, the vacancy formation *free energy* (no configurational entropy contribution, only vibrational entropy contribution). Similarly, the cohesive energy $e_1$ will be modified by vibrational energy contribution, $e_1 \to f_1^\circ$.

For sanity check, consider the special case of a Kossel crystal with nearest-neighbor springs $u(r) = -\epsilon + k(r-a_0)^2/2$ and $Z$ nearest neighbors ($Z = 4$ in 2D and 6 in 3D). At 0K, if there is no vacancy, each atom would have $e_1 = -Z\epsilon/2$ *cohesive energy* since each atom is connected to $Z$ springs, shared with another atom. By creating vacancy, the total energy would have risen by $e_V = Z\epsilon/2$ per vacancy created, since when plucking out an atom from Kossel crystal $Z$ springs are broken, but when we re-attach this atom to a surface ledge, $Z/2$ springs are formed anew.

We can define a dimensionless vacancy fraction as

$$X_\mathrm{V} \;\equiv\; \frac{N_\mathrm{V}}{N_1 + N_\mathrm{V}} \tag{3.6}$$

just like in A-B binary alloys, but with A=1 and B=Vacadium, $X_\mathrm{V}$ completely specify the macrostate of the system.

It should be clear that in the dilute limit ($X_\mathrm{V} \ll 1$), even with complicated interactomic

potentials, the total energy Vcan be written as

$$E(N_1, N_\mathrm{V}) \;=\; N_1 e_1 + N_V e_\mathrm{V}^\mathrm{f} \tag{3.7}$$

at 0K, so long as $N_V \ll N_1$ so the probability of two vacancies sitting side by side is small, where $e_1 = e_\mathrm{b} + e_{1,\mathrm{isolated}}$.

More generally, from solution thermodynamics, arbitrary extensive quantity $A$ (volume, energy, entropy, enthalpy, Helmholtz free energy, Gibbs free energy)

$$A(N_1, N_\mathrm{V}, T, P) \;=\; N_1 a_1 + N_\mathrm{V} a_\mathrm{V} \tag{3.8}$$

where "partial $A$" is defined as:

$$a_i \;\equiv\; \left.\frac{\partial A}{\partial N_i}\right|_{N_{j\neq i}, T, P}. \tag{3.9}$$

The meaning of $a_i$ is the increase in energy, enthalpy, volume, entropy, etc. when an additional type-$i$ atom (1 or V "Vacadium" species) is added into the system, keeping the temperature and pressure fixed. So this means we can write

$$E(N_1, N_\mathrm{V}) \;=\; N_1 e_1 + N_\mathrm{V} e_\mathrm{V} \tag{3.10}$$

$$V(N_1, N_\mathrm{V}) \;=\; N_1 v_1 + N_\mathrm{V} v_\mathrm{V} \tag{3.11}$$

$$S(N_1, N_\mathrm{V}) \;=\; N_1 s_1 + N_\mathrm{V} s_\mathrm{V} \tag{3.12}$$

even if the vacancy concentration is non-dilute. But in the expressions above,

$$e_1 = e_1(X_\mathrm{V}, T, P), \;\; v_1 = v_1(X_\mathrm{V}, T, P), \;\; s_1 = s_1(X_\mathrm{V}, T, P), \tag{3.13}$$

$$e_\mathrm{V} = e_\mathrm{V}(X_\mathrm{V}, T, P), \;\; v_\mathrm{V} = v_\mathrm{V}(X_\mathrm{V}, T, P), \;\; s_\mathrm{V} = s_\mathrm{V}(X_\mathrm{V}, T, P). \tag{3.14}$$

The "formation quantities" are defined in the dilute limit:

$$v_\mathrm{V}^\mathrm{f} \;\equiv\; v_\mathrm{V}(X_\mathrm{V} \to 0, T, P). \tag{3.15}$$

## 3.1 Formation Volume and Relaxation Volume

Let us inspect $v_{\rm V}^{\rm f}$ more carefully, because this part is critical for diffusion problem under stress, and for interaction of point defect with other defects.

For Kossel crystal, the vacancy formation volume $v_{\rm V}^{\rm f}$, a concept parallel to the vacancy formation energy $e_{\rm V}^{\rm f}$, is simply $v_{\rm V}^{\rm f} = \Omega$, where $\Omega$ is the **atomic volume**, defined as

$$\Omega \equiv v_1^{\rm f} \equiv \left.\frac{\partial V}{\partial N_1}\right|_{N_{\rm v}=0,T,P}. \tag{3.16}$$

That is to say, "Vacadium" is exactly as large as the solvent atom. Or, there is zero *vacancy relaxation volume* after we pluck out an atom, which is true in the Kossel crystal. This is because there is only NN springs, and all springs have zero force when at equilbiurm lattice constant (this is NOT so for general pair potentials, lest EAM potentials).

But for real crystal, there is a relaxation effect:

$$v_{\rm V}^{\rm f} = \Omega + v_{\rm V}^{\rm R} \tag{3.17}$$

with $v_{\rm V}^{\rm R}$ typically negative. As shown in the table, in BCC Li, $v_{\rm V}^{\rm R} \approx -0.8\Omega$, so there is a huge relaxation, and the "Schottky vacancy creation process" barely expand the crystal as much as one expected. So Li metal is very different from a Kossel crystal. In contrast, in FCC Cu, $v_{\rm V}^{\rm R} \approx -0.2\Omega$, so the relaxation effect is relatively small.

Intuitively, this relaxation displacement $u_r$ should have the asymptotic form that looks like

$$u_r = \frac{\beta}{r^2}, \quad \beta \propto v_{\rm V}^{\rm R} \tag{3.18}$$

in isotropic medium. This is so that if we track a spherical boundary surrounding the vacancy at center, the boundary would have sagged by a net volume of $4\pi\beta \propto v_{\rm V}^{\rm R}$ (typically negative) irrespective of $r$, which is a very good property. The reason $4\pi\beta$ is proportional to, but not exactly $v_{\rm V}^{\rm R}$ will be discussed later. The next thing is to check whether the above satisfies stress equilibrium in isotropic elastic medium.

The basic equations of linear elasticity are

$$\varepsilon_{ij} = \frac{1}{2}(u_{i,j} + u_{j,i}) \tag{3.19}$$

$$\sigma_{ij} \;=\; C_{ijkl}\varepsilon_{kl} \;=\; C_{ijkl}u_{k,l} \tag{3.20}$$

$$f_j + \sigma_{ij,i} = \rho[\partial_t^2 u_j + (\partial_t u_i)\partial_t u_{j,i}] \tag{3.21}$$

where Einstein summation rule is used, and $f_j$ is body force density like gravity. Equation (3.21) is just Newton's 2nd law for a continuum body:

$$\mathbf{f} + \nabla \cdot \boldsymbol{\sigma} \;=\; \rho[\partial_t \mathbf{v} + \mathbf{v} \cdot \nabla \mathbf{v}] \tag{3.22}$$

which is applicable to any solid/fluid. For a newtonian fluid, the stress is linearly related to the *strain rate*, not strain, and then plugging into Equation (3.21) would give us the famed Navier-Stokes equation. But for a linear elastic medium, the stress is linearly related to the strain, and not strain rate.

Assuming 3D isotropic medium

$$C_{ijkl} \;=\; \lambda\delta_{ij}\delta_{kl} + \mu(\delta_{ik}\delta_{jl} + \delta_{il}\delta_{jk}). \tag{3.23}$$

where $\mu$ is equivalent to $G$ (now the same no matter which direction the shear), we have

$$\sigma_{ij} \;=\; \lambda\varepsilon_{kk}\delta_{ij} + 2\mu\varepsilon_{ij}, \quad \boldsymbol{\sigma} \;=\; \lambda \mathrm{tr}(\boldsymbol{\varepsilon})\mathbf{I} + 2\mu\boldsymbol{\varepsilon} \tag{3.24}$$

we note that

$$3\lambda \mathrm{tr}(\boldsymbol{\epsilon}) + 2\mu \mathrm{tr}(\boldsymbol{\epsilon}) \;=\; \mathrm{tr}(\boldsymbol{\sigma}), \quad \mathrm{tr}(\boldsymbol{\epsilon}) \;=\; \frac{\mathrm{tr}(\boldsymbol{\sigma})}{3\lambda + 2\mu}, \tag{3.25}$$

so

$$\boldsymbol{\epsilon} \;=\; \frac{\boldsymbol{\sigma}}{2\mu} - \frac{\lambda}{2\mu}\frac{\mathrm{tr}(\boldsymbol{\sigma})}{3\lambda + 2\mu}\mathbf{I}. \tag{3.26}$$

From above, the relationship between the Lamé parameters $\lambda, \mu$ and $E, \nu, B$ can be derived:

$$\lambda = \frac{2\nu\mu}{1-2\nu} = \frac{E\nu}{(1+\nu)(1-2\nu)}, \quad \mu = \frac{E}{2(1+\nu)}, \quad B = \frac{E}{3(1-2\nu)} = \lambda + \frac{2\mu}{3}. \tag{3.27}$$

We then have

$$\sigma_{ij} \;=\; \lambda u_{k,k}\delta_{ij} + \mu u_{i,j} + \mu u_{j,i}, \tag{3.28}$$

and in elastostatic situation

$$f_j + \lambda u_{k,kj} + \mu u_{i,ji} + \mu u_{j,ii} \;=\; 0 \;=\; f_j + (\lambda + \mu)u_{i,ji} + \mu u_{j,ii} \tag{3.29}$$

In vector notation it is

$$(\lambda+\mu)\nabla(\nabla\cdot\mathbf{u})+\mu\nabla^2\mathbf{u} \;=\; -\mathbf{f} \tag{3.30}$$

which is the governing equation.

For $u_i \equiv r^{-3}x_i$, we have

$$u_{i,j} \;=\; r^{-3}\delta_{ij} - 3r^{-5}x_i x_j \;=\; u_{j,i} \tag{3.31}$$

$$u_{j,ii} \;=\; -3r^{-5}x_i\delta_{ij} + 15r^{-7}x_i x_i x_j - 3r^{-5}3x_j - 3r^{-5}x_i\delta_{ij} \;=\; 0 \tag{3.32}$$

$$u_{i,i} \;=\; 3r^{-3} - 3r^{-5}r^2 \;=\; 0. \tag{3.33}$$

so indeed $u_i = r^{-3}x_i$ satisfies

$$(\lambda+\mu)\nabla(\nabla\cdot\mathbf{u})+\mu\nabla^2\mathbf{u} \;=\; 0 \tag{3.34}$$

everywhere except $\mathbf{x} = 0$, where the differentibility of terms can give source terms at the origin, akin to the classic Coulombic potential ($\phi(r) \equiv \frac{1}{4\pi r}$):

$$\nabla^2\phi(r) \;=\; \nabla^2\frac{1}{4\pi r} \;=\; -\delta(\mathbf{x}) \tag{3.35}$$

which can be proven by applying the Gauss theorem:

$$\int dA\mathbf{n}\cdot(\nabla\phi) \;=\; \int d\mathbf{x}\nabla^2\phi \tag{3.36}$$

when the origin is included. Indeed what we are doing with the elasticity governing equation (3.30), since we seek vector $\mathbf{u}$ solution, is a hack on the electrostatic equation by re-differetiating the scalar potential:

$$-\nabla\delta(\mathbf{x}) \;=\; \nabla(\nabla^2\phi(r)) \;=\; \nabla^2(\nabla\phi) \tag{3.37}$$

so away from the origin, $\mathbf{u} \equiv -4\pi\nabla\phi$ is engineered to satisfy (3.30) because $\nabla^2\mathbf{u}$ would be zero, and so is $\nabla\cdot\mathbf{u}$ by definition, since according to (3.35):

$$\nabla\cdot\mathbf{u} \;=\; -4\pi\nabla^2\phi = 4\pi\delta(\mathbf{x}). \tag{3.38}$$

Right at the origin, though, we need to be very careful. Since analytically, by multiplying $-4\pi$ on both sides of (3.37)

$$\nabla^2\mathbf{u} \;=\; 4\pi\nabla\delta(\mathbf{x}) \tag{3.39}$$

we end up discovering that the external forcing density needs to be

$$-\mathbf{f} \;=\; (\lambda+\mu)\nabla(4\pi\delta(\mathbf{x})) + \mu 4\pi\nabla\delta(\mathbf{x}) \;=\; 4\pi(\lambda+2\mu)\nabla\delta(\mathbf{x}) \tag{3.40}$$

What, exactly, is the meaning of an external forcing density $\mathbf{f} = -4\pi(\lambda+2\mu)\nabla\delta(\mathbf{x})$? Consider the literal interpretation:

$$\mathbf{f} \;=\; \frac{4\pi(\lambda+2\mu)}{\Delta}\lim_{\Delta\to 0}\left[\begin{array}{c} \delta(\mathbf{x}-\frac{\Delta}{2}\mathbf{e}_1)-\delta(\mathbf{x}+\frac{\Delta}{2}\mathbf{e}_1) \\ \delta(\mathbf{x}-\frac{\Delta}{2}\mathbf{e}_2)-\delta(\mathbf{x}+\frac{\Delta}{2}\mathbf{e}_2) \\ \delta(\mathbf{x}-\frac{\Delta}{2}\mathbf{e}_3)-\delta(\mathbf{x}+\frac{\Delta}{2}\mathbf{e}_3) \end{array}\right] \tag{3.41}$$

So the interpretation of the $u_i \equiv r^{-3}x_i$ self-balancing displacement field is that it is generated by 3 self-balancing "force pairs" (for lack of better word), each with a moment of

$$M \;\equiv\; \frac{4\pi(\lambda+2\mu)}{\Delta}\cdot\Delta \;=\; 4\pi(\lambda+2\mu). \tag{3.42}$$

There is a very good physical interpretation: bonds in real metals are pre-stressed: that is, at the rest configuration, the NN bond is repulsive, whereas the 2NN and 3NN bonds are attractive. When we remove the center atom, the nearby $Z$ atoms lose their NN and the repulsive force, and the net effect would be these atoms feel inward "sagging" force.

To double check the above, we also invoke the Green's function solution derived in (A.68) by Fourier transform

$$\mathbf{u}_{\rm G}(\mathbf{x}) \;=\; \frac{\mathbf{F}}{4\pi\mu|\mathbf{x}|} - \frac{\alpha}{8\pi\mu}\nabla(\mathbf{F}\cdot\nabla|\mathbf{x}|), \quad \alpha \;\equiv\; \frac{\lambda+\mu}{\lambda+2\mu} = \frac{1}{2(1-\nu)}, \tag{3.43}$$

which solves

$$(\lambda+\mu)\nabla(\nabla\cdot\mathbf{u}) + \mu\nabla^2\mathbf{u} \;=\; -\mathbf{F}\delta(\mathbf{x}) \tag{3.44}$$

In index form and if the source is shifted to $\mathbf{x}'$, the solution is

$$u_{{\rm G},i}(\mathbf{x}) \;=\; \frac{F_i}{4\pi\mu|\mathbf{x}-\mathbf{x}'|} - \frac{1}{16\pi\mu(1-\nu)}\frac{\partial^2|\mathbf{x}-\mathbf{x}'|}{\partial x_i\partial x_j}F_j, \tag{3.45}$$

so the convolution kernel is

$$K_{ij} \;\equiv\; \frac{\delta_{ij}}{4\pi\mu|\mathbf{x}-\mathbf{x}'|} - \frac{1}{16\pi\mu(1-\nu)}\frac{\partial^2|\mathbf{x}-\mathbf{x}'|}{\partial x_i\partial x_j} \;=\; K_{ji} \tag{3.46}$$

which agrees with Eqn (2.5) of [18]. (3.46) is a very handy expression, not only for the point defect problem but in other context as well, since a general solution to (3.30) is

$$u_i(\mathbf{x}) \;=\; \int d\mathbf{x}' K_{ij}(\mathbf{x}-\mathbf{x}') f_j(\mathbf{x}') \tag{3.47}$$

Now imagine we have a bunch of forces near the origin ($|\mathbf{x}'|$ small) but we are looking at far-field effects ($|\mathbf{x}| \gg |\mathbf{x}'|$), then it is legitimate the do Taylor expansion of the kernel and take the leading order term:

$$u_i(\mathbf{x}) \;\approx\; -\int d\mathbf{x}' K_{ij,k}(\mathbf{x}) x'_k f_j \;=\; -K_{ij,k}(\mathbf{x}) \int d\mathbf{x}' x'_k f_j \;\equiv\; U_{ijk} P_{jk} \tag{3.48}$$

where

$$U_{ijk} \;\equiv\; -K_{ij,k}(\mathbf{x}) \;=\; \frac{\delta_{ij} x_k}{4\pi\mu|\mathbf{x}|^3} + \frac{1}{16\pi\mu(1-\nu)} \frac{\partial^3 |\mathbf{x}|}{\partial x_i \partial x_j \partial x_k} \tag{3.49}$$

$$P_{jk} \;\equiv\; \int d\mathbf{x}' x'_k f_j(\mathbf{x}') \tag{3.50}$$

So in the far field, the leading-order contribution comes from the force-dipole tensor, $\mathbf{P}$. The physical interpretation of $\mathbf{P}$ is that before adding the defect, the force on atoms are zero. After adding the defect (say removing an atom to create a vacancy), but before the atomic relaxation, there will be excess forces on the atoms surrounding the defect $\{\mathbf{x}^n, \mathbf{F}^n\}$. $\mathbf{F}^n$'s are called the Kanzaki forces, which satisfy

$$\sum_n^n \mathbf{F}^n \;=\; 0 \tag{3.51}$$

but with finite moments:

$$\mathbf{P} \;=\; \sum_n \mathbf{x}^n (\mathbf{F}^n)^T \tag{3.52}$$

This is the atomistic view. In order to relax the $\mathbf{F}^n$'s, the atoms need to move, and this can be done at the atomistic level by Lattice Green's function method. But if we coarse-grain the atoms into a continuum elastic medium, then the solution would be that shown in (3.48). $\mathbf{P}$ has the unit of eV.

We need to talk about the symmetry properties of these tensors. General speaking, $U_{ijk}$ is symmetric with respect to $ij$ permutation, but not symmetric with respect to $jk$ permutation. We would like to argue that under **normal circumstances**, not only are the forces self-balancing as expressed in (3.51), but also $\mathbf{P}$ should be a symmetric tensor

$$P_{jk} \;=\; P_{kj} \tag{3.53}$$

due to **zeroing of net torque**:

$$\mathbf{T} \equiv \sum_n \mathbf{x}^n \times \mathbf{F}^n = 0 \tag{3.54}$$

where in index form,

$$T_i \equiv \sum_n \epsilon_{ijk} x_j^n F_k^n = \sum_n \begin{bmatrix} \epsilon_{123} x_2^n F_3^n + \epsilon_{132} x_3^n F_2^n \\ \epsilon_{231} x_3^n F_1^n + \epsilon_{213} x_1^n F_3^n \\ \epsilon_{312} x_1^n F_2^n + \epsilon_{321} x_2^n F_1^n \end{bmatrix} = \sum_n \begin{bmatrix} x_2^n F_3^n - x_3^n F_2^n \\ x_3^n F_1^n - x_1^n F_3^n \\ x_1^n F_2^n - x_2^n F_1^n \end{bmatrix} \tag{3.55}$$

and $\epsilon_{ijk}$ is the Levi-Civita permutation symbol. By normal circumstances, we mean when the defect is at equilibrium. Imagine drawing a **free-body diagram** of a closed surface around the defect, that separates the "inside" with the "outside". There are inside-on-inside forces and outside-to-inside forces, but the sum of the outside-to-inside forces should be zero if the atoms enclosed are not gaining net momentum. But the outside-to-inside forces are just the negative of the inside-to-outside forces, i.e. Kanzaki forces. The Kanzaki forces are nothing other than what the defect's "inside" transmit to the "outside" continuum jelly through the dividing boundary. Thus, the sum of these Kanzaki forces are zero, and the torque vector should also be zero (which means $\mathbf{P}$ tensor has 9-3=6 degrees of freedom, and is a symmetric tensor - the same proof that stresss must be a symmetric tensor). The above argument does have an exception if there is very long-range interactions through gravity or electric field. Imagine a charged defect in insulator and there is electric field $\mathbf{E}$ that penetrates the boundary. In this case, one can say there is net force on the free-body diagram, or the better way to say it is that there are two kinds of forces: one is long-ranged interaction through the charge interaction with excess charges very far away on two parallel plates that generates the electric field, and one is through shorter-ranged "contact" forces through the bounday. The Kanzaki forces are the "contact" forces through the bounday (thus it has the concept of locality on the boundary), that needs to balance the long-ranged and remote-action forces if any. For such charged defect under external electric field, the general approach would be to first consider the situation without electric field, and then add on the electric field. In the first step, we still have (3.51) and $P_{jk} = P_{kj}$. In the second step, we may consider the charged driving force as a point force.

In the case of (3.41), it is clearly

$$P_{jk} = 4\pi(\lambda + 2\mu)\delta_{jk} \equiv M\delta_{jk} \tag{3.56}$$

and then the continuum relaxation field prediction is

$$u_i(\mathbf{x}) \;=\; \frac{Mx_i}{4\pi\mu|\mathbf{x}|^3} + \frac{M}{16\pi\mu(1-\nu)}\frac{\partial}{\partial x_i}(\nabla^2|\mathbf{x}|) \tag{3.57}$$

Recall that in spherical coordinate

$$\nabla^2 \;=\; r^{-2}\partial_r(r^2\partial_r) + r^{-2}(\sin\theta)^{-1}\partial_\theta(\sin\theta\partial_\theta) + (r\sin\theta)^{-2}\partial_\phi^2 \tag{3.58}$$

we get

$$\nabla^2 r \;=\; r^{-2}\partial_r(r^2\partial_r r) = \frac{2}{r}, \tag{3.59}$$

so we end up with

$$u_i(\mathbf{x}) \;=\; \frac{Mx_i}{4\pi\mu|\mathbf{x}|^3} - \frac{M}{8\pi\mu(1-\nu)}\frac{x_i}{|\mathbf{x}|^3} \;=\; \frac{x_i}{|\mathbf{x}|^3} \tag{3.60}$$

and double-checking is complete. That is, we've verfied the Green's function solution agrees totally with our guessed trial solution.

The stress field (3.28) can be computed, by using (3.31), (3.33), as

$$\sigma_{ij} \;=\; 2\mu(r^{-3}\delta_{ij} - 3r^{-5}x_ix_j) \tag{3.61}$$

which projected in the radial direction, is

$$\sigma_{rr} \;=\; r^{-2}x_ix_j 2\mu(r^{-3}\delta_{ij} - 3r^{-5}x_ix_j) = 2\mu(r^{-5}r^2 - 3r^{-7}r^2r^2) = -4\mu r^{-3}. \tag{3.62}$$

$r^{-3}$ is the scaling form of the long-range stress field of point defect with relaxation volume.

**Theorem:** In infinite isotropic medium, a $\frac{x_i}{|\mathbf{x}|^3}$ displacement field corresponds to a Kanzaki Force Dipole tensor $\mathbf{P} = 4\pi(\lambda+2\mu)\mathbf{I}$ at the origin, and long-range stress field $\sigma_{ij} = 2\mu(r^{-3}\delta_{ij} - 3r^{-5}x_ix_j)$ whose radial component is $-4\mu r^{-3}$.

The above did not consider the boundary condition of the medium. When there is free surface, there is an image effect just like the electric charges. Suppose there is a large sphere of radius $R \gg R_0 > r_0$ surrounding the point defect, which sits at the origin. At the boundary, the stress needs to be zero, which is clearly violated by the particular solution which gives $\sigma_{rr}(R) = -4\mu R^{-3}$. However, we can add a general solution, corresponding to **uniform dilation** of the sphere:

$$\boldsymbol{\sigma}^\circ \;=\; 4\mu R^{-3}\mathbf{I} \tag{3.63}$$

**everywhere inside the body**. Then the boundary traction would be zero when these two solutions are superimposed (added). The strain field is just, according to (3.26):

$$\boldsymbol{\epsilon}^{\circ} \;=\; \frac{4\mu R^{-3}\mathbf{I}}{2\mu} - \frac{\lambda}{2\mu}\frac{12\mu R^{-3}}{3\lambda+2\mu}\mathbf{I} \;=\; \frac{4\mu}{3\lambda+2\mu}R^{-3}\mathbf{I} \;=\; \frac{4\mu}{3B}R^{-3}\mathbf{I} \tag{3.64}$$

So the total displacement in this case becomes modified to

$$u_i \;=\; \frac{x_i}{|\mathbf{x}|^3} + \frac{4\mu}{3B}R^{-3}x_i. \tag{3.65}$$

If one multiplies $\beta$ onto the solution above, one would get

$$\Delta V_{\text{sphere}} \;=\; 4\pi\beta(1+\frac{4\mu}{3B}) \tag{3.66}$$

where the LHS is the volume change of sphere with traction-free surface in the relaxation process, and $4\pi\beta$ is the volume increase of a virtual boundary in infinite medium after the relaxation process (but stress is still transmitting through the virtual boundary). On first look this seems quite paradoxial. Is $\Delta V_{\text{sphere}}$ or $4\pi\beta$ the true relaxation volume we are going to use for thermodynamics?

The answer is that it should be $\Delta V_{\text{sphere}}$:

$$v_{\text{V}}^{\text{R}} \;=\; (1+\frac{4\mu}{3B})4\pi\beta \tag{3.67}$$

The reason is not as obvious as it seems. In the special image solution above, we put the vacancy at the center of the sphere, a very special position. Stress gradient exists at the longest lengthscale of the problem, which is $R$. The image correction is a response to that. If we place the single vacancy off-ceter, the total volume change of the sphere with traction-free surface might be different from (3.66).

Now consider populating the interior of the sphere with **regularly placed** vacancies, with regular spacing $L \ll R$, but both $L$ and $R$ going to $\infty$. $L$ is a **coarse-graining** unit. From our experience with coarse-gaining (after all, the electron density $\rho(\mathbf{x})$ have gradients on the order of $a_0$, but it does not prevent us from defining a uniform stress over a crystal), the **coarse-graining** unit at center is then no different from the other coarse-graining units (one cannot say this for the single-vacancy-in-sphere case). Then, at the sphere lengthscale level, there should be at most a uniform expansion with no coarse-grained stress gradient.

In other words, there should only be stress gradient at lengthscale $L$, but not at lengthscale $R$. Since the sphere is stress free, we therefore must have

$$0 \;=\; \bar{\boldsymbol{\sigma}} \tag{3.68}$$

where $\bar{\boldsymbol{\sigma}}$ is the supercell average stress, containing a single vacancy within $L^3$. Setting $\bar{\boldsymbol{\sigma}}$ to zero in a PBC supercell calculation is therefore the true definition of relaxation volume that one can use in thermodynamics. This brings a out a lesson: when one talks about chemical potential, formation volume etc. one is never talking about a single point defect, but a cloud of point defects.

The remaining work is to show that (3.68) gives as described above. Consider a unit volume containing $c_{\mathrm{V}}$ vacancies (a large number), randomly distributed inside. The sum of dipole-force tensors would be

$$\sum_n \int d\mathbf{x}' x'_k f_j(\mathbf{x}') \;=\; c_{\mathrm{V}} \beta 4\pi(\lambda + 2\mu)\mathbf{I} \tag{3.69}$$

But the LHS is actually an expression for the stress tensor (Virial stress summation [19]), now uniformly distributed inside the unit volume. Relaxing this uniformly distributed hydrostatic stress requires

$$\boldsymbol{\varepsilon}^{\mathrm{R}} \;=\; \frac{c_{\mathrm{V}} 4\pi\beta(\lambda + 2\mu)\mathbf{I}}{3B} \tag{3.70}$$

and total volume expansion

$$\frac{\Delta V}{1} \;=\; \frac{c_{\mathrm{V}} 4\pi\beta(\lambda + 2\mu)}{B} \;=\; \frac{c_{\mathrm{V}} 4\pi\beta(B + \frac{4\mu}{3})\mathbf{I}}{B} \;=\; c_{\mathrm{V}}(1 + \frac{4\mu}{3B})4\pi\beta \tag{3.71}$$

So finally, the elastic displacement and stress field associated with a high-symmetry vacancy configuration is

$$u_i \;=\; \beta \frac{x_i}{|\mathbf{x}|^3} + \text{image terms from BC} \tag{3.72}$$

$$\sigma_{ij} \;=\; 2\beta\mu(r^{-3}\delta_{ij} - 3r^{-5}x_i x_j) + \text{image terms from BC} \tag{3.73}$$

and the thermodynamic consequence is

$$v_{\mathrm{V}}^{\mathrm{f}} \;=\; \Omega + v_{\mathrm{V}}^{\mathrm{R}}, \quad v_{\mathrm{V}}^{\mathrm{R}} = (1 + \frac{4\mu}{3B})4\pi\beta, \quad \beta < 0 \tag{3.74}$$

with the first term corresponding to growing the crystal by 1 site (rigorous) and happening at the **boundary** of this block of single crystal, and the second term is **internal sagging**

and happening inside the crystal (especially near the point defect core).

## 3.2 Thermodynamics in Dilute Limit

The total thermodynamic potential for a variable-vacancy system looks like

$$\mathcal{G}(N_1, N_\mathrm{V}) \;=\; N_1 e_b - N_\mathrm{V}(\Omega t_{nn} + \mathrm{Tr}(\boldsymbol{\sigma}\boldsymbol{\omega}^\mathrm{R}\Omega)) + N_\mathrm{V}(h_\mathrm{V}^\mathrm{f} - T s_\mathrm{V}^\mathrm{f}) - T k_\mathrm{B} \ln \frac{(N_1+N_\mathrm{V})!}{N_1! N_\mathrm{V}!} \quad (3.75)$$

where $N_1 e_b$ refers to a $(N_1, 0)$ full dense system, $\Omega t_{nn}$ is the boundary work done, $h_\mathrm{V}^\mathrm{f}$ is the interal enthalpy to be defined later, $s_\mathrm{V}^\mathrm{f}$ is the vibrational excess entropy, and the last term is the configurational entropy term due to $\frac{(N_1+N_\mathrm{V})!}{N_1! N_\mathrm{V}!}$ number of microstates. Enthalpy, an **internal** quantity, is defined as $h = e + Pv$ in hydrostatic systems, but more generally can be defined by

$$h \;=\; e - \mathrm{Tr}(\boldsymbol{\sigma}\boldsymbol{\omega}^\mathrm{R}\Omega) \quad (3.76)$$

where $\boldsymbol{\sigma}$ is stress in the interior (close to the surface), and $\boldsymbol{\omega}^\mathrm{R}\Omega$ is called relaxation strain-volume. By definition, there will be for arbitrary defect

$$v^\mathrm{R} \;\equiv\; \mathrm{Tr}(\boldsymbol{\omega}^\mathrm{R}\Omega) \quad (3.77)$$

For vacancy, we therefore have

$$\boldsymbol{\omega}^\mathrm{R}\Omega \;=\; \frac{v_\mathrm{V}^\mathrm{R}}{3}\mathbf{I} \quad (3.78)$$

and therefore

$$h_\mathrm{V}^\mathrm{f} \;=\; e_\mathrm{V}^\mathrm{f} - \frac{v_\mathrm{V}^\mathrm{R}}{3}\mathrm{Tr}(\boldsymbol{\sigma}) \quad (3.79)$$

with $-\frac{\mathrm{Tr}(\boldsymbol{\sigma})}{3}$ recognized as $P$, agreeing with previous expression of internal enthalpy.

The effects of internal stress on $f_1^\circ$ and $f_V^f$ are 2nd order in stress (strain energy), which in most cases may be ignored, whereas stress come into the *boundary condition* as $f_V^f = t_{nn}\Omega$, which is linear order in stress if $t_{nn} \neq 0$. In the case of uniform hydrostatic pressure, $t_{nn} = -P$ for whichever exposed surface, so the solid body can be in global thermodynamic equilibrium if the vacancy density is uniform $X_V = \exp(-(f_V^f + P\Omega)/k_\mathrm{B}T)$. On the other hand, if the solid is in uniaxial tension or shear, the solid body can *never be* in global thermodynamic equilibrium. This is because the local equilibrium value of $X_V$ would depend on which surface the RVE is adjacent to (which "market" the RVE is "trading with", and like people, the

closest market is the most important one). There will be more vacancies near surface under tensile normal traction, and less vacancies near surface under compressive normal traction. The vacancy flux will move to surface under compression, which will drive deformation of the solid by diffusional creep.

We can define the "price" that the solid negotiates with the vacuum for Schottky vacancy creation to be

$$\tilde{\mu}_{\mathrm{V}} \;=\; h^{\mathrm{f}}_{\mathrm{V}} - T s^{\mathrm{f}}_{\mathrm{V}} + k_{\mathrm{B}} T \ln X_{\mathrm{V}} - \Omega t_{nn} - \mathrm{Tr}(\boldsymbol{\sigma}\boldsymbol{\omega}^{\mathrm{R}}\Omega) \tag{3.80}$$

which is the derivative of (3.75) with respect to $N_{\mathrm{V}} \to N_{\mathrm{V}} + 1$ (since Vacadium is not a real atom, this can be done if the vaccum is willing to lend some volume with price $t_{nn}$). So when the universe is happy (reflected by the total potential (3.75)), there is

$$0 \;=\; \tilde{\mu}_{\mathrm{V}} \;=\; h^{\mathrm{f}}_{\mathrm{V}} - T s^{\mathrm{f}}_{\mathrm{V}} + k_{\mathrm{B}} T \ln X_{\mathrm{V}} - \Omega t_{nn} - \mathrm{Tr}(\boldsymbol{\sigma}\boldsymbol{\omega}^{\mathrm{R}}\Omega) \tag{3.81}$$

so

$$X_{\mathrm{V}} \;=\; X^0_{\mathrm{V}} \exp\left(\frac{\Omega t_{nn} + \mathrm{Tr}(\boldsymbol{\sigma}\boldsymbol{\omega}^{\mathrm{R}}\Omega)}{k_{\mathrm{B}} T}\right) \tag{3.82}$$

where $X^0_{\mathrm{V}}$ is the reference vacancy fraction in the stress-free condition. Note however (3.81) is only for the deal struck at the particular boundary "market" (or "car dealership"). It provides boundary condition for $X_{\mathrm{V}}$, but does not describe possible other deals inside the crystal. In particular, once a vacancy is created (a car was sold to a customer at the boundary), it can migrate inside. The migration does not change $(N_1, N_{\mathrm{V}})$, but it can change the position of the vacancy, which gradually can experience a different $\boldsymbol{\sigma}(\mathbf{x})$, $T(\mathbf{x})$. Generally speaking, we will have the vacany flux $\mathbf{J}_{\mathrm{V}}(\mathbf{x})$ given by

$$\mathbf{J}_{\mathrm{V}}(\mathbf{x}) \;=\; c_{\mathrm{V}} M_{\mathrm{V}} \mathbf{v}_{\mathrm{V}}^{\mathrm{crystalframe}} \;=\; c_{\mathrm{V}} M_{\mathrm{V}} (-\nabla \mu_{\mathrm{V}}), \tag{3.83}$$

Now I want to argue that the universal "diffusional exchange potential" $\mu_{\mathrm{V}}$ is

$$\mu_{\mathrm{V}} \;=\; h^{\mathrm{f}}_{\mathrm{V}} - T s^{\mathrm{f}}_{\mathrm{V}} + k_{\mathrm{B}} T \ln X_{\mathrm{V}} - \mathrm{Tr}(\boldsymbol{\sigma}\boldsymbol{\omega}^{\mathrm{R}}\Omega) \tag{3.84}$$

**without** the $-\Omega t_{nn}$ term of (3.81). Another way to say this is that all that matters, as far as the interior diffusional PDE is concerned, is the gradient

$$\nabla \mu_{\mathrm{V}} \;=\; \nabla \left( h^{\mathrm{f}}_{\mathrm{V}} - T s^{\mathrm{f}}_{\mathrm{V}} + k_{\mathrm{B}} T \ln X_{\mathrm{V}} - \mathrm{Tr}(\boldsymbol{\sigma}\boldsymbol{\omega}^{\mathrm{R}}\Omega) \right) \tag{3.85}$$

The mathematical way to argue this is that $-\Omega t_{nn}$ is a boundary quantity (a constant) that

one does not bring into the interior **x**-dependency for the PDE. But the physical way is to argue the following: the car (vacancy) was sold at a particular dealership. The price that was struck depend on the local condition (principally, the moods of the salesman's boss and the customer), and that **do control how many cars get sold in that dealership**. But once there is a vacancy in the interior (someone takes ownership of the car and drives it away), whether the customer got a good deal or bad deal was in the past, and that should not affect how the car is driven in the future. Indeed, not all cars are sold in surface dealerships. There are also GB dealerships, dislocation climb dealerships, Frenkel (radiation) processes, etc. Once you have a vacancy in the interior, how it was created should no longer be material - in other words, it should not influence how this particular vacancy moves or reacts in the future. So the only potential that controls how the vacancy moves in the interior should be (3.84). The $-\Omega t_{nn}$ term does matter, but only through boundary condition for $X_{\mathrm{V}}(\mathbf{x})$.

The $-\Omega t_{nn}$ and $-\mathrm{Tr}(\boldsymbol{\sigma}\boldsymbol{\omega}^{\mathrm{R}}\Omega)$ terms are all linear in $\boldsymbol{\sigma}$. Occasionally we see second-order terms in $\boldsymbol{\sigma}$ in the thermodynamic driving force. This has to do with so-called "compliance change" term attributed to a defect. Indeed, unless otherwise specified (usually forbidden by symmetry), a defect will have excess in every physical characteristics, including 2nd-order elastic modulus (and 3rd,4th,5th-order moduli if you want). When we think of a point defect, the sum of contact Kanzaki forces and torques are generally zero, so the only **linear-order excess** that survives is **P**, and it indeed rules supreme in the theory of defects. We frequently ignore high-order excesses because they are asymptotically small. However, if the linear term **vanishes** ("the King dies"), we can no longer do so. And this is the case when we apply a tranverse load on the material, but only allowing horizontal surface to evolve kinetically,[20] in which case the linear term does vanish, so we need to consider 2nd-order elastic compliance effects on the evolution of solid morphology (Asaro-Tiller [21] / Srolovitz [20] instabilities).

### 3.2.1 Creep Rate of Single-crystalline Nanowire

Consider a single-crystalline cylindrical nanowire of diameter $d$ and height $H$, under uniform uniaxial stress $\sigma$, with no other vacancy sinks or sources inside like GBs and dislocations. To first order in $\sigma$, the equilibrium chemical potential of the loaded surface is $\mu_1 = \sigma\Omega$, where $\Omega$ is atomic/molecular volume, and the equilibrium chemical potential of the free surface is $\mu_0 = 0$ (there is 2nd-order stress contribution to $\mu_0$ which drives Asaro-Tiller [21] / Srolovitz [20] instabilities, but they should not contribute to the creep rate to the leading order in

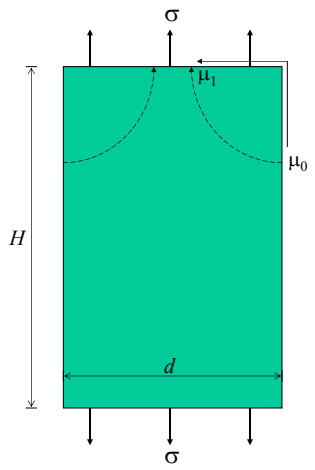


Figure 3.1: .

stress).

The bulk flux that drives Nabarro-Herring creep [22] is given by $J = \rho v$, where $\rho$ is atomic density in $\#/\mathrm{m}^3$, and $v$ is velocity. The velocity is given by $v = (D^*/k_\mathrm{B}T)\nabla\mu$, where $D^*$ is the self diffusivity. $\nabla\mu$ can be estimated to be $(\mu_1 - \mu_0)/d = \sigma\Omega/d$, as a scaling relation. Thus, the flux is $J = \rho D^*\sigma\Omega/dk_\mathrm{B}T = D^*\sigma/dk_\mathrm{B}T$, in unit of $\#/\mathrm{m}^2/\mathrm{s}$. Thus, per unit time, there are extra volume $J\Omega$ arriving per unit area of the loaded surface, so the surface displacement rate due to bulk flux is $\dot{H} = D^*\sigma\Omega/dk_\mathrm{B}T$. The strain rate due to Nabarro-Herring creep is then $\dot{\epsilon}_{\mathrm{Nabarro-Herring}} = D^*\sigma\Omega/dHk_\mathrm{B}T$.

## 3.3 Interstitials

Interstitial sites: octahedral (6 NN) and tetrahedral (4 NN), in FCC, BCC and HCP.

Consider a small atom like H occupying O and T positions in BCC Fe.

Self-interstitials (SIA) are usually very expensive, because of the insufficient volume inside the original lattice to accommodate an additional atom with the same size. We write their formation volume as

$$v^\mathrm{f}_\mathrm{SIA} \;=\; -\Omega + v^\mathrm{R}_\mathrm{SIA} \tag{3.86}$$

where the $-\Omega$ term corresponds to destruction of an atomic site on the surface/grain boundary. However the fact that the atoms are very uncomfortable is reflected in very large and

positive $v^{\rm R}_{\rm SIA}$ (see Table 4.1 of [23]), which makes $v^{\rm f}_{\rm SIA}$ positive overall.

The Kanzaki Force Dipole tensor is usually not an identity matrix, but looks like

$$\mathbf{P} \;=\; \begin{pmatrix} 15 & 0 & 0 \\ 0 & 16 & 0 \\ 0 & 0 & 16 \end{pmatrix} \text{ eV} \tag{3.87}$$

for $\langle 100 \rangle_{\rm FCC}$ dumbell in FCC Al [24], which is the ground-state SIA in FCC; and even more complicated-looking for $\langle 110 \rangle_{\rm BCC}$ type dumbells, which are ground-state in BCC crystals.

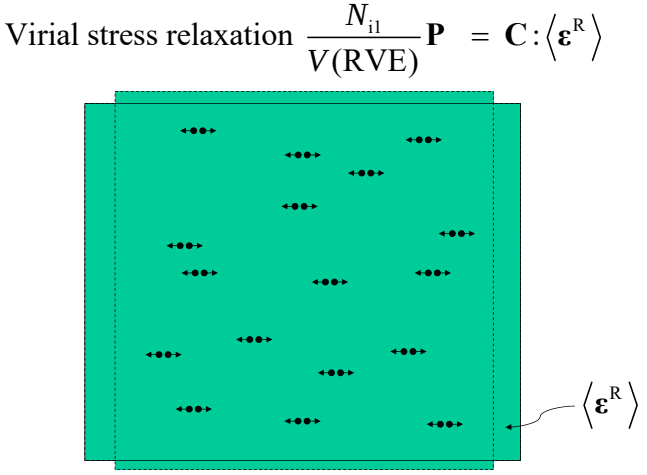


Figure 3.2: .

Suppose we have concentration $c_{\rm i1}$ of these $[100]_{\rm FCC}$ variant dumbels randomly distributed in a representative volume element (RVE). The sum of dipole-force tensors would be

$$\sum_n \int d\mathbf{x}' x'_k f_j(\mathbf{x}') \;=\; N_{\rm i1}\mathbf{P} \tag{3.88}$$

$$\frac{1}{V_{\rm RVE}} \sum_n \int d\mathbf{x}' x'_k f_j(\mathbf{x}') \;=\; c_{\rm i1}\mathbf{P} \tag{3.89}$$

But the LHS is actually an expression for the negative stress tensor (Virial stress summation [19]) applied by "God's hands". If we relax the stress to zero, the relaxation strain of the RVE would be

$$\mathbf{C} : \langle \boldsymbol{\varepsilon}^{\rm R} \rangle \;=\; c_{\rm i1}\mathbf{P} \tag{3.90}$$

or

$$\langle \boldsymbol{\varepsilon}^{\rm R} \rangle \;=\; c_{\rm i1}\mathbf{C}^{-1} : \mathbf{P} \;=\; \frac{N_{\rm i1}}{V_{\rm RVE}}\mathbf{C}^{-1} : \mathbf{P} \tag{3.91}$$

where $\mathbf{C}^{-1}$ is the elastic compliance tensor of the crystal (unit $\mathrm{GPa}^{-1}$). $\mathbf{C}^{-1} : \mathbf{P}$ has the unit of volume, but symmetry of rank-2 strain tensor, so we can define a **relaxation strain-volume** tensor $\boldsymbol{\omega}^{\mathrm{R}}\Omega$ as

$$\boldsymbol{\omega}^{\mathrm{R}}\Omega \;\equiv\; \mathbf{C}^{-1} : \mathbf{P} \tag{3.92}$$

Let us pick $\langle 100\rangle_{\mathrm{FCC}}$ dumbell. This will generate a stress field with tetragonal symmetry. If we believe isotropic elasticity works, then we can work out the stress field according to (3.48). But even if one has to use anisotropic elasticity, the analytical framework is already laid out.

We can work out the **relaxation strain-volume** tensor $\boldsymbol{\omega}^{\mathrm{R}}\Omega$ according to (3.92):

$$\boldsymbol{\omega}^{\mathrm{R}} \;=\; \begin{pmatrix} \omega_{11}^{\mathrm{R}} & 0 & 0 \\ 0 & \omega_{22}^{\mathrm{R}} & 0 \\ 0 & 0 & \omega_{33}^{\mathrm{R}} \end{pmatrix} \tag{3.93}$$

analytically, where the total relaxation volume is

$$v_{\mathrm{SIA}}^{\mathrm{R}} \;=\; \mathrm{Tr}(\boldsymbol{\omega}^{\mathrm{R}}\Omega) \;=\; (\omega_{11}^{\mathrm{R}} + \omega_{22}^{\mathrm{R}} + \omega_{33}^{\mathrm{R}})\Omega. \tag{3.94}$$

For $\langle 100\rangle_{\mathrm{FCC}}$ dumbell in FCC Al [24], the final outcome is

$$\boldsymbol{\omega}^{\mathrm{R}} \;=\; \begin{pmatrix} 0.5 & 0 & 0 \\ 0 & 0.7 & 0 \\ 0 & 0 & 0.7 \end{pmatrix} \;\rightarrow\; v_{\mathrm{SIA}}^{\mathrm{R}} \;=\; 1.9\Omega, \;\rightarrow\; v_{\mathrm{SIA}}^{\mathrm{f}} \;=\; 0.9\Omega \tag{3.95}$$

A stress field $\boldsymbol{\sigma}^{\mathrm{ext}}(\mathbf{x})$ on RVE at position $\mathbf{x}$ will modify the chemical potential of the defect at position $\mathbf{x}$ as:

$$\mu(\mathbf{x}) \;=\; \mu(\boldsymbol{\sigma}^{\mathrm{ext}} = 0) - \mathrm{Tr}(\boldsymbol{\sigma}^{\mathrm{ext}}(\mathbf{x})\boldsymbol{\omega}^{\mathrm{R}}\Omega) + \mathcal{O}((\boldsymbol{\sigma}^{\mathrm{ext}})^2) \tag{3.96}$$

analogous to the scalar form $G = E - TS + PV = F + PV$ or $\partial\mu/\partial P|_T = v$. The $\mathcal{O}((\boldsymbol{\sigma}^{\mathrm{ext}})^2)$ term is change in elastic compliance due to presence of defect, which is often ignored (unless the linear term vanishes). Note that $\boldsymbol{\sigma}^{\mathrm{ext}}(\mathbf{x})$ is the stress at $\mathbf{x}$, if the defect were not at $\mathbf{x}$: it can include the stress field from other defects, and this is how defects interact with each other.

The expression (3.96) describes the "interior" stress effect, which always accompany the

defect no matter where it goes, be it interstitial or vacancy. It is proportional to the relaxational Kanzaki Force Dipole tensor, because pulling on surrounding medium is how defects interact with each other. If there is no relaxation, then as far as continuum mechanics stress equilibiurm is concerned, there is no defect there (to leading order), like a submarine that generates no noise. $\mu(\mathbf{x})$ of (3.96), with concentration dependence also, is what drives diffusion in the interior.

There is also an exterior effect that sets the boundary condition for $\mu(\mathbf{x})$, with

$$\mu(\mathbf{x})|_{\rm BC} \;=\; f(T) + k_{\rm B}T \ln X(\mathbf{x}) - {\rm Tr}(\boldsymbol{\sigma}^{\rm ext}(\mathbf{x})\boldsymbol{\omega}^{\rm R}\Omega)\Big|_{\rm BC} \;=\; t_n \varepsilon_{nn}\Omega \tag{3.97}$$

where $f(T)$ is the Helmholtz free energy of formation that includes the vibrational excess entropy, but not the configurational excess entropy; $k_{\rm B}T\ln X(\mathbf{x})$ is the configurational excess entropy contribuion to the chemical potential; $t_n \equiv \mathbf{n}\boldsymbol{\sigma}^{\rm ext}\mathbf{n}|_{\rm BC}$ is the normal traction at the border, and $\varepsilon_{nn}$ is the **uniaxial** transformation strain of the surface source, which is $+1$ for vacancy surface source (Schottky), and $-1$ for interstitial surface source (this is not the Frenkel process). For Frenkel process, where vacancy and interstial are created simultaneously inside with no change of exterior sites, $\varepsilon_{nn} = 0$. Take $\varepsilon_{nn} = +1$ and $t_n > 0$, what (3.97) is saying is that because work gets done when the crystal surface pops out (site creation), the thermodynamic God is happy (accomplishing mechanical work) and so can tolerate a bit more expensive defect ($\mu(\mathbf{x})|_{\rm BC} > 0$) to be created inside (but very close to the surface), and a bit higher $X(\mathbf{x})|_{\rm BC}$.

(3.96) applies to arbitrary point defect of type $d$, and drive diffusion of such defects:

$$\mathbf{J}_d \;=\; c_d v_d \;=\; c_d(-M_d \nabla \mu_d(\mathbf{x})) \tag{3.98}$$

in any interior point of the domain, where $M_d$ is its mobility. This applies to anywhere inside the domain. (3.97) applies to boundary of the domain, and this completes the stress-diffusion problem for uncharged defects in metals, where the only long-ranged interaction is elastic.

The interior $\mu(\mathbf{x})$ in (3.96) will also cause an interstitial to re-orient itself, with an applied stress. Consider carbon interstitial in BCC iron lattice, with three variants of relaxation strain-volume tensor:

$$\boldsymbol{\omega}^{\rm R}_{\rm i1} \;=\; \begin{pmatrix} \lambda_1 & 0 & 0 \\ 0 & \lambda_2 & 0 \\ 0 & 0 & \lambda_2 \end{pmatrix}, \quad \boldsymbol{\omega}^{\rm R}_{\rm i2} \;=\; \begin{pmatrix} \lambda_2 & 0 & 0 \\ 0 & \lambda_1 & 0 \\ 0 & 0 & \lambda_2 \end{pmatrix}, \quad \boldsymbol{\omega}^{\rm R}_{\rm i3} \;=\; \begin{pmatrix} \lambda_2 & 0 & 0 \\ 0 & \lambda_2 & 0 \\ 0 & 0 & \lambda_1 \end{pmatrix}, \tag{3.99}$$

using the atomic volume of iron $\Omega$ as unit. Suppose we apply uniform but time-dependent $\sigma_{xx}^{\rm ext}(t)$, we will have energy of the three defects shifted as

$$-\lambda_1\Omega\sigma_{xx},\ \ -\lambda_2\Omega\sigma_{xx},\ \ -\lambda_2\Omega\sigma_{xx}, \tag{3.100}$$

and this will induce a net thermally activated transition rate of

$$r \ = \ 2\nu\exp\left(-\frac{Q_{\rm i1/i2}^{\rm rotate}}{k_{\rm B}T}\right)\left[\exp\left(\frac{\lambda_2\Omega\sigma_{xx}-\lambda_1\Omega\sigma_{xx}}{2k_{\rm B}T}\right)-\exp\left(\frac{\lambda_1\Omega\sigma_{xx}-\lambda_2\Omega\sigma_{xx}}{2k_{\rm B}T}\right)\right] \tag{3.101}$$

per i1 defect, where $Q_{\rm i1/i2}^{\rm rotate}$ is the rotational energy barrier that controls i1$\leftrightarrow$i2. The factor of 2 is to account for i1$\leftrightarrow$i3 exchanges as well. Suppose the initial concentration is $c_{\rm i1}^{\circ}$ (#/volume), we then have a net change of the **stress-free transformation strain** as:

$$\begin{aligned}\frac{d\boldsymbol{\varepsilon}_{\rm i}}{dt} \ &= \ \frac{rc_{\rm i1}^{\circ}\Omega}{2}\left[\begin{pmatrix}\lambda_2&0&0\\0&\lambda_1&0\\0&0&\lambda_2\end{pmatrix}-\begin{pmatrix}\lambda_1&0&0\\0&\lambda_2&0\\0&0&\lambda_2\end{pmatrix}+\begin{pmatrix}\lambda_2&0&0\\0&\lambda_2&0\\0&0&\lambda_1\end{pmatrix}-\begin{pmatrix}\lambda_1&0&0\\0&\lambda_2&0\\0&0&\lambda_2\end{pmatrix}\right]\\ &= \ rc_{\rm i1}^{\circ}\Omega(\lambda_2-\lambda_1)\begin{pmatrix}1&0&0\\0&-\frac{1}{2}&0\\0&0&-\frac{1}{2}\end{pmatrix} \ \approx \ \frac{2\nu\exp\left(-\frac{Q}{k_{\rm B}T}\right)(\lambda_2-\lambda_1)^2\Omega\sigma_{xx}}{k_{\rm B}T}\begin{pmatrix}1&0&0\\0&-\frac{1}{2}&0\\0&0&-\frac{1}{2}\end{pmatrix}\end{aligned} \tag{3.102}$$

where we have used the relation

$$c_{\rm i1}^{\circ} \ = \ \frac{1}{\Omega}\exp\left(-\frac{F_i^{\rm f}}{k_{\rm B}T}\right) \tag{3.103}$$

where $\frac{1}{\Omega}$ is the site concentration of the crystal lattice in FCC structure (each dumbell in FCC is centered at an original lattice site), and $F_i^{\rm f}$ is the formation Helmholtz free energy of this dumbbell. The effective activation energy is the sum of formation free energy (i1) plus rotational free-energy barrier (i1$\leftrightarrow$i2/i3):

$$Q \ = \ F_i^{\rm f}+Q_{\rm i1/i2}^{\rm rotate} \tag{3.104}$$

The linear relationship between plastic strain rate and stress is indicative a **linear viscoelastic** system, resembled by a spring connected to a dashpot. Generally speaking, we can represent a defected solid with internal "strain memory" by

$$\dot{\boldsymbol{\varepsilon}}_{\rm i}(t) \ = \ \boldsymbol{\eta}\boldsymbol{\sigma}(t) \tag{3.105}$$

where $\boldsymbol{\eta}$ has the unit of inverse viscosity.

The elastic strain is the difference between imposed total strain $\boldsymbol{\varepsilon}$ and the inelastic strain $\boldsymbol{\varepsilon}_{\mathrm{i}}$, and the stress is proportional to the elastic strain, so

$$\boldsymbol{\sigma} \;=\; \mathbf{C}(\boldsymbol{\varepsilon}(t) - \boldsymbol{\varepsilon}_{\mathrm{i}}(t)) \tag{3.106}$$

and

$$\dot{\boldsymbol{\sigma}} \;=\; \mathbf{C}(\dot{\boldsymbol{\varepsilon}}(t) - \dot{\boldsymbol{\varepsilon}}_{\mathrm{i}}(t)) \;=\; \mathbf{C}(\dot{\boldsymbol{\varepsilon}}(t) - \boldsymbol{\eta}\boldsymbol{\sigma}) \tag{3.107}$$

Suppose the externally applied strain is a sinusoidal function (displacement controlled boundary condition)

$$\dot{\boldsymbol{\varepsilon}}(t) \;=\; \tilde{\boldsymbol{\varepsilon}} e^{-i\omega t} \tag{3.108}$$

and $\boldsymbol{\sigma} = \tilde{\boldsymbol{\sigma}} e^{-i\omega t}$, we will have

$$(-i\omega + \boldsymbol{C\eta})\tilde{\boldsymbol{\sigma}} \;=\; -i\omega \mathbf{C}\tilde{\boldsymbol{\varepsilon}}, \tag{3.109}$$

or

$$\tilde{\boldsymbol{\sigma}} \;=\; (i\omega - \boldsymbol{C\eta})^{-1} i\omega \mathbf{C}\tilde{\boldsymbol{\varepsilon}} \tag{3.110}$$

We see there is an $\omega \to \infty$ response, which is purely elastic. But there is also a $\omega \to 0$ response, which is purely viscous. The complex modulus:

$$\frac{\tilde{\boldsymbol{\sigma}}}{\tilde{\boldsymbol{\varepsilon}}} \;=\; \frac{1}{1 + i\boldsymbol{C\eta}/\omega}\mathbf{C} \;=\; \frac{1 - i\boldsymbol{C\eta}/\omega}{1 + \boldsymbol{C^2\eta^2}/\omega^2}\mathbf{C} \tag{3.111}$$

has a real part

$$\mathrm{Re}\frac{\tilde{\boldsymbol{\sigma}}}{\tilde{\boldsymbol{\varepsilon}}} \;=\; \frac{1}{1 + \boldsymbol{C^2\eta^2}/\omega^2}\mathbf{C} \tag{3.112}$$

and an imaginary part

$$\mathrm{Im}\frac{\tilde{\boldsymbol{\sigma}}}{\tilde{\boldsymbol{\varepsilon}}} \;=\; -\frac{\boldsymbol{C\eta}/\omega}{1 + \boldsymbol{C^2\eta^2}/\omega^2}\mathbf{C} \tag{3.113}$$

The most rapid change in the real part, or the peak in the imaginary part, occurs at $\boldsymbol{C\eta}/\omega_{\mathrm{resonance}} = 1$. This is where the external agitation wave resonate with the internal "flopping around" rate.

Friction between two bodies is well known effect, but **internal friction** within a single solid body is a little bit less well known, which characterizes how much the solid deviates from perfect elastic body. Internal friction can be characterized by a torsion balance [25]. This

instrumentation, and the more general machinery of Dynamic Mechanical Analysis (DMA) spectroscopy, studies small-stress dynamical behavior of materials. Unlike plasticity which is large-stress nonlinear behavior, the DMA spectroscopy is linear-response but focusing on frequency space characteristics. Consider the following partition:

$$\varepsilon \;=\; \varepsilon_{\rm e} + \varepsilon_{\rm i} \tag{3.114}$$

where $\varepsilon_{\rm i}$ is the inelastic strain, also called stress-free strain, transformation strain. To appreciate this concept of transformation strain, consider the state of affairs of carbon interstitials in $\alpha$-iron. Without carbon, $\alpha$-iron would be perfectly cubic. With carbon, it is not necessarily so. The carbon can sit at edge centers or face centers, which are actually equivalent (octahedral site), so we only need consider edge center. Clearly, if the carbon is on [100]-bond, there will be uniaxial dilation in $x$. The only reason that ferrite (with carbon) is still cubic is because the three populations of carbon interstials have equal concentration:

$$c_{\rm C}^x \;=\; c_{\rm C}^y \;=\; c_{\rm C}^z \tag{3.115}$$

However, if somehow we can accomplish a population bias, then that configuration will no longer be cubic, and will have a transformation strain with respect to the cubic state. We can model this transformation strain as

$$\boldsymbol{\varepsilon}_{\rm i} \;=\; a \begin{pmatrix} c_{\rm C}^x - \frac{c_{\rm C}^x + c_{\rm C}^y + c_{\rm C}^z}{3} & 0 & 0 \\ 0 & c_{\rm C}^y - \frac{c_{\rm C}^x + c_{\rm C}^y + c_{\rm C}^z}{3} & 0 \\ 0 & 0 & c_{\rm C}^z - \frac{c_{\rm C}^x + c_{\rm C}^y + c_{\rm C}^z}{3} \end{pmatrix} + b(c_{\rm C}^x + c_{\rm C}^y + c_{\rm C}^z)\mathbf{I} \tag{3.116}$$

the second term above is irrelevant in the present discussion, because we presume the total carbon concentration in DMA experiment is unchanged.

To develop a model for torsion balance, we note that the amount of torsion $\theta \propto \varepsilon$, and to achieve apparent acceleration $\ddot{\theta}$ requires force $\propto m\ddot{\theta} \propto \sigma = G\varepsilon_{\rm e}$, where $G$ is the shear modulus, so the basic kinematic equation is

$$\ddot{\varepsilon} \;=\; kG\varepsilon_{\rm e} \;=\; \ddot{\varepsilon}_{\rm e} + \ddot{\varepsilon}_{\rm i} \tag{3.117}$$

where $k$ depends on the geometry. In above, the only question is how $\ddot{\varepsilon}_{\rm i}$ depends on $G\varepsilon_{\rm e}$. If we assume that

$$\dot{\varepsilon}_{\rm i} \;=\; \frac{G}{\nu}\varepsilon_{\rm e} \tag{3.118}$$

where $\nu$ is an apparent "viscosity" that relates the inelastic strain rate with stress.

In dynamical mechanical analysis (DMA), one applies a perturbational stress, of varying frequency $\omega$. We will see a peak corresponding to eigenvalues of $\boldsymbol{C\eta}$. These are called **internal friction peaks**, the location and amplitude characterizes the types and concentrations of defects inside the solid, whose has configuration mobility (either positional or orientation).

This is also called Zener peak, discovered by Clarence Zener (the namesake for Zener pinning as well) who first worked out so-called anelasticity kinetics in metals. This affects, among other things, how ultrasound is attenuated inside metals, and damping coefficient of springs and piano strings etc.

## 3.4 Elastic Interactions Between Defects

Even in anisotropic elastic continuum medium, we have Green's function

$$u_i(\mathbf{x}) \;=\; \int d\mathbf{x}' K_{ij}(\mathbf{x}-\mathbf{x}') f_j(\mathbf{x}') \tag{3.119}$$

with $K_{ij} = K_{ji}$. From this it is easy to derive

$$u_i(\mathbf{x}) \;=\; -K_{ij,k}(\mathbf{x}) P_{jk}. \tag{3.120}$$

for a single defect of Kanzaki force dipole tensor $\mathbf{P}$ at location $\mathbf{x} = 0$.

Consider point defect $n$ at position $\mathbf{x}_n$, which creates a long range elastic displacement field

$$\mathbf{u}_n(\mathbf{x}-\mathbf{x}_n) \;=\; \mathbf{U}(\mathbf{x}-\mathbf{x}_n) : \mathbf{P}_n \tag{3.121}$$

where $\mathbf{U}$ is a rank-3 tensor,

$$U_{ijk} \;\equiv\; -K_{ij,k}. \tag{3.122}$$

Then the unsymmetrized strain field (deformation gradient) is

$$\mathbf{s}_n(\mathbf{x}-\mathbf{x}_n) \;=\; -\mathbf{S}(\mathbf{x}-\mathbf{x}_n) : \mathbf{P}_n \tag{3.123}$$

where

$$S_{iljk} \;\equiv\; K_{ij,kl}. \tag{3.124}$$

It is easy to prove that $\mathbf{S}$ has the very good symmetry properties:

$$S_{iljk} \;=\; S_{jkil} \tag{3.125}$$

required for the order of its contraction, since $i \leftrightarrow j$ are symmtric and $k \leftrightarrow l$ are symmetric. $\mathbf{S}$ tensor is independent of the defect type. It has the unit of inverse energy.

The stress field would be

$$\boldsymbol{\sigma}_n(\mathbf{x}-\mathbf{x}_n) \;\propto\; \mathbf{C} : (-\mathbf{S}(\mathbf{x}-\mathbf{x}_n) : \mathbf{P}_n) \tag{3.126}$$

Now imagine creating a new defect $m$ at position $\mathbf{x}_m$, we will have the excess energy (or more appropriately, enthalpy $H_{\text{int}}$ if we think in terms of generalized ensemble) to be

$$E_{\text{int}} \;=\; -\text{Tr}(\boldsymbol{\sigma}_n(\mathbf{x}_m-\mathbf{x}_n)\boldsymbol{\omega}_m^{\text{R}}\Omega) \;=\; -\boldsymbol{\omega}_m^{\text{R}}\Omega : \boldsymbol{\sigma}_n(\mathbf{x}_m-\mathbf{x}_n) \tag{3.127}$$

This excess is in reference to when the two defects are infinitely separated $\mathbf{x}_m - \mathbf{x}_n \to \infty$ and non-interacting.

But recall that

$$\boldsymbol{\omega}_m^{\text{R}}\Omega \;=\; \mathbf{C}^{-1} : \mathbf{P}_m \tag{3.128}$$

so we get the interaction energy to be

$$E_{\text{int}} \;=\; \mathbf{P}_m : \mathbf{S}(\mathbf{x}_m-\mathbf{x}_n) : \mathbf{P}_n \tag{3.129}$$

which is a beautiful expression. $\mathbf{P}_m$ and $\mathbf{P}_n$ are symmetrical matrices, so the rank-4 tensor $\mathbf{S}$ can be further symmetrized to have the same symmetry as elastic constant tensor:

$$E_{\text{int}} \;=\; \mathbf{P}_m : \tilde{\mathbf{S}}(\mathbf{x}_m-\mathbf{x}_n) : \mathbf{P}_n \tag{3.130}$$

where

$$\tilde{S}_{iljk} \;=\; \frac{S_{iljk}+S_{lijk}+S_{ilkj}+S_{likj}}{4}, \tag{3.131}$$

with

$$\tilde{S}_{iljk} \;=\; \tilde{S}_{lijk} \;=\; \tilde{S}_{jkil} \;=\; \tilde{S}_{kjil} \tag{3.132}$$

(3.129) show that the defect-defect interaction energy is manifestly independent of the order of creation. That is, we can create defect $m$ first, and then defect $n$ later, and the interaction

energy would still be the same, because of the symmetry property we have derived for $\mathbf{S}(\mathbf{x}_m - \mathbf{x}_n)$.

Because we have a linear elastic system (quadratic energy landscape), the above process can be generalized to multiple defects:

$$\boldsymbol{\sigma}(\mathbf{x}) \;=\; \sum_n \boldsymbol{\sigma}_n(\mathbf{x} - \mathbf{x}_n) \;=\; -\mathbf{C} : \sum_n \mathbf{S}(\mathbf{x} - \mathbf{x}_n) : \mathbf{P}_n \tag{3.133}$$

and

$$E_{\text{int}} \;=\; \frac{1}{2} \sum_{n \neq m} \sum \mathbf{P}_m : \mathbf{S}(\mathbf{x}_m - \mathbf{x}_n) : \mathbf{P}_n \tag{3.134}$$

Again, $\mathbf{S}(\mathbf{x}_m - \mathbf{x}_n)$ is a universal function independent of defect type, and only depends on the elastic constants of the medium. This allows defect to align with each other, forming defect clusters of favorable configurations.

More explicitly, the impact of other defects on the chemical potential of defect $m$ is just:

$$\Delta\mu_m(\mathbf{x}_m) \;=\; \mathbf{P}_m : \sum_{n \neq m} \mathbf{S}(\mathbf{x}_m - \mathbf{x}_n) : \mathbf{P}_n \tag{3.135}$$

since defect $m$ (say interstitial dumbbell) can reorient, and this would cause $\mathbf{P}_m$ to change, we now have an explicit driving force and can derive the Transition State Theory (TST) expression for defect $m$'s reorientation kinetics, like what we did in Zener anelasticity.

The above is when the point defects are well separated ($|\mathbf{x}_m - \mathbf{x}_n| > R_0$). When they are close, there will be atomistic coordination interactions.

## 3.5 Ceramics

I adopt the Kroger-Vink notation [26, 27] system $S_P^C$, where $S$ is species, $P$ is position and $C$ is *excess* charge (positive: ˙; negative: '; neutral: x) except for the charge, which I found obstructive: the dot $\cdot$ invokes the image of an electron and should denote negative instead of positive charge; indeed chemists use $\cdot$ to denote Lewis electrons. But in the Kroger-Vink notation, it denotes a positive charge. Kroger-Vink also use ' to denote -e, and "' to denote -3e, which I found very awkward to use. So I use numeral 2+,+,0,-,2- instead.

Examples:

- $V_{Na}^{-}$: vacancy on Na site in NaCl, with excess electric charge -$e$.
- $V_{Cl}^{+}$: vacancy on Cl site in NaCl, with excess electric charge +$e$.
- $V_{Cl}^{0}$: vacancy on Cl site in NaCl, with an electron trapped inside. This is called F-center (F for German word *Farbe* or color). It is made by exposing NaCl to Na vapor, so one gets slight **off-stoichiometry** overall $NaCl_{1-y}$. The Na metal on the surface attracts $Cl^{-}$ to diffuse toward the surface. The Na metal atoms gets ionized to $Na^{+}$, and the free electrons diffuses inside to occupy the vacancy position. NaCl has band gap 8.5 eV, and is transparent in visible spectrum. However, the confined electron in the vacancy space has a number of additional levels, whose transition falls into the visible regime. This gives a greenish-yellow color. If one exposes NaCl to K vapor, this gives the same greenish-yellow color. But exposing KCl to K vapor, the color is violet. The F-center has an unpaired electron spin, and therefore can be detected by Electron paramagnetic resonance (EPR) or electron spin resonance (ESR) spectroscopy.
- $Cd_{Na}^{+}$: a $Cd^{2+}$ cation on a Na site in NaCl. This has net charge +$e$.
- $Ag_{i}^{+}$: a silver cation on an interstitial site in NaCl, net charge +$e$.
- $F_{i}^{-}$: a fluorine anion on an interstitial site, net charge -$e$.
- $e^{-}$: an excess **band electron** in conduction band, net charge -$e$.
- $h^{+}$: an excess **band hole** in valence band, net charge +$e$.

In my notation, I will use $V_{O}^{2+}$ instead of $V_{O}^{\cdot\cdot}$ to denote oxygen vacancy in ZnO, and $V_{Na}^{-}$ instead of $V_{Na}^{\prime}$ to denote sodium vacancy in NaCl. e and h denotes excess band electron and band hole, respectively. Since they are well known to carry charge $-1$ and $+1$, the charge is sometime omitted from the notation. It is important to remember that the Kroger-Vink charge is the *excess* charge. So $e^{-}$ here has different connotation from el, the latter being the abbreviation for a physical electron (could be bound to a molecule, could also be free, and can have a wide range of energies).

Consider $ZrO_2$ in cubic fluorite structure. I may have both $V_{O}^{2+}$ and $O_{i}^{2-}$ point defects in the lattice. When they are in equal numbers, this is called (anion) Frenkel disorder. I will

use $c_{\mathrm{V}_\mathrm{O}^{2+}}$ to denote the concentration (number of $\mathrm{V}_\mathrm{O}^{2+}$(RVE) / volume(RVE)). However, the subscript and superscript are bit too small to read. So we will also use chemists notation

$$[\mathrm{V}_\mathrm{O}^{2+}] \equiv c_{\mathrm{V}_\mathrm{O}^{2+}} \tag{3.136}$$

so you can read it clearer. Chemists' preferred unit for concentration is 1 molar (1 M), which equals to 1 mole/Liter $= 6.022 \times 10^{20}/\mathrm{cm}^3$.

Band electron e and band hole h are **delocalized**. They can be created in the following reaction:

$$base = \mathrm{e} + \mathrm{h} \tag{3.137}$$

where *base* is the reference perfect crystal. The mental picture is that e takes a quantum state $|\psi_\mathrm{e}\rangle$ from Conduction Band (CB), or h takes a quantum state $|\psi_\mathrm{h}\rangle$ from Valence Band (VB), both infinite Bloch waves (consisting of many planewaves) in this perfect crystal. A more sophisticated view is that we make a Gaussian wavepack of the Bloch wave, with wavepack width $\gg a_0$.

As a matter of notation, we use upright e to denote the physical object of a conduction band electron, and upright h to denote the physical object of a valence band hole. We use the italic $e$ to denote the absolute magnitude of elementary charge

$$e \equiv 1.60217662 \times 10^{-19}\mathrm{Coulombs} \tag{3.138}$$

So h carries **excess charge** $e$, and e carries **excess charge** $-e$. el carries **physical charge** $-e$ (but may be bound to something else). OK?

For simplicity, we will assume all e has the same energy (at the conduction band minimum, CBM) and all h has the same energy (at the valence band maximum, VBM). A reaction equilibrium can be established:

$$[\mathrm{e}][\mathrm{h}] = K_\mathrm{eh}(T) \tag{3.139}$$

where $K_\mathrm{eh}(T)$ is proportional to

$$K_\mathrm{eh}(T) \propto \exp\left(-\frac{E_\mathrm{g}}{k_\mathrm{B}T}\right) \tag{3.140}$$

where $E_\mathrm{g}$ is the band gap:

$$E_\mathrm{g} \equiv \mathrm{CBM} - \mathrm{VBM}. \tag{3.141}$$

$E_g$ varies from narrow bandgap of 0.17 eV of InSb used for infrared detectors (visible light spectrum is from 2-3 eV), to 7.8 eV of MgO and 8.8 eV of $Al_2O_3(\alpha)$.

Electrical **conductivity** is the relationship between current **j** and electric field **E**:

$$\mathbf{j} \equiv \sigma \mathbf{E}. \tag{3.142}$$

**If electronic carriers dominate**, then

$$\mathbf{j} = c_e \mathbf{v}_e(-e) + c_h \mathbf{v}_h(e) \tag{3.143}$$

But

$$\mathbf{v}_e = M_e(-e\mathbf{E}), \quad \mathbf{v}_h = M_h(e\mathbf{E}), \tag{3.144}$$

so we get

$$\sigma = e^2(c_e M_e + c_h M_h) \tag{3.145}$$

there are generally differences between $M_e$ and $M_h$ depending on the effective masses of CBM and VBM and scattering rates, but they usually do not differ by a large order of magnitude. So the question of whether e dominates ($n$-type) or h dominates ($p$-type) depends largely on whether $c_e \gg c_h$ or $c_e \ll c_h$, and this, as we shall see later, has a lot to do with charged point defects. If $c_e M_e \sim c_h M_h$, this is called **ambipolar**, meaning we cannot consider just one carrier species as the single dominant one. More generally, we can include the contribution of mobile charge defects:

$$\sigma = \sum_\alpha e^2 z_\alpha^2 c_\alpha M_\alpha \tag{3.146}$$

and **transference number**

$$t_\beta \equiv \frac{e^2 z_\beta^2 c_\beta M_\beta}{\sum_\alpha e^2 z_\alpha^2 c_\alpha M_\alpha}. \tag{3.147}$$

However, such delocalized e or h may also be captured by a localized defect. In the F-center example above, we can express this by:

$$V_{Cl}^+ + e = V_{Cl}^0 \tag{3.148}$$

The RHS may have the enthalpic advantage, but the LHS can have entropic advantage. We will end up with a reaction equilibrium

$$\frac{[V_{Cl}^0]}{[V_{Cl}^+][e]} = K(T), \tag{3.149}$$

where LHS is called the **reaction quotient**, and RHS is called the equilibrium constant, of this defect reaction. For this classic equation to hold, we assume (a) thermal equilibrium, (b) a dilute-solution expression for the configurational entropy (if not, then we have to use activity/activity coefficient language). With (a),(b) satisfied, $K(T)$ is defined as

$$K(T) \equiv K_0 \exp\left(-\frac{\Delta G^0_{\text{rxn}}(T)}{k_{\text{B}}T}\right) \tag{3.150}$$

where $\Delta G^0_{\text{rxn}}(T)$ is the driving force for the reaction without the configurational entropies contribution. $K_0$ is a site-density prefactor, that normalizes the left-hand side for the entropy.

Note that not only $\text{V}^+_{\text{Cl}}+\text{e} \rightarrow \text{V}^0_{\text{Cl}}$ (the **capture**) process is possible, the reverse $\text{V}^0_{\text{Cl}} \rightarrow \text{V}^+_{\text{Cl}}+\text{e}$ (the **ionization**) is also possible. This is what mainly happens when we put Phosphorus into Silicon:

$$\text{P}^+_{\text{Si}} + \text{e} = \text{P}^0_{\text{Si}} \tag{3.151}$$

Since diamond cubic Si is covalent and has 0 reference charge in the base structure (monatomic), the $\text{P}^0_{\text{Si}}$ state denotes an unionized neutral P atom stuck inside a vacant Si site (substitutional). The $\text{P}^+_{\text{Si}}$ is the post-ionized state, a local defect with positive charge (but low mobilty). e, however, can have very high band mobility (limited by electron-phonon / electron-electron scattering, etc., but moves ballistically as a band state and still has much higher mobility than that of localized defects). Whether the **capture** or the **ionization** dominates depends on the temperature, the nature of the trapping defect itself, and all other defects in the system which could trap/donate electrons. The ionization/trapping is also a self-stopping process. When there is too much ionization and electrons in the bands, the electrons chemical potential $\mu_{\text{el}} \equiv E_{\text{F}}$ rises:

$$c^\circ_{\text{el}}(\epsilon_{\text{el}}, T) = \text{DOS}(\epsilon_{\text{el}}) f^\circ(\epsilon_{\text{el}}, T), \quad f^\circ(\epsilon_{\text{el}}, T) = \frac{1}{e^{\frac{\epsilon_{\text{el}}-\mu_{\text{el}}}{k_{\text{B}}T}}+1} \tag{3.152}$$

Using the notation $E_{\text{F}}$ for the Fermi energy is a big notation mistake. The Fermi energy has the unit of eV, but is really a chemical potential which includes entropic contribution, and not just the energy (and not just the energy of any particular electron). This can be seen from the fact that $\mu_{\text{el}} \equiv E_{\text{F}} \equiv -eU$ falls in between [VBM, CBM] for ceramics, often in a no man's land for $\epsilon_{\text{el}}$. Being an intensive quantity, $E_{\text{F}}$ should really be called $\mu_{\text{F}}$, or $\epsilon_{\text{F}}$, if the latter is also understood to contain entropy/occupancy contribution.

To summarize, there are many physical electron states (el): the conduction band states $\text{e} \in$ el, the valance band states $\text{h} \in$ el, and even the defect-trapped electrons with mid-gap defect

charging level and exponentially localized wavefunction $\in$ el. We use $\epsilon_{\rm el}$ to denote their individual energy, $\mathrm{DOS}(\epsilon_{\rm el})$ to denote their energy degeneracy, and $f(\epsilon_{\rm el})$ to denote their occupation, which may or may not be at thermal equilibrium $f^\circ(\epsilon_{\rm el}, T)$. If not, then the process of $f(\epsilon_{\rm el}) \to f^\circ(\epsilon_{\rm el}, T)$ is called electronic relaxation, which is often on the order of nanoseconds or less, after external excitation like radiation is taken away. Once $f^\circ(\epsilon_{\rm el}, T)$ is reached, there is a global property called $\mu_{\rm el} \equiv E_{\rm F} \equiv -eU$ for *all* el's, irrespective of whether they are e, h, or defect-trapped local states. The reason that there should be a **collective constant** called $E_{\rm F}$ **at thermal equilibrium** for all electrons (those with higher $\epsilon_{\rm el}$ will be compensated by lower occupation, and those with lower $\epsilon_{\rm el}$ will be compensated by higher occuptation, just like air molecules at sea level vs at Mount Everest) if at thermal equilibrium, is because electrons interact with each other and exchange energy, and there is entropy/occupancy vs. energy tradeoff, so at equilibrium all electrons are "equally happy", since they are the same electrons (indistinguishable) to begin with, and constantly exchange energy/position anyway.

To connect with what we've done before, the rigorous definition of [e] and [h] are:

$$[\mathrm{e}] \equiv \int_{\rm CBM}^{\infty} d\epsilon_{\rm el} \mathrm{DOS}(\epsilon_{\rm el}) f^\circ(\epsilon_{\rm el}, T), \quad [\mathrm{h}] \equiv \int_{-\infty}^{\rm VBM} d\epsilon_{\rm el} \mathrm{DOS}(\epsilon_{\rm el})(1 - f^\circ(\epsilon_{\rm el}, T)) \tag{3.153}$$

There are two different modes of transport: band transport, vs. hopping transport. The mobilty of the former typically decreases with increasing temperature, due to higher probability of scattering. (So $M_{\rm e}$ and $M_{\rm h}$ decrease with $T$, usually in a power-law fashion $M_{\rm el} \propto T^{-\alpha}$ with $\alpha$ between 0.5 and 3). The mobility of hopping typically increases with temperature, due to thermally activated nature of the hopping, e.g. $M_{\mathrm{V}_{\mathrm{Cl}}^+}$ and $M_{\mathrm{V}_{\mathrm{Cl}}^0}$ should increase greatly with $T$ in the Arrhenius fashion $M \propto e^{-\frac{Q^{\rm m}(T)}{k_{\rm B}T}}$, where $Q^{\rm m}(T)$ is the migration free-energy barrier in transition-state theory (TST) for hopping transport. TST hopping transport (total-energy-below-the-barrier) is generally much slower and has much lower mobility than ballistic (total-energy-over-the-barrier) transport.

When a photon comes in, it can create e and h pair, if

$$h\nu \geq E_{\rm g} \tag{3.154}$$

In (3.137), even though people some time use the name "pair", they are physically well separated band states (or wide Gaussian packs). However, the e and h can also self-trap, and form an **association** called exciton, denoted by $(\mathrm{e}, \mathrm{h})$, which is a bound pair with distance

in between few-nm (small exciton) to hundred of nm (large exciton). We can express this association as:

$$\mathrm{e} + \mathrm{h} \;=\; (\mathrm{e}, \mathrm{h}) \tag{3.155}$$

$(\mathrm{e}, \mathrm{h})$ is charge neutral, but there are other associations like **trion** $(\mathrm{e}, \mathrm{e}, \mathrm{h})$ which would carry both charge, enthalpy and spin. With photons, or other ionizing radiation, the actual electronic distribution $f(\epsilon_{\mathrm{el}})$ can deviate from the thermal equilibrium distribution $f^{\circ}(\epsilon_{\mathrm{el}}, T)$ just like the point defects during temperature quenches. This is called electronic **out-of-equilibrium** (similar to plasma), and with time, the process of $f(\epsilon_{\mathrm{el}}) \to f^{\circ}(\epsilon_{\mathrm{el}}, T)$ is called **electronic relaxation**.

Reaction involving a generic electron of variable energy $\epsilon_{\mathrm{el}}$ looks like:

$$\mathrm{D}^{(n+1)+} + \mathrm{el} \;=\; \mathrm{D}^{n+} \tag{3.156}$$

The driving force for this reaction without the configurational entropies contribution, $\Delta G^{0}_{\mathrm{rxn}}(T)$, should look like

$$\Delta G^{0}_{\mathrm{rxn}}(T) \;=\; \epsilon_{\mathrm{D}^{(n+1)+/n+}}(T) - \epsilon_{\mathrm{el}} \tag{3.157}$$

where $\epsilon_{\mathrm{D}^{(n+1)+/n+}}(T)$ is called the charging level (the $T$-dependence can come from the vibrational entropy of the defect before and after electron capture), and is the free-energy difference of the lattice defect at electron-captured state (reduced) vs the same defect at oxidized state. By "same", we do not exclude some nuclear displacements or even reconstructions - loosely called "electron-phonon coupling" by some people - and thus $\mathrm{D}^{n+}$ and $\mathrm{D}^{(n+1)+}$ can have different Kanzaki force dipoles

$$\mathbf{P}(\mathrm{D}^{n+}) \;\neq\; \mathbf{P}(\mathrm{D}^{(n+1)+}) \tag{3.158}$$

and even different symmetries. $\epsilon_{\mathrm{D}^{(n+1)+/n+}}(T)$ can be computed in a supercell with $\mathrm{D}^{(n+1)+}$, and a supercell with $\mathrm{D}^{n+}$ (which is one electron heavier), and subtracting the free energies of the two. In a periodic boundary condition supercell calculation, to balance the charge brought by the real quantum electron to prevent Coulomb explosion, we also need to conceptually add a massless ether-like jellium that smears opposite charge uniformly in the supercell - but this is done automatically by planewave calculations by their $\mathbf{G} = 0$ non-treatment.

$\epsilon_{\mathrm{D}^{(n+1)+/n+}}(T)$ (sometimes abbrevated as $\epsilon_{n/n+1}$ if we understand it's about lattice defect D) is called the **defect charging level** of charged defect $D$ from $(n+1)+ \to n+$. It reflects the **composite property** of an electron trapped by phonon/defect, but it has the unit of

eV, and can be plotted on the $\epsilon_{\rm el}$ axis. In fact, if $\epsilon_{{\rm D}^{(n+1)+/n+}}(T)$ falls midway between CBM and VBM, then it can be proven that the trapped electronic wavefunction $|\psi_{\rm el}\rangle$ will have exponentially localized tail spatially (thus "trapped"). If $\epsilon_{\rm el}$ is close to the band edges (either CBM/VBM), then it is called a **shallow-level** donor/acceptor. If it is not close to either band edges, then this defect charging level is called a **deep level**. The key is to remember that $\epsilon_{{\rm D}^{(n+1)+/n+}}(T)$ is not the defect formation energy, but how much the defect formation energy would change if one more electron is added - thus $\epsilon_{{\rm D}^{(n+1)+/n+}}(T)$ has the connotation of *how happy one electron would be if trapped*, ie. marginal energy of the electron, thus this value can be and should be plotted on the $\epsilon_{\rm el}$-axis along with the band DOS features.

Now imagine el in the defect redox reaction (3.156) is sourced from the CBM of the ceramic,

$$\text{el} \;=\; \text{e}, \quad \epsilon_{\rm el} = \text{CBM} \tag{3.159}$$

then the configurational entropy of el can be well approximated by $-k_{\rm B}\ln[\text{e}]$, and we will have at thermal equilibrium

$$\frac{[{\rm D}^{n+}]}{[{\rm D}^{(n+1)+}][\text{el}]} \;=\; \text{const}_1 \times \exp\left(-\frac{\epsilon_{{\rm D}^{(n+1)+/n+}}(T) - \epsilon_{\rm el}}{k_{\rm B}T}\right) \tag{3.160}$$

$$\frac{[{\rm D}^{n+}]}{[{\rm D}^{(n+1)+}][\text{e}]} \;=\; \text{const}_1 \times \exp\left(-\frac{\epsilon_{{\rm D}^{(n+1)+/n+}}(T) - \text{CBM}}{k_{\rm B}T}\right) \tag{3.161}$$

But by the Fermi-Dirac distribution, and if $E_{\rm F}$ is in gap, we know [e] is basically

$$[\text{e}] \;\equiv\; \int_{\rm CBM}^{\infty} d\epsilon_{\rm el}\text{DOS}(\epsilon_{\rm el}) f^{\circ}(\epsilon_{\rm el}, T) \;\sim\; \text{const}_2 \times \exp\left(-\frac{\text{CBM} - E_{\rm F}}{k_{\rm B}T}\right) \tag{3.162}$$

so we get

$$\begin{aligned}\frac{[{\rm D}^{n+}]}{[{\rm D}^{(n+1)+}]} \;&=\; \text{const} \times \exp\left(-\frac{\text{CBM} - E_{\rm F}}{k_{\rm B}T}\right)\exp\left(-\frac{\epsilon_{{\rm D}^{(n+1)+/n+}}(T) - \text{CBM}}{k_{\rm B}T}\right)\\ &=\; \text{const} \times \exp\left(-\frac{\epsilon_{{\rm D}^{(n+1)+/n+}}(T) - E_{\rm F}}{k_{\rm B}T}\right)\end{aligned} \tag{3.163}$$

. Thus the **reduction fraction** of the defect would be

$$\frac{[{\rm D}^{n+}]}{[{\rm D}^{n+}] + [{\rm D}^{(n+1)+}]} \;=\; \frac{1}{1 + \frac{[{\rm D}^{(n+1)+}]}{[{\rm D}^{n+}]}} \;=\; \frac{1}{1 + \text{const}^{-1} \times \exp\left(\frac{\epsilon_{{\rm D}^{(n+1)+/n+}}(T) - E_{\rm F}}{k_{\rm B}T}\right)} \tag{3.164}$$

Obviously, const $\equiv$ const$_1$const$_2$ should be equal to 1, and a more physically motivated way is to think of the reduced defect as a *trapped electron* with marginal price $\epsilon_{\rm el} = \epsilon_{{\rm D}^{(n+1)+/n+}}(T)$, and then applying the **same Fermi-Dirac distribution** as for other band electrons:

$$\frac{[{\rm D}^{n+}]}{[{\rm D}^{n+}] + [{\rm D}^{(n+1)+}]} \;=\; \frac{1}{e^{\frac{\epsilon_{{\rm D}^{(n+1)+/n+}}(T) - E_{\rm F}}{k_{\rm B}T}} + 1} \tag{3.165}$$

even though the trapped electron is in reality an electron-phonon/defect coupled composite particle. D in fact can also be a perfect lattice site, in which case such trapped electron is called a polaron. For example in battery material LiCoO2, where all Co cations are $Co^{3+}$. But suppose there happens to be a $Co^{4+}$ with a localized hole. This localized hole will polarize the lattice, generating a Kanzaki force dipole $\mathbf{P}(Co^{4+})$. This trapped hole can hop from place to place, and this will be the main contribution to electronic conduction in LiCoO2 (there can also polaron on Oxygen, but that is much less likely). On the other hand, there are special layered planes for Li cations to hop, so the $Li^+$ ion mobility is also good. A good electronic conductivity and a good ionic conductivity (both relative to other ceramics) is the fundamental reason that LiCoO2 is used as battery cathode material.

From the defect reduction fraction (3.165), whether the defect is mostly oxidized or reduced depends on where the voltage is ($E_{\rm F} \equiv \mu_{\rm el} = -eU$) compared to the defect charging levels.

In a "normal" (positive-$U$) defect, we should have

$$\epsilon_{{\rm D}^{n+/(n-1)+}} \;>\; \epsilon_{{\rm D}^{(n+1)+/n+}} \tag{3.166}$$

In other words, as we raises $E_{\rm F}$, the defect taking ${\rm D}^{(n+1)+}$ state will first reduce to ${\rm D}^{n+}$, and later if we keep increasing $E_{\rm F}$, ${\rm D}^{n+}$ will reduce to ${\rm D}^{(n-1)+}$. We see that the above equation means

$$F({\rm D}^{(n-1)+}) - F({\rm D}^{n+}) \;>\; F({\rm D}^{n+}) - F({\rm D}^{(n+1)+}) \tag{3.167}$$

where $F$ is the Helmholtz free energy of the supercell, and we omitted the temperature dependence, or

$$F({\rm D}^{(n-1)+}) - 2F({\rm D}^{n+}) + F({\rm D}^{(n+1)+}) \;>\; 0 \tag{3.168}$$

This means if we interpolate the defect free energy with its charge number, we get positive curvature. (This curvature is the "electronic stiffness" or "hardness", or how much the going price of electrons is changing with more and more acquired). We can define

$$U \;\equiv\; F({\rm D}^{(n-1)+}) - 2F({\rm D}^{n+}) + F({\rm D}^{(n+1)+}) \;>\; 0 \tag{3.169}$$

A positive $U$ means the electronic subsystem is locally stable. This would be same as mechanical system with positive modulus, or chemical system before spinodal decomposition. But what happens with negative $U$? We would have

$$\epsilon_{\mathrm{D}^{n+/(n-1)+}} < \epsilon_{\mathrm{D}^{(n+1)+/n+}}, \quad F(\mathrm{D}^{(n-1)+}) - 2F(\mathrm{D}^{n+}) + F(\mathrm{D}^{(n+1)+}) \; < \; 0 \tag{3.170}$$

Suppose we have two $\mathrm{D}^{n+}$, it would actually choose to change to

$$\mathrm{D}^{n+} + \mathrm{D}^{n-} \; \rightarrow \; \mathrm{D}^{(n+1)+} + \mathrm{D}^{(n-1)+} \tag{3.171}$$

In other words, negative-$U$ defects would be locally unstable in charge, and would spontaneoulsy takes on charge state above and below.

There are really lots of parallels between **electronic disorder** and **point-defect disorder**, and the two are intimately coupled. Indeed, $\mu_{\mathrm{el}} \equiv E_{\mathrm{F}}$ controls what kind of charged defects exist in a dominant fashion in the lattice, and their populations, as we will see later in the **Brouwer diagram** section. The biggest difference is in the mobility, and the temperature dependence of mobility.

### Schottky disorder

This is expressed as

$$base \; = \; \mathrm{V}^{-}_{\mathrm{Na}} + \mathrm{V}^{+}_{\mathrm{Cl}} + \mathrm{Na}^{0}_{\mathrm{Na}'} + \mathrm{Cl}^{0}_{\mathrm{Cl}'} \tag{3.172}$$

where a $\mathrm{Na}^{0}_{\mathrm{Na}}(base)$ atom is moved to a new surface site and becomes $\mathrm{Na}^{0}_{\mathrm{Na}'}$, and a $\mathrm{Cl}^{0}_{\mathrm{Cl}}(base)$ atom is moved to a new surface site and becomes $\mathrm{Cl}^{0}_{\mathrm{Cl}'}$. We can also express $\mathrm{Na}^{0}_{\mathrm{Na}'} + \mathrm{Cl}^{0}_{\mathrm{Cl}'}$ as simply NaCl to resemble a newly grown piece of crystal, and reexpress (3.172) as

$$base \; = \; \mathrm{V}^{-}_{\mathrm{Na}} + \mathrm{V}^{+}_{\mathrm{Cl}} + \mathrm{NaCl}. \tag{3.173}$$

Since the LHS contains just *base*, the RHS may have different energy/entropy, but its chemistry will be unchanged from perfect crystalline *base*. This is called stoichiometric defect reaction. Some people also choose to write (3.173) as

$$nil \; = \; \mathrm{V}^{-}_{\mathrm{Na}} + \mathrm{V}^{+}_{\mathrm{Cl}} \tag{3.174}$$

In this notation, the charge is obviously balanced, and mass is balanced, but the site creation part (and surface traction sensitivity) is not easily seen. So I prefer (3.173) notation over (3.174) notation.

The defect equilibrium at zero stress would give us

$$[\mathrm{V}^-_{\mathrm{Na}}][\mathrm{V}^+_{\mathrm{Cl}}] \;=\; K(T) \tag{3.175}$$

where

$$K \;=\; c_{\mathrm{Na}} c_{\mathrm{Cl}} \exp\left(-\frac{f_{\mathrm{S}}(T)}{k_{\mathrm{B}}T}\right), \tag{3.176}$$

where $f_{\mathrm{S}}(T)$ is the Helmholtz free energy of creation, that includes the energy cost of creating two well-separated vacancies, as well as the vibrational entropy gain (not configurational) when that happens; $c_{\mathrm{Na}}$ is the concentration of Na-sublattice sites; $c_{\mathrm{Cl}}$ is the concentration of Cl-sublattice sites. (these are not defect concentrations, but site concentrations). If we call the volume per formula unit of NaCl $\Omega_{\mathrm{NaCl}}$, we should have $c_{\mathrm{Na}} = c_{\mathrm{Cl}} = 1/\Omega_{\mathrm{NaCl}}$.

**Frenkel disorder**

Many ceramics has smaller cations than anions, for example AgBr (ionic radius $\mathrm{Br}^-$: 1.96Å, $\mathrm{Ag}^+$: 1.26Å). They tend to have cation Frenkel disorder:

$$base \;=\; \mathrm{Ag}^+_{\mathrm{i}} + \mathrm{V}^-_{\mathrm{Ag}} \tag{3.177}$$

with equilibrium

$$[\mathrm{Ag}^+_{\mathrm{i}}][\mathrm{V}^-_{\mathrm{Ag}}] \;=\; K(T) \;=\; c_{\mathrm{Ag}} c_{\mathrm{i}} \exp\left(-\frac{f_{\mathrm{F}}(T)}{k_{\mathrm{B}}T}\right) \tag{3.178}$$

where $c_{\mathrm{i}}$ is the number of possible interstial sites, that may be different from $c_{\mathrm{Ag}} = 1/\Omega_{\mathrm{AgBr}}$ but fractional multiples. This can be proven by looking at the total energy - entropy tradeoff:

$$N_{\mathrm{F}} f_{\mathrm{F}}(T) - T k_{\mathrm{B}} \ln \frac{N_{\mathrm{Ag}}!}{(N_{\mathrm{Ag}} - V^-_{\mathrm{Ag}})! V^-_{\mathrm{Ag}}!} \times \frac{N_{\mathrm{i}}!}{(N_{\mathrm{i}} - \mathrm{Ag}^+_{\mathrm{i}})! \mathrm{Ag}^+_{\mathrm{i}}!} \tag{3.179}$$

when one extra $\mathrm{Ag}^+_{\mathrm{i}}, \mathrm{V}^-_{\mathrm{Ag}}$ is introduced into the system, the differential cost is

$$f_{\mathrm{F}}(T) + k_{\mathrm{B}}T \ln \frac{V^-_{\mathrm{Ag}}}{N_{\mathrm{Ag}}} + k_{\mathrm{B}}T \ln \frac{\mathrm{Ag}^+_{\mathrm{i}}}{N_{\mathrm{i}}} \;=\; 0 \tag{3.180}$$

so we get

$$K(T) \;=\; \frac{N_{\rm Ag}}{V_{\rm RVE}}\frac{N_{\rm i}}{V_{\rm RVE}}\exp\left(-\frac{f_{\rm F}(T)}{k_{\rm B}T}\right) \tag{3.181}$$

In AgCl, each cube has 4 Ag and 4 Cl. Each cube can take one interstitial, so $N_{\rm i}$ is the number of cubes. However, each cube has half Na atom (or each Na atom owns two cubes). So $N_{\rm i} = 2N_{\rm Ag}$. One can therefore also write, in the case of Schottky disorder:

$$[{\rm Ag}_{\rm i}^{+}] \;=\; [{\rm V}_{\rm Ag}^{-}] \;=\; \sqrt{\alpha}c_{\rm Ag}\exp\left(-\frac{f_{\rm F}(T)}{2k_{\rm B}T}\right) \tag{3.182}$$

where $\alpha = 2$, the ratio of interstitial sites to silver sublattice sites.

$\rm Ag_i^+$ is exceptionally mobile in silver halide crystals. When light is absorbed, it can create well-separated e and h. Then, this electronic disorder can induce

$$\rm Ag_i^+ + e \;=\; Ag_i^0 \tag{3.183}$$

which can migrate to the surface of a Ag(Br,I) grain. This is how traditional photography works. As the film containing colloidal suspension of the Ag(Br,I) grains (in gelatin) were exposed to light, as few as four Ag atoms on the surface of forms a neutral Ag metal cluster, which becomes the **latent image** (the holes are collected by the $\rm Br^-$, oxidizing them and forming $\rm Br_2(g)$, which leaves from the surface, making this photo-decomposition irreversible). Later, in developing the film by exposing the grains to a reducing solution of hydroquinone, the remaining silver cations in Ag(Br,I) will be reduced to silver metal, but they preferentially precipitate and grow at regions with pre-existing Ag clusters (serving as nuclei), forming the image consisting of metallic $\{\rm Ag_{\it n}\}$ clusters. (If one exposes to hydroquinone for too long, eventually all region would turn black). Afterwards, one washes away the unreduced Ag(Br,I) by exposing to "hypo".

**Anion Frenkel** disorder however are found in fluorite structures like $\rm CaF_2$, $\rm UO_2$, $\rm ZrO_2$, $\rm ThO_2$, etc. One reason is that the fluorite structure has open cubic holes in 50% of the anion cubes (the other 50% was filled by cations, so the cube is **large**). The other reason is that the anion charge is half that of the cation charge, and therefore the anion-anion electrostatic repulsion is less than the cation-cation electrostatic repulsion. So we can have $\rm O_i^{2-}$ in cubic $\rm ZrO_2$, alongside $\rm V_O^{2+}$. There are cation interstitials $\rm Zr_i^{\it x+}$, but they are not dominant anywhere with changing $E_{\rm F}$ (Fig. 4 of [28]).

There is no site creation in Frenkel disorder, thus no traction dependence in $K(T)$. There is

however interior stress dependence, and they bias the internal diffusion potentials for both cation and anion, by the relaxation strain-volumes of each, $\boldsymbol{\omega}^{\mathrm{R}}_{\mathrm{O}^{2-}_{\mathrm{i}}}\Omega_{\mathrm{ZrO_2}}$ and $\boldsymbol{\omega}^{\mathrm{R}}_{\mathrm{V}^{2+}_{\mathrm{O}}}\Omega_{\mathrm{ZrO_2}}$. $K(T)$ would be affected by interior stress $\boldsymbol{\sigma}$ according to

$$\boldsymbol{\omega}^{\mathrm{R}}_{\mathrm{Frenkel}}\Omega_{\mathrm{ZrO_2}} \;=\; \boldsymbol{\omega}^{\mathrm{R}}_{\mathrm{O}^{2-}_{\mathrm{i}}}\Omega_{\mathrm{ZrO_2}} + \boldsymbol{\omega}^{\mathrm{R}}_{\mathrm{V}^{2+}_{\mathrm{O}}}\Omega_{\mathrm{ZrO_2}} \tag{3.184}$$

Similarly, we can have antisite disorder

$$base \;=\; \mathrm{Na}^{2+}_{\mathrm{Cl}} + \mathrm{Cl}^{2-}_{\mathrm{Na}} \tag{3.185}$$

These are all stoichiometric disorders. One can think of stoichiometric disordering as "civil war". Non-stoichiometric disordering would be like with additional combatants (reactants) from foreign countries.

### Non-stoichiometric disorders

Consider FeO as our base structure. It turns out that this base is fictional, as there is always cation deficiency $\mathrm{Fe}_{1-x}\mathrm{O}$, with cation vacancies. This is created by the further oxidation of FeO:

$$base + \frac{1}{2}\mathrm{O_2}(g) \;=\; 2\mathrm{Fe}^{+}_{\mathrm{Fe}} + \mathrm{V}^{2-}_{\mathrm{Fe}} + \mathrm{O}^{0}_{\mathrm{O}} + \mathrm{FeO} \tag{3.186}$$

where we first invoke stoichiometric

$$base \;=\; \mathrm{V}^{2-}_{\mathrm{Fe}} + \mathrm{V}^{2+}_{\mathrm{O}} + \mathrm{FeO} \tag{3.187}$$

to create the site for incorporating external oxygen (mass action). But then we have a charge compensation problem (see 3.5.1), so we use $\mathrm{Fe}^{+}_{\mathrm{Fe}}$, which is just $\mathrm{Fe}^{3+}$ cation! (Ferric: $\mathrm{Fe}^{3+}$ or iron(III); Ferrous: $\mathrm{Fe}^{2+}$ or iron(II))

The equilibrium is just

$$\frac{[\mathrm{Fe}^{+}_{\mathrm{Fe}}]^2[\mathrm{V}^{2-}_{\mathrm{Fe}}]}{p^{1/2}_{\mathrm{O_2}}} \;=\; K(T) \tag{3.188}$$

The $\mathrm{Fe}^{+}_{\mathrm{Fe}}$, or trapped hole, is not as mobile as the band hole h, but is probably still more mobile than ionic defect since its motion requires only small ionic motion followed by eletron tunneling (Rudolph A. Marcus won Chemistry Nobel Prize in 1992 for coming up with rate expression for such electron transfer reactions). Thus, it is reasonable to postulate that $p_{\mathrm{O_2}}$

will impact the electronic conductivity of this material.

Alternatively, one can think of the process to be dissolving $Fe_2O_3$ into base:

$$base + Fe_2O_3 \;=\; V_{Fe}^{2-} + 2Fe_{Fe}^{+} + 3O_O^0 + 3FeO \tag{3.189}$$

which is an equivalent way to think about the mass action. In above we don't seem to have $p_{O_2}$ in the equation, though. Later, when we reveal the relationship between various point-defect disorders and phase free energy $g^\alpha(X_O)$ in (3.5.2), it will be obvious that when we put $Fe_2O_3$ phase in contact with FeO phase, the $p_{O_2}$ will be pinned by the common tangent between $Fe_{1-x}O$ and $Fe_2O_{3-y}$ single phases. This is often written in abbreviation as

$$\frac{1}{2}O_2(g) + 2FeO \;=\; Fe_2O_3 \tag{3.190}$$

which gives an equilibrium (pinned) $p_{O_2}$ value. But the notation in the reaction (3.190) above is a bit of simplification, because in individual crystalline phases of FeO and $Fe_2O_3$, there are defect disorders. The rigorous notation would think of both as **alloy phases** with degrees of **off-stoichiometry**, albeit small.

The reaction

$$base + h \;=\; Fe_{Fe}^{+} \tag{3.191}$$

converts delocalized band hole to a localized polaron. Rigorously speaking, polaron is not an ionic disorder, because unlike $V_{Cl}^0$ or $Ag_i^0$, the hole is not trapped by a lattice defect. However, there is some phonon (elastic displacement) that is dressing the localized hole. $Fe_{Fe}^{+}$ moves faster than normal lattice defects, but is much slower than a normal band hole, since its motion does involve some small lattice motion.

Another polaron example is $Li_{1-x}CoO_2$ that is used as cathode in Li-ion batteries. When $x = 0$, the lithium cobalt(III) oxide is easy to handle in air. Then once sealed in the battery, we can delithiate it:

$$base \;=\; Li^{+}(electrolyte) + e(metal\ current\ collector) + V_{Li}^{-} + h \tag{3.192}$$

but the hole is likely trapped by Co cation at room temperature:

$$base + h \;=\; Co_{Co}^{+} \tag{3.193}$$

which is really cobalt(IV). The multi-valency of Co,Ni,Mn,Fe first-row transition metals

supports the Li-ion battery technology today. When $V_{Li}^{-}$ diffuses in and out of the cathode, it needs to be accompanied by equal amount of polaron motion localized on the transition metal cations.

### Cation Interstitials

Cation interstitial becomes possible for ZnO, since $Zn^{2+}$ has very small ionic radius, 0.74Å, and the Frenkel disorder energy is only 2.51 eV (table 11.8 of [29]). Let us exclude the possibility of vacancies (either $V_O^{2+}$ or $V_M^{2-}$) for the moment. (They are still there, but are "deep under the ocean" that they don't matter)

Consider a base crystal ZnO exposed to Zn vapor:

$$base + \mathrm{Zn}(g) \;=\; 2\mathrm{e} + \mathrm{Zn}_\mathrm{i}^{2+} \tag{3.194}$$

This creates off-stoichiometry, $Zn_{1+x}O$. Note that in our notation, subscript $1-x$ implies vacancies and $1+x$ implies interstials. Even though $M_{1-x}O_{1+y}$ is chemically identical to $M_{(1-x)/(1+y)}O_1$, the former notation gives richer information about the point-defect disorder inside.

Also, the e find it easier to be trapped by $Zn_i^{2+}$, and turn into $Zn_i^{+}$ (a $Zn^{+}$ or zinc(I) cation), and so we also have

$$base + \mathrm{Zn}(g) \;=\; \mathrm{e} + \mathrm{Zn}_\mathrm{i}^{1+} \tag{3.195}$$

and

$$[\mathrm{e}][\mathrm{Zn}_\mathrm{i}^{1+}]p_\mathrm{Zn}^{-1} \;=\; K \tag{3.196}$$

The trapping energy is sufficiently large that $[Zn_i^{2+}] \ll [Zn_i^{1+}]$, so we get

$$[\mathrm{e}] \;\sim\; [\mathrm{Zn}_\mathrm{i}^{1+}] \tag{3.197}$$

and so

$$[\mathrm{e}] \;\sim\; [\mathrm{Zn}_\mathrm{i}^{1+}] \;\propto\; p_\mathrm{Zn}^{1/2} \;\propto\; p_{\mathrm{O}_2}^{-1/4}. \tag{3.198}$$

In above we have used the relation $p_{Zn}p_{O_2}^{1/2} = K$, derived from

$$\mathrm{Zn}(g) + \frac{1}{2}\mathrm{O}_2(g) \;=\; \mathrm{ZnO} \tag{3.199}$$

Alternatively, we may also write

$$base \;=\; \mathrm{Zn_i^{2+}} + \frac{1}{2}\mathrm{O_2}(g) + 2\mathrm{e} - \mathrm{ZnO} \tag{3.200}$$

$$base \;=\; \mathrm{Zn_i^{1+}} + \frac{1}{2}\mathrm{O_2}(g) + \mathrm{e} - \mathrm{ZnO} \tag{3.201}$$

where the -ZnO is to denote the destruction of lattice sites at surface. From above we can also see that

$$[\mathrm{Zn_i^{2+}}]p_{\mathrm{O_2}}^{1/2}[\mathrm{e}]^2 \;=\; K_2, \quad [\mathrm{Zn_i^{1+}}]p_{\mathrm{O_2}}^{1/2}[\mathrm{e}] \;=\; K_1 \tag{3.202}$$

Indeed $\sigma_{\mathrm{el}} \propto p_{\mathrm{O_2}}^{-1/4}$ is what is experimentally found, so $[\mathrm{Zn_i^{1+}}] \sim [\mathrm{e}]$ is the actual situation. If $2[\mathrm{Zn_i^{2+}}] \sim [\mathrm{e}]$, then we should have $\sigma_{\mathrm{el}} \propto p_{\mathrm{O_2}}^{-1/6}$ instead.

ZnO is n-type semiconductor ($E_{\mathrm{F}}$ high and likely larger than $\varepsilon_{1/2}(\mathrm{Zn_i})$), and used to make sensors like variable resistor (varistor). Since the electronic conductivity $\propto [\mathrm{e}]$, we will have its total electrical conductivity decreases with increasing $p_{\mathrm{O_2}}$, which makes it a possible oxygen gas sensor.

**To summarize**

Ceramics entertain a richer zoo of electronic and ionic disorder. For electronic disorder, in metals there is just "el" around the Fermi energy (so-called Landau-Fermi liquid theory, think of it as an ocean, with "foams" at sea level). In ceramics, "el" breaks up into two levels, e and h. Think of it as stone slab separating ground water below from dry floor above. e,h can associate with each other (excitons, trions) and with ionic defects (color centers like $\mathrm{V_{Cl}^0}$ and diamond $\mathrm{NV^-}$, non-Kroger Vink charged $\mathrm{Ag_i^0}$ for photography and $\mathrm{Zn_i^+}$ for gas sensing, polarons like $\mathrm{Fe_{Fe}^+}$ in FeO and $\mathrm{Co_{Co}^+}$ in $\mathrm{Li_{1-x}CoO_2}$ for battery). With association, the enthalpy, entropy and mobility all tends to reduce.

### 3.5.1 Charge compensation

The excess charge density $\rho^{\mathrm{excess}}(\mathbf{x})$ defined in (1.1), which consists of ionic and electronic contributions:

$$\rho^{\mathrm{excess}}(\mathbf{x}) \;\equiv\; \rho_{\mathrm{ion}}(\mathbf{x}) + \rho_{\mathrm{el}}(\mathbf{x}) \tag{3.203}$$

needs to respect certain constraints. $\rho_{\mathrm{ion}}(\mathbf{x})$ consists of the formal charge of all localized ionic defects ($\mathrm{V_M^{2-}}$, $\mathrm{V_O^{2+}}$, $\mathrm{M_i^{2+}}$, $\mathrm{O_i^{2-}}$, etc). $\rho_{\mathrm{el}}(\mathbf{x})$ consists of delocalized band electrons (e) and

holes (h):

It turns out that the positive cloud of $\rho^{\text{excess}}(\mathbf{x})$ has to be screened by equal and opposite cloud. In other words, the positive cloud cannot be infinitely separated from the negative cloud, otherwise something called **Coulombic explosion** would happen. Suppose a region of positive average

$$\langle \rho^{\text{excess}}(\mathbf{x}) \rangle \;=\; \bar{\rho} \;>\; 0 \tag{3.204}$$

extends to a sphere of radius $R$:

$$E_{\text{interaction}} \;=\; \int d\mathbf{x} \int d\mathbf{x}' \frac{\bar{\rho} \times \bar{\rho}}{4\pi\varepsilon\varepsilon_0 |\mathbf{x} - \mathbf{x}'|} \;\propto\; R^5 \tag{3.205}$$

so the interaction energy density actually scales as

$$\frac{E_{\text{interaction}}}{R^3} \;=\; R^2 \;\to\; \infty \tag{3.206}$$

In other words, it becomes infinitely costly to insert the same charge in the same voume. The only way to avoid Coulombic explosion is therefore to have

$$\langle \rho^{\text{excess}}(\mathbf{x}) \rangle \;=\; 0 \tag{3.207}$$

which includes the sum of charged defect (localized), and electrons and holes (delocalized band transport). Coulombic explosion actually happens in materials under ultrahigh powered laser, where some electrons are instantaneously excited out of the material, and the remainder crystal would just have to explode over picoseconds timescale.

Consider Schottky disorder in $M_2O_3$:

$$2\mathrm{M}_{\mathrm{M}}^{0} + 3\mathrm{O}_{\mathrm{O}}^{0} \;=\; 2\mathrm{V}_{\mathrm{M}}^{3-} + 3\mathrm{V}_{\mathrm{O}}^{2+} + \mathrm{M_2O_3} \tag{3.208}$$

When we write down the chemical potential balance, we get:

$$0 \;=\; \Delta G^{\circ} + 2k_{\mathrm{B}}T \ln \frac{N_{\mathrm{V}_{\mathrm{M}}^{3-}}}{N_{\mathrm{M}}} + 3k_{\mathrm{B}}T \ln \frac{N_{\mathrm{V}_{\mathrm{O}}^{2+}}}{N_{\mathrm{O}}} \tag{3.209}$$

where $N_{\mathrm{M}}$ is the number of metal sites in a certain volume:

$$\frac{N_{\mathrm{V}_{\mathrm{M}}^{3-}}}{N_{\mathrm{M}}} \;\equiv\; \frac{[\mathrm{V}_{\mathrm{M}}^{3-}]}{c_{\mathrm{M}}^{\circ}}, \qquad \frac{N_{\mathrm{V}_{\mathrm{O}}^{2+}}}{N_{\mathrm{O}}} \;\equiv\; \frac{[\mathrm{V}_{\mathrm{O}}^{2+}]}{c_{\mathrm{O}}^{\circ}} \tag{3.210}$$

which gives us

$$[\mathrm{V}_{\mathrm{M}}^{3-}]^2[\mathrm{V}_{\mathrm{O}}^{2+}]^3 \;=\; K_{\mathrm{S}}(T) \tag{3.211}$$

where

$$K \;\equiv\; c_{\mathrm{M}}^{\circ 2} c_{\mathrm{O}}^{\circ 3} \exp\left(-\frac{\Delta G^{\circ}}{k_{\mathrm{B}}T}\right) \tag{3.212}$$

is temperature and surface traction $t_{nn}$ dependent.

(3.211) is true, but it does not fully close the problem. If we assume the charge compensation is done only between $\mathrm{V}_{\mathrm{O}}^{2+}$ and $\mathrm{V}_{\mathrm{M}}^{3-}$, that there are **no other** significant contributors to $\bar{\rho}$ (the essence of "Schottky disorder" dominant), then we will have

$$2[\mathrm{V}_{\mathrm{O}}^{2+}] - 3[\mathrm{V}_{\mathrm{M}}^{3-}] \;=\; 0, \tag{3.213}$$

and then we can close the equation

$$(\frac{2}{3}[\mathrm{V}_{\mathrm{M}}^{3-}])^2[\mathrm{V}_{\mathrm{O}}^{2+}]^3 \;=\; K \tag{3.214}$$

or

$$[\mathrm{V}_{\mathrm{O}}^{2+}] \;\propto\; K^{1/5} \;\propto\; \exp\left(-\frac{\Delta G^{\circ}}{5k_{\mathrm{B}}T}\right). \tag{3.215}$$

But if the system is *electronically compensated*, the above would not be true. When we consider ceramics or semiconductor:

$$[\mathrm{e}][\mathrm{h}] \;=\; K_{\mathrm{eh}}(T) \;\propto\; \exp\left(-\frac{E_{\mathrm{gap}}}{k_{\mathrm{B}}T}\right). \tag{3.216}$$

and the difference between majority carrier and minority carrier is usally pretty stark. (If [e] is the majority carrier, it is called n-typed, and if [h] is the majority carrier, it is called p-typed). *Electronically compensated* means the magnitude of the majority carrier becomes comparable to that of the highest-concentration charged defect, and must be taken into consideration. So in principle we could have for example

$$2[\mathrm{V}_{\mathrm{O}}^{2+}] - 3[\mathrm{V}_{\mathrm{M}}^{3-}] + [\mathrm{h}] - [\mathrm{e}] \;=\; 0, \tag{3.217}$$

or even more ionic defects in the above, and the equation is dominated by $[\mathrm{V}_{\mathrm{M}}^{3-}]$ and [h], for instance, instead of the other terms.

For stoichiometric situation, we have three equations, (3.217), (3.211) and (3.216) and what appears to be four variables. But those four variables are given by two reaction progress

variables: $[\mathrm{e}] = [\mathrm{h}] = \lambda_{\mathrm{eh}}$, $[\mathrm{V}_{\mathrm{M}}^{3-}] = 2\lambda_{\mathrm{S}}$, $[\mathrm{V}_{\mathrm{O}}^{2+}] = 3\lambda_{\mathrm{S}}$, so the charge balance equation is doubly satisfied (one has an intrinsic semiconductor with $E_{\mathrm{F}}$ perfectly midgap, and the ionic disorder and the electronc disorder are individually charge balanced), and because these reaction progress variables individually satisfy charge balance, the total charge balance equation is not a true equation, so we have two true equations ($K_{\mathrm{S}}(T)$ and $K_{\mathrm{eh}}(T)$) and two true unknowns ($\lambda_{\mathrm{S}}(T)$ and $\lambda_{\mathrm{eh}}(T)$). But for non-stoichiometric (NS) situation, there is foreign combatant, with price controlled by $p_{\mathrm{O}_2}$. One adds another reaction progress variable $\lambda_{\mathrm{O}}$:

$$base + \frac{3}{2}\mathrm{O}_2(g) \;=\; 2\mathrm{V}_{\mathrm{M}}^{3-} + 6h + \mathrm{M}_2\mathrm{O}_3 \tag{3.218}$$

One also gets one more equation $K_O(T)$, so there are three true equations and three true unknowns, each derived from one independent reaction. Here, because of the introduction of foreign combatant (more oxygen would make the environment more oxidative, favoring more holes), the semiconductor is no longer "intrinsic", and since

$$[\mathrm{e}] \;=\; const \times \exp(-\frac{\mathrm{CBM} - E_{\mathrm{F}}}{k_{\mathrm{B}}T}),\;\; [\mathrm{h}] \;=\; const \times \exp(\frac{\mathrm{VBM} - E_{\mathrm{F}}}{k_{\mathrm{B}}T}), \tag{3.219}$$

changing $p_{\mathrm{O}_2}$ would shift $E_{\mathrm{F}}$.

### 3.5.2 Brouwer diagram

Suppose a metal oxide of base form MO can have vacancy disorder $\mathrm{V}_{\mathrm{M}}^{2-}$ or $\mathrm{V}_{\mathrm{O}}^{2+}$, but the interstials are so expensive that they are forbidden. Thus, the actual metal oxide can deviate from its base and become off-stoichiometric $\mathrm{M}_{1-x}\mathrm{O}_{1-y}$, where $x \propto [\mathrm{V}_{\mathrm{M}}^{2-}]$ and $y \propto [\mathrm{V}_{\mathrm{O}}^{2+}]$. When $x = y$, we say **stoichiometry is maintained** (Schottky disorder), but clearly, a very large or very small $p_{\mathrm{O}_2}$ can drive the system off-stoichiometry. In reality, materials are not isolated: they are open systems where mass action (like immigration) is kinetically possible, in particular the exchange of oxygen with the air bath environment. In considering charge compensation:

$$2[\mathrm{V}_{\mathrm{O}}^{2+}] - 2[\mathrm{V}_{\mathrm{M}}^{2-}] + [\mathrm{h}] - [\mathrm{e}] \;=\; 0 \tag{3.220}$$

there are multiple possibilities:

- $2[\mathrm{V}_{\mathrm{O}}^{2+}] \;\sim\; 2[\mathrm{V}_{\mathrm{M}}^{2-}]$
- $2[\mathrm{V}_{\mathrm{O}}^{2+}] \;\sim\; [\mathrm{e}]$

- $2[\mathrm{V}_\mathrm{M}^{2-}] \sim [\mathrm{h}]$
- $[\mathrm{e}] \sim [\mathrm{h}]$

where $\sim$ denotes the **two major actors**, fighting to a near draw. The remaining two **minor actors** may have large ratio amongst themselves, but it won't matter because they are of minor concentrations. When we plot the four actors on log-axis, we get the Brouwer diagrams as shown in FIGURE 11.4 of [29], which have three regimes as a function of $p_{\mathrm{O}_2}$.

Clearly, when $p_{\mathrm{O}_2}$ is humongous, $[\mathrm{V}_\mathrm{O}^{2+}] \ll [\mathrm{V}_\mathrm{M}^{2-}]$. When $p_{\mathrm{O}_2}$ is tiny (on the log-scale), $[\mathrm{V}_\mathrm{O}^{2+}] \gg [\mathrm{V}_\mathrm{M}^{2-}]$. So there must exist a special $p_{\mathrm{O}_2}$, where

$$[\mathrm{V}_\mathrm{O}^{2+}] = [\mathrm{V}_\mathrm{M}^{2-}] \tag{3.221}$$

exactly. This special $p_{\mathrm{O}_2}$ is defined as $p_{\mathrm{O}_2}^\mathrm{S}$, which may stand for either Schottky or stoichiometry in this context.

To orient ourselves, let us distinguish two situations A and B, at the stoichiometric $p_{\mathrm{O}_2}^\mathrm{S}$. Since by definition $[\mathrm{V}_\mathrm{O}^{2+}] = [\mathrm{V}_\mathrm{M}^{2-}]$, there must also be $[\mathrm{e}] = [\mathrm{h}]$ exactly. If there are **more ionic disorder** than electronic disorder at point of stoichiometry, then we call this situation A. Otherwise, we call this situation B. Whether A/B pretty much depends on whether $f_\mathrm{S}(T) < E_\mathrm{g}$ or not.

Take situation A, we have regime I and III where one vacancy defect is compensated electronically. Consider the reaction:

$$base = \mathrm{V}_\mathrm{O}^{2+} + \frac{1}{2}\mathrm{O}_2(g) + 2\mathrm{e} \tag{3.222}$$

$$base = \mathrm{V}_\mathrm{O}^{2+} + \mathrm{V}_\mathrm{M}^{2-} + \mathrm{MO} \tag{3.223}$$

$$base + \frac{1}{2}\mathrm{O}_2(g) = 2\mathrm{h} + \mathrm{O}_\mathrm{O}^0 + \mathrm{V}_\mathrm{M}^{2-} + \mathrm{MO} \tag{3.224}$$

The first equation is oxygen release, whereas the third equation is oxidation. There is

$$[\mathrm{V}_\mathrm{O}^{2+}][\mathrm{e}]^2 p_{\mathrm{O}_2}^{1/2} = K_1 \tag{3.225}$$

$$[\mathrm{V}_\mathrm{O}^{2+}][\mathrm{V}_\mathrm{M}^{2-}] = K_\mathrm{S} \tag{3.226}$$

$$[\mathrm{V}_\mathrm{M}^{2-}][\mathrm{h}]^2 p_{\mathrm{O}_2}^{-1/2} = K_3 \tag{3.227}$$

In the very low $p^{\mathrm{S}}_{\mathrm{O}_2}$ regime, we will have a lot of reaction 1, and as a result we will have

$$2[\mathrm{V}^{2+}_{\mathrm{O}}] \sim [\mathrm{e}] \tag{3.228}$$

so with

$$[\mathrm{V}^{2+}_{\mathrm{O}}](2[\mathrm{V}^{2+}_{\mathrm{O}}])^2 p^{1/2}_{\mathrm{O}_2} \sim K_1 \tag{3.229}$$

we get $[\mathrm{V}^{2+}_{\mathrm{O}}], [\mathrm{e}] \propto p^{-1/6}_{\mathrm{O}_2}$. Then, $[\mathrm{V}^{2-}_{\mathrm{M}}], [\mathrm{h}] \propto p^{1/6}_{\mathrm{O}_2}$ even though they are much lower than [e]. This is regime I.

For scenario A, because $K_{\mathrm{S}}$ is big, $[\mathrm{V}^{2-}_{\mathrm{M}}]$ is not very low to begin with and catches up fast with decreasing [e]. Once we get to a cross-over point where $[\mathrm{V}^{2-}_{\mathrm{M}}]$ becomes comparable to [e], we change from electronically compensated to ionically compensated: $2[\mathrm{V}^{2+}_{\mathrm{O}}] \sim 2[\mathrm{V}^{2-}_{\mathrm{M}}]$. Then, for a while $[\mathrm{V}^{2+}_{\mathrm{O}}]$ no longer changes with $p_{\mathrm{O}_2}$, and we get $[\mathrm{e}] \propto p^{-1/4}_{\mathrm{O}_2}$, and $[\mathrm{h}] \propto p^{1/4}_{\mathrm{O}_2}$. This is called regime II. Even though we introduce foreign combatant and the external condition changes quite a lot, the two majority combatants populations are basically pinned. This is similar to a **chemical buffer solution**. The trick is to introduce other players in the phase of interest that are locked in combat.

The situation has mirror symmetry afterwards. With the continuous rise of [h], eventually [h] catches up to $[\mathrm{V}^{2+}_{\mathrm{O}}]$, and the system becomes electronically compensated again, this time between [h] and $[\mathrm{V}^{2-}_{\mathrm{M}}]$. We get

$$2[\mathrm{V}^{2-}_{\mathrm{M}}] \sim [\mathrm{h}] \tag{3.230}$$

and

$$[\mathrm{V}^{2-}_{\mathrm{M}}](2[\mathrm{V}^{2-}_{\mathrm{M}}])^2 p^{-1/2}_{\mathrm{O}_2} = K_3 \tag{3.231}$$

so $[\mathrm{V}^{2-}_{\mathrm{M}}], [\mathrm{h}] \propto p^{1/6}_{\mathrm{O}_2}$. This is regime III.

The Brouwer diagram shows the degree and nature of the non-stoichiometry of an oxide as $p_{\mathrm{O}_2}$ is varied. The above illustrates the situation with $\mathrm{M}_{1-x}\mathrm{O}_{1-y}$ where interstitials are scarce, but interstitial concentration can also show up in the Brouwer diagram [28] (see next subsection), and then maybe the oxide can be denoted as $\mathrm{M}_{1+x}\mathrm{O}_{1-y}$. Generally speaking, the range of continuously varying $x$ and $y$ that $\mathrm{M}_{1\pm x}\mathrm{O}_{1\pm y}$ can exist stably in the same lattice structure is called the **solubility range** of the MO phase, just like the solubility range of metallic alloy phases. Typically one thinks of the ceramic as **compounds**, because the solubility range tends to be much smaller than that of metallic alloys. Still, there is always a small amount of defects in a large enough crystal, and this crystal will breathe in and out small amount of oxygen depending on the $p_{\mathrm{O}_2}$ of the environment. This means the solubility

range of any compound may be very small, but not perfect zero. And defects is what we deal with in this course, so we must face up to this reality.

We see from FIGURE 11.4 of [29] that the dominant defect concentration would shift up or down depending on $f_{\rm S}(T)$. Thus, for MgO which has a huge $f_{\rm S}(T) = 6.6$eV, the solubility range is tiny (less than tens of ppm), so for most practical purposes people call MgO "stoichiometric oxide". On the other hand, well-known oxides $TiO_2$, VO, FeO, $Fe_3O_4$, etc. have solubility range exceeding tens of ppm (see TABLE 6.1 of [30]), and thus are called "nonstoichiometric oxides". (even though in principles everyone is nonstoichiometric). The difference lies in the **magnitude** of the defect formation energies. This is because the actual way the lattice can accommodate a chemical composition expression like $M_{1\pm x}O_{1\pm y}$ is through the physical creation of point defects, and it is more costly in some materials than others.

We can now apply solution thermodynamics to analyze the stability of any $M_{m\pm x}O_{n\pm y}$ phase. There is a **local stability** analysis where $M_{m\pm x}O_{n\pm y}$ is just competing with small variations of itself, either vibrational perturbations to its own structure, or composition perturbations like the spinodal instability. The **local stability range** $X$,$Y$ is probably quite large, like tens of percent. However, there is also a **global stability** analysis where $M_{m\pm x}O_{n\pm y}$ has to compete with far-away phases $\{M_{m'\pm x}O_{n'\pm y}\}$ that have very dissimilar lattice structures and chemistries, by mass action. The basic tool one uses in this is the tangent theorem, where the tangent extrapolation of $g(\mathbf{X}, T, P)$ to $\mathbf{X} = \mathbf{p}_i$ is identified to be the chemical potential $\mu_i(\mathbf{X}, T, P)$. If we take $i$=Oxygen, and use ideal $O_2$ gas as reference, then

$$\mu_{\rm O} \;=\; \tilde{\mu}_{\rm O}(T) + \frac{1}{2} k_{\rm B} T \ln p_{\rm O_2} \tag{3.232}$$

where more generally $p_{\rm O_2}$ is the gas fugacity of $O_2(g)$. Thus, according to the Gibbs phase rule, at an arbitrary temperature $T$, the competition of different forms of $\{M_{m\pm x}O_{n\pm y}\}$ gives either 1-phase or 2-phase regions. The 2-phase region is denoted by a constant $p_{\rm O_2}$, given by the **common tangent construction**. At this $p_{\rm O_2}$, there is a jump from $M_{m-x}O_n$ to $M_{m'}O_{n'-y}$, say, i.e. there is a sharp change of oxygen ratio. For oxygen ratio in between, it is a 2-phase mixture rather than 1-phase. Below and above that fixed $p_{\rm O_2}$, there are two single-phase regions, where $p_{\rm O_2}$ varies continuously and $x$ or $y$ varies continuously also.

### 3.5.3 Diffusion in Nonstoichiometric Ceramics

**Stabilized Cubic** $ZrO_2$

Stoichiometric cubic fluorite $ZrO_2$ does not compete well with monoclinic $ZrO_2$ (stable below 1170 °C) or tetragonal $ZrO_2$ (stable between 1170-2370 °C). But by mixing in CaO, MgO or $Y_2O_3$ on the order of few percent up to 20%, the fluorite structure can be stablized to room temperature. We have

$$\mathrm{CaO} + base \;=\; \mathrm{Ca}_{\mathrm{Zr}}^{2-} + \mathrm{O}_{\mathrm{O}}^{0} + V_{\mathrm{O}}^{2+} + \mathrm{ZrO}_2 \tag{3.233}$$

So if we have a few percent $\mathrm{Ca}_{\mathrm{Zr}}^{2-}$, we will have a few percent $V_{\mathrm{O}}^{2+}$, with a chemical formula that reads $\mathrm{Ca}_x\mathrm{Zr}_{1-x}\mathrm{O}_{2-x}$. Naively, one can think of this composition as $x\mathrm{CaO}\cdot(1-x)\mathrm{ZrO}_2$, but this notation seems to suggest 2-phase mixture, whereas in reality we are talking about a single-phase solid solution, so I prefer the $\mathrm{Ca}_x\mathrm{Zr}_{1-x}\mathrm{O}_{2-x}$ notation. If necessary, we can write down

$$x\mathrm{CaO} + (1-x)\mathrm{ZrO}_2 \;\rightarrow\; \mathrm{Ca}_x\mathrm{Zr}_{1-x}\mathrm{O}_{2-x}. \tag{3.234}$$

The above is called Calcia-Stabilized Zirconia. One can also have similar $Y_2O_3$ mixing and Yttria-stabilized zirconia (YSZ) like 8YSZ where 8% of the original Zr site is taken up by Y, and there are 4% vacancies on the oxygen sublattice.

The mobility of $V_{\mathrm{O}}^{2+}$ is quite high in the fluorite structure. So YSZ is used as the solid electrolyte in high temperature fuel cells. The basic idea of fuel cell (and battery) is pretty much the same as **burning the fuel**, where one needs to either bring the oxygen to the fuel, or the fuel (like hydrogen fuel cell) to oxygen, with only one additional trick: so-called **electrolyte contrast** in transference number. Solid electrolyte like YSZ conduct ions ($V_{\mathrm{O}}^{2+}$) but not e. Metal wire conducts e but not ions. So the neutral $\mathrm{O}_2(g)$ would split up into oxygen ion and electrons, and go separate ways. The electrons that goes through the metal wire will be "taxed" to drive the outer circuit.

In such case, there is clearly $D_{\mathrm{O}} \propto [\mathrm{Ca}_{\mathrm{Zr}}^{2-}]$, since the probability of any particular oxygen tracer moving is proportional to the probability there is an oxygen vacancy sitting next to it.

**KCl doped by** $CaCl_2$

KCl is still dominated by vacancies. We have

$$CaCl_2 + base \;=\; Ca_K^+ + V_K^- + 2Cl_{Cl}^0 + 2KCl \tag{3.235}$$

$$base \;=\; 2V_K^- + 2V_{Cl}^+ + 2KCl \tag{3.236}$$

We can define two reaction progress variables, $\lambda_1$ and $\lambda_2$, that describes how much cases of reaction (3.235) and reaction (3.236) have occured. The former is called **extrinsic**, whereas the latter is called **intrinsic**. Extrinsic cases requires external "intervention". In most situations, the extrinsic contribution ($\lambda_1$) can dominate over the intrinsic contribution. So $D_K \propto [Ca_K^+]$. This relation works because (a) the intrinsic vacancies, due to thermal fluctuations, is quite low and not comparable with the amount of Ca dopants in the system. (b) the mobility of $V_K^-$ has a limiting value in the dilute $[Ca_K^+]$ limit.

It is interesting that the transport of K can be dominated by externally added impurities like Ca. In Fig. 11.11 of [29], we see that going from high temperature to low temperature, there are three ranges of $\log D_K$ vs. $1/T$. At very high temperature, the intrinsic behavior dominates, and the slope is $h_S/2k_B + h_m/k_B$, where $h_m$ is the saddle-point enthalpy change (migration enthalpy) of $V_K^-$. $h_S/2$ is just 1.3eV, as shown in the inset. In intermediate temperature, the slope is just $h_m/k_B$, but with the intercept influenced by whether [Ca] is $10^{-4}c_K$ or $10^{-5}c_K$. In very low temperature, we see a break again. This is due to the association reaction:

$$Ca_K^+ + V_K^- \;=\; (Ca_K^+, V_K^-) \tag{3.237}$$

The LHS represents two well-separated (divorced) point defects. The RHS represents a defect association, where the two are tightly bound together. The RHS has an enthalpy advantage of $h_P$ =0.8eV, as shown in the inset, but the LHS has entropy advantage. We can write down

$$\frac{[Ca_K^+][V_K^-]}{[(Ca_K^+, V_K^-)]} \;=\; K(T) \tag{3.238}$$

where $K(T)$ has $1/T$ sensitivity of $h_P$. This is exactly like an exciton - an electron tied to a hole - but for ionic disorder. (3.237) is very similar to a evaporation/condensation reaction. When the temperature reachs a certain level, the water molecule would evaporate despite higher enthalpy. So $(Ca_K^+, V_K^-)$, despite Coulombic binding, might self-ionize. This is the same story with exciton $(e, h)$, etc.

When temperature is in regime III, we are going to assume that the RHS of (3.237) is immobile, and we still need to rely on the LHS of (3.237) for shuffling of K. (In reality, the $(\mathrm{Ca}_\mathrm{K}^+, \mathrm{V}_\mathrm{K}^-)$ of course also has certain rotational and translational mobility, but that could be very low.) In this case, most of the $10^{-4}$ or $10^{-5}$ of [Ca] is tied down by vacancy, and free vacancy concentration (LHS of (3.237)) needs to be thermally activated, with a population that goes as $10^{-5} c_\mathrm{K} \exp(-h_\mathrm{P}/2k_\mathrm{B}T)$. Thus the third segement of Fig. 11.11 of [29] has yet another slope of $h_\mathrm{P}/2k_\mathrm{B} + h_\mathrm{migration}/k_\mathrm{B}$.

It is reasonable to ask what is the scale of binding energy to temperature that one needs to consider something as clearly tight bound. Consider we have a Avogadro number of atoms (e.g. 12 grams of carbon). This is a macroscopic piece with cm dimension. What is the temperature at which there is just a single vacancy in the piece? We have

$$6.022 \times 10^{23} \exp(-\frac{h_\mathrm{V}}{k_\mathrm{B}T}) \ \sim \ 1 \tag{3.239}$$

and this gives $h_\mathrm{V} = \ln(6.022 \times 10^{23}) k_\mathrm{B}T = 55 k_\mathrm{B}T$. For $T_\mathrm{room} = 300\mathrm{K}$, we get 1.4 eV; so for 600K it is 2.8 eV; 1000K it is 4.7 eV, etc.

### 3.5.4 Ambipolar transport of oxygen

Consider a binary oxide $\mathrm{M}_m\mathrm{O}_n$, where $n$, $m$ are the formal valence charge (absolute value) of the cation and anion, respectively. Usually $m = 2$, and $\mathrm{M}_m\mathrm{O}_n$ may be further factorized like $\mathrm{Zn_2O_2} = \mathrm{ZnO}$, but here we just keep them unfactorized. The following defects (and their ionized versions perhaps) are usual suspects: $\mathrm{V}_\mathrm{M}^{n-}$, $\mathrm{V}_\mathrm{O}^{m+}$, $\mathrm{M}_\mathrm{i}^{n+}$, $\mathrm{O}_\mathrm{i}^{m-}$. The presence of an oxidizing environment may bias the stoichiometry of the crystal, in the following ways:

$$\frac{1}{2}\mathrm{O}_2(g) + \mathrm{V}_\mathrm{O}^{m+} + m\mathrm{e} \ = \ \mathrm{O}_\mathrm{O}, \tag{3.240}$$

or

$$\frac{1}{2}\mathrm{O}_2(g) \ = \ \mathrm{O}_\mathrm{i}^{m-} + m\mathrm{h}. \tag{3.241}$$

Consider the permeation of $\mathrm{O}_2(g)$ from $p_{\mathrm{O}_2}^\mathrm{H}$ at $x = H$ to $\mathrm{O}_2(g)$ from $p_{\mathrm{O}_2}^\mathrm{L}$ at $x = L$ through an oxide membrane. The physical reality is that $\mathrm{O}_2/2$ must be disassembled into a charged defect plus excess band e/h in order to be transported through. After disassembly, there is no reason microscopically that the e/h must move in lock step with the charged defect;

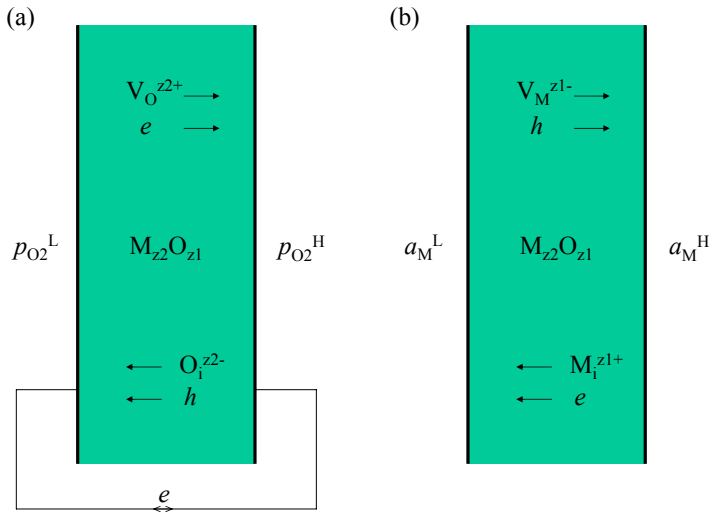


Figure 3.3: Permeation across oxide layer.

they can go their separate ways. Indeed, if there is an external circuit as shown in Fig. 3.3, the e/h would go through that external circuit as shortcut. But, if no such electrical circuit exist as in most cases of metal oxidation, the e/h must go through the same oxide scale as the charged defect. Usually there are large differences in the mobilities of e/h and charged defect, so the center-of-mass of e/h cloud will initially have a relative velocity versus that of the charged defect cloud. This would establish an electric field across the entire scale which would accelerate one cloud and decelerate the other, until eventually the two centers-of-mass have a finite but no longer increasing separation. This coupling of two mobile species, through the same electrostatic potential $\phi(x)$ that they must share inside the oxide, is called ambipolar diffusion [30].

The dynamics of ambipolar diffusion is quite complex, so we will only solve for the steady-state in the case of $O_2$ permeation [31]. Consider the situation where $V_O^{m+}$ is the dominant species. On either surface where $V_O^{m+}$ is able to equilibrate with $O_2(g)$, we would have:

$$p_{O_2}^{1/2} c_{V_O^{m+}} c_e^m \;=\; K_1. \tag{3.242}$$

Electro-neutrality condition is only broken at the surface, and even there only slightly, $\propto \log(p_{O_2}^{H}/p_{O_2}^{L})$. In the spirit of 1st-order perturbation theory, we can ignore this and assume:

$$m c_{V_O^{m+}} \;=\; c_e. \tag{3.243}$$

Thus,

$$p_{\mathrm{O}_2}^{1/2} c_{\mathrm{V}_\mathrm{O}^{m+}}^{1+m} m^m \;=\; K_1 \;\;\rightarrow\;\; c_{\mathrm{V}_\mathrm{O}^{m+}} \;=\; K_1^{1/(1+m)} m^{-m/(1+m)} p_{\mathrm{O}_2}^{-1/2(1+m)}. \tag{3.244}$$

In other words with increasing $p_{\mathrm{O}_2}$, $c_{\mathrm{V}_\mathrm{O}^{m+}}$ goes down, and so does $c_e$.

With an external electric field $\mathbf{E} \equiv -\nabla\phi$ in a compositionally homogeneous oxide, the current carried by $\mathrm{V}_\mathrm{O}^{m+}$ is

$$\mathbf{v}_{\mathrm{V}_\mathrm{O}^{m+}} \;=\; M_{\mathrm{V}_\mathrm{O}^{m+}} me\mathbf{E} \;\;\rightarrow\;\; \mathbf{I}_{\mathrm{V}_\mathrm{O}^{m+}} \;=\; c_{\mathrm{V}_\mathrm{O}^{m+}} me M_{\mathrm{V}_\mathrm{O}^{m+}} me\mathbf{E}. \tag{3.245}$$

So the electrical conductivity contribution from $\mathrm{V}_\mathrm{O}^{m+}$ is

$$\sigma_{\mathrm{V}_\mathrm{O}^{m+}} \;=\; M_{\mathrm{V}_\mathrm{O}^{m+}} c_{\mathrm{V}_\mathrm{O}^{m+}} m^2 e^2. \tag{3.246}$$

Similarly,

$$\mathbf{v}_e \;=\; -M_e e\mathbf{E}, \;\; \sigma_e \;=\; M_e c_e e^2. \tag{3.247}$$

The transference numbers are

$$t_{\mathrm{V}_\mathrm{O}^{m+}} \;=\; \frac{M_{\mathrm{V}_\mathrm{O}^{m+}} c_{\mathrm{V}_\mathrm{O}^{m+}} m^2}{M_{\mathrm{V}_\mathrm{O}^{m+}} c_{\mathrm{V}_\mathrm{O}^{m+}} m^2 + M_e c_e}, \quad t_e \;=\; \frac{M_e c_e}{M_{\mathrm{V}_\mathrm{O}^{m+}} c_{\mathrm{V}_\mathrm{O}^{m+}} m^2 + M_e c_e}. \tag{3.248}$$

Eq. 3.240 has no meaning physically far away from the surface, but we can use $p_{\mathrm{O}_2}$ as a fictitious tracking variable, which however must be reconciled with real $p_{\mathrm{O}_2}^{\mathrm{H}}$ and $p_{\mathrm{O}_2}^{\mathrm{L}}$ at $x = H$ and $x = L$. With a varying concentration, we should have

$$\mathbf{j}_{\mathrm{V}_\mathrm{O}^{m+}} \;=\; c_{\mathrm{V}_\mathrm{O}^{m+}} M_{\mathrm{V}_\mathrm{O}^{m+}} (-\nabla\mu_{\mathrm{V}_\mathrm{O}^{m+}} - me\nabla\phi) = \frac{\sigma t_{\mathrm{V}_\mathrm{O}^{m+}}}{m^2 e^2} (-\nabla\mu_{\mathrm{V}_\mathrm{O}^{m+}} - me\nabla\phi) \tag{3.249}$$

$$\mathbf{j}_\mathrm{e} \;=\; c_\mathrm{e} M_\mathrm{e} (-\nabla\mu_\mathrm{e} + e\nabla\phi) = \frac{\sigma t_e}{e^2} (-\nabla\mu_\mathrm{e} + e\nabla\phi). \tag{3.250}$$

At steady state, the net electrical current should be zero,

$$0 = me\mathbf{j}_{\mathrm{V}_\mathrm{O}^{m+}} - e\mathbf{j}_\mathrm{e} \;=\; \sigma(-\nabla\phi) + \frac{\sigma t_{\mathrm{V}_\mathrm{O}^{m+}}}{me} (-\nabla\mu_{\mathrm{V}_\mathrm{O}^{m+}}) + \frac{\sigma t_e}{e} \nabla\mu_\mathrm{e}, \tag{3.251}$$

or

$$me\sigma(-\nabla\phi) \;=\; \sigma t_{\mathrm{V}_\mathrm{O}^{m+}} \nabla\mu_{\mathrm{V}_\mathrm{O}^{m+}} - m\sigma t_e \nabla\mu_\mathrm{e}, \tag{3.252}$$

in other words, the electric-field driven electrical current should balance the chemically driven

electrical current. Then,

$$\begin{aligned}
\mathbf{j}_{\mathrm{V}_\mathrm{O}^{m+}} &= \frac{t_{\mathrm{V}_\mathrm{O}^{m+}}}{m^2e^2}(-\sigma\nabla\mu_{\mathrm{V}_\mathrm{O}^{m+}} - me\sigma\nabla\phi) \\
&= \frac{t_{\mathrm{V}_\mathrm{O}^{m+}}}{m^2e^2}(-\sigma t_e\nabla\mu_{\mathrm{V}_\mathrm{O}^{m+}} - m\sigma t_e\nabla\mu_\mathrm{e}) \\
&= \frac{\sigma t_e t_{\mathrm{V}_\mathrm{O}^{m+}}}{m^2e^2}(-\nabla\mu_{\mathrm{V}_\mathrm{O}^{m+}} - m\nabla\mu_\mathrm{e}).
\end{aligned} \tag{3.253}$$

We have, from Eq. 3.240,

$$\frac{k_\mathrm{B}T}{2}\log p_{\mathrm{O}_2} + \mu_{\mathrm{V}_\mathrm{O}^{m+}} + m\mu_\mathrm{e} = \text{const}, \tag{3.254}$$

so

$$\mathbf{j}_{\mathrm{V}_\mathrm{O}^{m+}} = \frac{k_\mathrm{B}T\sigma t_e t_{\mathrm{V}_\mathrm{O}^{m+}}}{2m^2e^2}\nabla\log p_{\mathrm{O}_2}. \tag{3.255}$$

Inside the scale, $p_{\mathrm{O}_2}$ as a variable is a patsy: it adjust itself so that $\mathbf{j}_{\mathrm{V}_\mathrm{O}^{m+}}$ is a constant. But we can pretend to play this game by:

$$\begin{aligned}
\int_L^\mathrm{H}\mathbf{j}_{\mathrm{V}_\mathrm{O}^{m+}}dx = \mathbf{j}_{\mathrm{V}_\mathrm{O}^{m+}}(H-L) &= \int_{p_{\mathrm{O}_2}^\mathrm{L}}^{p_{\mathrm{O}_2}^\mathrm{H}}\frac{k_\mathrm{B}T\sigma t_e t_{\mathrm{V}_\mathrm{O}^{m+}}}{2m^2e^2}\nabla\log p_{\mathrm{O}_2}dx \\
&= \int_{p_{\mathrm{O}_2}^\mathrm{L}}^{p_{\mathrm{O}_2}^\mathrm{H}}\frac{k_\mathrm{B}T\sigma t_e t_{\mathrm{V}_\mathrm{O}^{m+}}}{2m^2e^2}d\log p_{\mathrm{O}_2} \\
&\equiv k.
\end{aligned} \tag{3.256}$$

The nice thing is that $k$ is apparently independent of oxide thickness.

The parabolic scale growth law [32] can then be derived straightforwardly,

$$(H-L)^2 = 2kt. \tag{3.257}$$

An interesting fact [33] about $\mathrm{V}_\mathrm{O}^{m+}$ dominated diffusion is that $k$ is almost independent of $p_{\mathrm{O}_2}^\mathrm{H}$. This is because $c_{\mathrm{V}_\mathrm{O}^{m+}}, c_e, \sigma \propto p_{\mathrm{O}_2}^{-1/2(1+m)}$ in Eq. (3.244). The transference numbers are dimensionless and should only depend weakly on $p_{\mathrm{O}_2}$. So,

$$k \propto \int_{p_{\mathrm{O}_2}^\mathrm{L}}^{p_{\mathrm{O}_2}^\mathrm{H}} p_{\mathrm{O}_2}^{-1/2(1+m)}p_{\mathrm{O}_2}^{-1}dp_{\mathrm{O}_2} \propto (p_{\mathrm{O}_2}^\mathrm{L})^{-1/2(1+m)} - (p_{\mathrm{O}_2}^\mathrm{H})^{-1/2(1+m)}. \tag{3.258}$$

Since the solubility of O in metal is very small, $p_{\mathrm{O}_2}^\mathrm{L}$ is millions of times smaller than $p_{\mathrm{O}_2}^\mathrm{H}$, so

the first term dominates over the second term. Therefore, by doubling $p^{\mathrm{H}}_{\mathrm{O}_2}$, it can only make very small impact on $k$.

### 3.5.5 Coulomb interaction and Electrolyte theory

We have seen how elastic interactions impact point defects in metals. Their $r^{-3}$ stress field governs the long-range attraction/repulsion. This begs the question of how charged defects in ceramics interact, since we expect a long-range Coulombic interaction behavior like

$$V(r) \;=\; \sum_{n<m}\sum \frac{q_n q_m}{4\pi\varepsilon\varepsilon_0|\mathbf{x}_n-\mathbf{x}_m|} \tag{3.259}$$

on top of the elastic interactions, where $q_n$, $q_m$ are the Kroger-Vink formal charges of the point defects, and $\varepsilon$ is the zero-frequency dielectric constant of the *base* insulator medium (including both electronic polarization and ionic relaxation effects, but both for completely bound charges).

The above assumes we have negligible amount of free [e], [h] compensation. If there are, then we need to bring $\rho_{\text{electronic}}(\mathbf{x}) \equiv (c_{\mathrm{h}}(\mathbf{x}) - c_{\mathrm{e}}(\mathbf{x}))e$ into the interaction. Classical electrostatics would do a good job.

Here it is important to distinguish between

- **free charge / monopole / mobility / electrolyte / metal**
- **bound charge / dipole / polarizability / dielectric / dielectric breakdown**

The dielectric constant characterizes the second group. The utility of this quantity can be seen in the definition of a parallel plate capacitor:

$$C \;\equiv\; \frac{Q}{U} \;=\; \frac{\varepsilon\varepsilon_0 A}{d} \tag{3.260}$$

where a dielectric medium of thickness $d$ separates two sides with $-Q$ and $Q$ charges. In such ideal capacitor, the ideal dielectric should not allow to leak current (in other words, it can sustain a finite electric field $\mathbf{E} = -\nabla\phi$ through itself without a current). Although in real gate "dielectric" material, especially when it's very thin, the charge leakage through point defects could be a real problem.[34]

With the first group, one gets **complete screening** of arbitrary external charge. With the second group, one gets only **partial screening** by an amount $1/\varepsilon$. Even though $\varepsilon$ can vary from 1.00059 for air, to 233 for $SrTiO_3$ at RT and even up to $10^4$ near its ferroelectric phase transition, there is always a difference with the first group. It's like the difference between "free lunch" and "discounted cheaper lunch".

When free charge / monopole has mobility and can move by an unbounded distance (sample size), this enables modern wonders like the electric grid, where free charges circulate over thousands of miles and energy flows. If the free charge / monopole is band electron, this is called a **metal** or **semiconductor**. If the **free charge / monopole** is charged ionic defect like charged vacancies or interstitials, this is called an **ionic conductor** or electrolyte. One may also have the possibility of **mixed ionic-electronic conductors (MIEC)**. The relative contribution of different physical carriers of charge to the total conductivity is described by the transference number $t$.

When free charges, say ionic defects, can arbitrarily redistribute, how would they respond to an inhomogeneity like a grain boundary? It turns out there will be an entropy-energy trade-off also, giving rise to the Poisson-Boltzmann equation (called Poisson-Fermi for electronic carriers, since the electrons satisfy Fermi statistics instead of Boltzmann statistics).

Suppose that due to segregation (short-range coordination action), the grain boundary acquires positive excess charge density $\rho_{\text{GB}} > 0$ in NaCl. NaCl is traditionally considered an insulator, but suppose there are enough Schottky disorder in the system, which becomes possible when the temperature rises to like 800K. Before the introduction of the inhomogeneity, there is

$$[\text{V}^+_{\text{Cl}}] \;=\; [\text{V}^-_{\text{Na}}] \tag{3.261}$$

But with a positively charged GB, it will repel $\text{V}^+_{\text{Cl}}$ while attract $\text{V}^-_{\text{Na}}$, and this would build up an excess of negative charge around the GB. (alternatively, one can think that some $\text{V}^+_{\text{Cl}}$ gets attached to the GB in the first place to create the positive $\rho_{\text{GB}} > 0$). One should have

$$\frac{d^2\phi}{dx^2} \;=\; -\frac{\rho^{\text{excess}}}{\varepsilon\varepsilon_0} \tag{3.262}$$

But

$$\rho^{\text{excess}} \;=\; e(\Delta c_{\text{V}^+_{\text{Cl}}} - \Delta c_{\text{V}^-_{\text{Na}}}). \tag{3.263}$$

Under external potential $\phi$ (reference $\phi = 0$ is for $x \to \infty$), we should have simple

$$c_{\mathrm{V}^+_{\mathrm{Cl}}} \;=\; c^\circ_{\mathrm{V}^+_{\mathrm{Cl}}} \exp\left(-\frac{e\phi}{k_{\mathrm{B}}T}\right), \quad c_{\mathrm{V}^-_{\mathrm{Na}}} \;=\; c^\circ_{\mathrm{V}^-_{\mathrm{Na}}} \exp\left(\frac{e\phi}{k_{\mathrm{B}}T}\right), \tag{3.264}$$

Thus

$$\frac{d^2\phi}{dx^2} \;=\; -\frac{ec^\circ_{\mathrm{V}^+_{\mathrm{Cl}}}(\exp\left(-\frac{e\phi}{k_{\mathrm{B}}T}\right) - \exp\left(\frac{e\phi}{k_{\mathrm{B}}T}\right))}{\varepsilon\varepsilon_0}. \tag{3.265}$$

The above is the nonlinear Poisson–Boltzmann equation. In regions with $e\phi \ll k_{\mathrm{B}}T$, we can further linearize it

$$\frac{d^2\phi}{dx^2} \;=\; \frac{2e^2c^\circ_{\mathrm{V}^+_{\mathrm{Cl}}}}{\varepsilon\varepsilon_0 k_{\mathrm{B}}T}\phi \tag{3.266}$$

Clearly, we can define a length scale

$$\lambda_{\mathrm{D}} \;\equiv\; \sqrt{\frac{\varepsilon\varepsilon_0 k_{\mathrm{B}}T}{2e^2c^\circ_{\mathrm{V}^+_{\mathrm{Cl}}}}}, \tag{3.267}$$

and get

$$\frac{d^2\phi}{dx^2} \;=\; \frac{\phi}{\lambda_{\mathrm{D}}^2} \tag{3.268}$$

and since we need to go to $x \to \infty$, the only allowed asymptote would be

$$\phi(x) \;=\; \phi_0 e^{-\frac{x}{\lambda_{\mathrm{D}}}} \tag{3.269}$$

The above linearized form can also be apply to 3D for screening a point charge itself, and one gets

$$\phi(r) \;=\; \frac{e^{-\frac{r}{\lambda_{\mathrm{D}}}}}{4\pi\varepsilon\varepsilon_0 r} \tag{3.270}$$

that has the same form as the Yukawa potential in particle physics.

When there are multiple species of mobile charge carriers in the system, the most general form of the Debye length is

$$\lambda_{\mathrm{D}} \;\equiv\; \sqrt{\frac{\varepsilon\varepsilon_0 k_{\mathrm{B}}T}{\sum_n z_n^2 e^2 c_n^\circ}} \tag{3.271}$$

the bottom is also called the **ionic strength**, describing the strength of ionic screening in the system (if free electronic carrier density is negligle). In metals, where free electronic carrier density is dominant, $\lambda_{\mathrm{D}}$ is called the Thomas–Fermi screening distance, usually of the order

of Angstroms. $\lambda_{\mathrm{D}}$ is much larger in ceramics, that can range from tens of nanometers to infinity, since $c_n^{\circ}$ appear in the denominator. This is the distance the electric field line can penetrate an ionic conductor.

(3.271) is a very fundamental relation in charged matter. It says that even though the mobile carriers has the **ability** to go very far indidually, **as a collective** the **cloud of positive charge** does not want to separate from the **cloud of negative charge** by more than a few $\lambda_{\mathrm{D}}$. So screening is always complete in an electrolyte/metal, if we give it enough time and space to occur. (In (3.271) there is no hard requirement on mobility, only that it can move over the observation time).

# Chapter 4

# Dislocations

## 4.1 Branch cut

Just like point defects can be represented by Eshelby operation of cutting a hole in continuous medium (jellium), and sticking in an ellipsoid and sewing them back together, dislocations (stacking faults), disclinations (grain boundaries) and cracks (surfaces) can also be represented by some operations on continuous medium called Branch cut. These operations are extremely violent on the branch cut plane, B, like surgery knife on tissue cells that the plane happens to pass - totally splattered - or think of a war zone. We call this set of points on the 2D plane the **trauma zone**. But the knife is often wielded by a plastic surgeon - so after the cut, the surgeon may pull the tissue on both sides in a certain way (like in a facelift), then sew the cut back. Two things will then happen: (a) the tissue right at the cut may "heal" after sewing back, even though cells on two sides of the cut were initially "strangers" (before the cut and shift, those cells were not the the same kind of NN). (b) Many many other cells will also feel the long-range effect of the cut and shift ("Nip/Tuck"). After all, this is the point of **plastic surgery**: not to mangle up a small number of cells and leave a scar (although sometimes do happen), but to make a large number of cells look better. If we speak of elasticity RVE instead of cells, then the original ERVE that B happens to passes are **destroyed** (**inelastic**), while the rest of the ERVEs are preserved and deforming in a diffuse way (**elastic**).

Mathematically, branch cut is a 2D plane B $\{\mathbf{x}_{\mathrm{B}}\}$ embedded in 3D space. It can be a curved plane, and terminate at a line denoted by $\beta$. $\beta$ is certainly curved in general and can

form a loop, but it can contain piecewise straight segements. B is the trauma zone, where **inelasticity happens** (so inelasticity is local) with **areal energy penalty** (unit J/m$^2$). The rest of the 3D space is called $\bar{\text{B}}$, and are elastic. There is a normal direction $\mathbf{n}$, and $\mathbf{x}_\text{B}^+$ and $\mathbf{x}_\text{B}^-$ which are infinitely close to $\mathbf{x}_\text{B}$.

To illustrate the generality of this language, a **crack** is a produced by branch cut. Imagine before the cracking, the material is whole, and suppose there is far-field stress $\boldsymbol{\sigma}^\infty$ pulling on the jellium. One can consider a ERVE straddling $\mathbf{x}_\text{B}$, and this ERVE would be transmitting stress:

$$\mathbf{n} \cdot \boldsymbol{\sigma} \equiv \mathbf{T}_n \neq 0 \tag{4.1}$$

we use capital $\mathbf{T}_n$ to denote traction that's transmitted inside the jellium (and $\mathbf{t}_n$ to denote traction that's transmitted across surface or interface). Since $\boldsymbol{\sigma} \propto \nabla \mathbf{u}$ in ERVE, a finite $\mathbf{T}_n$ would mean finite $\nabla \mathbf{u}$, or

$$\mathbf{u}(\mathbf{x}_\text{B}^+) = \mathbf{u}(\mathbf{x}_\text{B}^-). \tag{4.2}$$

since $\mathbf{u}(\mathbf{x}_\text{B}^+) - \mathbf{u}(\mathbf{x}_\text{B}^-) = \frac{\partial \mathbf{u}}{\partial l} dl$, where $\frac{\partial \mathbf{u}}{\partial l} = \mathbf{n} \cdot \nabla \mathbf{u}$ is finite, with infinitesimal $dl$.

But once a crack has occured, the ERVE straddling $\mathbf{x}_\text{B}$ are destroyed and lose their load-carrying ability completely (100% $\to$ 0%). We **open up two new boundaries**, the free surfaces on $\mathbf{x}_\text{B}^+$ and $\mathbf{x}_\text{B}^-$, and the new boundary conditions are

$$\mathbf{n} \cdot \boldsymbol{\sigma}(\mathbf{x}_\text{B}^+) = 0, \quad \mathbf{n} \cdot \boldsymbol{\sigma}(\mathbf{x}_\text{B}^-) = 0 \tag{4.3}$$

since free surfaces can not take load (0%) and are traction free. Since $\boldsymbol{\sigma} \propto \nabla \mathbf{u}$, these new BCs are like the Neumann boundary condition in PDEs. If the crack front $\beta$ moves and B expands, one has to solve a Stefan problem which moving boundaries. In a finite element calculation, what one usually has to do is to *delete* the elastic elements straddling an expanding B.

It turns out, from fracture mechanics, one can derive that

$$\mathbf{u}(\mathbf{x}_\text{B}^+) - \mathbf{u}(\mathbf{x}_\text{B}^-) \equiv \mathbf{v}(\mathbf{x}_\text{B}) \propto |\mathbf{x}_\text{B} - \mathbf{x}_\beta|^{\frac{1}{2}} \tag{4.4}$$

where $\mathbf{x}_\beta$ is the closest point on $\beta$ to $\mathbf{x}_\text{B}$. The above says there will be a singular jump in $\mathbf{u}$ across the branch-cut plane, with an amount that is square root of the distance to the crack tip. $\mathbf{v}(\mathbf{x}_\text{B})$ can be called branch-cut displacement, or "$\mathbf{v}$ for Violence". From fracture

mechanics, one can also derive that

$$\boldsymbol{\sigma} \ \propto \ f(\theta)|\mathbf{x}-\mathbf{x}_\beta|^{-1/2} \tag{4.5}$$

where the angle $\theta$ is defined with respect to the branch cut. In cracks, the branch cut plane B obviously **matters**. So $f(\theta)$ for crack goes like $\cos(\theta/2)$, when $\theta$ for $\mathbf{x}_{\bar{\mathrm{B}}}$ goes from -180° to 180° (0° belong to $\mathbf{x}_{\bar{\mathrm{B}}}$, the good material, whereas ±180° belongs to $\mathbf{x}_{\mathrm{B}}$, the bad material). Consider $(\boldsymbol{\sigma}^\infty)_{yy} > 0$, whether B is aligned with $x$ or $y$ matter, not only with regard to where the "trauma zone" is, but also with regard to stress distribution in the rest of the material.

The crack plane and crack-front singularity is easy to understand. But there are other branch-cut inelastic operations on elastic jellium that is slightly more difficult to explain. In 1907, Volterra envisioned 6 new classes of operations on aether he called *distorsioni*, three of which are dislocations, and the other three are disclinations. They are defined by Dirichlet type boundary condition of the discontinuous $\mathbf{u}$ on B. Dislocations are 1D bounding rim $\beta$ of $\mathbf{v}(\mathbf{x}_{\mathrm{B}}) = \mathbf{b}$ type displacement discontinuity on B: on B there is a translational fault of magnitude $\mathbf{b}$. Disclinations are 1D bounding rim $\beta$ of $\mathbf{v}(\mathbf{x}_{\mathrm{B}}) = (\mathbf{R}^+ - \mathbf{R}^-)\mathbf{x}_{\mathrm{B}}$ type displacement discontinuity on B: where $\mathbf{R}^+$ and $\mathbf{R}^-$ are rotational matrices. So on B there is a rotational fault, a **grain boundary**. In the Volterra sense, the cut B matters **locally**, since both translational fault (aka stacking fault) and rotational fault (aka grain boundary) - the trauma zone - costs areal energy. But Volterra showed that the rest of the ERVEs actually does not care how the branch cut was made (aligned with $x$ or $y$, or even curved). The elastic strain and stress in the remaining ERVEs just care about $\beta$, $\mathbf{b}$ or $\mathbf{R}^+$,$\mathbf{R}^-$, and not about details of B, which is a great simplification. Later, we will demonstrate this by a loop intergral form of the strain:

$$\oint_C dl \left(\frac{\partial \mathbf{u}}{\partial l}\right)_{\text{elastic}} \ = \ \mathbf{b} \tag{4.6}$$

where the branch cut has been removed from the specification.

Finally, it turns out that for the dislocations, if $\mathbf{b} = \mathbf{a}$, where $\mathbf{a}$ is any of the Bravais lattice vectors, then the local trauma disappears once sewed back, so even the **local** trauma does not care about B any more. (The **global** strain still cares about details of B, though).

Dislocation is a finely crafted machine to achieve inelastic deformation of **crystals**. In above we pretend the medium is continuum jellium, and ignored the discrete-atom character of the medium. In reality $\mathbf{x}_{\mathrm{B}}^+$, $\mathbf{x}_{\mathrm{B}}^-$ cannot be infinitely close to each other, but separated by a

**single** atomic plane distance $d_0$, usually. This indicates it is probably meaningless to talk about a core that is infinitely narrow. So unlike a *Volterra dislocation* where the core is infinitely narrow, in reality the core of $\beta$ is probably spread over a few atomic distances in B and over 1 atomic distance exactly perpendicular to B. This means the singularity (in the continuum sense) is not really singular at the atomic scale. Section 4.6 discusses about a semi-continuum version of the dislocation core, mixing inelastic interactions on B with elastic interactions in $\bar{\text{B}}$.

Suppose B lies on a crystallographic flat plane for a moment. We can have a "phase field" description of the branch cut, by defining an order parameter for each $\mathbf{x}_{\text{B}}$:

$$\mathbf{v}(\mathbf{x}_{\text{B}}) \;=\; \eta(\mathbf{x}_{\text{B}})\mathbf{a} \tag{4.7}$$

where $\eta$ is a continuous variable. This may not seem to be doing much, except the following. Previously B is a half-plane that terminates at $\beta$. Now $\eta(x, y)$ is defined on the full-plane, and we use $(\partial_x^2 + \partial_y^2)\eta$ to track where $\beta$ is. The width of the core can be introduced in phase field model, by adding local gradient terms like $\int_{\text{B}} dA\kappa((\partial_x\eta)^2 + (\partial_y\eta)^2)/2$, or more realistic nonlocal gradient terms like in the Peierls model.

Since Volterra inelastic operation for disclination/grain boundary is defined by a linearly growing cut displacement:

$$\mathbf{v}(\mathbf{x}_{\text{B}}) \;=\; \mathbf{A}\mathbf{x}_{\text{B}} \tag{4.8}$$

we see that it can be understood, at the continuum mechanics level, by a regularly space array of dislocations, with gradually increasing (step wise) order parameter. In other words, a roational fault (a grain boundary) can be understood as a combination of dislocations. So, a grain boundary contains so-called **Frank-Bilby** dislocation content, and this is the basis for the **Read-Shockley** model of GB energy. For low-angle grain boundaries, the atomistic versions of the dislocation cores can be visualized directly. Even for high-angle grain boundaries, even though the atomistic versions of the dislocation cores cannot be made out, they are still there. For example, if a GB absorbs a lattice dislocation, the local lattice misorientation angle would change a bit, according to the Frank-Bilby equation. This **Frank-Bilby** dislocation content is similar to the concept of "money". Money is not real (it's just a piece of paper), except it is used to track the exchange of real products and services.

For both dislocation and disclination, B still carries load, so $f(\theta)$ for both dislocation and disclination goes like $\cos(\theta)$, when $\theta$ for $\mathbf{x}_{\bar{\text{B}}}$ goes from -180° to 180° (0° belong to $\mathbf{x}_{\bar{\text{B}}}$, the

good material, whereas $\pm 180^\circ$ belongs to $\mathbf{x}_\mathrm{B}$, the bad material).

## 4.2 Dislocation Geometry and Process of Creation

Consider 3D space $\mathbf{x}$ and a closed loop C in the jellium. Now imagine a branch cut plane B that penetrates C but terminates inside. Let us denote points on branch cut plane B by $\mathbf{x}_\mathrm{B}$, and those slightly above B as $\mathbf{x}_\mathrm{B}^+$ and slightly below B as $\mathbf{x}_\mathrm{B}^-$. Then consider achieving the following displacement:

$$\mathbf{u}(\mathbf{x}) \;=\; \mathbf{u}^\mathrm{B}(\mathbf{x}) + \mathbf{u}^\mathrm{R}(\mathbf{x}) \tag{4.9}$$

where $\mathbf{u}^\mathrm{R}(\mathbf{x})$ is relaxational displacement, but one enforces

$$\mathbf{u}^\mathrm{B}(\mathbf{x}_\mathrm{B}^+) - \mathbf{u}^\mathrm{B}(\mathbf{x}_\mathrm{B}^-) \;=\; \mathbf{v}(\mathbf{x}_\mathrm{B}) \tag{4.10}$$

Note that $\mathbf{x}_\mathrm{B}^+$ and $\mathbf{x}_\mathrm{B}^-$ are limiting to the same point $\mathbf{x}_\mathrm{B}$, so (4.10) enforces a sharp discontinuity in $\mathbf{u}^\mathrm{B}(\mathbf{x})$ on the branch-cut plane, with branch-cut amount $\mathbf{v}(\mathbf{x}_\mathrm{B})$, **guaranteed by the "hands of God"**. In all the other point besides $\mathbf{x}_\mathrm{B}$, $\mathbf{u}^\mathrm{B}(\mathbf{x})$ is set to be continuous and differentiable. So $\nabla\mathbf{u}^\mathrm{B}$ is finite everywhere else, except a delta function like feature at $\mathbf{x}_\mathrm{B}$. Note that while $\mathbf{u}^\mathrm{R}(\mathbf{x})$ can be finite everywhere else (and they depend on how $\mathbf{u}^\mathrm{B}(\mathbf{x})$ is set outside of the branch-cut plane), by definition

$$\mathbf{u}^\mathrm{R}(\mathbf{x}_\mathrm{B}^+) \;=\; \mathbf{u}^\mathrm{R}(\mathbf{x}_\mathrm{B}^-) \;=\; 0 \tag{4.11}$$

because that is where the "hands of God" enforces. And so

$$\mathbf{u}(\mathbf{x}_\mathrm{B}^+) - \mathbf{u}(\mathbf{x}_\mathrm{B}^-) \;=\; \mathbf{v}(\mathbf{x}_\mathrm{B}) \tag{4.12}$$

By imposing different $\mathbf{v}(\mathbf{x}_\mathrm{B})$ functions and letting $\mathbf{u}^\mathrm{R}(\mathbf{x})$ run its course, we can get the dislocations (if $\mathbf{v}(\mathbf{x}_\mathrm{B}) = \mathbf{b}$), the disclinations (if $\mathbf{v}(\mathbf{x}_\mathrm{B}) = \mathbf{A}\mathbf{x}_\mathrm{B}$), and other kinds of defects. $\mathbf{u}^\mathrm{B}(\mathbf{x})$ is like the **guess** solution, and $\mathbf{u}^\mathrm{R}(\mathbf{x})$ is like the **correction**, in an iterative numerical solver. Despite the slight arbitrariness of the guess solution, the final solution $\mathbf{u}^\mathrm{B}(\mathbf{x}) + \mathbf{u}^\mathrm{R}(\mathbf{x})$ removes this arbitrariness by adjusting $\mathbf{u}^\mathrm{R}(\mathbf{x})$ correspondingly.

Now further consider the scenario where

$$\mathbf{v}(\mathbf{x}_\mathrm{B}) \;\equiv\; \mathbf{b} \;=\; \lambda\mathbf{a} \tag{4.13}$$

where **a** is a Bravais lattice vector, and $\lambda$ continuously changes from 0 to 1. In other words, we imposes a **translational fault** pattern on the branch cut plane B. One can come up with some reasonable $\mathbf{u}^{\mathrm{B}}(\mathbf{x})$ initialization like that rendered in Fig. 4 or Fig. 5 of Balluffi (3D version), and then let the material respond to that imposed $\mathbf{u}^{\mathrm{B}}(\mathbf{x})$ displacement by a corrective $\mathbf{u}^{\mathrm{R}}(\mathbf{x})$. All this will have to be supported by **finite** forces on $\mathbf{x}_{\mathrm{B}}^{+}$ and $\mathbf{x}_{\mathrm{B}}^{-}$ from the "hands of God" (in atomistic simulation, one can just compute these forces), except at $\lambda = 0$, and at $\lambda = 1, 2, 3, ....$ The reason that for integer values of $\lambda = n$, the **enforcing hands on $\mathbf{x}_{\mathrm{B}}^{\pm}$ can let go**, is because the "trauma" across the branch cut periodically heals. The material that we obtain across the branch cut, **as long as it stays a short distance away from the edge of B** (i.e. $\beta$), is a perfect crystal again based on any kind of NN bond topology characterization with the newly shifted-in neighbors, despite the sharp discontinuity in $\mathbf{u}^{\mathrm{B}}(\mathbf{x})$ and $\mathbf{u}(\mathbf{x})$. In fact, stress $\boldsymbol{\sigma}$ can transmit perfectly (100%) across this reformed perfect crystal, and while the branch cut imposes some kind of global boundary condition (the dislocation), locally the crystal would be completely unaware of the particular details of the branch cut. Note that **b** does not have to be parallel to the branch-cut plane. If **b** has some perpendicular component to the branch-cut plane, one just needs to add or remove atoms as needed, and still obtains a **seamless perfect crystal**.

If we ponder on the nature of $\mathbf{u}(\mathbf{x})$ and $\nabla\mathbf{u}(\mathbf{x})$ away from the dislocation, we can decompose it into

$$\nabla\mathbf{u}(\mathbf{x}) \;\equiv\; \nabla\mathbf{u}_{\mathrm{elastic}}(\mathbf{x}) + \nabla\mathbf{u}_{\mathrm{inelastic}}(\mathbf{x}) \tag{4.14}$$

where $\nabla\mathbf{u}_{\mathrm{inelastic}}(\mathbf{x})$ is a delta funciton like quantity that is localized on $\mathbf{x}_{\mathrm{B}}$, and $\nabla\mathbf{u}_{\mathrm{elastic}}(\mathbf{x})$ is diffuse but long-ranged. Note that it is initially quite challenging to write the above as $\mathbf{u}(\mathbf{x}) = \mathbf{u}_{\mathrm{elastic}}(\mathbf{x}) + \mathbf{u}_{\mathrm{inelastic}}(\mathbf{x})$ and then differentiate. It is only possible to first differentiate and then decompose into elastic and inelastic strains. Mathematically, let us define

$$\nabla\mathbf{u}_{\mathrm{inelastic}}(\mathbf{x}) \;\equiv\; \int_{\mathrm{B}} dA\delta(\mathbf{x} - \mathbf{x}_{\mathrm{B}})\mathbf{n}^T\mathbf{b} \tag{4.15}$$

so

$$\int d\mathbf{l}\cdot\nabla\mathbf{u}_{\mathrm{inelastic}}(\mathbf{x}) \;=\; \int\int_{\mathrm{B}} dA\delta(\mathbf{x} - \mathbf{x}_{\mathrm{B}})(d\mathbf{l}\cdot\mathbf{n}^T)\mathbf{b} \;=\; \mathbf{b}. \tag{4.16}$$

This fully account for the branch cut discontinuity. Therefore

$$\int d\mathbf{l}\cdot\nabla\mathbf{u}_{\mathrm{elastic}}(\mathbf{x}) \;=\; 0 \tag{4.17}$$

and the value of $\nabla\mathbf{u}_{\mathrm{elastic}}(\mathbf{x})$ is therefore finite across the branch cut. Furthermore, when

$\lambda = n$, the perfect crystal which has 100% load-bearing ability (no damage) sustains

$$\boldsymbol{\sigma}(\mathbf{x}_{\mathrm{B}}^{+}) \;=\; \boldsymbol{\sigma}(\mathbf{x}_{\mathrm{B}}^{-}) \tag{4.18}$$

so

$$\nabla \mathbf{u}_{\mathrm{elastic}}(\mathbf{x}_{\mathrm{B}}^{+}) \;=\; \nabla \mathbf{u}_{\mathrm{elastic}}(\mathbf{x}_{\mathrm{B}}^{-}). \tag{4.19}$$

Thus, despite the branch cut, $\nabla \mathbf{u}_{\mathrm{elastic}}(\mathbf{x}_{\mathrm{B}})$ itself is analytical function in all space away from the dislocation, even though integration of it would give a discontinuity across B. An analogy would be that a constant 1 is clearly an analytical function in all space. But if $\partial f/\partial\theta = 1$, $f(\theta) = \theta$ would be a multiple-valued function. The key point is that we are not interested in $f$ (or $\mathbf{u}_{\mathrm{elastic}}(\mathbf{x})$), but only $\nabla \mathbf{u}_{\mathrm{elastic}}(\mathbf{x})$ because it has to do with stress, and $\mathbf{u}(\mathbf{x})$ occasionally if we are interested in the process.

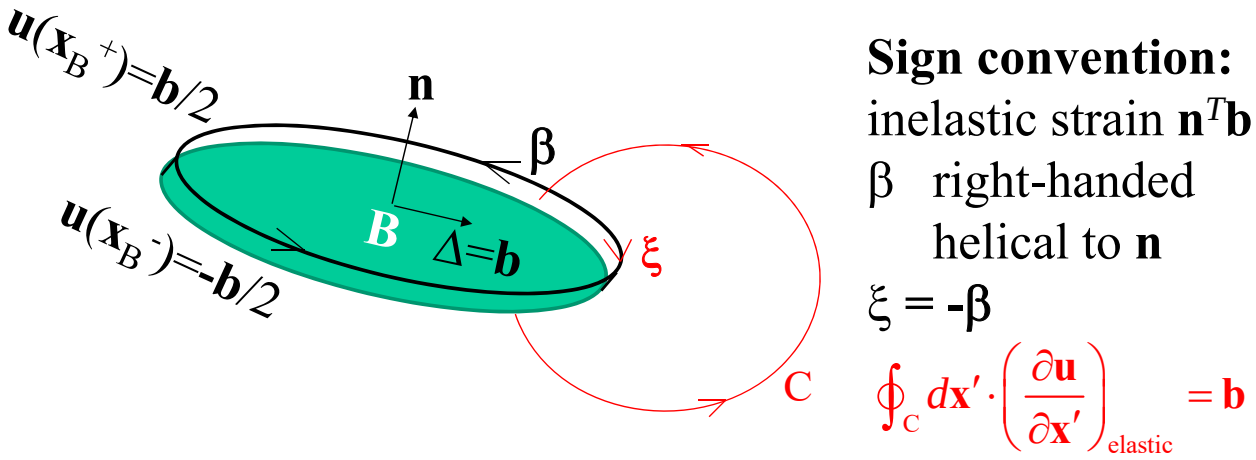


Figure 4.1: It is necessary to have $\boldsymbol{\beta}$ running opposite to $\boldsymbol{\xi}$ to respect all the right-handed sign conventions for defining the normal $\mathbf{n}$ of B, the inelastic strain of B as $\mathbf{n}^T\mathbf{b}$, the loop integral form $\mathbf{b} = \oint_{\mathrm{C}} \frac{\partial \mathbf{u}}{\partial l} dl$, and that C is a right-handed loop around $\boldsymbol{\xi}$.

A dislocation is characterized by its line direction $\boldsymbol{\xi}$, $|\boldsymbol{\xi}| = 1$, and the Burgers vector $\mathbf{b}$, with

$$\mathbf{b} \;=\; \oint_{\overline{\mathrm{C}}} \frac{\partial \mathbf{u}}{\partial l} dl \;=\; \oint_{\mathrm{C}} \left(\frac{\partial \mathbf{u}}{\partial l}\right)_{\mathrm{elastic}} dl \tag{4.20}$$

where the line integral is taken in a right-handed sense relative to $\boldsymbol{\xi}$. C is a closed loop in an original perfect crystal far from the dislocation core (the Lagrangian frame of reference), and $\mathbf{u}$ is the total displacement after the dislocation has sheared into inside the loop, creating a branch cut. $\overline{\mathrm{C}}$ is the same loop as C, except it is open and avoiding the branch cut. $\frac{\partial \mathbf{u}}{\partial l}$ is a

strain-like quantity, so we have

$$\frac{\partial \mathbf{u}}{\partial l} = \left(\frac{\partial \mathbf{u}}{\partial l}\right)_{\text{elastic}} + \left(\frac{\partial \mathbf{u}}{\partial l}\right)_{\text{inelastic}} \tag{4.21}$$

where $\left(\frac{\partial \mathbf{u}}{\partial l}\right)_{\text{elastic}}$ is small-amplitude but diffuse (away from the core), and $\left(\frac{\partial \mathbf{u}}{\partial l}\right)_{\text{inelastic}}$ is a delta-function like quantity in space, tracking the 2D branch cut. (The 2D branch cut ends at the 1D dislocation core.) Since stress $\boldsymbol{\sigma} \propto \left(\frac{\partial \mathbf{u}}{\partial l}\right)_{\text{elastic}}$, and the material at the branch cut is perfectly repaired and has the same load-bearing ability as the uncut material, $\boldsymbol{\sigma}$ is continuous across the branch cut and in fact is not even aware of its existence. (We will later see this from the stress solution of screw and edge dislocations). Because $\left(\frac{\partial \mathbf{u}}{\partial l}\right)_{\text{inelastic}}$ is a delta-function like quantity, it is zero away from the branch cut, so $\frac{\partial \mathbf{u}}{\partial l} = \left(\frac{\partial \mathbf{u}}{\partial l}\right)_{\text{elastic}}$ away from the branch cut, and

$$\oint_{\overline{\text{C}}} \frac{\partial \mathbf{u}}{\partial l} dl = \oint_{\overline{\text{C}}} \left(\frac{\partial \mathbf{u}}{\partial l}\right)_{\text{elastic}} dl. \tag{4.22}$$

The second equality in (4.20) holds because in the continuum representation of $\mathbf{u}(\mathbf{x})$, the 2D branch cut is infinitely thin, and since $\left(\frac{\partial \mathbf{u}}{\partial l}\right)_{\text{elastic}}$ is finite, integrating $\left(\frac{\partial \mathbf{u}}{\partial l}\right)_{\text{elastic}}$ across the zero-thickness branch cut gives zero anyway. In the literature, one often sees

$$\mathbf{b} = \oint_{\text{C}} \frac{\partial \mathbf{u}}{\partial l} dl \tag{4.23}$$

But one must understand this is an abbreviated notation due to "notational laziness". The branch cut unaware second equality in (4.20) is my favorite version because of its subtlety, and to make it even more subtle we can even use the (4.23) form, but keeping in mind that $\mathbf{u}$ there is the elastic component, i.e. modulo $\mathbf{b}$ at the branch cut plane (wherever it is) to make $\frac{\partial \mathbf{u}}{\partial l}$ not divergent.

From (4.20) we see that $\boldsymbol{\xi}$ definition and $\mathbf{b}$ definition is related. $(-\boldsymbol{\xi}, -\mathbf{b})$ actually describes the same dislocation as $(\boldsymbol{\xi}, \mathbf{b})$. To make the whole thing work in a right-handed manner, we need to have $\boldsymbol{\xi} = -\boldsymbol{\beta}$, though. So once we have chosen the direction of $\mathbf{n}$ ("up"), we have chosen $\boldsymbol{\beta}$ and therefore $\boldsymbol{\xi}$. (For a physical slip operation, we can either say $(\mathbf{n}, \mathbf{b})$, or call it $(-\mathbf{n}, -\mathbf{b})$, so this binary-choice gauge freedom is not removed, but to make everything consistent we need to always have $\boldsymbol{\xi} = -\boldsymbol{\beta}$). We need to maintain right-handed loop between $\mathbf{n}$ and $\boldsymbol{\beta}$ because we will use the Stokes theorem later.

If $\mathbf{b} \parallel \boldsymbol{\xi}$, it is called screw dislocation. If $\mathbf{b} \perp \boldsymbol{\xi}$, it is called edge dislocation. Otherwise it is called mixed dislocation.

Because a loop integral of purely elastic displacements $\oint_{\mathrm{C}} \left(\frac{\partial \mathbf{u}}{\partial l}\right)_{\text{elastic}} dl$ should always give 0 (imagine we apply a diffuse but single-valued elastic distortion field in which C is embedded), (4.20) gives the *purely inelastic* excess displacement, which is the slip displacement $\mathbf{b}$ between two adjacent atomic planes (in continuum mechanics, this is idealized as infinitely sharp slip fault). Because of this, there should be Burgers vector conservation law:

$$\mathbf{b}_1 \;=\; \mathbf{b}_2 + \mathbf{b}_3. \tag{4.24}$$

as one could distort C purely elastically from one location to another in Fig. 1-24 of [35].

To prove that

$$\mathbf{b} \;=\; \oint_{\mathrm{C}} \left(\frac{\partial \mathbf{u}}{\partial l}\right)_{\text{elastic}} dl \tag{4.25}$$

enables one to completely determine the stress-elastic strain field around $\beta$ regardless of B, let us consider a screw dislocation

$$\mathbf{b} \;=\; b\mathbf{e}_z, \quad \boldsymbol{\xi} \;=\; \mathbf{e}_z. \tag{4.26}$$

In isotropic medium we have

$$(\lambda + \mu)\nabla(\nabla \cdot \mathbf{u}) + \mu\nabla^2\mathbf{u} \;=\; 0 \tag{4.27}$$

Note that above applies only to the elastic region. We seek solution of the type

$$\mathbf{u} \;=\; \mathbf{e}_z h(x, y) \tag{4.28}$$

so the first term drops out, and we end up with

$$(\partial_x^2 + \partial_y^2)h \;=\; 0 \tag{4.29}$$

a Poisson equation. In the rest of the branch cut, let us use radial coordinate:

$$r^{-1}\partial_r(r\partial_r h) + r^{-2}\partial_\theta^2 h \;=\; 0. \tag{4.30}$$

Suppose the branch cut is flat, and we call that $\theta = 0$, then we need to satisfy

$$h(r, 2\pi) - h(r, 0) \;=\; b \tag{4.31}$$

so our guess would be

$$h(r,\theta) \;=\; h(\theta) = \frac{\theta b}{2\pi} \tag{4.32}$$

which satisfy stress-equilibrium. There is a jump in displacement at the branch cut, but the stress above the cut and below the cut depends only on $\nabla\mathbf{u}$, not $\mathbf{u}$. $\nabla\mathbf{u}$ is **continuous** in the solution above:

$$\nabla\mathbf{u} \;=\; \begin{pmatrix} 0 & 0 & \partial_x h \\ 0 & 0 & \partial_y h \\ 0 & 0 & 0 \end{pmatrix} \;=\; \frac{b}{2\pi}\begin{pmatrix} 0 & 0 & \partial_x \theta \\ 0 & 0 & \partial_y \theta \\ 0 & 0 & 0 \end{pmatrix} \;=\; \frac{b}{2\pi r}\begin{pmatrix} 0 & 0 & -\sin\theta \\ 0 & 0 & \cos\theta \\ 0 & 0 & 0 \end{pmatrix} \tag{4.33}$$

So

$$\sigma_{xz} = -\frac{\mu b}{2\pi}\frac{y}{x^2+y^2}, \quad \sigma_{yz} = \frac{\mu b}{2\pi}\frac{x}{x^2+y^2}, \quad \sigma_{xy} = \sigma_{xx} = \sigma_{yy} = \sigma_{zz} = 0 \tag{4.34}$$

and since $\mathbf{n}_\theta = -\sin\theta\mathbf{e}_x + \cos\theta\mathbf{e}_y$, $\mathbf{n}_r = \cos\theta\mathbf{e}_x + \sin\theta\mathbf{e}_y$, we have

$$\sigma_{\theta z} \;=\; -\sin\theta\sigma_{xz} + \cos\theta\sigma_{yz} \;=\; \frac{b}{2\pi r}, \;\; \sigma_{rz} = \sigma_{zz} = \sigma_{rr} = \sigma_{\theta\theta} = 0 \tag{4.35}$$

We then noticed the above solution is "seamless", that is the stress and the elastic strain field has excellent analytical properties away from $\beta$, regardless of B. We can cut a curvy B, and still the same solution would apply. This is because $\nabla\mathbf{u}$, or actually $(\nabla\mathbf{u})_{\text{elastic}}$, by setup has such analytical seamless property. We can convert a $\mathbf{u}(\mathbf{x})$ solution from a simple branch cut B to $\tilde{\mathbf{u}}(\mathbf{x})$ of a more complex branch cut $\tilde{\text{B}}$ by simply adding

$$\tilde{\mathbf{u}}(\mathbf{x}) \;=\; \mathbf{u}(\mathbf{x}) + \begin{cases} -\mathbf{b}, & \mathbf{x} \in \text{wedge} \\ \\ 0, & \text{otherwise} \end{cases} \tag{4.36}$$

where the wedge is the sliver of material between B and $\tilde{\text{B}}$. The above operation would not cause any change to the self-equilibrating stress field, and therefore is a valid solution for the new branch cut condition.

The stress solution of edge dislocation is a bit more challenging. So we proceed to derive the general expression for a curved dislocation loop! Recall that the interaction energy between two point defects are **independent of the order** of which they are created. Imagine the following two process, which should give the same interaction energy (**reciprocity**) regardless of the order of two operations. In process I, one first imposes a point force $\mathbf{F}$ on

$\mathbf{x}$ in a perfect jellium, which creates

$$\tilde{u}_i(\mathbf{x}') \;=\; K_{ij}(\mathbf{x}'-\mathbf{x})F_j, \quad \tilde{u}_{i,k}(\mathbf{x}') \;=\; K_{ij,k}(\mathbf{x}'-\mathbf{x})F_j, \tag{4.37}$$

and stress

$$\sigma_{ml}(\mathbf{x}') \;=\; C_{mlik}K_{ij,k}(\mathbf{x}'-\mathbf{x})F_j \tag{4.38}$$

at $\mathbf{x}'$. We then induce the branch-cut strain

$$\nabla\mathbf{u}_{\text{inelastic}}(\mathbf{x}') \;\equiv\; \int_{\text{B}} dA'\delta(\mathbf{x}'-\mathbf{x}_{\text{B}})\mathbf{n}^T\mathbf{b} \tag{4.39}$$

so the interaction (additional work of creation) energy would be

$$W \;=\; \int_{\text{B}} dA' n_m b_l C_{mlik}K_{ij,k}(\mathbf{x}'-\mathbf{x})F_j \tag{4.40}$$

On the other hand, in process II, one first creates the dislocation loop with self-equilibriating displacement field $u_i(\mathbf{x})$ (what we want to solve), and then, if one adds the force, this would cause additional work

$$W \;=\; F_j u_j(\mathbf{x}) \tag{4.41}$$

Equating the $W$ in process I and II, we would get

$$u_j(\mathbf{x}) \;=\; \int_{\text{B}} dA' n_m b_l C_{mlik}K_{ij,k}(\mathbf{x}'-\mathbf{x}) \;=\; -\int_{\text{B}} dA' n_m b_l C_{mlik}K_{ij,k}(\mathbf{x}-\mathbf{x}') \tag{4.42}$$

This is **reconnaissance by fire** using a small point force! So the strain field is:

$$u_{j,s}(\mathbf{x}) \;=\; -\int_{\text{B}} dA'_m b_l C_{mlik}K_{ij,ks}(\mathbf{x}-\mathbf{x}') \tag{4.43}$$

where we removed the Branch cut label B and define $dA'_m \equiv dA' n_m$. The above trick is actually very general, and can apply to all different kinds of transformations. We will define

$$\mathbf{R} \;\equiv\; \mathbf{x}-\mathbf{x}', \quad R \;\equiv\; |\mathbf{R}| \tag{4.44}$$

From now on, by default $f = f(\mathbf{R})$. We define

$$f_{,m} \;\equiv\; \frac{\partial f}{\partial(\mathbf{R})_m} \;=\; \frac{\partial f}{\partial x_m}, \quad f^{,m} \;\equiv\; \frac{\partial f}{\partial x'_m} \;=\; -f_{,m}. \tag{4.45}$$

Later, we will use the following variant of Stokes' theorem:

$$\int_{\mathrm{B}} dA'_s f_{,m} - dA'_m f_{,s} \;=\; \int_{\mathrm{B}} dA'(n_s f_{,m} - n_m f_{,s}) \;=\; \epsilon_{msp} \oint_\beta f dx'_p \tag{4.46}$$

This is because $\oint_\beta \mathbf{g} \cdot d\mathbf{x}' = \int_{\mathrm{B}} d\mathbf{A}' \cdot (\nabla' \times \mathbf{g})$ and

$$\oint_\beta f dx'_p \;=\; \oint_\beta f \delta_{pq} dx'_q \;=\; \int_{\mathrm{B}} dA' n_w \epsilon_{wvq} f^{,v} \delta_{pq} \;=\; \int_{\mathrm{B}} dA' n_w \epsilon_{vwp} f_{,v} \tag{4.47}$$

$$\epsilon_{msp}\epsilon_{vwp} \;=\; \delta_{sw}\delta_{mv} - \delta_{sv}\delta_{mw} \tag{4.48}$$

So

$$\epsilon_{msp} \oint_\beta f dx'_p \;=\; \int_{\mathrm{B}} dA'(\delta_{sw}\delta_{mv} - \delta_{sv}\delta_{mw}) n_w f_{,v} \;=\; \int_{\mathrm{B}} dA'(n_s f_{,m} - n_m f_{,s}) \tag{4.49}$$

QED.

For isotropic medium, we have

$$C_{mlik} \;=\; \lambda\delta_{ml}\delta_{ik} + \mu\delta_{mi}\delta_{lk} + \mu\delta_{mk}\delta_{li}, \quad -K_{ij,k}(\mathbf{x}) \;=\; \frac{\delta_{ij}x_k}{4\pi\mu|\mathbf{x}|^3} + \frac{1}{16\pi\mu(1-\nu)} \frac{\partial^3|\mathbf{x}|}{\partial x_i \partial x_j \partial x_k} \tag{4.50}$$

So the contraction over $i, k$ gives

$$-C_{mlik}K_{ij,k} \;=\; \frac{\lambda\delta_{ml}x_j + \mu\delta_{mj}x_l + \mu\delta_{lj}x_m}{4\pi\mu|\mathbf{x}|^3} + \frac{\lambda\delta_{ml}}{16\pi\mu(1-\nu)} \frac{\partial\nabla^2|\mathbf{x}|}{\partial x_j} + \frac{1}{8\pi(1-\nu)} \frac{\partial^3|\mathbf{x}|}{\partial x_m \partial x_j \partial x_l} \tag{4.51}$$

Since $\nabla^2|\mathbf{x}| = 2/|\mathbf{x}|$, and

$$\frac{\lambda}{\mu} \;=\; \frac{2\nu}{1-2\nu}, \tag{4.52}$$

the first two big terms are grouped as

$$\begin{aligned} & \frac{\lambda\delta_{ml}x_j + \mu\delta_{mj}x_l + \mu\delta_{lj}x_m}{4\pi\mu|\mathbf{x}|^3} - \frac{\nu\delta_{ml}x_j}{4\pi(1-2\nu)(1-\nu)|\mathbf{x}|^3} \\ = \;& \frac{\delta_{mj}x_l + \delta_{lj}x_m}{4\pi|\mathbf{x}|^3} + \frac{2\nu\delta_{ml}x_j}{4\pi(1-2\nu)|\mathbf{x}|^3} - \frac{\nu\delta_{ml}x_j}{4\pi(1-2\nu)(1-\nu)|\mathbf{x}|^3} \\ = \;& \frac{\delta_{mj}x_l + \delta_{lj}x_m}{4\pi|\mathbf{x}|^3} + \frac{\nu\delta_{ml}x_j}{4\pi(1-\nu)|\mathbf{x}|^3} \end{aligned} \tag{4.53}$$

So finally we get

$$-C_{mlik}K_{ij,k}(\mathbf{x}) \;=\; \frac{\delta_{mj}x_l + \delta_{lj}x_m}{4\pi|\mathbf{x}|^3} + \frac{\nu\delta_{ml}x_j}{4\pi(1-\nu)|\mathbf{x}|^3} + \frac{1}{8\pi(1-\nu)} \frac{\partial^3|\mathbf{x}|}{\partial x_m \partial x_j \partial x_l} \tag{4.54}$$

The beautiful contraction (4.54) can also be used in (4.42)

$$\begin{aligned} u_j(\mathbf{x}) &= -\int_{\mathrm{B}} dA' n_m b_l C_{mlik} K_{ij,k}(\mathbf{R}) \\ &= \int_{\mathrm{B}} dA' n_m b_l \left[ \frac{\delta_{mj} R_l + \delta_{lj} R_m}{4\pi |\mathbf{R}|^3} + \frac{\nu \delta_{ml} R_j}{4\pi(1-\nu)|\mathbf{R}|^3} + \frac{1}{8\pi(1-\nu)} \frac{\partial^3 |\mathbf{R}|}{\partial R_m \partial R_j \partial R_l} \right] \\ &= \int_{\mathrm{B}} dA' \left[ \frac{n_j b_l R_l + b_j \mathbf{n}\cdot\mathbf{R}}{4\pi |\mathbf{R}|^3} + \frac{\nu n_l b_l R_j}{4\pi(1-\nu)|\mathbf{R}|^3} + \frac{n_m b_l}{8\pi(1-\nu)} \frac{\partial^3 |\mathbf{R}|}{\partial R_m \partial R_j \partial R_l} \right] \end{aligned} \tag{4.55}$$

We are going to take out the 2nd term separately, which is

$$\frac{\mathbf{b}}{4\pi} \int_{\mathrm{B}} dA' \frac{\mathbf{n}\cdot\mathbf{R}}{|\mathbf{R}|^3} = \frac{\mathbf{b}}{4\pi} \Omega \tag{4.56}$$

where

$$\Omega \equiv \int_{\mathrm{B}} dA' \frac{\mathbf{n}\cdot\mathbf{R}}{|\mathbf{R}|^3} \tag{4.57}$$

is the solid angle extended by the branch cut: $2\pi$ when $\mathbf{x}$ is a little bit above B, and $-2\pi$ when $\mathbf{x}$ is a little bit below B, thus giving the sharp discontinuity in displacement. The rest of the terms should be continuous and branch cut independent:

$$u_j(\mathbf{x}) = \frac{b_j}{4\pi}\Omega + \int_{\mathrm{B}} dA' \left[ \frac{n_j b_l R_l}{4\pi |\mathbf{R}|^3} + \frac{\nu n_l b_l R_j}{4\pi(1-\nu)|\mathbf{R}|^3} + \frac{n_m b_l}{8\pi(1-\nu)} \frac{\partial^3 |\mathbf{R}|}{\partial R_m \partial R_j \partial R_l} \right] \tag{4.58}$$

We note that

$$\frac{\nu n_l b_l R_j}{4\pi(1-\nu)|\mathbf{R}|^3} = -\frac{n_l b_l R_j}{4\pi |\mathbf{R}|^3} + \frac{n_l b_l R_j}{4\pi(1-\nu)|\mathbf{R}|^3} = -\frac{n_l b_l R_j}{4\pi |\mathbf{R}|^3} - \frac{n_l b_l \partial_j \partial_m \partial_m |\mathbf{R}|}{8\pi(1-\nu)} \tag{4.59}$$

So we can group above as

$$\begin{aligned} u_j(\mathbf{x}) &= \frac{b_j}{4\pi}\Omega + \int_{\mathrm{B}} dA' \left[ \frac{n_j b_l R_l - n_l b_l R_j}{4\pi |\mathbf{R}|^3} + \frac{n_m b_l |\mathbf{R}|_{,mjl} - n_l b_l |\mathbf{R}|_{,mjm}}{8\pi(1-\nu)} \right] \\ &= \frac{b_j}{4\pi}\Omega + \int_{\mathrm{B}} dA' \left[ \frac{n_l b_l (|\mathbf{R}|^{-1})_{,j} - n_j b_l (|\mathbf{R}|^{-1})_{,l}}{4\pi} + \frac{n_m b_l |\mathbf{R}|_{,mjl} - n_l b_l |\mathbf{R}|_{,mjm}}{8\pi(1-\nu)} \right] \\ &= \frac{b_j}{4\pi}\Omega + \oint_\beta \left[ \frac{\epsilon_{jlp} b_l (|\mathbf{R}|^{-1})}{4\pi} + \frac{\epsilon_{lmp} b_l |\mathbf{R}|_{,mj}}{8\pi(1-\nu)} \right] dx'_p \end{aligned} \tag{4.60}$$

The above can be written in vector format as

$$\mathbf{u}(\mathbf{x}) = \frac{\mathbf{b}}{4\pi}\Omega + \oint_\beta \frac{\mathbf{b}\times d\mathbf{x}'}{4\pi|\mathbf{R}|} + \nabla \oint_\beta \mathbf{b}\cdot \frac{\mathbf{R}\times d\mathbf{x}'}{8\pi(1-\nu)|\mathbf{R}|} \tag{4.61}$$

This agrees with Equation (4-20) of [35] but with the following translations: in [35] $\mathbf{R}$ is defined as $\mathbf{x}' - \mathbf{x}$ (Equation (4-16)) which I think is awkward. In Figure 4-4 of [35], $\mathbf{n}$ is defined to form right-handed loop to $\boldsymbol{\xi}$, so it is opposite to our $\mathbf{n}$. Their $\boldsymbol{\xi}$ and $\boldsymbol{b}$ are the same as our $\boldsymbol{\xi}$ and $\boldsymbol{b}$.

(4.61) was first worked out by Johannes Martinus Burgers in 1939. It is clear that $\mathbf{u}(\mathbf{x})$ has a B dependent part, and a $\beta$-dependent but B-independent part. Later, we will show that $\nabla\mathbf{u}(\mathbf{x})$ consists of the $\int_{\mathrm{B}} dA\delta(\mathbf{x}-\mathbf{x}_{\mathrm{B}})\mathbf{n}^T\mathbf{b}$ singular piece that is B dependent, but the rest is $\beta$-dependent but B-independent.

Let us consider a screw dislocation loop with $\xi$ running from $(0,0,-\infty) \to (0,0,\infty) \to (-\infty,0,\infty) \to (-\infty,0,-\infty) \to (0,0,-\infty)$, and $\mathbf{b} = b\mathbf{e}_z$. Note that the branch cut B has $\mathbf{n} = \mathbf{e}_y$. In the loop integral, only the $(0,0,-\infty) \to (0,0,\infty)$ segment matters because of closer distance. But the second and third terms are zero, because $\mathbf{b} /\!/ d\mathbf{x}'$. It's easy to see that the first term gives what we want, with $\mathbf{u}(\mathbf{x}_{\mathrm{B}}^+) = \mathbf{b}\frac{2\pi}{4\pi}$ and $\mathbf{u}(\mathbf{x}_{\mathrm{B}}^-) = \mathbf{b}\frac{-2\pi}{4\pi}$.

Now consider the edge dislocation loop with $\xi$ running from $(0,0,-\infty) \to (0,0,\infty) \to (-\infty,0,\infty) \to (-\infty,0,-\infty) \to (0,0,-\infty)$, and $\mathbf{b} = b\mathbf{e}_x$. In our notation system this has $\beta$ running backwards and $\mathbf{n} = \mathbf{e}_y$. Then for the 2nd term:

$$\oint_\beta \frac{\mathbf{b}\times d\mathbf{x}'}{4\pi|\mathbf{R}|} \;=\; b\mathbf{e}_y \int_{-\infty}^{\infty} \frac{dl'}{4\pi|\mathbf{R}|} \;=\; b\mathbf{e}_y\left(-\frac{\ln r}{2\pi} + \text{const}\right) \tag{4.62}$$

where $dl' > 0$ always. Some explanation is needed for the 2nd equality, where the minus sign can be really surprising since we are integrating a positive integrand.

$$\int \frac{dl'}{4\pi|\mathbf{R}|} \;=\; \int_{-\infty}^{\infty} \frac{dz'}{4\pi\sqrt{(x-0)^2+(y-0)^2+(z-z')^2}} \tag{4.63}$$

is the same form as the repulsive electrostatic potential between a point charge and a line of charges (if $\varepsilon\varepsilon_0 = 1$). In electrostatics, one applies Gauss theorem to $\nabla\cdot\mathbf{E} = \rho$ ($\mathbf{E} \equiv -\nabla\phi$, $\nabla^2\phi = -\rho$), so for a wire with uniform charge density of 1, $\mathbf{E} = \frac{\mathbf{e}_r}{2\pi r}$ (which is one order longer-ranged than point-charge), and

$$\phi(r) - \phi(r_0) \;=\; -\int_{r_0}^{r} \frac{dr'}{2\pi r'} \;=\; -\frac{1}{2\pi}\ln\frac{r}{r_0} \tag{4.64}$$

There is clearly a divergence problem, however. Indeed, it is clear that when $l' \to \pm\infty$, the vector integral $\int_{-\infty}^{\infty} \frac{dl'}{4\pi|\mathbf{R}|}$ won't converge unconditionally. Nontheless, careful analysis

shows that this conditional convergence just results in a different const, which is rigid-body translation and immaterial to the solution, and won't really affect the active term, which is $-\frac{\ln r}{2\pi}$.

The 3rd term is easy too, we have

$$\frac{\mathbf{R}\times d\mathbf{x}'}{|\mathbf{R}|} \;=\; \frac{r dl'}{|\mathbf{R}|}\mathbf{e}_\theta \tag{4.65}$$

so the integral gives

$$\oint_\beta \mathbf{b}\cdot\frac{\mathbf{R}\times d\mathbf{x}'}{8\pi(1-\nu)|\mathbf{R}|} \;=\; = \; \frac{r\mathbf{b}\cdot\mathbf{e}_\theta}{2(1-\nu)}\left(-\frac{\ln r}{2\pi}\right) \;=\; br\sin\theta\frac{\ln r}{4\pi(1-\nu)} \;=\; \frac{by\ln r}{4\pi(1-\nu)} \tag{4.66}$$

so

$$\nabla\frac{by\ln r}{4\pi(1-\nu)} \;=\; \frac{b\mathbf{e}_y\ln r}{4\pi(1-\nu)} + \frac{by\mathbf{e}_r}{4\pi(1-\nu)r} \tag{4.67}$$

Thus the total displacement is

$$\mathbf{u}(\mathbf{x}) \;=\; \frac{b\mathbf{e}_x}{2\pi}\theta + \frac{b\mathbf{e}_y}{2\pi}\ln r\times\frac{2\nu-1}{2(1-\nu)} + \frac{by\mathbf{e}_r}{4\pi(1-\nu)r} \tag{4.68}$$

So

$$u_x \;=\; \frac{b\theta}{2\pi} + \frac{bxy}{4\pi(1-\nu)r^2} \;=\; \frac{b}{2\pi}\left[\theta + \frac{b\sin(2\theta)}{4(1-\nu)}\right] \tag{4.69}$$

$$u_y \;=\; \frac{(2\nu-1)b\ln r}{4\pi(1-\nu)} + \frac{by^2}{4\pi(1-\nu)r^2} \tag{4.70}$$

To make the symmetry more apparent, we can subtract $r^2/2$ from the numerator of the second term (a constant), and get

$$u_y \;=\; \frac{(2\nu-1)b\ln r}{4\pi(1-\nu)} + \frac{b(y^2-x^2)}{8\pi(1-\nu)r^2} \;=\; \frac{b}{4\pi(1-\nu)}\left[(2\nu-1)\ln r - \frac{\cos(2\theta)}{2}\right] \tag{4.71}$$

## 4.3 Stress and Strain of Arbitrary Loop

For dislocation loop, we would like to transform (4.43) to a 1D loop integral ($\beta$) instead of 2D area integral (B). Mura came up with the following transformation. He noticed that **as**

**along as x is not on B**, we have

$$C_{mlik}K_{ij,km}(\mathbf{x}-\mathbf{x}') \;=\; 0 \tag{4.72}$$

for all $l, j$ due to self-balancing nature of the Green's function displacement. So there is

$$\int_{\mathrm{B}} dA'_s b_l C_{mlik}K_{ij,km}(\mathbf{x}-\mathbf{x}') \;=\; 0 \tag{4.73}$$

and we get

$$u_{j,s}(\mathbf{x}) \;=\; b_l C_{mlik}\left(\int_{\mathrm{B}} dA'_s K_{ij,km}(\mathbf{R}) - \int_{\mathrm{B}} dA'_m K_{ij,ks}(\mathbf{R})\right) \tag{4.74}$$

But then applying (4.49),

$$u_{j,s}(\mathbf{x}) \;=\; b_l C_{mlik}\epsilon_{msp}\oint_\beta K_{ij,k}(\mathbf{R})dx'_p, \quad \forall \mathbf{x} \notin \mathrm{B} \tag{4.75}$$

The above is called Mura's formula, which works in anisotropic medium. There is a delta-function singularity in $u_{j,s}(\mathbf{x})$ at $\mathbf{x} = \mathbf{x}_{\mathrm{B}}$ as we have discussed before (see Branch cut setup (4.14)). But after getting rid of that singularity, we get the elastic part:

$$(u_{j,s})_{\text{elastic}}(\mathbf{x}) \;=\; b_l C_{mlik}\epsilon_{msp}\oint_\beta K_{ij,k}(\mathbf{R})dx'_p, \quad \forall \mathbf{x} \tag{4.76}$$

It is clear that $(u_{j,s})_{\text{elastic}}(\mathbf{x})$ is B independent, which is the main result of the previous section.

Plugging in the beautiful contraction (4.54) for isitropic medium,

$$u_{j,s}(\mathbf{x}) \;=\; b_l\epsilon_{msp}\oint_\beta \left[\frac{\delta_{mj}R_l + \delta_{lj}R_m}{4\pi|\mathbf{R}|^3} + \frac{\nu\delta_{ml}R_j}{4\pi(1-\nu)|\mathbf{R}|^3} + \frac{1}{8\pi(1-\nu)}\frac{\partial^3|\mathbf{R}|}{\partial R_m \partial R_j \partial R_l}\right] dx'_p. \tag{4.77}$$

For stress field,

$$\sigma_{wv}(\mathbf{x}) \;=\; C_{wvjs}u_{j,s} \;=\; (\lambda\delta_{wv}\delta_{js} + \mu\delta_{wj}\delta_{vs} + \mu\delta_{ws}\delta_{vj})u_{j,s} \tag{4.78}$$

and

$$C_{wvjs}\epsilon_{msp}\delta_{mj} \;=\; C_{wvjs}\epsilon_{sjp} \;=\; 0 \tag{4.79}$$

$$C_{wvjs}b_l\epsilon_{msp}\delta_{lj} \;=\; b_j(\lambda\delta_{wv}\delta_{js}+\mu\delta_{wj}\delta_{vs}+\mu\delta_{ws}\delta_{vj})\epsilon_{msp} \;=\; b_j\lambda\delta_{wv}\epsilon_{jmp}+b_j\mu\delta_{wj}\epsilon_{vmp}+b_j\mu\delta_{vj}\epsilon_{wmp} \tag{4.80}$$

$$
\begin{aligned}
C_{wvjs}b_l\epsilon_{msp}\delta_{ml} &= C_{wvjs}b_l\epsilon_{slp} = (\lambda\delta_{wv}\delta_{js} + \mu\delta_{wj}\delta_{vs} + \mu\delta_{ws}\delta_{vj})b_l\epsilon_{slp} \\
&= \lambda\delta_{wv}b_l\epsilon_{jlp} + \mu\delta_{wj}b_l\epsilon_{vlp} + \mu\delta_{vj}b_l\epsilon_{wlp} \qquad (4.81)
\end{aligned}
$$

$$
\begin{aligned}
C_{wvjs}b_l\epsilon_{msp}R_{,mjl} &= (\lambda\delta_{wv}\delta_{js} + \mu\delta_{wj}\delta_{vs} + \mu\delta_{ws}\delta_{vj})b_l\epsilon_{msp}R_{,mjl} \\
&= \lambda\delta_{wv}\delta_{js}\epsilon_{msp}R_{,mjl}b_l + \mu\delta_{wj}\delta_{vs}b_l\epsilon_{msp}R_{,mjl} + \mu\delta_{ws}\delta_{vj}b_l\epsilon_{msp}R_{,mjl} \\
&= \mu b_l\epsilon_{vmp}R_{,mwl} + \mu b_l\epsilon_{wmp}R_{,mvl} \qquad (4.82)
\end{aligned}
$$

So the first two terms give

$$
\begin{aligned}
& \oint_\beta \frac{\mu}{4\pi R^3}[\frac{2\nu}{1-2\nu}b_j\delta_{wv}\epsilon_{jmp}R_m + b_j\delta_{wj}\epsilon_{vmp}R_m + b_j\delta_{vj}\epsilon_{wmp}R_m + \\
& \frac{2\nu^2}{(1-2\nu)(1-\nu)}\delta_{wv}b_l\epsilon_{jlp}R_j + \frac{\nu}{1-\nu}\delta_{wj}b_l\epsilon_{vlp}R_j + \frac{\nu}{1-\nu}\delta_{vj}b_l\epsilon_{wlp}R_j]dx'_p \\
= \quad & \oint_\beta \frac{\mu}{4\pi R^3}[\frac{2\nu}{1-2\nu}b_j\delta_{wv}\epsilon_{jmp}R_m + b_w\epsilon_{vmp}R_m + b_v\epsilon_{wmp}R_m + \\
& \frac{2\nu^2}{(1-2\nu)(1-\nu)}\delta_{wv}b_l\epsilon_{jlp}R_j + \frac{\nu}{1-\nu}b_l\epsilon_{vlp}R_w + \frac{\nu}{1-\nu}b_l\epsilon_{wlp}R_v]dx'_p \\
= \quad & \oint_\beta \frac{\mu}{4\pi R^3}[\frac{2\nu}{1-\nu}b_j\delta_{wv}\epsilon_{jmp}R_m + b_w\epsilon_{vmp}R_m + b_v\epsilon_{wmp}R_m + \\
& \frac{\nu}{1-\nu}b_l\epsilon_{vlp}R_w + \frac{\nu}{1-\nu}b_l\epsilon_{wlp}R_v]dx'_p \qquad (4.83)
\end{aligned}
$$

So the total stress is

$$
\begin{aligned}
\sigma_{wv}(\mathbf{x}) = \quad & \oint_\beta \frac{\mu}{4\pi R^3}[\frac{2\nu}{1-\nu}b_j\delta_{wv}\epsilon_{jmp}R_m + b_w\epsilon_{vmp}R_m + b_v\epsilon_{wmp}R_m + \\
& \frac{\nu}{1-\nu}b_l\epsilon_{vlp}R_w + \frac{\nu}{1-\nu}b_l\epsilon_{wlp}R_v + \frac{b_l\epsilon_{vmp}R_{,mwl} + b_l\epsilon_{wmp}R_{,mvl}}{2(1-\nu)}]dx'_p \qquad (4.84)
\end{aligned}
$$

## 4.4 Peach-Koehler force, Glide vs Climb

The so-called Peach-Koehler force on a dislocation can be derived by virtual work:

$$
\delta W = V\mathrm{Tr}(\boldsymbol{\sigma}\delta\boldsymbol{\epsilon}_{\text{inelastic}}) = \mathbf{b}^T\boldsymbol{\sigma}(\boldsymbol{\xi}dl\times\delta\mathbf{x}) = dl(\mathbf{b}\cdot\boldsymbol{\sigma})\cdot(\boldsymbol{\xi}\times\delta\mathbf{x}) = dl\delta\mathbf{x}\cdot((\mathbf{b}\cdot\boldsymbol{\sigma})\times\boldsymbol{\xi}) \quad (4.85)
$$

since $\mathbf{a} \cdot (\mathbf{b} \times \mathbf{c}) = \mathbf{c} \cdot (\mathbf{a} \times \mathbf{b})$. So the force per unit length of dislocation is

$$\frac{d\mathbf{F}}{dl} \;=\; (\mathbf{b} \cdot \boldsymbol{\sigma}) \times \boldsymbol{\xi}. \tag{4.86}$$

In index form this would be

$$\frac{dF_i}{dl} \;=\; \epsilon_{ijk} b_l \sigma_{lj} \xi_k. \tag{4.87}$$

where repeated indices are summed over, and $\epsilon_{ijk}$ is the Levi-Civita permutation symbol:

$$\epsilon_{123} = \epsilon_{231} = \epsilon_{312} = 1, \quad \epsilon_{213} = \epsilon_{132} = \epsilon_{321} = -1, \quad \text{all others} = 0. \tag{4.88}$$

This force is always perpendicular to $\boldsymbol{\xi}$. For a non-screw dislocation, the slip plane would have normal

$$\mathbf{m} \;=\; \frac{\boldsymbol{\xi} \times \mathbf{b}}{|\boldsymbol{\xi} \times \mathbf{b}|} \tag{4.89}$$

with $\mathbf{m} \perp \boldsymbol{\xi}$, and gliding direction

$$\mathbf{g} \;=\; \mathbf{m} \times \boldsymbol{\xi}. \tag{4.90}$$

So the total force can be written as

$$\frac{d\mathbf{F}}{dl} \;=\; \frac{d\mathbf{F}_{\text{glide}}}{dl} + \frac{d\mathbf{F}_{\text{climb}}}{dl} \tag{4.91}$$

with

$$\frac{d\mathbf{F}_{\text{glide}}}{dl} \;=\; \mathbf{g}(\mathbf{g} \cdot ((\mathbf{b} \cdot \boldsymbol{\sigma}) \times \boldsymbol{\xi})), \quad \frac{d\mathbf{F}_{\text{climb}}}{dl} \;=\; \mathbf{m}(\mathbf{m} \cdot ((\mathbf{b} \cdot \boldsymbol{\sigma}) \times \boldsymbol{\xi})). \tag{4.92}$$

Generally speaking, dislocation climb is called "non-conservative" process, because a net flux of atoms toward the core by diffusion is needed in order to drive climb. Thus at lower temperatures when long-range diffusion is impossible, even with finite driving force $\frac{d\mathbf{F}_{\text{climb}}}{dl}$, dislocation won't climb.

Dislocation glide, however, is called "conservative" or displacive process, where all that is needed is for the atoms that are already there to shift their positions by a small and semi-deterministic amount. Dislocation glide is much more ready process when $\frac{d\mathbf{F}_{\text{glide}}}{dl}$ exceeds some threshold.

## 4.5 Ideal Strength vs Actual Strength

The ideal strength $\boldsymbol{\sigma}_{\text{ideal}}$ is defined by the following thought experiment (Gedankenexperiment). Imagine a perfect crystal without any defects and at $T = 0$. Now we gradually elastically strain up the lattice, according to a path $\boldsymbol{\epsilon}(\lambda)$, which could be a simple straight line in the 6D strain space

$$\boldsymbol{\epsilon}(\lambda) \;=\; \lambda\boldsymbol{\epsilon}_0, \quad \lambda = [0, \lambda_{\text{C}}), \tag{4.93}$$

at what point would a critical $\lambda_{\text{C}}$ be reached, that the homogeneity of the lattice can no longer be maintained, and the deformation loses reversibility?

We could imagine that along the $\epsilon_{\text{shear}}$ axis, we can shear the bonds more and more, until at some point, the original set of nearest-neighbor bonds snap, or break spontaneously. Then we reach the ideal shear strength $\sigma_{\text{ideal}}^{\text{shear}}$ and ideal shear strain $\epsilon_{\text{ideal}}^{\text{shear}}$. We could also imagine that along the $\epsilon_{\text{hydro}}$ axis, we stretch the bonds more and more, until the nearest-neighbor bonds snap; then we reach the ideal hydrostatic tensile strength $\sigma_{\text{ideal}}^{\text{hydro}}$ and ideal hydrostatic tensile strain $\epsilon_{\text{ideal}}^{\text{hydro}}$. Generally speaking, $\boldsymbol{\epsilon}_{\text{ideal}}$ is a 5-dimensional surface in the 6-dimensional strain space. Moving the strain path $\boldsymbol{\epsilon}(\lambda)$ anyway inside the $\boldsymbol{\epsilon}_{\text{ideal}}$ surface is completely reversible - one can fully recover the perfect crystal upon unloading (all at 0K). But if the path ever touches the surface, BOOM!

Ab initio calculations can be used to calculate $\boldsymbol{\epsilon}_{\text{ideal}}$ and $\boldsymbol{\sigma}_{\text{ideal}}$. The results tend to be huge values [36]. For instance, BCC Fe has $\epsilon_{\text{ideal}}^{\text{shear}} = 0.178$ and $\sigma_{\text{ideal}}^{\text{shear}} = 8$ GPa. (Have you ever seen a piece of bulk Fe that can elastically shear 17% and sustain critical resolved shear stress (CRSS) of 8 GPa reversibly? The key, however, is the qualifier **bulk** Fe and what defects may be contained in your typical polycrystalline bulk Fe: dislocations, GBs, inclusions, surface damages, voids, microcracks, outright macrocracks...)

If you don't believe the numerical ab initio calculations, the large ideal strength can be still be justified on theoretical grounds. The renowned physicist Yakov Frenkel proposed the famous "Frenkel sinusoid"[37] in 1926. Imagine a material whose electron glue is local, i.e., its energy response only cares about the atomic plane immediately above, and the atomic plane immediately below. We can then perform the so-called generalized stacking fault (GSF) energy calculation, which characterize a sharp slip between two rigidly upright blocks of crystals. Let us define the slip displacement as $\mathbf{x}$ (note $\mathbf{x}$ does not mean position here!), and we can calculate the energy increase as the top plane rides above the bottom plane, $\Delta E_1(\mathbf{x})$, the subscript 1 denotes there is just one glue layer that is being sheared (between

just two planes). Clearly, $\Delta E_1(\mathbf{x})$ is extensive quantity and needs to be normalized by the slip plane area $A_0$, and we can define an intensive quantity called one-layer GSF:

$$\gamma_1(\mathbf{x}) \;=\; \frac{\Delta E_1(\mathbf{x})}{A_0} \tag{4.94}$$

We note that $\gamma_1(\mathbf{x})$ resembles the most localized deformation possible in the vertical direction, **very distinct** from the elastic deformation before. We will address this difference later. Right now, however, focus on $\gamma_1(\mathbf{x})$, which has the unit of energy per area, same as the surface or interfacial energies (it is a kind of stacking fault). We note that $\gamma_1(\mathbf{x})$ must be a periodic function:

$$\gamma_1(\mathbf{x}+\mathbf{b}) \;=\; \gamma_1(\mathbf{x}) \tag{4.95}$$

where $\mathbf{b}$ is a Bravais translational vector. And

$$\gamma_1(0) \;=\; \gamma_1(n\mathbf{b}) \;=\; 0 \tag{4.96}$$

where for a simple cubic solid, one likely have a very high energy for $\mathbf{x} \sim \mathbf{b}/2$, since we will have an energy saddle point. Thus, a most crude fitting form for the slip-shear response would be

$$\gamma_1(x) \;=\; \frac{\gamma_1^*}{2}[1-\cos\left(\frac{2\pi x}{b}\right)] \tag{4.97}$$

where $\gamma_1^*$ is the unstable stacking energy. We can also define

$$\frac{d\gamma_1(x)}{dx} \;=\; \frac{\pi\gamma_1^*}{b}\sin\left(\frac{2\pi x}{b}\right), \tag{4.98}$$

which can be regarded as the **traction-displacement** response of the **local** electron glue. (The "metallic bonding" really comes from the electron glue, as we have seen before). $\frac{d\gamma_1(x)}{dx}$ has the unit of stress.

Now consider a series of constrained deformation, $E_2(\mathbf{x})$, $E_3(\mathbf{x})$, $E_4(\mathbf{x})$, ..., $E_n(\mathbf{x})$, where the deformation is more and more delocalized (diffuse) in the $z$-direction. But we can normalize the energy by $n$, the number of glue layers being sheared:

$$\gamma_n(\mathbf{x}) \;=\; \frac{\Delta E_n(\mathbf{x})}{nA_0}. \tag{4.99}$$

There is clearly also:

$$\gamma_n(\mathbf{x}+\mathbf{b}) \;=\; \gamma_n(\mathbf{x}) \tag{4.100}$$

and we can now directly compare intensive quantity $\gamma_n(\mathbf{x})$ with intensive quantity $\gamma_1(\mathbf{x})$. As it turns out, in FCC Cu,

$$\gamma_n(\mathbf{x}) \approx \gamma_1(\mathbf{x}) \tag{4.101}$$

indicating the electron glue in Cu is indeed quite local [13]. In FCC Al, $\gamma_n(\mathbf{x})$ and $\gamma_1(\mathbf{x})$ differ somewhat - the difference thus indicates the glue is not entirely local, there is some bond angle dependence in the energy which generate triple-layer interactions. Nontheless, $\gamma_n(\mathbf{x})$ (up to $\gamma_\infty(\mathbf{x})$, which characterizes elastic deformation) are of similar magnitude with $\gamma_1(\mathbf{x})$. For pedagogical simplicity, let us pretend

$$\gamma_\infty(\mathbf{x}) = \gamma_1(\mathbf{x}) \tag{4.102}$$

and the electron glue is very local in this course.

From (2.8), we see that

$$\sigma_{\text{shear}} = \lim_{n\to\infty} \frac{1}{V_n}\frac{\partial E_n}{\partial \epsilon_{\text{shear}}} = \frac{1}{nA_0 d_0}\frac{\partial nA_0\gamma_n(x)}{\partial(x/d_0)} = \frac{d\gamma_\infty(x)}{dx} \tag{4.103}$$

From (4.102) and (4.98), we then get

$$\sigma_{\text{shear}} = \frac{d\gamma_1(x)}{dx} = \frac{\pi\gamma_1^*}{b}\sin\left(\frac{2\pi x}{b}\right). \tag{4.104}$$

From the very simple physical reasoning above, two conclusions can be drawn:

1. For small deformation, $x \ll b$,

$$\sigma_{\text{shear}} \approx \frac{\pi\gamma_1^*}{b}\frac{2\pi x}{b} = \frac{\pi\gamma_1^*}{b}\frac{2\pi\epsilon_{\text{shear}} d_0}{b} \tag{4.105}$$

so we get

$$G = \frac{2\pi^2\gamma_1^* d_0}{b^2} \tag{4.106}$$

or

$$\gamma_1^* = \frac{Gb^2}{2\pi^2 d_0}. \tag{4.107}$$

as an estimate of the energy barrier (actually energy/area) for localized shear, or **slip**.

2. The peak shear stress is obtained at:

$$\sigma_{\text{shear}}^{\text{ideal}} \;=\; \frac{\pi\gamma_1^*}{b} \;=\; \frac{Gb}{2\pi d_0} \tag{4.108}$$

when $x = b/4$ and

$$\epsilon_{\text{shear}}^{\text{ideal}} \;=\; \frac{b}{4d_0}. \tag{4.109}$$

At this point,

$$\frac{\partial^2 E}{\partial \epsilon_{\text{shear}}^2} \;=\; 0, \tag{4.110}$$

and one enters into the non-convex region of the PEL. The local elastic stability is lost, and homogeneity of the lattice can no longer be maintained.

(4.108) is called the Frenkel ideal shear strength estimate. Generally speaking, in a simple metal, $b = |\mathbf{b}|$ is the nearest-neighbor distance. With respect to the reference atom on one plane, the adjacent plane below should also have one of its nearest neighbors, but the separation is not perfectly parallel to the plane normal $\mathbf{n}$, so there tends to be

$$b \;>\; d_0 \tag{4.111}$$

Thus, a reasonable estimate for the ideal shear strength is

$$\sigma_{\text{shear}}^{\text{ideal}} \;\approx\; \frac{G}{5} \tag{4.112}$$

from the Frenkel sinusoid model. However, as we have mentioned before, metals are "shear-soft", and the sinusiod is actually **tilted** [38] and **peaks earlier** than $b/4$, so a better approximation for metals might be

$$\sigma_{\text{shear}}^{\text{ideal}} \;\approx\; \frac{G}{10}. \tag{4.113}$$

Thus, if we take the $\{0001\}\langle 11\bar{2}0\rangle$ shear system of HCP Mg, $G = 19.2$ GPa, the ideal shear strength should be around 2 GPa, which is close to the density functional theory (DFT) calculated value of 1.84 GPa[39].

In an actual experiment on a bulk metal, say HCP Mg, what one gets is a plastically flowing

metal at much lower stresses than the ideal strength:

$$\sigma \;=\; \sigma(\epsilon), \quad \epsilon = \dot{\epsilon} t \tag{4.114}$$

where a typical applied strain rate is $\dot{\epsilon} = 10^{-4}/\mathrm{s}$. A notable bend occurs in the curve at $\sigma = \sigma_{\mathrm{y}}$. People usually define $\sigma_{\mathrm{y}}$ by the "0.2% offset strain" rule. The rationale for this is that the unloading modulus is often a good (sometimes even better) estimate of the elastic modulus as the loading modulus, so if one imagines unloading, the amount of residual plastic strain at zero load would be 0.2%, which is **small but measurable** amount of sample-scale plasticity. Thus, the point of $\sigma_{\mathrm{y}}$ can be considered to have initiated measurable sample-scale plasticity, on top of whatever elasticity that have occurred. Hollomon's equation is

$$\sigma \;=\; K\epsilon_{\mathrm{p}}^{n}, \tag{4.115}$$

where $n$ is the (plastic) **strain hardening exponent** (between 0.1 and 0.5 for most metals), and $\epsilon_{\mathrm{p}}$ is the plastic strain component of the total applied strain

$$\epsilon \;=\; \epsilon_{\mathrm{e}} + \epsilon_{\mathrm{p}} \tag{4.116}$$

and $\epsilon_{\mathrm{e}}$ is the elastic component of the total applied strain. Also, for traditional macroscopic experiments, it is a very good approximation to have

$$\sigma \;=\; E\epsilon_{\mathrm{e}} \tag{4.117}$$

where $E$ is the Young's modulus. Thus, combining the equations, we have

$$\sigma \;=\; K\left(\epsilon - \frac{\sigma}{E}\right)^{n}, \tag{4.118}$$

which gives the total stress-strain curve.

$\sigma_{\mathrm{y}}$ is very small for pure bulk Mg, if we align $(0001)_{\mathrm{Mg}}$ 45° to the uniaxial pulling direction. The contrast between $\sigma_{\mathrm{y}} \sim 0.7$ MPa and $\sigma_{\mathrm{ideal}}^{\mathrm{shear}} = 1.8$ GPa is really stark, off by a factor of more than 2000! Has Frenkel gone mad?

## 4.6 Peierls-Nabarro Model of Dislocation Core and Lattice Friction

In 1934, G. I. Taylor [40], Egon Orowan [41] [1] and Michael Polanyi [42] simultaneously introduced the concept of dislocations, which resolve the paradox or discord between ideal strength and practically observed strength of bulk metals. If we regard Frenkel's estimate as pure physicists' answer to strength of crystals, the answer by Taylor, Orowan and Polanyi has more pessimistic realism in it, which is the typical view of material scientists. The 2000-fold difference is attributed to initial condition in the material, ie. *microstructures* or defects, namely dislocations. These dislocations are line defects that move inside the crystal, like crawling caterpillars or rolling carpet creases [43]. Dislocations are giant atomic-bond harvesting machines: as a dislocation core move in the crystal, it cuts some old bonds but also simultaneously stitches some new bonds together, promoting so-called **bond-switching** (not permanent **bond-loss** as in crack propagation), which is the essence of inelastic or plastic shear. Dislocations are not thermal-equilibrium defects: they must be generated by "beating".

Let us back up a little. Scientists in the 1800s have envisioned elastic distortions on aether [43] that contain localized defects. Anton Timpe [44] and Vito Volterra [45] indeed solved the elastic stress fields of these defects. Volterra further classified these line defects into six types of *distorsioni*, three turns out to be dislocations, and three turns out to be disclinations. The dislocations are the 1D edges of a 2D translational fault ($\Delta\mathbf{x} = \mathbf{b}$ to $\Delta\mathbf{x} = 0$ ), or slip fault. The disclinations are the 1D edges of a 2D rotational fault ($\Delta\theta = 10°$, a grain boundary, to $\Delta\theta = 0$, no grain boundary). Disclinations are prohibitively expensive in 3D crystals, but they can exist in 2D crystals embedded in 3D [46, 47] and liquid crystals [48, 49].

Dislocations were first directly observed by transmission electron microscopy (TEM) by the team led by Sir Peter B. Hirsch at Oxford in 1956. [50] Thus, in this case, materials theory was ahead of experimentation by more than 20 years!

Dislocations are created to relax (gradually reduce) elastic strain energy. As previously mentioned, elastic strain energy is small (small amplitude) but diffuse (long wavelength) "pain" inside the crystal. The most common treatment of such small-amplitude, long-wavelength pain is so-called linear elasticity theory, where stress-strain relation is linear but energy is approximately by quadratic fitting of the bottom. Basically one attempts to fit the PEL by a

[1] Orowan was a professor of metallurgy at the MIT from 1950.

quadratic expansion near the local minimum. But even if the strain amplitude is somewhat larger and needs to go beyond the quadratic fitting (so-called nonlinear elasticity), the main toplogical features of crystal bonding remains as at the bottom of the energy basin, and reversibility is ensured upon unloading. In contrast, dislocations represent extremely localized, large-amplitude, highly nonlinear (convex→concave→convex) and metastable deformation. The key to plasticity is the lock-in effect, which can be seen from (4.95) and (4.100) already. Namely, if one abuses a crystal by shearing, initially the crystal will cry out for pain, but if one keeps up the abuse, and push it through the nonlinear regime, then the crystal will start to feel less pain, and in the end would see no difference from its comfort zone. Until the next round of abuse starts. This "locks in" the large-amplitude, highly localized slip displacement. **Nonlinearity and non-convexity in the PEL is the essence of plasticity.** (as versus elasticity, which focusses on and is limited by the quadratic fit).

Why then, is dislocation slip preferred over, say, shearing 3 layers together? (From here on, slip means most localized, large shearing between two atomic planes.) We notice even that the generalized stacking fault calculation of $\gamma_1(\mathbf{x})$ looks kind of "unnatural", in that one must rigidly constrains the top and bottom blocks, and only allow relative displacement between the two rigid block. Why would one artificially apply such constraint?

The reason turns out to have more to do with the nonlinear response, than with the linear response of the crystal. If one fixes the external displacement $\Delta$ that spreads over $n$ layers, one should plot and compare $\gamma_1(\Delta)$ with $n\gamma_n(\Delta/n)$ (From now on, we use $\Delta$ to denote shear displacement instead of $\mathbf{x}$, since we will talk about spatially dependent displacement $\Delta(\mathbf{x})$). It turns out that, if we assume the local electron glue, (4.101), then for small $\Delta$:

$$\gamma_1(\Delta) \ll n\gamma_n(\Delta/n) \tag{4.119}$$

Indeed, the curvature of the former is $n$ times larger than that of the latter. So, for small $\Delta$, diffuse deformation is preferred, the more diffuse, the better. However, once we requires large shear offset $\Delta$, the situation is seen to be reversed. The saddle-point energy to overcome a diffuse barrier is $n$ times larger than that of $\gamma_1(\Delta)$! Thus, for the most localized slip deformation, the pain comes quickly, but peaks earlier; whereas for the delocalized deformation, the pain comes later, but is ultimately greater. This basically says that, if one must cuts bonds to achieve large traction relaxation, then doing the bond cutting on one atomic plane is the best choice.

The above is the argument for the strongest possible localization in the $z$-direction, which

is localizing down to a single slip plane between two adjacent atomic planes. There is also an argument for localization in the $xy$-plane, the so-called Peierls-Nabarro theory of the dislocation core. [51, 52] Basically, Peierls argues that if only pain on the slip plane ("localized pain") is counted:

$$\frac{E_{\text{slip}-\text{inelastic}}}{L} \;=\; \sum_{\text{atom } i \text{ in core}} \gamma_1(\Delta_i) \;\approx\; \int_{-\infty}^{\infty} dx \gamma_1(\mathbf{v}(x)) \tag{4.120}$$

this energy would prefer a core as narrow as possible. In above we have made a discrete to continuum mapping $\{\Delta_i\} \to \mathbf{v}(\mathbf{x})$

However, since a dislocation must make the transition from $\mathbf{v} = 0$ (outside of slipped plate) to $\mathbf{v} = \mathbf{b}$ (inside slipped plate), the slip offset $\mathbf{v}$ changes with position $\mathbf{x}$, and therefore elastic energy in other places ("diffuse pain") must also be involved. One could show it is of the form

$$\frac{E_{\text{elastic}}}{L} \;=\; \frac{1}{2}\int_{-\infty}^{\infty} dx \int_{-\infty}^{\infty} dx' \frac{d\mathbf{v}(x)}{dx}(-K \ln|x-x'| + \text{const})\frac{d\mathbf{v}(x')}{dx'}, \tag{4.121}$$

where $K$ depends on the elastic constants only. The floating constant that accompanies $-K \ln|x-x'|$ does not matter, since we have the constraint:

$$\int_{-\infty}^{\infty} dx \frac{d\mathbf{v}(x)}{dx} \;=\; \mathbf{v}(x=\infty) - \mathbf{v}(x=-\infty) = \mathbf{b} \tag{4.122}$$

The above is a quadratic form: it is easy to show that if the dislocation core is wider by 2:

$$\mathbf{v}(x) \;\to\; \mathbf{v}\left(\frac{x}{2}\right) \tag{4.123}$$

$E_{\text{elastic}}$ would drop by a factor of 4. Therefore $E_{\text{elastic}}$ prefers as wide core as possible. The competition of the two gives the equilibrium core width of dislocation.

Peierls solved the variational problem:

$$\frac{E_{\text{dislocation}}}{L} \;=\; \int_{-\infty}^{\infty} dx \gamma_1(\mathbf{v}(x)) - \frac{1}{2}\int_{-\infty}^{\infty} dx \int_{-\infty}^{\infty} dx' \frac{d\mathbf{v}(x)}{dx} K \ln|x-x'| \frac{d\mathbf{v}(x')}{dx'}, \tag{4.124}$$

and obtained the in-plane size of the dislocation core.[51] Imagine a variation $\mathbf{v}(x) \to \mathbf{v}(x) + \delta\mathbf{v}(x)$. One gets:

$$\frac{\partial \gamma_1}{\partial \mathbf{v}} + \frac{d}{dx}\int_{-\infty}^{\infty} K \ln|x-x'| \frac{d\mathbf{v}(x')}{dx'} dx' \;=\; 0. \tag{4.125}$$

The above is an integral equation. Suppose we take the Frenkel form of the non-linear glue

(4.97):

$$\gamma_1(v) = \frac{\gamma_1^*}{2}[1-\cos\left(\frac{2\pi v}{b}\right)] \tag{4.126}$$

$$\frac{\partial\gamma_1}{\partial\mathbf{v}} = \frac{\pi\gamma_1^*}{b}\sin\left(\frac{2\pi v}{b}\right)\mathbf{e}_x \tag{4.127}$$

and $\mathbf{v} = v(x)\mathbf{e}_x$, we get

$$\sin\left(\frac{2\pi v}{b}\right) = \frac{Kb}{\pi\gamma_1^*}\int_{-\infty}^{\infty}\frac{1}{x'-x}\frac{dv(x')}{dx'}dx' \tag{4.128}$$

For edge dislocation in simple cubic (or simple tetragonal with $d_0 > b$) material,

$$K = \frac{\mu}{2\pi(1-\nu)},\ \ \gamma_1^* = \frac{\mu b^2}{2\pi^2 d_0},\ \ d_0 = b. \tag{4.129}$$

so the dimensionless number

$$\kappa \equiv \frac{Kb}{\pi\gamma_1^*} = \left(\frac{1}{1-\nu}\right)\frac{d_0}{b} \tag{4.130}$$

and is $\frac{d_0}{b}$ for screw dislocation. So we get

$$\sin\left(\frac{2\pi v}{b}\right) = \kappa\int_{-\infty}^{\infty}\frac{1}{x'-x}\frac{dv(x')}{dx'}dx'. \tag{4.131}$$

$\kappa$ is a dimensionless constant symbolizing the ratio of strength of delocalized elastic constant ($\gamma_\infty$) to localized glue ($\gamma_1$ [13]). The larger is $\kappa$, the wider the dislocation core should be from previous discussions.

We first get rid of all the constants, by defining

$$V \equiv \frac{2\pi v}{b}, \tag{4.132}$$

so

$$\sin V = \frac{\kappa b}{2\pi}\int_{-\infty}^{\infty}\frac{1}{x'-x}\frac{dV(x')}{dx'}dx'. \tag{4.133}$$

and then we rescale the distance

$$X \equiv \frac{2\pi x}{\kappa b} \tag{4.134}$$

so integral equation is as simple as possible

$$\sin V \;=\; \int_{-\infty}^{\infty} \frac{1}{X'-X}\frac{dV(X')}{dX'}dX'. \tag{4.135}$$

$\frac{dV(X')}{dX'}$ is the core spread function: it be a smooth peaked function like a Gaussian, which also decays as $X \to \pm\infty$. The above looks awfully like a contour integral, if we identify $z = X'$, and assume $\frac{dV(z)}{dz}$ to contain one pole $z_p$ in the upper complex plane and vanishes in the big arc (we are already guessing $\frac{dV(X')}{dX'}$ to look like a Lorentzian shaped function with algebraic decay at least, and possibly even faster), so

$$\int_{-\infty}^{X-\epsilon} + \int_{X+\epsilon}^{\infty} \frac{1}{z-X}\frac{dV(z)}{dz}dz - i\pi\frac{dV(X)}{dX} + 0 \;=\; \frac{2\pi i}{z_p - X}\lim_{z\to z_p}(z-z_p)\frac{dV}{dz} \tag{4.136}$$

or

$$\sin V - i\pi\frac{dV(X)}{dX} \;=\; \frac{2\pi i}{z_p - X}a_p \tag{4.137}$$

We are not in bad shape, because the above is ODE. If

$$V(X) = 2\arctan\left(\frac{X}{\pi}\right) + \pi \tag{4.138}$$

which satisfied the boundary conditions, then

$$\frac{dV(X)}{dX} \;=\; \frac{2}{\pi}\frac{1}{1+(X/\pi)^2} \;=\; \frac{2\pi}{X^2+\pi^2} \;=\; \frac{2\pi}{(X+i\pi)(X-i\pi)} \tag{4.139}$$

then $z_P = i\pi$ and $a_p = \frac{1}{i}$, and

$$\sin V(X) = -2\frac{X/\pi}{\sqrt{1+(X/\pi)^2}}\frac{1}{\sqrt{1+(X/\pi)^2}}, \quad \frac{2\pi i}{z_p - X}a_p = \frac{2\pi}{i\pi - X} \tag{4.140}$$

so we get

$$-2\frac{X/\pi}{(1+(X/\pi)^2)} - \frac{2i}{1+(X/\pi)^2} \;=\; -2\frac{X/pi+i}{(X/\pi+i)(X/\pi-i)} = \frac{-2}{X/\pi - i} \;=\; \frac{2\pi}{i\pi - X} \tag{4.141}$$

QED. The above solution to (4.135) can be verified numerically.

```
mesh = 1024;
Xmax = 60;
Xmin = -Xmax;
```

```
Xdel = (Xmax - Xmin)/1024;
X = Xmin+Xdel/2 : Xdel : Xmax;
V = pi + 2 * atan(X / pi);

plot(X,V);
dVdX = 2/pi./(1+(X/pi).^2);
n = floor(mesh * 2.7/5);
plot(X,dVdX, X(n),(V(n+1)-V(n-1))/2/Xdel,'ro');

kernel = 1./(X-X(n));
kernel(n) = 0;
plot(X,sin(V), X(n),kernel*dVdX'*Xdel,'ro');
```

So the Peierls solution gives

$$\frac{2\pi v}{b} = 2\arctan\left(\frac{2x}{\kappa b}\right) + \pi \tag{4.142}$$

or

$$v(x) \;=\; \frac{b}{\pi}\arctan\left(\frac{x}{w}\right) + \frac{b}{2}. \tag{4.143}$$

where the core width $w$ (one half of Full Width at Half Maximum (FWHM)) is given by

$$w \;=\; \frac{\kappa b}{2} \;=\; \frac{Kb^2}{2\pi\gamma_1^*} \tag{4.144}$$

in this particular case.

The problem with (4.124) is that there is no barrier against the translation

$$\mathbf{v}(x) \;\rightarrow\; \mathbf{v}(x-s) \tag{4.145}$$

for arbitrary shift $s$ of the dislocation core, forming so-called Goldstone mode, due to the continuum formulation. This is not true in reality, because so-called lattice friction does exist on all dislocations, for example screw dislocation in BCC metal, and dislocations in semiconductors, are known to have very significant lattice frictions.

Nabarro removed the zero-friction problem by resorting back to the atomistic sum:

$$\frac{E_{\text{slip}-\text{inelastic}}}{L} = \int_{-\infty}^{\infty} dx\gamma_1(\mathbf{v}(x)) \;\;\rightarrow \sum_{\text{atom } i \text{ in core}} \gamma_1(\mathbf{v}_i)a \tag{4.146}$$

using the Peierls core solution, where $a$ is the distance between atoms on the slip plane that is sampling the $\mathbf{v}(x)$. For simple 2D lattice and edge dislocation, there should be $a = b$, but we will keep using $a$ for conceptual clarity (in 3D solid, the sampling can get more interesting). We have

$$\begin{aligned}
\frac{E_{\text{slip}-\text{inelastic}}}{La} &= \sum_{n=-\infty}^{\infty} \frac{\gamma_1^*}{2}\left[1-\cos\left(\frac{2\pi(\frac{b}{\pi}\arctan\left(\frac{x_n}{w}\right)+\frac{b}{2})}{b}\right)\right] \\
&= \sum_{n=-\infty}^{\infty} \frac{\gamma_1^*}{2}\left[1+\cos\left(2\arctan\left(\frac{x_n}{w}\right)\right)\right] \\
&= \sum_{n=-\infty}^{\infty} \gamma_1^*\cos^2\left(\arctan\left(\frac{x_n}{w}\right)\right) \\
&= \gamma_1^* \sum_{n=-\infty}^{\infty} \frac{1}{1+\left(\frac{x_n}{w}\right)^2}
\end{aligned} \tag{4.147}$$

Since

$$x_n \;=\; (n+s)b, \quad s=[0,1) \tag{4.148}$$

we have

$$\frac{E_{\text{slip}-\text{inelastic}}(s)}{La} \;=\; \gamma_1^* \sum_{n=-\infty}^{\infty} \frac{1}{1+\left(\frac{b(n+s)}{w}\right)^2} \tag{4.149}$$

The summation can be mappled to a contour integral, and one gets

$$\sum_{n=-\infty}^{\infty} \frac{1}{1+c^2(n+s)^2} \;=\; \frac{1}{c}\frac{\pi\cosh(\frac{\pi}{c})\sinh(\frac{\pi}{c})}{\cosh^2(\frac{\pi}{c})-\cos^2(\pi s)} \tag{4.150}$$

```
>> pi/c*cosh(pi/c)*sinh(pi/c)/(cosh(pi/c)^2-cos(pi*s)^2)
>> c=3; s=0.34; n = -10000:10000; sum(1./(1+c^2*(n+s).^2))
```

We have

$$c \;=\; \frac{b}{w} \tag{4.151}$$

here, so the lattice friction barrier can be written as

$$\frac{E_{\text{slip}-\text{inelastic}}(s)}{La} \;=\; \frac{\gamma_1^*\pi w}{b}\frac{\cosh(\frac{\pi w}{b})\sinh(\frac{\pi w}{b})}{\cosh^2(\frac{\pi w}{b})-\cos^2(\pi s)} \tag{4.152}$$

Recall that

$$\sinh(x) \equiv \frac{e^x-e^{-x}}{2}, \;\; \cosh(x) \equiv \frac{e^x+e^{-x}}{2} \tag{4.153}$$

so when $\pi w/b \to \infty$ (in simple cubic it is 1.57 for screw and 2.3 for edge), we would have

$$\frac{E_{\text{slip}-\text{inelastic}}(s)}{La} \sim \frac{\gamma_1^* \pi w}{b}\left(1+\frac{\cos^2(\pi s)}{\cosh^2(\frac{\pi w}{b})}\right) \sim \frac{\gamma_1^* \pi w}{b}\left(1+\frac{\cos^2(\pi s)}{e^{\frac{2\pi w}{b}}/4}\right) \tag{4.154}$$

That is, the barrier height scales as

$$\frac{W_{\text{m}}}{L} = \frac{4\pi\gamma_1^* w a}{b} e^{-\frac{2\pi w}{b}} \tag{4.155}$$

The key results from Nabarro's work [52] are: (a) Nabarro obtained an energy barrier for dislocation translation, paradoxially called the Peierls energy barrier (in terms of stress needed to overcome this barrier, the **Peierls stress**), and (b) the Peierls barrier has strong (exponential) dependence on the core size. The wider the dislocation core, the lower the Peierls barrier. So, dislocations in FCC metals have wider cores (due to Shockley partials splitting), and the lattice friction is small. But screw dislocation in BCC crystals have narrow cores, and therefore the lattice friction can be very large, with the **Peierls stress** as high as on the order of 1GPa, so large that it can dominate the overall plastic flow strength.

This turns out to be general for all extensive defects. The narrower the core, the stronger the lattice pins it, and the more difficult it is to move. This is even true for "electronic" defects, e.g. polarons. Small polarons have low mobility and is strongly trapped and required $T$ to activate its hopping, where large polarons have high mobility and is more band transport or ballistic like.

This kind of discrete sampling trapping also occurs in numerical simulations and causes "numerical friction" as well. That is, when we use PDE solver, we need a mesh to discretize and represent the continuum field by a discrete points, and invariably such representation error causes "artificial" undulation of the numerical Hamiltonian when the field solution is being translated in space.

So dislocation is basically a machine to cut bonds on one plane, and then re-stitch them together. It should not be surprising that dislocation is the fundamental agent of plastic deformation, which is basically irreversible shape change, because dislocation slip gives the most localized (in $z$ and in $x$) way to cut the bonds.

We know that $\kappa \equiv \frac{Kb}{\pi\gamma_1^*}$ is the dimensionless "ratio" of $\gamma_\infty(\mathbf{v})$ to $\gamma_1(\mathbf{v})$, and the dislocation half-FWHM $w = \frac{\kappa b}{2}$ will depend on this material-dependent ratio. For simplicity let us assume $\kappa = 2$ and $w = b$. In this case, $e^{-\frac{2\pi w}{b}} = e^{-2\pi} = 0.00186$, and this is before the

thermal activation effect (double kink mechanism) kicks in. Furthermore, when $w$ increases by 50%, $e^{-\frac{2\pi w}{b}} = e^{-3\pi} = 8 \times 10^{-5}$. These factors are indeed what one needs to compare the experimentally observed "Peierls stress" (to move a single glissible dislocation, in say, in situ TEM) with the ideal strength. In reality, the Peiels-Nabarro model is not that numerically precise, and also we have ignored thermal activation, so these numbers should not be taken literally, but the $10^{-3} - 10^{-4}$ order of magnitude, and the fact that even small changes in $w$ results in huge variation in the lattice friction, are the take-home messages.

## 4.7 Line Defect Picture and Equation of Motion

For an infinite straight dislocation in isotropic elastic medium, the stress field is

$$\sigma_{xz} = -\frac{\mu b}{2\pi}\frac{y}{x^2+y^2}, \quad \sigma_{yz} = \frac{\mu b}{2\pi}\frac{x}{x^2+y^2}, \quad \sigma_{xy} = \sigma_{xx} = \sigma_{yy} = \sigma_{zz} = 0 \tag{4.156}$$

for "positive" screw dislocation:

$$\boldsymbol{\xi} \;=\; \frac{\mathbf{b}}{|\mathbf{b}|} \;=\; \mathbf{e}_z. \tag{4.157}$$

where $\mu$ is the shear modulus (we use $G$ for crystallographic shear modulus). In cylindrical coordinate, this is

$$\sigma_{\theta z} \;=\; \frac{\mu b}{2\pi r}, \quad \sigma_{rz} = \sigma_{r\theta} = \sigma_{rr} = \sigma_{\theta\theta} = \sigma_{zz} = 0. \tag{4.158}$$

For edge dislocation,

$$\boldsymbol{\xi} \;=\; \mathbf{e}_z, \;\; \mathbf{b} \;=\; b\mathbf{e}_x \tag{4.159}$$

the formula is a little bit more complicated:

$$\sigma_{xx} \;=\; -\frac{\mu b}{2\pi(1-\nu)}\frac{y(3x^2+y^2)}{(x^2+y^2)^2}, \;\; \sigma_{yy} \;=\; \frac{\mu b}{2\pi(1-\nu)}\frac{y(x^2-y^2)}{(x^2+y^2)^2}, \;\; \sigma_{xz} = \sigma_{yz} = 0 \tag{4.160}$$

$$\sigma_{xy} \;=\; \frac{\mu b}{2\pi(1-\nu)}\frac{x(x^2-y^2)}{(x^2+y^2)^2}, \;\; \sigma_{zz} \;=\; \nu(\sigma_{xx}+\sigma_{yy}) \;=\; -\frac{\mu b\nu}{\pi(1-\nu)}\frac{y}{x^2+y^2}, \tag{4.161}$$

In cylindrical coordinates:

$$\sigma_{rr} = \sigma_{\theta\theta} \;=\; -\frac{\mu b \sin\theta}{2\pi(1-\nu)r}, \quad \sigma_{r\theta} \;=\; \frac{\mu b\cos\theta}{2\pi(1-\nu)r}, \tag{4.162}$$

$$\sigma_{zz} \;=\; \nu(\sigma_{rr}+\sigma_{\theta\theta}) \;=\; -\frac{\mu b\nu\sin\theta}{\pi(1-\nu)r}, \quad \sigma_{rz}=\sigma_{\theta z}=0. \tag{4.163}$$

Taking the screw dislocation as example (the edge dislocation has the same scaling, but is algebraically more complex). We note in above that the dislocation stress field decays as $r^{-1}$. This means the elastic strain field decays also as $r^{-1}$, and the elastic strain energy density behaves like

$$e_{\rm elastic}(\mathbf{x}) \;=\; \frac{\sigma_{\theta z}^2}{2\mu} \;=\; \frac{\mu^2 b^2}{8\pi^2\mu}r^{-2} \tag{4.164}$$

Thus, with a standalone dislocation, the total elastic energy per length scales as

$$\frac{E_{\rm elastic}}{L} \;=\; \int_{R_0}^{R_1} dr 2\pi r\frac{\mu b^2}{8\pi^2}r^{-2} \;=\; \int_{R_0}^{R_1} dr\frac{\mu b^2}{4\pi}r^{-1} = \frac{\mu b^2}{4\pi}\ln\frac{R_1}{R_0}, \tag{4.165}$$

which is the diffuse "pain" in a ring of materials between $R_0$ and $R_1$. Obviously there is a problem with convergence in both the inner cutoff $R_0$ and the outer cutoff $R_1$. The inner cutoff can be handled by recognizing that elastic strain has a limit of $\sim 10\%$. Once that limit is reached, we get into the inelastic region of the core, and the pure elasticity theory no longer applies, and one has to use the Peierls-Nabarro theory of the dislocation core that has some handle on the nonlinear non-convex part of PEL, the $E_{\rm slip-inelastic}$ term in (4.120). [51, 52]. When that nonlinear energy inside $R_0$ is included, the self energy can be written as

$$\frac{E_{\rm self}}{L} \;=\; \frac{\mu b^2}{4\pi}\ln\frac{R_1}{R_0} + e_{\rm inelastic} \;\equiv\; \frac{\mu b^2}{4\pi}\ln\frac{R_1}{\tilde{R}_0}. \tag{4.166}$$

Quite often people find $\tilde{R}_0$ to be around the order of $b$ from exact atomistic calculations. [53].

There is also a problem with the outer cutoff $R_1$. This in fact means the dislocation cares about its environment. If a single screw dislocation exists in the center of a nanowire [54], then one can expect $R_1$ to be of the order the cylinder radius $R$. Generally speaking, in a bulk metal, if there are other dislocations which screen the field of the dislocation in question, and those nearest-neighbor screening dislocations are of the order $R_{\rm screen}$, we would have the dislocation self energy as

$$\frac{E_{\rm self}}{L} \;=\; \frac{\mu b^2}{4\pi}\ln\frac{R_{\rm screen}}{\tilde{R}_0}. \tag{4.167}$$

A rule of thumb in the literature is to take

$$\eta \;\equiv\; \frac{E_{\rm self}}{L} \;\sim\; \alpha\mu b^2 \tag{4.168}$$

with $\alpha \sim 0.5 - 1$. From (4.167), we see this implies the screening distance is of the order

$$\alpha = 0.5 : R_{\text{screen}} \sim e^{2\pi}\tilde{R}_0 = 535\tilde{R}_0, \quad \alpha = 1 : R_{\text{screen}} \sim e^{4\pi}\tilde{R}_0 = 286751\tilde{R}_0 \tag{4.169}$$

Assuming $\tilde{R}_0 = b = a_0/\sqrt{2} = 2.556$Å in Cu, this converts to $R_{\text{screen}} = 137$nm for $\alpha = 0.5$, to $R_{\text{screen}} = 73\mu$m for $\alpha = 1$, which covers most of the physically sensible ranges, from heavily work-hardened metal (a mediumly cold-worked Cu has dislocation density $\rho = 4 \times 10^{14}/\text{m}^2$ [55], which implies a characteristic spacing of 50 nm), to highly annealed metal.

Below we look at glide-only motion. Consider a pure applied shear stress $\sigma_{xy} = \tau$ for a curved dislocation on $y$-plane with $\mathbf{b} = b\mathbf{e}_x$, and

$$\boldsymbol{\xi}(l) = \xi_x \mathbf{e}_x + \sqrt{1 - \xi_x^2}\mathbf{e}_z. \tag{4.170}$$

$$\frac{d\mathbf{F}_{\text{climb}}}{dl} = 0, \quad \frac{d\mathbf{F}_{\text{glide}}}{dl} = b\tau \mathbf{e}_y \times \boldsymbol{\xi}, \tag{4.171}$$

We can call $\eta$ in (4.168) the *line tension* of a dislocation. If we pretend

1. $\eta$ to be independent of $\boldsymbol{\xi}$. (In reality $\eta$ depends on $\boldsymbol{\xi}$.)
2. Besides the self energy, the dislocations do not interact with each other elastically. (In reality, they do).

we come to the so-called line tension model of a dislocations. This is an extremely simple model because it is local.

Consider the line direction $\boldsymbol{\xi}(l)$ as a function of the dislocation length $l$. If the dislocation is a straight line, then locally we have force equilibrium from the line tension. But, if $\boldsymbol{\xi}(l)$ has curvature, this would generate

$$d\mathbf{F} = \eta\boldsymbol{\xi}(l + dl) - \eta\boldsymbol{\xi}(l) = \eta\frac{d\boldsymbol{\xi}}{dl}dl = \eta\frac{\mathbf{e}_R(l)}{R(l)}dl \tag{4.172}$$

where $R(l)$ is the radius of curvature, and $\mathbf{e}_R$ points towards the center of the local tangent circle.

If a dislocation is pinned between two fixed ends with distance $2c$, then we would have a

circular segment, with line tension balancing the PK force:

$$b\tau \;=\; \frac{\eta}{R(l)} \quad \rightarrow \quad R(l) = \frac{\eta}{b\tau} \tag{4.173}$$

From the derivation above, we see $R$ is actually independent of $l$ when the dislocation reaches equilibrium. This means at equilibrium, the dislocation is always arc of a *perfect circle* in the isotropic line tension model.

The critical configuration is actually when $R = c$ ($R$ first decreases with $\tau \uparrow$, but after reaching the minimum value of $c$, would start to increase again, so $R = c$ is the "saddle" configuration), so the critical external stress for bow-out is

$$\tau_{\mathrm{C}} \;=\; \frac{\eta}{bc} = \frac{\alpha G b^2}{bc} = \frac{\alpha G b}{c}. \tag{4.174}$$

In reality, $c = 10^{-6}$m, but $b \sim 2 \times 10^{-10}$m, so we get

$$\tau_{\mathrm{C}} \;\sim\; 10^{-4} G. \tag{4.175}$$

The above immediately explains the $1000\times$ difference with Frenkel estimate of ideal shear strength.

The dislocation density $\rho$ [unit $1/\mathrm{m}^2$] is defined as the total length of all dislocations in a unit volume of material. $\rho$ in mediumly work-hardened Cu is typically on the order of $4 \times 10^{14}/\mathrm{m}^2$ (number of etch pits per unit area) $= 4 \times 10^{14}\mathrm{m}/\mathrm{m}^3$ (dislocation line length per $\mathrm{m}^3$ of material - in reference, circumference of earth is $4 \times 10^7$m, circumference of sun is $4 \times 10^9$m - it would take light 15 days to traverse the dislocation line in $1\mathrm{m}^3$ of copper! so to simulate plasticity by tracking dislocations is quite a challenge). We can estimate the mean spacing between between dislocations to be

$$2c \;=\; \rho^{-1/2} \tag{4.176}$$

Plugging into (4.174), we get

$$\tau_{\mathrm{C}} \;=\; 2\alpha G b \rho^{1/2} \tag{4.177}$$

The above $\rho^{1/2}$ dependence is called the Taylor hardening law. It comes from forest dislocation resistance. There can be other sources of plastic flow resistance, for example lattice friction, solute hardening, precipitate/dispersion hardening, grain boundary hardening etc.

The typical way of modeling them is to add all together:

$$\tau_{\rm C} \;=\; 2\alpha G b\rho^{1/2} + \tau_{\rm LatticeFriction} + \tau_{\rm solute} + \tau_{\rm precipitate/dispersion} + \tau_{\rm GB} \tag{4.178}$$

$\tau_{\rm C}$ is called the critical resolved shear stress (CRSS). The resolved shear stress $\tau$ on a slip system is generally computed as

$$\tau \;\equiv\; \frac{(\mathbf{b}\cdot\boldsymbol{\sigma})\cdot\mathbf{n}}{|\mathbf{b}|} \;=\; \frac{b_i\sigma_{ij}n_j}{b} \tag{4.179}$$

If we put uniaxial tension/compression along a direction $\mathbf{u}$, we have

$$\boldsymbol{\sigma} \;=\; \sigma\mathbf{u}\mathbf{u}^T \tag{4.180}$$

we have

$$\tau \;=\; \frac{\sigma(\mathbf{b}\cdot\mathbf{u})(\mathbf{n}\cdot\mathbf{u})}{b} \;=\; \sigma\cos(\theta_b)\cos(\theta_n) \tag{4.181}$$

where $\theta_b$ is angle between $\mathbf{u}$ and $\mathbf{b}$, and $\theta_n$ is angle between $\mathbf{u}$ and $\mathbf{n}$. $\cos(\theta_b)\cos(\theta_n)$ is called the Schmid factor. Since $\mathbf{n}\perp\mathbf{b}$, the maximum Schmid factor is $\frac{1}{2}$, when $\mathbf{u}$ is 45° between $\mathbf{n}$ and $\mathbf{b}$.

The so-called Schmid's Law means all that matter is scalar CRSS $\tau_{\rm C}$, no matter what is the tensor $\boldsymbol{\sigma}$ that generates this scalar.

So far we considered stationary dislocation. To establish an **equation of motion** for gliding dislocation, we need to consider **elastodynamic** equation:

$$\nabla\cdot\boldsymbol{\sigma} \;=\; \rho\mathbf{u}_{,tt} \tag{4.182}$$

where $\rho$ is the mass density (unit kg/m$^3$). For isotropic medium we have

$$(\lambda+\mu)\nabla(\nabla\cdot\mathbf{u}) + \mu\nabla^2\mathbf{u} \;=\; \rho\partial_t^2\mathbf{u} \tag{4.183}$$

For simplicity, let us consider a moving straight screw dislocation. We are going to assume the property of

$$u_z \;=\; u_z(x,y,t),\;\; u_x = u_y = 0, \tag{4.184}$$

so the divergence-free property $\nabla\cdot\mathbf{u}=0$ stays even in transients. Let us then ignore the

subscript and define $u = u_z$. Then

$$\frac{\mu}{\rho}(\partial_x^2 + \partial_y^2)u \;=\; \partial_t^2 u \tag{4.185}$$

Without the dislocation singularity, the above defines transverse shear waves, with wave speed

$$c \;\equiv\; \sqrt{\frac{\mu}{\rho}}. \tag{4.186}$$

The stationary singularity would posses displacement field

$$u \;=\; \frac{b\theta}{2\pi}, \quad \theta = -\pi..\pi \tag{4.187}$$

if the branch cut is from $(-\infty, 0)$ to $(0, 0)$.

Now consider a uniformly moving dislocation singularity with speed $v$. We would like to comove with the dislocation, so we will perform Galileo transform

$$t' \;=\; t, \quad x' = x - vt, \quad y' = y \tag{4.188}$$

and we want to re-express

$$f(x, y, t) \;=\; f(x', y', t') = f(x - vt, y, t) \tag{4.189}$$

So the idea is someone gives you the explicit form for the 2nd expression, and you wonder about the sensitivity of $f$ to the former arguments. We then have

$$\partial_x \;=\; \partial_{x'}, \;\; \partial_y \;=\; \partial_{y'}, \;\; \partial_t \;=\; \partial_{t'} - v\partial_{x'}, \tag{4.190}$$

so we get

$$c^2(\partial_x^2 + \partial_y^2)u \;=\; (\partial_{t'} - v\partial_{x'})^2 u \tag{4.191}$$

Now suppose we have reached stationary speed, then $\partial_{t'} u = 0$, so we end up with

$$(c^2 - v^2)\partial_x^2 u + c^2\partial_y^2 u \;=\; 0 \tag{4.192}$$

If we define dimensionless speed

$$\beta \;\equiv\; \frac{v}{c} \tag{4.193}$$

then

$$(1-\beta^2)\partial_x^2 u + \partial_y^2 u \;=\; 0 \tag{4.194}$$

So we see the structure of the steady-state equation is the same as that of the stationary equation, if we just perform Lorentz contraction of $x$:

$$\tilde{x} \;\equiv\; \frac{x}{\sqrt{1-\beta^2}} \tag{4.195}$$

$$\partial_{\tilde{x}}^2 u + \partial_y^2 u \;=\; 0 \tag{4.196}$$

then **everything stays the same** (including the essential branch cut discontinuity condition). In other words, in the $\tilde{x}-y$ frame, we can define

$$\tilde{\theta} \;\equiv\; \arctan\left(\frac{y}{\tilde{x}}\right) \tag{4.197}$$

and

$$u_z \;=\; \frac{b\tilde{\theta}}{2\pi}. \tag{4.198}$$

This moving dislocation has both kinetic and elastic energy. The stationary elastic energy was

$$E_0 \;=\; \alpha\mu b^2 \;=\; \int dxdy \frac{\mu(\partial_x u)^2 + \mu(\partial_y u)^2}{2} \tag{4.199}$$

so

$$\int dxdy \frac{\mu(\partial_x u)^2}{2} \;=\; \int dxdy \frac{\mu(\partial_y u)^2}{2} \;=\; \frac{\alpha\mu b^2}{2} \tag{4.200}$$

and with the Lorentz contraction, the first term is scaled by

$$\sqrt{1-\beta^2} \times \left(\frac{1}{\sqrt{1-\beta^2}}\right)^2 \;=\; \frac{1}{\sqrt{1-\beta^2}} \tag{4.201}$$

whereas the second term is scaled only by $\sqrt{1-\beta^2}$, so the new potential energy is

$$\alpha\mu b^2 \left(\frac{1}{2\sqrt{1-\beta^2}} + \frac{\sqrt{1-\beta^2}}{2}\right) \;=\; \alpha\mu b^2 \frac{2-\beta^2}{2\sqrt{1-\beta^2}}. \tag{4.202}$$

But there is also kinetic energy

$$\int dxdy \frac{\rho(\partial_t u)^2}{2} \;=\; \int dxdy \frac{\rho v^2(\partial_x u)^2}{2} \;=\; \beta^2 \alpha\mu b^2 \frac{1}{2\sqrt{1-\beta^2}} \tag{4.203}$$

So the total energy is now

$$E(v) \;=\; \frac{\alpha\mu b^2}{\sqrt{1-v^2/c^2}} \;=\; \frac{E_0}{\sqrt{1-v^2/c^2}} \tag{4.204}$$

In the small $v$ limit, we get

$$E(v) - E_0 \;=\; E_0(1+\frac{v^2}{2c^2}) \tag{4.205}$$

so we can identify "inertial mass" of the dislocation (if we want to have $E(v)-E_0 = \frac{1}{2}m_0v^2$) to be

$$m_0 \;=\; \frac{E_0}{c^2} \;=\; \frac{\alpha\mu b^2}{\mu/\rho} \;=\; \rho b^2 \frac{\ln \frac{R_{\text{screen}}}{R_0}}{4\pi}. \tag{4.206}$$

The interpretation of the above is that as far as inertial mass goes, those near the core are more important than those far away from the core (by $(r^{-1})^2$).

Energy conservation tells us that for a straight dislocation

$$\mathbf{f}_{\text{glide}} \cdot (\mathbf{x}_{\text{f}} - \mathbf{x}_{\text{i}})) = (\mathbf{g} \cdot (\mathbf{x}_{\text{f}} - \mathbf{x}_{\text{i}}))(\mathbf{g} \cdot ((\mathbf{b} \cdot \boldsymbol{\sigma}) \times \boldsymbol{\xi})) \;=\; E(v) - E_0 + W_{\text{dissipation}} \tag{4.207}$$

We can convert the above to an ordinary differential equation:

$$m\frac{dv}{dt} \;=\; f_{\text{glide}} + f_{\text{dissipation}} \tag{4.208}$$

$f_{\text{dissipation}}$ consists of lattice friction (section 4.6), solute drag (section 4.10), and phonon drag, where

$$f_{\text{dissipation/phonon}} \;=\; -Bv \tag{4.209}$$

with

$$B \;=\; B_0 + \frac{B_1 k_{\text{B}} T}{\omega_{\text{Debye}}\Omega}. \tag{4.210}$$

where $B_0$ is phonon emission (1-phonon process) and $B_1$ is phonon scattering (2-phonon process). The linear scaling with temperature of the phonon scattering process is due to the fact that the higher the phonons, the more phonons there are per volume and the more phonon "raindrops" would bounce off the moving dislocation.

If we have an edge dislocation initially lined along $\boldsymbol{\xi}_0 = \mathbf{e}_x$, with $\mathbf{b} = b\mathbf{e}_y$, under shear stress $\sigma_{yz}$, then

$$\mathbf{b} \cdot \boldsymbol{\sigma} \;=\; b\sigma_{yz}\mathbf{e}_z \tag{4.211}$$

$$(\mathbf{b}\cdot\boldsymbol{\sigma})\times\boldsymbol{\xi}_0 \;=\; b\sigma_{yz}\mathbf{e}_y \;=\; \mathbf{f}_{\text{glide}} \tag{4.212}$$

Then for a gentle variation in the dislocation profile $y(x)$:

$$\left|\frac{dy}{dx}\right| \;\ll\; 1 \tag{4.213}$$

the equation of motion would read:

$$m\frac{d^2y}{dt^2} \;=\; b\sigma_{yz} + \eta\frac{d^2y}{dx^2} - b\tau_{\text{LatticeFriction}} - B\frac{dy}{dt} + f_{\text{fluctuation}} \tag{4.214}$$

The LHS is "inertial". On the RHS, the first term is Peach-Koehler, the 2nd term is line tension, the 3rd term is from atomic nature of lattice, the 4th term is from phonon scattering, and the 5th term is the random thermal force fluctuation (Langevin equation), usually modelled as white noise

$$\langle f_{\text{fluctuation}}(t) f_{\text{fluctuation}}(t')\rangle \;\propto\; \frac{\delta(t-t')}{dl} \tag{4.215}$$

where all the forces above are averaged over segement length $dl$.

## 4.8 Crystallographic Effects

From (4.168), we see the cost of creating a dislocation scales with $b^2$. Thus, whenever possible, the dislocation tends to split into the smallest crystallographic unit. Also, if the interplanar spacing $d_0$ is large, one tends to have smaller shear moduli. So to minimize the cost of dislocation $\mu b^2$, the preferred slip system tend to have (a) the smallest Burgers vector, and (b) the widest planar spacing. (a) and (b) are in fact not unrelated, because the smallest Burgers vector tend to occur on in the closest packing plane. But since the atomic density (a scalar) is the same no matter which planes and corresponding normal direction we count, the *closest packing plane* also tends to be the *loosest stacking plane*. All these point to choice of slip plane with the largest $d_0$ and smallest $b$.

Thus, in HCP metals, when the $c/a$-ratio is significantly smaller than the ideal value of $\sqrt{8/3} = 1.633$, like in Ti and Zr, the prismatic slip $\{10\bar{1}0\}\langle 1\bar{2}10\rangle$ is triggered, instead of basal slip $\{0001\}\langle 1\bar{2}10\rangle$.

The above logic naturally leads to Shockley partials. Assuming $G$ is isotropic in plane (it is

if the plane has 3-fold symmetry), the **Frank's rule** says that whenever

$$\mathbf{b}_1 \;=\; \mathbf{b}_2 + \mathbf{b}_3, \quad |\mathbf{b}_1|^2 \;>\; |\mathbf{b}_2|^2 + |\mathbf{b}_3|^2 \tag{4.216}$$

the $\mathbf{b}_1$ dislocation can reduce its energy by splitting into a $\mathbf{b}_2$ dislocation separated some distance from the $\mathbf{b}_3$ dislocation.

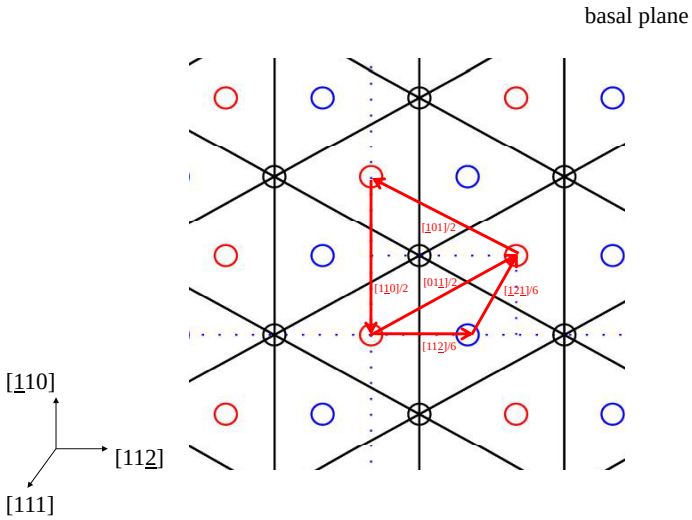


Figure 4.2: Looking down onto the (111) plane.

Consider (111) plane. The normal of this plane is $\mathbf{n} = [111]/(\sqrt{3}a_0)$. To orient ourselves (see Fig.4.2), we can take

$$\mathbf{e}_{x'} \;=\; \frac{[11\bar{2}]}{\sqrt{6}a_0}, \quad \mathbf{e}_{y'} \;=\; \frac{[\bar{1}10]}{\sqrt{2}a_0}, \quad \mathbf{e}_{z'} \;=\; \frac{[111]}{\sqrt{3}a_0} \tag{4.217}$$

we can check that $\mathbf{e}_{x'} \times \mathbf{e}_{y'} = \mathbf{e}_{z'}$. On this plane, there are six full Burgers vectors:

$$\mathbf{b}_1 \;\equiv\; \frac{[01\bar{1}]}{2}, \quad \mathbf{b}_2 \;\equiv\; \frac{[\bar{1}01]}{2}, \quad \mathbf{b}_3 \;\equiv\; \frac{[1\bar{1}0]}{2}, \tag{4.218}$$

and $-\mathbf{b}_1$, $-\mathbf{b}_2$, $-\mathbf{b}_3$. Generally,

$$\boldsymbol{\epsilon}^{\text{unsymmetrized}}_{\text{inelastic}} \;=\; \frac{A_{\text{slip}}\mathbf{n}\mathbf{b}^T}{V} \tag{4.219}$$

where $V$ is the total same volume, $A_{\text{slip}}$ is how much area has slip occurred on this slip plane,

and the superscript "unsymmetrized" means we have not carried out the symmetrization process in computing strain:

$$\boldsymbol{\epsilon}_{\text{inelastic}} \;=\; \frac{\boldsymbol{\epsilon}^{\text{unsymmetrized}}_{\text{inelastic}} + (\boldsymbol{\epsilon}^{\text{unsymmetrized}}_{\text{inelastic}})^T}{2}. \tag{4.220}$$

So $(\mathbf{n}, -\mathbf{b})$ are often considered to be a different slip system from $(\mathbf{n}, \mathbf{b})$.

Bruce Lee: *Now you put water in a cup, it becomes the cup; You put water into a bottle it becomes the bottle; You put it in a teapot it becomes the teapot. Now water can flow or it can crash. Be water, my friend.* One needs 5 indepedent slip systems to be able to deform arbitrarily.

The point here is that

$$\mathbf{b}_1 \;=\; \mathbf{b}_{\text{p1}} + \mathbf{b}_{\text{p2}}, \tag{4.221}$$

where the partial dislocations

$$\mathbf{b}_{\text{p1}} \;=\; \frac{[11\bar{2}]}{6}, \quad \mathbf{b}_{\text{p2}} \;=\; \frac{[\bar{1}2\bar{1}]}{6} \tag{4.222}$$

Since

$$|\mathbf{b}_{\text{p1}}|^2 \;=\; |\mathbf{b}_{\text{p2}}|^2 \;=\; \frac{a_0^2}{6}, \tag{4.223}$$

we have

$$|\mathbf{b}_{\text{p1}}|^2 + |\mathbf{b}_{\text{p2}}|^2 \;=\; \frac{a_0^2}{3} \tag{4.224}$$

which is smaller than

$$|\mathbf{b}_1|^2 \;=\; \frac{a_0^2}{2}. \tag{4.225}$$

Thus, two partials, separated far away, would have smaller energy than a full dislocation. In reality, they will not separate infinitely far apart because of the stacking fault ribbon they generated. Roughly speaking, the reduction in elastic energy is proportional to

$$\propto \;\; \frac{G\Delta(b^2)}{4\pi} \ln \frac{s}{\tilde{R}_0} \tag{4.226}$$

where $s$ is the splitting separation between the two partials, so the total energy is like

$$E \;=\; -\frac{G\Delta(b^2)}{4\pi} \ln \frac{s}{\tilde{R}_0} + s\gamma_{\text{ISF}}, \tag{4.227}$$

where $\gamma_{\rm ISF}$ is the intrinsic stacking fault energy. So the equilibrium splitting distance scales as

$$s_{\rm eq} \;=\; \frac{G\Delta(b^2)}{4\pi\gamma_{\rm ISF}}. \tag{4.228}$$

For low-stacking fault FCC crystal like pure Cu, $\gamma_{\rm ISF} = 40$ mJ/m$^2$, the splitting distance is large, like $s = 2$nm. For high-stacking fault FCC crystal like pure Al, $\gamma_{\rm ISF} = 160$ mJ/m$^2$, the splitting distance is small, like $s = 4$Å. This has severe consequences on the dislocation dynamics. For example, it is much more difficult for screw dislocations in Cu to cross-slip, because in order to do so, it must first constrict. But a widely separated ribbon would make the energy barrier for constriction larger.

The so-called Thompson tetrahedron describes the arrangement of full and partial Burgers vectors on slip planes. There are four faces (ABC$\delta$, BCD$\alpha$, CDA$\beta$, DAB$\gamma$, the last Greek letter is the center of each equilateral triangle), representing the {111} planes. Clearly, if we want to have $\overrightarrow{\rm DA}$ slip on DAB$\gamma$ slip plane, we can go:

$$\overrightarrow{\rm DA} \;=\; \overrightarrow{\rm D\gamma} + \overrightarrow{\gamma\rm A} \tag{4.229}$$

or

$$\overrightarrow{\rm DA} \;=\; \overrightarrow{\gamma\rm A} + \overrightarrow{\rm D\gamma} \tag{4.230}$$

where $\overrightarrow{\rm DA} \equiv {\rm A} - {\rm D}$ denotes the translation direction of the top block versus the bottom block across the slip plane ($\gamma_1$). The order of the decomposition matters, as one moves from $\Delta = 0$ region across the dislocation core, to the $\Delta = \overrightarrow{\rm DA}$ region. Only one choice among (4.229), (4.230) would be allowed. For (4.229), the atom at D site in the top block would be translated to

$${\rm D} + \overrightarrow{\rm D\gamma} \;=\; \gamma \tag{4.231}$$

at the intermediate state. For (4.230), the atom at D site in the top block would be translated to

$${\rm D} + \overrightarrow{\gamma\rm A} \tag{4.232}$$

which is also a crystallographic site. The key question here is whether $\gamma$ or ${\rm D} + \overrightarrow{\gamma\rm A}$ is on top of a - site, or on top of an $\bigcirc$ site. The former (intrinsic stacking fault) is the much lower in energy than the latter on-top configuration. Since $\gamma$ is on top of C when we look down on the DAB$\gamma$ plane of a Thompson's tetrahedron, we can determine that (4.230) is always right, when we perceive DAB$\gamma$ to be the top (+) plane. There is no $\mathbf{b}_{\rm p} \leftrightarrow -\mathbf{b}_{\rm p}$ symmetry in FCC or HCP crystals.

The Lomer-Cottrell (LC) lock is formed by the following reaction:

$$\frac{[11\bar{2}]_{(111)}}{6} + \frac{[\bar{1}\bar{2}1]_{(\bar{1}11)}}{6} \;=\; \frac{[0\bar{1}\bar{1}]}{6} \equiv \mathbf{b}_{\mathrm{LC}}, \tag{4.233}$$

since

$$\frac{a_0^2}{6} + \frac{a_0^2}{6} \;>\; \frac{a_0^2}{18}. \tag{4.234}$$

However, note that $\mathbf{b}_{\mathrm{LC}} = \frac{[0\bar{1}\bar{1}]}{6}$ is not our usual Burgers vector. Slip by $\frac{[0\bar{1}\bar{1}]}{6}$ on *any* atomic plane is likely to creates a very high energy stacking fault. Furthermore, there is another fundamental conflict if the Lomer-Cottrell dislocation is to move by glide. Note that by the way LC is formed, its line direction $\boldsymbol{\xi}_{\mathrm{LC}}$ must be a common direction on both (111) and $(\bar{1}11)$ planes, namely $\boldsymbol{\xi}_{\mathrm{LC}} \parallel [111] \times [\bar{1}11] \parallel [01\bar{1}]$. However, $\mathbf{b}_{\mathrm{LC}} = \frac{[0\bar{1}\bar{1}]}{6}$ does not belong to either (111) or $(\bar{1}11)$ "old" planes. It does belong to the $(11\bar{1})$ and $(\bar{1}1\bar{1})$ "new" planes, but $\boldsymbol{\xi}_{\mathrm{LC}}$ does not belong to these "new" planes. Thus, there is no $\{111\}$ plane where the LC dislocation could move as edge dislocation. That plane should be $\boldsymbol{b}_{\mathrm{LC}} \times \boldsymbol{\xi}_{\mathrm{LC}} = (100)$, but this cube plane is unusual for slip. For this reason, the Lomer-Cottrell dislocation is called "sessile", or "lock" or "junction", meaning it is a low-energy trap state, but once formed, it would be difficult to move. The LC dislocations are important for dislocation storage and forest dislocation hardening in FCC metals. [2]

## 4.9 Shear-Cleavage Competition

In above we have been talking about shear, i.e. bond switching, where there is transient loss of coordination for the atoms involved, but over long timescale no net loss of total coordination (or very little). This is fundamentally different from the cleavage process, where there is often irreversible loss of metal-metal coordination [3] Shear and cleavage are the two fundamental categories of inelastic events inside the solid. For small elastic deformation, they are roughly characterized by $G$ and $B$, respectively. Then for ideal strength calculation, there is no formal distinction, but practially the tensile and shear ideal strength and strains can be used to characterize the intrisic brittleness of materials [39, 36]. But for large nonlinear inelasticity, the inelastic shear and inelastic cleavage are very different. The metal-metal

[2] It is not impossible to move, or at least remove LC dislocations, however, if we consider dislocation reactions under stress, or dislocation climb.

[3] Imagine, that, once two metal surfaces are opened by the Griffith process [56], the metal surfaces are passivated by oxygen, and one cannot recover the metal-metal coordination even if the crack is closed later.

bond switching is a reversible source of dissipation: an arrays of bond switched this way can be reswitched later, converting mechanical energy to heat many many times. But if there is a loss of coordination, for example by voiding and surface creation, then this can only be used one time. For this reason, metals which are shear soft have a larger fracture toughness, because the soft shear entices the shear relaxation again and again. Bonding shearing is a *sustainable* way of dissipating energy, whereas cleavage is basically a one-off thing.

Just like the Frenkel relation for shear, there is a popular form for fitting decohesion called Universal Binding Energy Relation (UBER)[57]. The details are not that important, the key is that $e_{\mathrm{b}}(\epsilon_{\mathrm{hydro}})$ is not a periodic function, but is a function with a minimum, followed by a turning point where the 2nd derivative vaishes. So $\sigma_{\mathrm{hydro}}(\epsilon_{\mathrm{hydro}})$ has a maximum, then decays to zero as $\epsilon_{\mathrm{hydro}} \to 0$. Also, it can be shown that to separate a material, the best way is to localize the bond cutting on one plane. In other words, consider a crystal with $10^{24}$ atoms, thus $10^8$ planes on each side. It takes only cutting the bonds on one plane out of the $10^8$ to achieve separation. Brittle ceramics basically do this. It turns out that metals are wily, and do not fall for this generally. It takes a whole lot of bond shearing in metals before one coordination loss is achieve in metals, by for instance dislocation emission in front of the crack tip.

Having reconciled the $\sigma_{\mathrm{shear}}^{\mathrm{ideal}} = 2\mathrm{GPa}$ for Mg vesus the measured CRSS = 0.35 MPa for Mg (Basically dislocation is like a lever, that breaks bond in its core, and then restitches them back together), I would like to mention an interesting possibility of elastic strain engineering [58, 59]. All physical properties are function of the elastic strain. Because "smaller is stronger", nanostructured materials such as nanowires, nanotubes, nanoparticles, thin films, atomic sheets etc. can dynamically withstand non-hydrostatic (e.g. tensile and shear) stresses up to a significant fraction of its ideal strength without inelastic relaxation by plasticity or fracture. For example, large elastic strains can be generated by epitaxy in thin films, or by static or dynamical external loading on small-volume materials, and can be spatially homogeneous or inhomogeneous. This leads to new possibilities for tuning the physical and chemical (e.g. electronic, optical, magnetic, phononic, catalytic, etc.) properties of a material, by varying the 6-dimensional elastic strain as continuous variables. By controlling the elastic strain field statically or dynamically, one opens up a much larger parameter space (probably on par with chemical alloying) for optimizing functional properties of materials, imparting a new meaning to Feynman's statement "there's plenty of room at the bottom".

## 4.10 Dislocation-Point Defect Coupling

When point defects are mobile, they would be able to respond to fields. In the case of electric field, we have seen how mobile charge defects can screen out any imposed electric field **completely** given sufficient time and space to do so, which is the property of an **electrolyte**. This is because a point defect carries charge monopole that couples to the electric potential as $-\nabla(z_i e\phi)$. The same thing can happen to an imposed stress, as (3.96) show us that there is a driving force $-\nabla(-\mathrm{Tr}(\boldsymbol{\sigma}^{\mathrm{ext}}(\mathbf{x})\boldsymbol{\omega}^{\mathrm{R}}\Omega))$ for indiviual (isolated) point defects to move in the interior. Suppose $\boldsymbol{\omega}^{\mathrm{R}}$ is identity matrix, then $\mathrm{Tr}(\boldsymbol{\sigma}^{\mathrm{ext}}(\mathbf{x}))$ plays the role of $\phi$, and the mobile defects would completely screen out internal pressure gradient, if given sufficient time and space to do so. Also, point defects can **plate out** on surfaces and dislocation half-planes to give **uniaxial** transformation strain, even for isotropic vacancies (because when they plate out, they are densely packed ranks which has packing direction, and no longer isolated individuals).

Note that $\boldsymbol{\sigma}^{\mathrm{ext}}$ is in paralell position to scalar electric potential $\phi$ in the energy expression, not $\mathbf{E}$. ($\boldsymbol{\omega}^{\mathrm{R}}\Omega$ is similar to $q$). In electrolyte theory between two parallel plates, $\mathbf{E}$ is screened exponentially in the far-field, not $\phi$. So given infinite supply of point defects, the exponentially screened is not in the value of stress, but the **stress gradient** that can drive point-defect flux (like $\mathbf{E}$ that drives electrical current, which needs to be zeroed deep inside a bulk metal). Also, only certain component of the stress gradient can be screened by a certain type of point defect. For example, isotropic vacancy can only screen pressure gradient, but cannot do much to the shear stress. Therefore, Cottrell/Suzuki atmosphere of $\mathrm{V_{Cu}}$ may change the pressure distribution around a dislocation somewhat, but cannot really screen the $1/r$ screw dislocation-screw dislocation long-range interaction that is mediated by pure shear stress, nor can they screen the $1/r$ edge dislocation - screw dislocation interaction. Substitutional solutes like $\mathrm{Al_{Cu}}$ would be similar as they have isotropic $\boldsymbol{\omega}^{\mathrm{R}}\Omega$. Interstitial solutes like $\mathrm{H_{Cu}}$, $\mathrm{O_{Cu}}$, $\mathrm{C_{Cu}}$ may have somewhat richer behavior, but remember they can only screen flux-driving stress gradient component, but not necessarily stress. Another thing I should mention is that Cottrell/Suzuki atmosphere involve many-body interactions between point-defects, and not just between point-defect and dislocation, and such many-body entanglement can have more complex correlation effect beyond the mean-field "Debye"-type treatment. The treatment that follows are effective two-body simplification (even without the "Debye" screening), that I will further comment at the end.

Interstitials are very mobile. And radiation generates a lot of self-interstials. In addition to

hydrostatic component, they also possess several orientational variants, and therefore they would be able to screen out more stress components inside the solid. This is indeed the lesson we've learned from anelastic relaxation. This means therefore long-range dislocation-dislocation interactions can be partially screened by redistribution of point defects.

There are roughly speaking two kinds of point defect - dislocation coupling. One is long-ranged (LR), and one is short-ranged (SR), like solute segregation in the dislocation core. The LR coupling, which induces a "cloud" effect, changes the long-range interactions. The SR or coordination interaction changes dislocation mobility significantly. Suppose $b = a_0/\sqrt{2} = 2.556$Å as in copper, a LR intraction would be something like 200 lattice spacing away, or 50nm. SR interaction would be like 0, 1 or 2 lattice spacing away. For discussion below, it is also useful to define something called thermal-escape (TE) point-defect / dislocation distance, where the elastic interaction energy is significantly less than $k_{\mathrm{B}}T$. Suppose the vacancy relaxation volume is $v_{\mathrm{V}}^{\mathrm{R}} = 0.1\Omega = 1.18\text{Å}^3$, we have

$$\frac{k_{\mathrm{B}}T_{\mathrm{room}}}{v_{\mathrm{V}}^{\mathrm{R}}} \;=\; 3.5\mathrm{GPa}, \tag{4.235}$$

(A very useful number to keep in mind is $k_{\mathrm{B}}T_{\mathrm{room}}/\text{Å}^3 = 4.14$ GPa). Therefore, the hydrostatic stress of an edge dislocation

$$\frac{\sigma_{xx}+\sigma_{yy}+\sigma_{zz}}{3} \;=\; -\frac{\mu b(1+\nu)}{3\pi(1-\nu)}\frac{y}{x^2+y^2} \;\sim\; -\frac{\mu b}{5y} \tag{4.236}$$

we see that if the interaction energy is $0.01k_{\mathrm{B}}T$ which would only cause 1% change in population ($e^{-0.01} = 0.9900498$), $y \sim \frac{\mu b}{5\times 0.01\times 3.5\mathrm{GPa}} = 45/0.175 = 250b$. The thermal-escape range $r_{\mathrm{TE}}$ obviously belongs to LR, and can be used as a reference energy position for point defects. When point defects gets closer than $r_{\mathrm{TE}}$, we need continuum solution to consider their coupling, and if still closer, we need atomistics. $r_{\mathrm{TE}}$ is fortunately shorter than $\rho_{\mathrm{dislocation}}^{1/2}$ in most situations.

Imagine a RVE containing a mixed dislocation with

$$\boldsymbol{\xi} \;=\; \begin{bmatrix} 0 & 0 & 1 \end{bmatrix}, \quad \mathbf{b} \;=\; \begin{bmatrix} b_{\mathrm{e}} & 0 & b_{\mathrm{s}} \end{bmatrix} \tag{4.237}$$

and consider the RVE to be under a shear stress

$$\boldsymbol{\sigma} \;=\; \begin{pmatrix} 0 & 0 & \sigma_{xz} \\ 0 & 0 & 0 \\ \sigma_{xz} & 0 & 0 \end{pmatrix} \tag{4.238}$$

so

$$\mathbf{b}\cdot\boldsymbol{\sigma} \;=\; \begin{bmatrix} \sigma_{xz}b_{\mathrm{s}} & 0 & \sigma_{xz}b_{\mathrm{e}} \end{bmatrix} \tag{4.239}$$

and the Peach-Koehler force would be

$$(\mathbf{b}\cdot\boldsymbol{\sigma})\times\boldsymbol{\xi} \;=\; \begin{pmatrix} \mathbf{e}_x & \mathbf{e}_y & \mathbf{e}_z \\ \sigma_{xz}b_{\mathrm{s}} & 0 & \sigma_{xz}b_{\mathrm{e}} \\ 0 & 0 & 1 \end{pmatrix} \;=\; -\sigma_{xz}b_{\mathrm{s}}\mathbf{e}_y. \tag{4.240}$$

The above shows that shear stress (not necessarily normal stress) can drive dislocation climb.

In monatomic metal, we have previous derived

$$c_{\mathrm{V}}^{\circ}(T) \;=\; \frac{e^{-f_{\mathrm{V}}^{\mathrm{f}}(T)/k_{\mathrm{B}}T}}{\Omega} \tag{4.241}$$

by considering a free surface or a grain boundary "market" for atomoporosity. But with dislocations as markets, these 2D markets are not really necessary. One can consider trading atomoporosity directly with dislocation. The kinematics of the trading process is the following. For the dislocation above to move by $-\delta\mathbf{e}_y$, the branch-cut equation would give transformation strain-volume contribution from the core region:

$$\Delta\boldsymbol{\omega}^{\mathrm{R}}\Omega \;=\; \mathrm{Symmetrize}((dl\boldsymbol{\xi}\times(-\delta\mathbf{e}_y))\mathbf{b}) \;=\; \delta dl\,\mathrm{Symmetrize}(\mathbf{e}_x\mathbf{b}) \;=\; \delta dl\begin{pmatrix} b_{\mathrm{e}} & 0 & \frac{b_{\mathrm{s}}}{2} \\ 0 & 0 & 0 \\ \frac{b_{\mathrm{s}}}{2} & 0 & 0 \end{pmatrix} \tag{4.242}$$

and indeed this is the basis for deriving the Peach-Koehler force, both the coupling to the shear stress, and the normal strain response in the core region. However, it is noted that the $xx$ component cannot be accomplished without increasing atomoporosity within the RVE, so the total transformation strain-volume of the process is actually

$$\boldsymbol{\omega}^{\mathrm{R}}\Omega \;=\; \delta dl\begin{pmatrix} b_{\mathrm{e}} & 0 & \frac{b_{\mathrm{s}}}{2} \\ 0 & 0 & 0 \\ \frac{b_{\mathrm{s}}}{2} & 0 & 0 \end{pmatrix} + \frac{\delta dl b_{\mathrm{e}}}{\Omega}\times\boldsymbol{\omega}_{\mathrm{V}}^{\mathrm{R}}\Omega, \tag{4.243}$$

where $\frac{\delta dlb_{\rm e}}{\Omega}$ is the number of isolated vacancies that needs to be injected. If the above were accomplished by absorbing interstitials instead, then the corresponding transformation strain-volume of the RVE would be

$$\boldsymbol{\omega}^{\rm R}\Omega \;=\; \delta dl\begin{pmatrix} b_{\rm e} & 0 & \frac{b_{\rm s}}{2} \\ 0 & 0 & 0 \\ \frac{b_{\rm s}}{2} & 0 & 0 \end{pmatrix} - \Delta_{\rm i1}\boldsymbol{\omega}^{\rm R}_{\rm i1}\Omega - \Delta_{\rm i2}\boldsymbol{\omega}^{\rm R}_{\rm i2}\Omega - \Delta_{\rm i3}\boldsymbol{\omega}^{\rm R}_{\rm i3}\Omega, \quad \Delta_{\rm i1}+\Delta_{\rm i2}+\Delta_{\rm i3} = \frac{\delta dlb_{\rm e}}{\Omega}. \tag{4.244}$$

When the above processes occur at zero external stress, the above transformations can happen without penalty/reward, and the entropy-energy balance (same as the free-surface market) gives:

$$0 + \frac{\delta dlb_{\rm e}}{\Omega} \times \left(f^{\rm f}_{\rm V}(T) + k_{\rm B}T\ln X_{\rm V}\right) \;=\; 0 \tag{4.245}$$

Note that the $X^{\circ}_{\rm V}$ that we consider should be **outside the stress range** of the dislocation, since rigorously speaking a vacancy within the stress range of a dislocation is a (vacancy, dislocation) complex, and not an isolated vacancy. Thus, the market operates between the dislocation core and perfect crystal $r_{\rm TE} \sim 50$nm distance away from it.

But then, suppose there is **external stress $\boldsymbol{\sigma}$** added to both RVE and RVE', then things get interesting, and the total balance reads:

$$-\boldsymbol{\sigma} : \boldsymbol{\omega}^{\rm R}\Omega + \frac{\delta dlb_{\rm e}}{\Omega} \times \left(f^{\rm f}_{\rm V}(T) + k_{\rm B}T\ln X_{\rm V}\right) \;=\; 0 \tag{4.246}$$

so

$$c^{\rm eq}_{\rm V}(T) \;=\; c^{\circ}_{\rm V}(T)\exp\left(\frac{\boldsymbol{\sigma} : \boldsymbol{\omega}^{\rm R}\Omega}{\frac{\delta dlb_{\rm e}}{\Omega}k_{\rm B}T}\right) \tag{4.247}$$

The above is actually the most general expression and works for surfaces/dislocations/GBs. $\boldsymbol{\omega}^{\rm R}\Omega$ includes both the "core plating" part (which is uni-axial) and the isolated vacancy relaxation in the interior (which is tri-axial). If we take the (4.244) example, we get

$$\frac{\boldsymbol{\sigma} : \boldsymbol{\omega}^{\rm R}\Omega}{\frac{\delta dlb_{\rm e}}{\Omega}} \;=\; \frac{\Omega}{b_{\rm e}}\boldsymbol{\sigma} : \begin{pmatrix} b_{\rm e} & 0 & \frac{b_{\rm s}}{2} \\ 0 & 0 & 0 \\ \frac{b_{\rm s}}{2} & 0 & 0 \end{pmatrix} + \boldsymbol{\sigma} : \boldsymbol{\omega}^{\rm R}_{\rm V}\Omega \;=\; \frac{\Omega}{b_{\rm e}}(\sigma_{xx}b_{\rm e} + \sigma_{xz}b_{\rm s}) + \boldsymbol{\sigma} : \boldsymbol{\omega}^{\rm R}_{\rm V}\Omega \tag{4.248}$$

The first term is just the Peach-Koehler force we have derived time and again (now prorated to a single vacancy), and the second term is the hydrostatic coupling used for driving PDE. So essentially all we have done is to replace the free surface by the branch cut! For

interstitial, this stress biasing is

$$\frac{\boldsymbol{\sigma}:\boldsymbol{\omega}^{\mathrm{R}}\Omega}{\frac{\delta dlb_{\mathrm{e}}}{\Omega}} \;=\; \frac{\Omega}{b_{\mathrm{e}}}\boldsymbol{\sigma}:\begin{pmatrix} b_{\mathrm{e}} & 0 & \frac{b_{\mathrm{s}}}{2} \\ 0 & 0 & 0 \\ \frac{b_{\mathrm{s}}}{2} & 0 & 0 \end{pmatrix} - \boldsymbol{\sigma}:\boldsymbol{\omega}^{\mathrm{R}}_{\mathrm{i1}}\Omega \;=\; \frac{\Omega}{b_{\mathrm{e}}}(\sigma_{xx}b_{\mathrm{e}}+\sigma_{xz}b_{\mathrm{s}}) - \boldsymbol{\sigma}:\boldsymbol{\omega}^{\mathrm{R}}_{\mathrm{i1}}\Omega \qquad (4.249)$$

and there needs to be an extra - factor if put inside the exponential, since we would be pro-rating to **adding** an i1.

Suppose one is in an out-of-equilibrium situation, where the actual $c_{\mathrm{V}}$ in surrounding RVE's are smaller than the $c_{\mathrm{V}}^{\mathrm{eq}}$, then the net thermodynamic benefit for the $-\delta\mathbf{e}_y$ climb would be

$$\frac{\delta dlb_{\mathrm{e}}}{\Omega}k_{\mathrm{B}}T\ln\frac{c_{\mathrm{V}}^{\mathrm{eq}}}{c_{\mathrm{V}}} \;\equiv\; -\delta dl f_{\mathrm{climb}} \qquad (4.250)$$

so

$$f_{\mathrm{climb}} \;\equiv\; \frac{b_{\mathrm{e}}}{\Omega}k_{\mathrm{B}}T\ln\frac{c_{\mathrm{V}}}{c_{\mathrm{V}}^{\mathrm{eq}}} \;=\; \frac{b_{\mathrm{e}}k_{\mathrm{B}}T}{\Omega}\ln\frac{c_{\mathrm{V}}}{c_{\mathrm{V}}^{\circ}} - \frac{b_{\mathrm{e}}}{\Omega}\boldsymbol{\sigma}:\boldsymbol{\omega}^{\mathrm{R}}_{\mathrm{V}}\Omega - (\sigma_{xx}b_{\mathrm{e}}+\sigma_{xz}b_{\mathrm{s}}) \qquad (4.251)$$

The last term is the familiar Peach-Koehler force. The first term is defined as **osmotic force** on climb. The second term is due to the internal stress effect on vacancy formation **Gibbs free energy** which would show up regardless of vacancy source.

To appreciate how large the osmotic force is, we know that

$$\frac{k_{\mathrm{B}}T_{\mathrm{room}}}{\mathring{\mathrm{A}}^{3}} \;=\; 4.14\mathrm{GPa} \qquad (4.252)$$

so with $\Omega = 11.8\mathring{\mathrm{A}}^{3}$ in Cu, we get

$$\frac{k_{\mathrm{B}}T_{\mathrm{room}}}{\Omega} \;=\; 350\mathrm{MPa} \qquad (4.253)$$

so with $\frac{c_{\mathrm{V}}}{c_{\mathrm{V}}^{\circ}} = 2$, we will need the equivalence of 243 MPa of Peach-Koehler force to balance the osmotic force that would otherwise drive the edge dislocation "up" in $y$. So this is not a small effect.

If $\sigma_{xx} = 0$, then we are lucky because $\boldsymbol{\omega}^{\mathrm{R}}_{\mathrm{V}}$ does not couple to shear stress, and the third term vanishes. Then

$$f_{\mathrm{climb}} \;=\; \frac{b_{\mathrm{e}}k_{\mathrm{B}}T}{\Omega}\ln\frac{c_{\mathrm{V}}}{c_{\mathrm{V}}^{\circ}} - \sigma_{xz}b_{\mathrm{s}} \qquad (4.254)$$

which agrees with (15-77) to (15-80) of [35]. The only nitpick would be that I would call $F_{\mathrm{el}}$

in (15-77) of [35] $F_{\text{mechanical}}$, since this term derives from the inelastic "plating" operation performed on the branch cut!

But it turns out even if the vacancy feel the interaction stress with the dislocation, the formalism do not change. From the market trading virtual work, we can rewrite

$$f_{\text{climb}} \equiv \frac{b_{\text{e}}k_{\text{B}}T}{\Omega}\ln\frac{c_{\text{V}}}{c_{\text{V}}^{\circ}} - \frac{b_{\text{e}}}{\Omega}\boldsymbol{\sigma}(\mathbf{x}) : \boldsymbol{\omega}_{\text{V}}^{\text{R}}\Omega - (\sigma_{xx}b_{\text{e}} + \sigma_{xz}b_{\text{s}}) \tag{4.255}$$

where $\boldsymbol{\sigma}(\mathbf{x})$ includes both the externally applied stress, and the stress of the dislocation on RVE'. That is, the atomoporosity is created under the influence of the pre-existing dislocation stress field, and this describes the interaction energy. Note however, that we can combine the first and second term as:

$$f_{\text{climb}} \equiv \frac{b_{\text{e}}k_{\text{B}}T}{\Omega}\ln\frac{\tilde{c_{\text{V}}}(\boldsymbol{\sigma})}{c_{\text{V}}^{\circ}} - (\sigma_{xx}b_{\text{e}} + \sigma_{xz}b_{\text{s}}) \tag{4.256}$$

and it is $\tilde{c_{\text{V}}}(\boldsymbol{\sigma})$ that drives diffusion equation in any case. So we would get the same result to leading order.

Now consider this market to be highly efficient, so the dislocation can shed vacancies and climb to a position with surrounding RVE's that has

$$f_{\text{climb}} = 0 \quad \rightarrow \quad \frac{c_{\text{V}}}{c_{\text{V}}^{\circ}} = \exp\left(\frac{\sigma_{xz}b_{\text{s}}\Omega}{b_{\text{e}}k_{\text{B}}T}\right). \tag{4.257}$$

This is assuming SR process is efficient relative to LR transport. (not necessarily true always) But far field has just $c_{\text{V}} = c_{\text{V}}^{\circ}$ because they were not aware of this dislocation (and the opposite dislocation in a dipole, for simplicity let us assume that one is pinned somehow). Then, we can use cylindrical coordinate to solve the **LR transport limited** climb rate:

$$r^{-1}\partial_r(rD_{\text{V}}\partial_r c_{\text{V}}) = 0 \tag{4.258}$$

The above has some assumptions: (a) there is no stress gradient, and (b) we are assuming that even though the center is translating, this translation has no effect on the diffusion equation. As a general remark, the flux expression changes from **crystal lattice frame**:

$$\mathbf{J} = c_{\text{V}}M_{\text{V}}(-\nabla k_{\text{B}}T\ln c_{\text{V}}) \tag{4.259}$$

upon Galileo transformation $t' = t, \mathbf{x}' = \mathbf{x} - \mathbf{v}t$, to

$$\mathbf{J}' \;=\; c_{\mathrm{V}} M_{\mathrm{V}}(-\nabla k_{\mathrm{B}} T \ln c_{\mathrm{V}}) - c_{\mathrm{V}}\mathbf{v} \tag{4.260}$$

We note that $\mathbf{v}$ is supported by vacancy diffusion, and the rate is proportional to $c_{\mathrm{V}}^{\circ}$, so the 2nd term is actually proportional to $(c_{\mathrm{V}}^{\circ})^2$. Thus, **in the dilute vacancy limit, the effect of Galileo transformation on the diffusion equation can be ignored.**

Thus, we derive a steady-state (but out-of-equilibrium) vacancy distribution of

$$-2\pi r D_{\mathrm{V}} \partial_r c_{\mathrm{V}} \;=\; \frac{v_{\mathrm{climb}} b_{\mathrm{e}}}{\Omega} \tag{4.261}$$

and so

$$c_{\mathrm{V}}(r) \;=\; c_{\mathrm{V}}(R) + \frac{v_{\mathrm{climb}} b_{\mathrm{e}}}{2\pi D_{\mathrm{V}} \Omega} \ln \frac{R}{r_{\mathrm{TE}}} \tag{4.262}$$

We have the customary divergence problem at both small $r$ and large $R$ again! These dislocation lines are real divas.

If we identify $c_{\mathrm{V}}(r)$ as

$$c_{\mathrm{V}}(r) \;=\; \exp\left(\frac{\sigma_{xz} b_{\mathrm{s}} \Omega}{b_{\mathrm{e}} k_{\mathrm{B}} T}\right) c_{\mathrm{V}}^{\circ} \tag{4.263}$$

and $c_{\mathrm{V}}(R)$ as $c_{\mathrm{V}}^{\circ}$, and also assuming

$$\frac{\sigma_{xz} b_{\mathrm{s}} \Omega}{b_{\mathrm{e}} k_{\mathrm{B}} T} \;\ll\; 1 \tag{4.264}$$

we can derive the standard climbing rate law:

$$v_{\mathrm{climb}} \;=\; \frac{2\pi D_{\mathrm{V}} \Omega}{b_{\mathrm{e}} \ln \frac{R}{r_{\mathrm{TE}}}} c_{\mathrm{V}}^{\circ} \frac{\sigma_{xz} b_{\mathrm{s}} \Omega}{b_{\mathrm{e}} k_{\mathrm{B}} T} \;=\; (\sigma_{xz} b_{\mathrm{s}}) \times \frac{2\pi D_{\mathrm{V}} c_{\mathrm{V}}^{\circ} \Omega^2}{b_{\mathrm{e}}^2 k_{\mathrm{B}} T \ln \frac{R}{r_{\mathrm{TE}}}} \tag{4.265}$$

The latter object is defined as the **climbing mobility** (but note this mobility is long-range diffusion controlled, not short-range reaction controlled)

$$M_{\mathrm{climb}} \;=\; \frac{2\pi D_{\mathrm{V}} c_{\mathrm{V}}^{\circ} \Omega^2}{b_{\mathrm{e}}^2 k_{\mathrm{B}} T \ln \frac{R}{r_{\mathrm{TE}}}} \;=\; \frac{2\pi D^{*} \Omega}{b_{\mathrm{e}}^2 k_{\mathrm{B}} T \ln \frac{R}{r_{\mathrm{TE}}}} \tag{4.266}$$

where we identify $c_{\mathrm{V}}^{\circ} \Omega D_{\mathrm{V}} = X_{\mathrm{V}}^{\circ} \Omega D_{\mathrm{V}}$ as the self- or tracer diffusivity (which is directly measurable, unlike $D_{\mathrm{V}}$ itself).

In solving the above diffusion equation, we ignored (a) vacancy-vacancy interactions ("Debye screening" effect), (b) vacancy-dislocation stress term, and (c) transport resistance from SR to $r_{\rm TE}$. Now let us try to add these effects back, by talking about what happens when a vacancy gets inside $r_{\rm TE}$. When we examine (a) and (b), it is like adding an effective potential $U(\mathbf{x})$ to the diffusion potential of a single vacancy

$$\mu_{\rm V}(\mathbf{x}) \;=\; k_{\rm B}T\ln X_{\rm V}(\mathbf{x}) + U(\mathbf{x}) \tag{4.267}$$

the $k_{\rm B}T\ln X_{\rm V}(\mathbf{x})$ term is the thermodynamic entropy term, the second term is the mechanical work term that includes both self-interaction and external stress-vacancy interaction. The diffusion flux in the PDE is

$$\mathbf{J}_{\rm V} = c_{\rm V}M_{\rm V}(-\nabla\mu_{\rm V}) \;=\; -c_{\rm V}M_{\rm V}(k_{\rm B}Tc_{\rm V}^{-1}\nabla c_{\rm V} + \nabla U(\mathbf{x})) \;=\; -M_{\rm V}k_{\rm B}T\nabla c_{\rm V} - c_{\rm V}M_{\rm V}\nabla U(\mathbf{x}) \tag{4.268}$$

Before we suddenly increase the externally applied stress and the Peach-Koehler mechanical driving force $\Delta{\rm PK} \equiv \sigma_{xx}^{\rm ext}b_{\rm e} + \sigma_{xz}^{\rm ext}b_{\rm s}$, there is already self-equilibrating $U(\mathbf{x}) = U_0(\mathbf{x})$, $c_{\rm V}(\mathbf{x})$ and $\mathbf{J}_{\rm V} = 0$, i.e. at equilibrium. With the additional $U(\mathbf{x}) = U_0(\mathbf{x}) + \delta U$ inside the PDE where $\delta U = -{\rm Tr}(\boldsymbol{\sigma}^{\rm ext}\boldsymbol{\omega}^{\rm R}\Omega)$, therefore,

$$\mathbf{J}_{\rm V} = 0+\delta\mathbf{J}_{\rm V} \;=\; -M_{\rm V}k_{\rm B}T\nabla\delta c_{\rm V} - c_{\rm V}M_{\rm V}\nabla\delta U - \delta c_{\rm V}M_{\rm V}\nabla U_0 \;=\; -M_{\rm V}k_{\rm B}T\nabla\delta c_{\rm V} - \delta c_{\rm V}M_{\rm V}\nabla U_0, \tag{4.269}$$

where the first term is no different from without (a),(b), the second term is zero for uniform external stress. Let us define effective concentration

$$\tilde{c} \;\equiv\; (\delta c_{\rm V})e^{\frac{U_0}{k_{\rm B}T}} \tag{4.270}$$

we then have

$$\mathbf{J}_{\rm V} \;=\; -M_{\rm V}k_{\rm B}Te^{-\frac{U_0}{k_{\rm B}T}}\nabla\tilde{c} \tag{4.271}$$

and since

$$\partial_t(\delta c_{\rm V}) \;=\; -\nabla\cdot\mathbf{J}_{\rm V} \;=\; \nabla\cdot M_{\rm V}k_{\rm B}Te^{-\frac{U_0}{k_{\rm B}T}}\nabla\tilde{c} \;=\; \partial_t(\tilde{c}e^{-\frac{U_0}{k_{\rm B}T}}) \tag{4.272}$$

there is

$$\partial_t\tilde{c} \;=\; e^{\frac{U_0}{k_{\rm B}T}}\nabla\cdot M_{\rm V}k_{\rm B}Te^{-\frac{U_0}{k_{\rm B}T}}\nabla\tilde{c} = M_{\rm V}k_{\rm B}T(\nabla^2\tilde{c} - \frac{\nabla U_0\cdot\nabla\tilde{c}}{k_{\rm B}T}) \tag{4.273}$$

which gracefully recovers to the equation without (a),(b) effects at large $\mathbf{x}$. Furthermore, at steady state, we just have

$$2\pi r D_{\rm V}e^{-\frac{U_0(r)}{k_{\rm B}T}}\partial_r\tilde{c}(r) \;=\; {\rm const} \tag{4.274}$$

It is basically saying that mass diffusivity is not a constant near the core. But as we have seen before, this modification effect is really quite small for vacancies.

Thus, even though the system has (a),(b), because we start the external stress jump from an already self-equilibrated system, the diffusion equation for $\delta c_{\mathrm{V}}$ is not much different from the reference system without (a),(b). Therefore, to include (c), all we need to do is to add the transport impedance from SR to $r_{\mathrm{TE}}$, and we get

$$M_{\mathrm{climb}} \;=\; \frac{2\pi D_{\mathrm{V}} c_{\mathrm{V}}^{\circ} \Omega^2}{b_{\mathrm{e}}^2 k_{\mathrm{B}} T \ln \frac{R}{r_{\mathrm{TE}}}} \;=\; \frac{2\pi D^* \Omega}{b_{\mathrm{e}}^2 k_{\mathrm{B}} T \ln \frac{R}{R_0}} \tag{4.275}$$

where $R_0$ is on the order of $b$.

Next, we employ the usual trick-of-hat that

$$\frac{\ln \frac{R}{R_0}}{4\pi} \;\equiv\; \alpha \tag{4.276}$$

with $\alpha$ likely ranging between 0.5 and 1, and very insensitive to the choice of $R$ and $r$. So we end up with

$$M_{\mathrm{climb}} \;=\; \frac{D^* \Omega}{2\alpha b_{\mathrm{e}}^2 k_{\mathrm{B}} T} \tag{4.277}$$

which agrees with equation (15-91) of ([35]), if we take $\alpha = \frac{1}{2}$. The above equation looks very similar to the fluctuation-dissipation theorem, where one relates random-walk kind of "diffusivity" with driven "mobility" for the defect. This kind of random-walk formula also applies to other extended defects like grain boundaries.[60] Indeed grain boundaries can be thougt of as regularly spaced dislocations.

In radiation damage, we create a lot of interstitials. These interstials interact with each other strongly, and since they have high mobility, they will aggregate into plates. When the plates are small, we have a nucleation problem of Frank loop by point defect aggregation, that can later be unfaulted into a stacking fault tetrahedron. [61]

# Chapter 5

# Interfaces

Interfaces such as grain boundaries, phase boundaries (free surface is the phase boundary between condensed and vapor phase), stacking faults, domain walls are locations where 3D order parameter field (phase field) sustains a finite jump. They are **extended defects** like the dislocations, and therefore do not have an equilibrium distribution. In other words, they must be produced as a cause of dissipative processes (mechanical work done, radiation, thermal quench) that gives rise to emergent behavior.

## 5.1 Interfacial Segregation

Gibbs developed the theory of chemical potential for homogeneous 3D phases in 1870s at Yale, but he also thought about the problem of interfaces very carefully. At his time there was no instrument that could directly visualize the atoms in the interface. But by the power of imagination Gibbs developed the concept of **interfacial excesses** and Gibbs Adsorption Equation.

Gibbs developed the theory for interface between $\alpha, \beta$ phases under the following assumptions: (a) spatial inhomogeneity only exists near the physical interface region, which is very thin; away from the interfaces, both phases are homogeneous with particle concentrations $\mathbf{c}^\alpha$ and $\mathbf{c}^\beta$, respectively. (b) both $\alpha$ and $\beta$ are fluid phases that can only sustain hydrostatic pressures. Away from the physical interface region, the hydrostatic pressures are $P^\alpha$ and $P^\beta$, respectively.

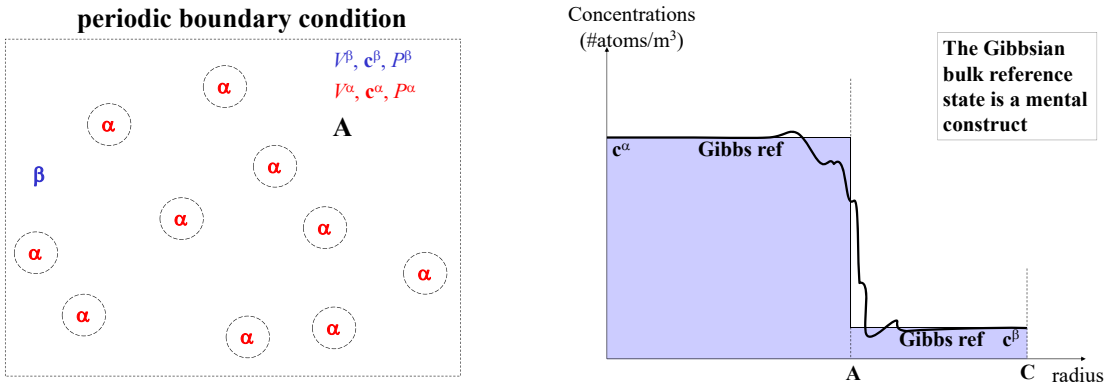


(a) (b)

Figure 5.1: Gibbs excess.

The Gibbs interfacial excess is defined by (a) consider a cutout region $\mathbf{C}$: the cutout exists in mind only and not in reality. Or we could consider periodic bondary condition (PBC), where the $\alpha$ phase is encased in $\beta$ phase matrix, so we can forget about free surfaces all together. (b) choose an arbitrary geometric partition surface $\mathbf{A}$ between $\alpha$ and $\beta$, as long as the arbitrary choice is consistently applied and near the physical interface region. Thus, we have volume partition $\mathbf{C} = V^\alpha + V^\beta$. The Gibbs bulk reference state is a state with $\mathbf{c}^\alpha V^\alpha + \mathbf{c}^\beta V^\beta$ particles, which is different from $\mathbf{N}$, what the system really has inside $\mathbf{C}$, as Fig. 5.1(b) illustrates. The difference is defined as the Gibbs excess:

$$\mathbf{N}^\alpha \equiv \mathbf{c}^\alpha V^\alpha, \quad \mathbf{N}^\beta \equiv \mathbf{c}^\beta V^\beta, \quad \mathbf{N} \equiv \mathbf{N}^\alpha + \mathbf{N}^\beta + \mathbf{N}^\gamma. \tag{5.1}$$

Note that $\mathbf{N}$ is real, but $\mathbf{N}^\alpha$ and $\mathbf{N}^\beta$ are not, and only serve in the bulk reference state. Define interfacial excesses:

$$E^\gamma \equiv E - E^\alpha(\mathbf{N}^\alpha, V^\alpha, S^\alpha) - E^\beta(\mathbf{N}^\beta, V^\beta, S^\beta) \tag{5.2}$$

$$S^\gamma \equiv S - S^\alpha - S^\beta \tag{5.3}$$

The point is that there is a unique mapping from $(\mathbf{N}, E, \mathbf{C}) \to (\mathbf{N}^\alpha, E^\alpha, V^\alpha) + (\mathbf{N}^\beta, E^\beta, V^\beta) + (\mathbf{N}^\gamma, E^\gamma, \mathbf{A})$, once an arbitrary but consistent choice (a gauge choice) for $\mathbf{A}$ is taken, that the physical system "naturally" lends itself to such decomposition under the assumptions stated above.

For the physical system, when **C** and **A** is fixed,

$$dE \;=\; TdS + \sum_i \mu_i dN_i, \tag{5.4}$$

for the injection of heat and particles into **C**. Let them equilibrate inside **C**, and remeasure $(S^\alpha, \mathbf{N}^\alpha)$, $(S^\beta, \mathbf{N}^\beta)$, and recalculate the tracking reference quantities:

$$dE^\alpha \;=\; TdS^\alpha + \sum_i \mu_i dN_i^\alpha, \qquad dE^\beta \;=\; TdS^\beta + \sum_i \mu_i dN_i^\beta \tag{5.5}$$

recognizing the intensive quantities $T$ and $\mu_i$ are the same everywhere in the physical system, and that the reference system and the physical system agree in these intensive quantities. So we have:

$$dE^\gamma \;=\; TdS^\gamma + \sum_i \mu_i dN_i^\gamma. \tag{5.6}$$

In essence, the perspective is to map the physical system, which has small but finite interfacial thickness, to a fictitious system of three phases $\alpha, \beta, \gamma$, where $\gamma$ has zero volume but finite particle number and energy as well as entropy.

The $\gamma$ phase does have finite area **A**, which can vary as shown in Fig. 5.1(a). Drawing analogy to isotropic $PdV$ term for $\alpha, \beta$ phases, one can propose $\gamma dA$ term for **A** variations:

$$dE^\gamma \;=\; TdS^\gamma + \sum_i \mu_i dN_i^\gamma + \gamma dA, \tag{5.7}$$

where $\gamma$ is called the interfacial tension [62], and like $P$ has the connotation of force.

The above allows **A** to change. If we also allow **C** to change, we should have:

$$dE^\alpha \;=\; TdS^\alpha + \sum_i \mu_i dN_i^\alpha - P^\alpha dV^\alpha, \qquad dE^\beta \;=\; TdS^\beta + \sum_i \mu_i dN_i^\beta - P^\beta dV^\beta \tag{5.8}$$

Thus, the total differential in **C** is:

$$dE \;=\; TdS + \sum_i \mu_i dN_i - P^\alpha dV^\alpha - P^\beta dV^\beta + \gamma dA. \tag{5.9}$$

For fixed **C**, but $dV^\alpha = -dV^\beta$, it is then easy to show the Young-Laplace relation:

$$P^\alpha \;=\; P^\beta + \gamma \frac{dA}{dV^\alpha} \;=\; P^\beta + \gamma(\kappa_1 + \kappa_2) \;=\; P^\beta + \gamma\left(\frac{1}{R_1} + \frac{1}{R_2}\right), \tag{5.10}$$

where $\kappa_1$ and $\kappa_2$ are the two principal curvatures.

Consider a 2-phase emulsion illustrated in Fig. 5.1(a), imagine instead of 1 liter of such emulsion, we create $\lambda$ liters of such emulsion, we will have

$$E(\lambda S, \lambda \mathbf{N}, \lambda V^\alpha, \lambda V^\beta, \lambda A) \;=\; \lambda E(S, \mathbf{N}, V^\alpha, V^\beta, A). \tag{5.11}$$

In other words, we keep the **same microstructure** (denoted by vector $\hat{\mathbf{A}} \equiv \mathbf{A}/A$) and the same **interfacial-area-to-volume ratio**, and just make more quantity of this composite materials, then we have:

$$E \;=\; TS + \sum_i \mu_i N_i - P^\alpha V^\alpha - P^\beta V^\beta + \gamma A. \tag{5.12}$$

The grand potential for the system is:

$$\Omega(T, \{\mu_i\}, \mathbf{C}, \mathbf{A}) \;\equiv\; F - \sum_i \mu_i N_i \;=\; \gamma A - P^\alpha V^\alpha - P^\beta V^\beta, \tag{5.13}$$

whereas for the Gibbs bulk reference states:

$$\Omega^\alpha \;\equiv\; F^\alpha - \sum_i \mu_i N_i^\alpha = -P^\alpha V^\alpha, \quad \Omega^\alpha \;\equiv\; F^\alpha - \sum_i \mu_i N_i^\alpha = -P^\alpha V^\alpha \tag{5.14}$$

so $\gamma$, the tension, can be understood as the excess grand potential per unit area:

$$\Omega^\gamma \;\equiv\; F^\gamma - \sum_i \mu_i N_i^\gamma \;=\; \Omega - \Omega^\alpha - \Omega^\beta \;=\; \gamma A. \tag{5.15}$$

It is clear that the $V^\alpha \to A^{\alpha\beta}$ and $-P^\alpha \to \gamma^{\alpha\beta}$ analogy holds exactly between 3D bulk and 2D interfacial area in the free energy expression. Thus, we can simply regard the interface between $\alpha\beta$ as zero-volume, finite-area 2D phase, and $\gamma$ as the "minus pressure" of this **infinitely thin 2D phase**. The interpretation of the Gibbs isotherm is that it is exactly the same analog to the Gibbs-Duhem relation in 3D bulk system.

$\gamma$ is also an excess Helmholtz free energy density, but one must take a homogeneous bulk reference state (JL ref) that has the same number of atoms as $\mathbf{N}$, as illustrated in Fig. 5.1(a), instead of the Gibbs bulk reference state that has different number of atoms. This is only reasonable, since to obtain a measurable energy difference/change one should compare two systems with the same number of atoms, so the Einstein $E = mc^2$ does not come into play.

It is clear from Fig. 5.1(a) that

$$F^{\alpha}_{\mathrm{JL}} \;=\; F^{\alpha} + \sum_i N_i^{\gamma\alpha}\mu_i, \tag{5.16}$$

since

$$\left.\frac{\partial F^{\alpha}}{\partial N_i}\right|_{N^{\alpha}_{j\neq i},T,V^{\alpha}} \;=\; \mu_i \tag{5.17}$$

for a homogeneous bulk phase, where $N_i^{\gamma\alpha}$ is the Gibbs particle excess to the left of the geometric cut $\mathbf{A}$, so $F^{\alpha}_{\mathrm{JL}}$ has the same number of atoms as the physical system to the left of $\mathbf{A}$. Similarly

$$F^{\beta}_{\mathrm{JL}} \;=\; F^{\beta} + \sum_i N_i^{\gamma\beta}\mu_i, \tag{5.18}$$

so the JL ref state is different from the Gibbs ref state

$$F_{\mathrm{JL}} \;=\; F^{\alpha}_{\mathrm{JL}} + F^{\beta}_{\mathrm{JL}} = F^{\alpha} + F^{\beta} + \sum_i N_i^{\gamma}\mu_i, \tag{5.19}$$

by $\sum_i N_i^{\gamma}\mu_i$. Thus,

$$F - F_{\mathrm{JL}} \;=\; F^{\gamma} - \sum_i N_i^{\gamma}\mu_i \;=\; \Omega^{\gamma} \;=\; \gamma A. \tag{5.20}$$

In the context of the JL reference state, then, interfacial tension is also understood as the interfacial free energy (excess Helmholtz free energy).

Differentiating (5.12) and subtracting off (5.9):

$$0 \;=\; SdT + \sum_i N_i d\mu_i - V^{\alpha}dP^{\alpha} - V^{\beta}dP^{\beta} + Ad\gamma. \tag{5.21}$$

We also have Gibbs-Duhem relations for the Gibbs ref states:

$$0 \;=\; S^{\alpha}dT + \sum_i N_i^{\alpha}d\mu_i - V^{\alpha}dP^{\alpha}, \quad 0 \;=\; S^{\beta}dT + \sum_i N_i^{\beta}d\mu_i - V^{\beta}dP^{\beta}, \tag{5.22}$$

so the **"Gibbs-Duhem analog"** relation for the infinitely thin 2D $\gamma$ phase is just:

$$0 \;=\; S^{\gamma}dT + \sum_i N_i^{\gamma}d\mu_i + Ad\gamma, \tag{5.23}$$

thus

$$d\gamma \;=\; -\frac{S^{\gamma}}{A}dT - \sum_i \frac{N_i^{\gamma}}{A}d\mu_i \tag{5.24}$$

is called the Gibbs adsorption equation [62]. One can define interfacial excess as

$$\Gamma_i \equiv \frac{N_i^\gamma}{A} \tag{5.25}$$

which has unit of mol/m$^2$.

So we have

$$\left.\frac{\partial\gamma}{\partial T}\right|_{\{\mu_j\}} = -\frac{S^\gamma}{A}, \tag{5.26}$$

and

$$\left.\frac{\partial\gamma}{\partial\mu_i}\right|_{\{\mu_{j\neq i}\},T} = -\frac{N_i^\gamma}{A} = -\Gamma_i. \tag{5.27}$$

$\Gamma_i$ can be measured by so-called contact angles. Suppose we have three phases $\alpha$, $\beta$, $\delta$, then by force balance we should have

$$\frac{\gamma^{\alpha\beta}}{\sin\theta^{\alpha\beta}} = \frac{\gamma^{\alpha\delta}}{\sin\theta^{\alpha\delta}} = \frac{\gamma^{\beta\delta}}{\sin\theta^{\beta\delta}}. \tag{5.28}$$

By studying the contact-angle change with respect to temperature and chemical environment, we can infer about the entropy excess and particle excess on the interface.

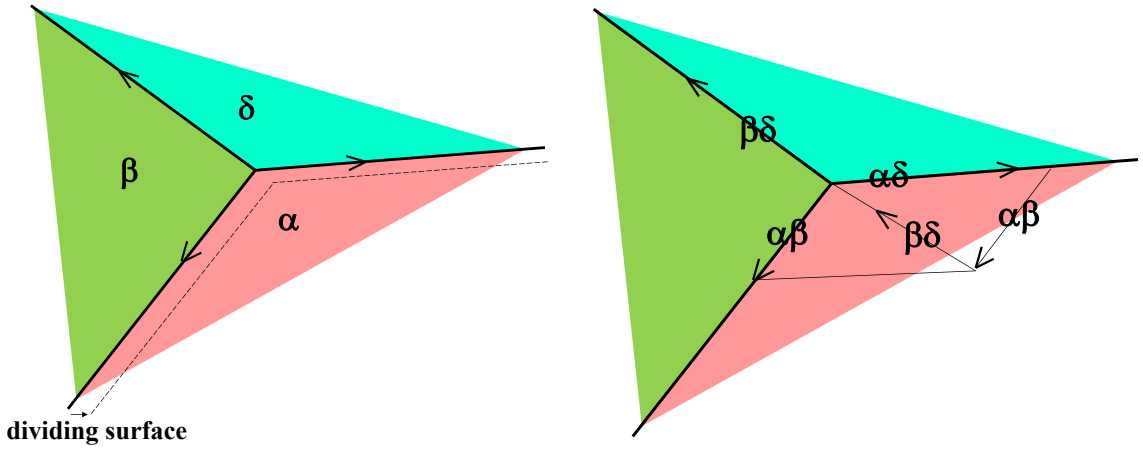


(a) (b)

Figure 5.2: (a) Consistency needs to be maintained in defining the Dividing Surface. (b) Measuring how interfacial energies change with $T$ and $\{\mu_j\}$

We note that in the original definition, $\Gamma_i$ depends on the exact location of the dividing surface (a gauge freedom). In the contact angle experiment, say between $\alpha$, $\beta$, $\delta$, with $\alpha\beta$, $\alpha\delta$, $\beta\delta$ interfaces, this depth has to be consistent though across different phase boundaries. In other words, if we retreat the dividing surface location with respect to the actual $c_i^{\alpha\beta}(\mathbf{x})$ toward the $\alpha$ side, then it has to retreat by the same distance with respect to $c_i^{\alpha\delta}(\mathbf{x})$ toward the $\alpha$ side as well, otherwise there will be a gap left at the triple junction. Indeed, while interfacial excess entropy $S^\gamma/A$, excess energy $E^\gamma/A$, and excess masses $\Gamma_i$ are **gauge**-dependent, macro-measurables like the liquid-air surface tensions $\gamma^{\alpha\beta}$, $\gamma^{\alpha\delta}$, $\gamma^{\beta\delta}$ and dihedral angles are **gauge-independent** (and this have to do with the fact that when changing the dividing surface by a few Angstroms, the former atomistic-scale quantities change a lot and can go from positive to negative, while the numerical value of $A$ will change relatively little, and $\gamma$, which is like a "pressure"-conjugate to $A$ in the free energy, won't change much with respect to the definition of the dividing surface).

To remove this uncertainty in the dividing surface location, one can define **relative surface excess**:

$$\Gamma_i^1 \;\equiv\; \Gamma_i - \Gamma_1 \frac{c_i^\alpha - c_i^\beta}{c_1^\alpha - c_1^\beta} \tag{5.29}$$

When there is shift in the dividing surface toward $\alpha$ by $\Delta$, the actual number of atoms does not change, but the reference state changes, with $(c_1^\beta - c_1^\alpha)\Delta$ more type-1 atoms in the reference state, and $(c_i^\beta - c_i^\alpha)\Delta$ more type-$i$ atoms in the reference state, so we will get:

$$\Gamma_1 \;\to\; \Gamma_1 + (c_i^\alpha - c_i^\beta)\Delta,\;\; \Gamma_i \;\to\; \Gamma_i + (c_i^\alpha - c_i^\beta)\Delta,\;\; \gamma^{\beta\delta} \;\to\; \gamma^{\beta\delta} + \sum_{i=1}^{C}(c_i^\alpha - c_i^\beta)\Delta\mu_i \tag{5.30}$$

and it is easy to see that $\Gamma_i^1$ is independent of $\Delta$. Type-1 is usually chosen to the solvent molecule. Alternatively, we can just define the dividing surface so that

$$\Gamma_1 \;=\; 0 \tag{5.31}$$

so there is no solvent-molecule excess at the interface. When we take a dividing surface so (5.31) is true, we can directly read off the dividing-surface-independent $\Gamma_i^1$ by $\Gamma_i$ (which is dividing-surface-dependent) at that particular dividing surface. This is the dividing surface we will choose next.

Soap molecules like sodium dodecyl sulfate (SDS) has a hydrophilic head and a fatty hydrophobic tail. It dissolves in water, but prefers to segregate to the water-air interface, to

reduce the pain of loss of hydrogen bonds, thus

$$\Gamma_{\mathrm{SDS}} \ > \ 0 \tag{5.32}$$

From the Gibbs adsorption equation, we see that

$$d\gamma \ \approx \ -\Gamma_{\mathrm{SDS}} dk_{\mathrm{B}} T \ln a_{\mathrm{SDS}}(aq) \tag{5.33}$$

where $a_{\mathrm{SDS}}(aq)$ is the activity of the SDS molecule solvated in the water, which is close to the mole fraction when dilute. Then

$$d\gamma \ \approx \ -\frac{\Gamma_{\mathrm{SDS}} k_{\mathrm{B}} T}{c_{\mathrm{SDS}}(aq)} dc_{\mathrm{SDS}}(aq). \tag{5.34}$$

Experimentally, the surface tension of the aqueous phase can be reduced by as much as 70% from that of plain water. This allows the aqueous solution to wet solids and spread on solid surfaces more easily. Also, because the soap water has lower surface tension, it delays the Rayleigh-Plateau instability, and cause soap bubble to be more stable (it also reduces the rate of water evaporation kinetically).

Also, by varying the temperature or composition spatially, the surface tension $\gamma(T(\mathbf{x}), \mathbf{X}(\mathbf{x}))$ can change, and this gradient in $\gamma$ induces so-called **Gibbs-Marangoni flow** or convection of the fluid:

$$\nabla\gamma \ = \ -s^{\gamma}\nabla T - \sum_i \Gamma_i \nabla\mu_i \tag{5.35}$$

since $\nabla\gamma$ causes direct imbalance of force per length. The first term above is called *thermo-capillary force*, while the rest are called *chemo-capillary force*. Such transient imbalance imposes a calming effect on the surface wave, which is used by spear fisherman: they throw grease into the water, and this calm the water (transiently) so they could see inside the ocean. According to Franklin's 1774 paper, "*not more than a tea spoonful produced an instant calm over a space of several yards square, . . . , making all that quarter of the pond, perhaps half an acre, as smooth as a looking-glass.*" [63] This effect can be explained by greatly increased shear-dissipation due to Gibbs-Marangoni flow.[64]

To explain Franklin's and other experiments, let us define $\alpha \equiv$ oil phase, $\beta \equiv$ water phase, $\alpha' \equiv$ vapor phase, and solutes like SDS can dissolve in $\beta$ as well as segregate into $\alpha\beta$ interface. Oil phase wets water, meaning:

$$\gamma^{\beta\alpha'} \ > \ \gamma^{\beta\alpha} + \gamma^{\alpha\alpha'} \tag{5.36}$$

So there is an effective reduction of surface energy after the oil wetting. However, with SDS dissolved in $\beta$ (soap water), $\gamma^{\beta\alpha}$ can drop even more, as the polar head of SDS likes water, and the non-polar tail of SDS likes oil. This further reduced $\gamma^{\beta\alpha}$ would make it even easier for water solvent ($\beta$ phase) to surround oil phase ($\alpha$ phase) under washing conditions. Thus SDS is a detergent, that helps to remove oil patches on cloth.

When there is a sinusoidal water ($\beta$) wave, even when the $\alpha$ phase is very thin, the density of oil molecules in flat interfacial region and the curved interfacial region will be different. This difference in oil molecule density will cause $\nabla\mu_i$, and will actuate the chemo-capillary force gradient in (5.35), which will then drag the oil film and shear the water beneath it. The sliding and slippage of $\beta$ beneath $\alpha$ film will induce a much larger dissipation rate than a bare $\gamma^{\alpha\alpha'}$ interface would - it is like a moving solid on top of fluid[64] Only about 15% of the enhanced water wave damping comes directly from reduced surface tension value. In other words, the gradient in surface tension is more important than the value of surface tension in this problem.

The above discussions all assume the interfacial excess free energy (if we take (5.12) to be definition of $\gamma$ and think $\sum_i \mu_i dN_i$ as the "free energy"). What if the excess energy is a function of inclination angle $\phi$? Consider the following classic problem of optimizing $\int dl\gamma(\phi)$:

$$F[\phi(x)] \equiv \int_{x_i}^{x_f} dx \frac{\gamma(\phi)}{\cos\phi} \tag{5.37}$$

subjected to the constraint that the curve must pass through $(x_i, y_i)$ and $(x_f, y_f)$:

$$y_f - y_i \;=\; \int_{x_i}^{x_f} dy \;=\; \int_{x_i}^{x_f} dx \frac{\sin\phi}{\cos\phi} \tag{5.38}$$

Imagine any arbitrary change $\phi(x) \to \phi(x) + \delta\phi(x)$ that satisfies the constraint:

$$0 \;=\; \int_{x_i}^{x_f} dx \left[\frac{\cos\phi}{\cos\phi} - \frac{\sin\phi}{\cos^2\phi}(-\sin\phi)\right]\delta\phi(x) = \int_{x_i}^{x_f} dx \frac{\delta\phi(x)}{\cos^2\phi} \tag{5.39}$$

which will cause

$$0 \;=\; \int_{x_i}^{x_f} dx \left[\frac{\gamma'(\phi)}{\cos\phi} + \frac{\gamma(\phi)\sin\phi}{\cos^2\phi}\right]\delta\phi(x). \tag{5.40}$$

The above can only be correct, if

$$\frac{\gamma'(\phi)}{\cos\phi} + \frac{\gamma(\phi)\sin\phi}{\cos^2\phi} \;=\; \frac{\lambda}{\cos^2\phi} \tag{5.41}$$

where $\lambda$ is a *position-independent* Lagrange multiplier. Therefore, mechanical equilibrium is achieved only if

$$\gamma'(\phi)\cos\phi + \gamma(\phi)\sin\phi \;=\; \lambda \tag{5.42}$$

for all $x$. Since in this example, the interface is just a line, force equilibrium along a line suggest $\lambda$ is exactly this force. $\gamma(\phi)\sin\phi$ is the traditional line tension, projected in the $y$-direction. If $\gamma'(\phi) \equiv \frac{d\gamma}{d\phi} = 0$, then solving (5.42) as an ODE would give us

$$\sin\phi(x) \;=\; \frac{\lambda}{\gamma} \;\;\rightarrow\;\; \phi(x) = \text{const} \tag{5.43}$$

e.g. a straight line. But if $\gamma(\phi)$ then generally it will be a curved, or even kinked line. The $\gamma'(\phi)\cos\phi$ is easily explained as torque term. So the *surface tension* is just

$$\mathbf{t} \;=\; \frac{d\gamma}{d\phi}\mathbf{m} + \gamma\xi \tag{5.44}$$

for a 1D line, where $\xi$ is the line direction and $\mathbf{m} \perp \xi$.

### 5.1.1 McLean Isotherm for Interfacial Segregation

The interfacial excess of a solute $\Gamma_i$ usually takes a "Fermi-Dirac" shape when $\mu_i$ is varied ($k_\mathrm{B}T\ln\gamma_i X_i$). That is, for very small or very large $\mu_i$, there is vanishing slope:

$$\frac{d\Gamma_i}{d\ln\gamma_i X_i} \;\rightarrow\; 0 \tag{5.45}$$

indicating there is a fixed number of sites in the solid interface that is either all empty ("0") or all occupied ("1"). Thus there is a peak slope location:

$$\max\frac{d\Gamma_i}{d\ln\gamma_i X_i} \tag{5.46}$$

Imagine a dilute 1-2 solid solution in the bulk lattice:

$$X_2 \;\ll\; 1 \tag{5.47}$$

and a grain boundary. Suppose the GB has a site density $\Gamma^\circ$ (mole/area, or #/area), forming

a **monolayer**. So at most, we have occupancy:

$$\max \Gamma_2 \;=\; \Gamma^\circ \tag{5.48}$$

(In above, we ignore the dividing plane choice, since $X_2$ is very small in either side of the interface). We can define interfacial composition to be

$$X_2^\gamma \;\equiv\; \frac{\Gamma_2}{\Gamma^\circ}. \tag{5.49}$$

We can also define **solute enrichment factor** $s$ to be

$$s \;\equiv\; \frac{\Gamma_2}{\Gamma^\circ X_2} \;=\; \frac{X_2^\gamma}{X_2} \tag{5.50}$$

Suppose these sites are either occupied by 1 or 2, and cannot be vacant (e.g. the energy penalty is too high, or the barrier is too sluggish since this requires long-range transport). In other words, we should only consider 1-2 exchanges with the bulk. The equilibrium of this facile exchange requires:

$$\mu_2^\gamma - \mu_1^\gamma \;=\; \mu_2 - \mu_1 \tag{5.51}$$

We model the right-hand side by an ideal solution:

$$\mu_2 - \mu_1 \;=\; \left.\frac{\partial g}{\partial X_2}\right|_T \;=\; a(T) + k_\mathrm{B}T \ln \frac{\gamma_2 X_2}{\gamma_1(1-X_2)} \tag{5.52}$$

with $\gamma_2 = \gamma_1 = 1$. We will model the left hand side by a regular solution. Basically, let us assume the interfacial site lattice has coordination number $Z$ ($Z = 4$ if simple cubic, and 6 if close packed), and suppose only NN interaction on the interfacial site layer is important, then

$$g^\gamma(X_2^\gamma) \;=\; X_2^\gamma g^\gamma(1) + (1-X_2^\gamma) g^\gamma(0) + k_\mathrm{B}T\left[X_2^\gamma \ln X_2^\gamma + (1-X_2^\gamma)\ln(1-X_2^\gamma)\right] + f^\mathrm{excess} \tag{5.53}$$

where

$$f^\mathrm{excess} \;=\; Z\theta X_2^\gamma(1-X_2^\gamma) \;=\; \frac{Z}{2} \times \theta \times 2X_2^\gamma(1-X_2^\gamma), \tag{5.54}$$

in which $\theta$ is the excess bonding energy between 1-2:

$$\theta \;\equiv\; -\epsilon_{12} + \frac{\epsilon_{11}+\epsilon_{22}}{2}. \tag{5.55}$$

where $-\epsilon_{12}$ is the amount of energy stablization gained by a 1-2 bond, and $2X_2^\gamma(1-X_2^\gamma)$ is the probability that a certain bond is a 1-2 bond in the mean-field approximation.

If $\theta < 0$, then the system prefers to mix in 2D inside the interface layer. If $\theta > 0$, it prefers to 2D phase separate (inside the interface layer). Then

$$\left.\frac{\partial g^\gamma}{\partial X_2^\gamma}\right|_T \;=\; g^\gamma(1) - g^\gamma(0) + k_{\rm B}T\ln\frac{X_2^\gamma}{1-X_2^\gamma} + (1-2X_2^\gamma)Z\theta \tag{5.56}$$

therefore we get the isotherm:

$$\frac{X_2}{1-X_2}e^{-\frac{b(T)}{k_{\rm B}T}} \;=\; \frac{X_2^\gamma}{1-X_2^\gamma}e^{-\frac{2Z\theta X_2^\gamma}{k_{\rm B}T}} \tag{5.57}$$

with

$$b(T) \;\equiv\; g^\gamma(1) - g^\gamma(0) + Z\theta - a(T) \tag{5.58}$$

If we define

$$\alpha \;\equiv\; -\frac{2Z\theta}{k_{\rm B}T},\;\; w \;\equiv\; \frac{X_2}{1-X_2}e^{-\frac{b(T)}{k_{\rm B}T}} \tag{5.59}$$

then

$$\ln X_2^\gamma - \ln(1-X_2^\gamma) + \alpha X_2^\gamma \;=\; \ln w \tag{5.60}$$

so

$$dX_2^\gamma\left(\frac{1}{X_2^\gamma} + \frac{1}{1-X_2^\gamma} + \alpha\right) \;=\; d\ln w \tag{5.61}$$

so

$$\frac{dX_2^\gamma}{d\ln w} \;=\; \frac{1}{\frac{1}{X_2^\gamma} + \frac{1}{1-X_2^\gamma} + \alpha}. \tag{5.62}$$

We see from above that indeed when $X_2^\gamma \to 0$,

$$\frac{dX_2^\gamma}{d\ln w} \;\to\; 0^+ \tag{5.63}$$

and when $X_2^\gamma \to 1$,

$$\frac{dX_2^\gamma}{d\ln w} \;\to\; 0^+ \tag{5.64}$$

which are saturation behaviors. The peak slope is always reached at $X_2^\gamma = 0.5$. We see that if

$$\alpha \;>\; -4 \tag{5.65}$$

or

$$\frac{2Z\theta}{k_{\mathrm{B}}T} \;<\; 4 \tag{5.66}$$

we will always have a single "solid-solution" interface. But otherwise the interface could phase separate in 2D (Fig. 7.11 of [65]).

## 5.2 Moire Bicrystallography, Coincidence Site Lattice, O-Lattice

A lattice is described by

$$\mathbf{g}_i \cdot \mathbf{a}_j \;=\; 2\pi\delta_{ij} \tag{5.67}$$

where $\mathbf{a}_1, \mathbf{a}_2, \mathbf{a}_3$ are the primitive cell vectors, and $\mathbf{g}_1, \mathbf{g}_2, \mathbf{g}_3$ are the corresponding primitive reciprocal vectors. (in Bragg diffraction, we see $m_1\mathbf{g}_1 + m_2\mathbf{g}_2 + m_3\mathbf{g}_3$). We use $\mathbf{b}$ to denote a certain integer combination of the primitive vectors:

$$\mathbf{b} = n_1\mathbf{a}_1 + n_2\mathbf{a}_2 + n_3\mathbf{a}_3 \tag{5.68}$$

and the fundamental relation

$$\mathbf{g}_i \cdot \mathbf{b} \;=\; 2\pi n_i \tag{5.69}$$

More generally, we use

$$\Delta s_i \;\equiv\; \mathbf{g}_i \cdot \Delta\mathbf{x} \tag{5.70}$$

to measure the change in internal coordinate. $\{s_i\}$ can be futher expressed as

$$s_i \;=\; 2\pi\left(\left\lfloor\frac{s_i}{2\pi}\right\rfloor + v_i\right) \tag{5.71}$$

so $v_i \in [0, 1)$. Clearly, two different $\mathbf{s}$ with the same $\mathbf{v}$ are equivalent cell interior positions.

Now consider two lattices $\{\mathbf{g}_i^\alpha, \mathbf{a}_i^\alpha\}$, $\{\mathbf{g}_i^\beta, \mathbf{a}_i^\beta\}$. $\alpha$ and $\beta$ can be **rotationally related**:

$$\mathbf{a}_i^\beta \;=\; \mathbf{R}\mathbf{a}_i^\alpha \tag{5.72}$$

where

$$\mathbf{R}^T\mathbf{R} \;=\; \mathbf{R}\mathbf{R}^T \;=\; \mathbf{I} \tag{5.73}$$

which is the situation for a grain boundary, or they may not (in which case we have a phase

boundary, and $\alpha$ and $\beta$ are phase labels).

With 2D grids, we can do an experiment, where as we rotate $\beta$, a pattern **coarser** than either $\alpha$ and $\beta$ are sometime clearly discernible by the human eye. Such pattern is called the **Moire pattern**. Aside from lattices in materials science, Moire pattern also arises in digitial photography, when we try to tilt a digital photograph on an upright pixelated display.

A coarse Moire pattern arises when the magnitude of one or more **Moire reciprocal vector**:

$$\mathbf{g}^{\mathrm{M}} \equiv \mathbf{g}^{\beta} - \mathbf{g}^{\alpha} \tag{5.74}$$

where

$$\mathbf{g}^{\beta} = l_1\mathbf{g}_1^{\beta} + l_2\mathbf{g}_2^{\beta} + l_3\mathbf{g}_3^{\beta}, \quad \mathbf{g}^{\alpha} = m_1\mathbf{g}_1^{\alpha} + m_2\mathbf{g}_2^{\alpha} + m_3\mathbf{g}_3^{\alpha} \tag{5.75}$$

gets **much smaller** than the primitives:

$$|\mathbf{g}^{\mathrm{M}}| \ll |\mathbf{g}_1^{\alpha}|, |\mathbf{g}_2^{\alpha}|, |\mathbf{g}_3^{\alpha}|, \quad |\mathbf{g}_1^{\beta}|, |\mathbf{g}_2^{\beta}|, |\mathbf{g}_3^{\beta}|. \tag{5.76}$$

This is shown by considering the **interference** between two periodic patterns $f^{\alpha}(\mathbf{x})$, $f^{\beta}(\mathbf{x})$ with lattice periods. To leading order, two pattern interact through **multiplication**:

$$f_{\text{interaction}}(\mathbf{x}) \propto f^{\alpha}(\mathbf{x})f^{\beta}(\mathbf{x}) \tag{5.77}$$

Consider a black-and-white image where $f^{\alpha}(\mathbf{x})$ and $f^{\beta}(\mathbf{x})$ is either 0 (white) or 1 (black). A combined picture has a black pixel at $\mathbf{x}$ if either $f^{\alpha}(\mathbf{x})$ is 1 or $f^{\beta}(\mathbf{x})$ is 1, so that is expressed as

$$\text{image}(\mathbf{x}) = 1 - (1 - f^{\alpha}(\mathbf{x}))(1 - f^{\beta}(\mathbf{x})) = f^{\alpha}(\mathbf{x}) + f^{\beta}(\mathbf{x}) - f^{\alpha}(\mathbf{x})f^{\beta}(\mathbf{x}) \tag{5.78}$$

The first two terms are superposition without interaction. The third term represents the interaction effect. (This is also true for the elastic energy between two defects).

With Fourier transformation,

$$f^{\alpha}(\mathbf{x}) = \sum f_{\mathbf{g}^{\alpha}} e^{i\mathbf{g}^{\alpha}\cdot\mathbf{x}}, \quad f^{\beta}(\mathbf{x}) = \sum f_{\mathbf{g}^{\beta}} e^{i\mathbf{g}^{\beta}\cdot\mathbf{x}} \tag{5.79}$$

It is clear that

$$f^{\alpha}(\mathbf{x})f^{\beta}(\mathbf{x}) = f^{\alpha *}(\mathbf{x})f^{\beta}(\mathbf{x}) \tag{5.80}$$

will generate various harmonic waves containing $-\mathbf{g}^\alpha + \mathbf{g}^\beta$ with amplitude $f^*_{\mathbf{g}^\alpha} f_{\mathbf{g}^\beta}$. Indeed, the above conclusion is still true for arbitrary interaction of the form $(f^\alpha(\mathbf{x}))^n (f^\alpha(\mathbf{x}))^m$ which we will obtain in a Taylor expansion of arbitrary nonlinear interaction

$$U(f^\alpha(\mathbf{x}), f^\beta(\mathbf{x})) \;=\; \sum_{n,m} U_{nm} (f^\alpha(\mathbf{x}))^n (f^\alpha(\mathbf{x}))^m. \tag{5.81}$$

Since human eyes pick out long-range patterns very well, we notice these very small $\mathbf{g}^{\mathrm{M}}$'s, **if the amplitude is not too small**. So the composite image after interference consists of **multiple scattering** of the **crystal momenta** of both crystals.

All possible $\{\mathbf{g}^{\mathrm{M}}\}$'s form a "group", that is, arbitrary integer combinations of arbitrary $\mathbf{g}^{\mathrm{M}}$ vectors still belongs to the set, since $\mathbf{g}^\beta$'s and the $\mathbf{g}^\alpha$ also form "groups". The key question is how many integers are needed to basis-expand entire $\{\mathbf{g}^{\mathrm{M}}\}$. If $\beta = \alpha$ (self multiple scattering), the answer is 3. For arbitrary $\alpha, \beta$, however, the answer is unfortunately 6 and not 3 (if 3, then it is a **lattice**, since we would be able to expand every $\mathbf{g}^{\mathrm{M}}$ as $n_1\mathbf{g}^{\mathrm{M}}_1 + n_2\mathbf{g}^{\mathrm{M}}_2 + n_3\mathbf{g}^{\mathrm{M}}_3$). You can convince yourself of this by considering 1D, with two irrationally incommensurate $g^\alpha$, $g^\beta$:

$$\frac{g^\beta}{g^\alpha} \;\neq\; \frac{m}{n}, \quad \forall n, m \tag{5.82}$$

Since one can use rational number to infinitely approach irrational number

$$\frac{g^\beta}{g^\alpha} \;=\; \frac{m}{n} + \epsilon \tag{5.83}$$

where $\epsilon$ is small number, it is possible to imagine a situation where:

$$g^{\mathrm{M}} \;=\; ng^\beta - mg^\alpha \;=\; n\epsilon g^\alpha \tag{5.84}$$

gets really small. But note that just small $|\mathbf{g}^{\mathrm{M}}|$ does not necessarily this interaction will be important, since the amplitude of pre-interaction Fourier components could decay rapidly with $n$, $m$ respectively. The most conspicuous Moire wave component **visually** should be the one with (a) small $\mathbf{g}^{\mathrm{M}}$, and (b) its generators, $\mathbf{g}^\beta$ and $\mathbf{g}^\alpha$ are themselves not too big.

Now consider a special **rational** situation, where there exists a "relatively small" $\mathbf{g}^{\mathrm{M}}$ that is

a rational fraction of a certain crystal momentum $\tilde{\mathbf{g}}^\beta$ of $\beta$:

$$\mathbf{g}^{\mathrm{M}} \equiv \mathbf{g}^\beta - \mathbf{g}^\alpha = \frac{l}{n}\tilde{\mathbf{g}}^\beta, \quad l < n. \tag{5.85}$$

Note that $\tilde{\mathbf{g}}^\beta$ is some not-too-big brother of $\mathbf{g}^\beta$.

In 2D square lattice of lattice constant $a$ (with square reciprocal lattice of lattice constant $g = 2\pi/a$), for example, by rotating $\alpha$ downward by $-\frac{\theta}{2}$ and $\beta$ upward by $\frac{\theta}{2}$, we create

$$\mathbf{g}^{\mathrm{M}} \;=\; \mathbf{e}_y 2g \sin\frac{\theta}{2} \tag{5.86}$$

if we use $g[1,0]^\alpha$ and $g[1,0]^\beta$ as generators.

We may indeed get lucky, for example, so **rational** multiples of $\mathbf{g}^{\mathrm{M}}$ hits one of $\{\mathbf{g}_i^\beta\}$:

$$\mathbf{g}^{\mathrm{M}} \;=\; \frac{l}{n}\tilde{\mathbf{g}}^\beta \tag{5.87}$$

where $l < n$ are both integers. Since

$$\mathbf{g}_1^\beta \;=\; g\begin{bmatrix} \cos\frac{\theta}{2} \\ \sin\frac{\theta}{2} \end{bmatrix}, \quad \mathbf{g}_2^\beta \;=\; g\begin{bmatrix} -\sin\frac{\theta}{2} \\ \cos\frac{\theta}{2} \end{bmatrix} \tag{5.88}$$

We need

$$\tilde{\mathbf{g}}^\beta \;=\; \tilde{n}^1\mathbf{g}_1^\beta + \tilde{n}^2\mathbf{g}_2^\beta \;=\; g\begin{bmatrix} \tilde{n}^1\cos\frac{\theta}{2} - \tilde{n}^2\sin\frac{\theta}{2} \\ \tilde{n}^1\sin\frac{\theta}{2} + \tilde{n}^2\cos\frac{\theta}{2} \end{bmatrix} \tag{5.89}$$

We need $\tilde{\mathbf{g}}^\beta$ to be parallel to $\mathbf{e}_y$ in this particular construction (doing so, because choosing a small $\theta$ is a sure-fire way to generate small $\mathbf{g}^{\mathrm{M}}$ using not-too-large generators). Thus:

$$\frac{\tilde{n}^1}{\tilde{n}^2} \;=\; \tan\frac{\theta}{2} \tag{5.90}$$

and

$$2g\sin\frac{\theta}{2} \;=\; \frac{l}{n}g(\tilde{n}^1\sin\frac{\theta}{2} + \tilde{n}^2\cos\frac{\theta}{2}) \tag{5.91}$$

or

$$\frac{(\tilde{n}^1)^2 + (\tilde{n}^2)^2}{\tilde{n}^1} \;=\; \frac{2n}{l} \tag{5.92}$$

So this amazing construction is indeed **achievable** for a number of $\tilde{n}^1$, $\tilde{n}^2$, $l$, $n$ choices. We can select arbitrary $\tilde{n}^1$, $\tilde{n}^2$ tuple, then compute the integer $(\tilde{n}^1)^2 + (\tilde{n}^2)^2$. If it is even, then

we identify

$$n \;=\; \frac{(\tilde{n}^1)^2+(\tilde{n}^2)^2}{2}, \quad l \;=\; \tilde{n}^1 \tag{5.93}$$

because we want $l, n$ to be integer but **as small as possible**. Note that when $(\tilde{n}^1)^2+(\tilde{n}^2)^2$ is even, it can be (a) $\tilde{n}^1, \tilde{n}^2$ both even, or (b) $\tilde{n}^1, \tilde{n}^2$ both odd. But (a) can be reduced to (b), because before meeting that long $\tilde{\mathbf{g}}^\beta$, the Moire vector is in resonance with another shorter $\tilde{\mathbf{g}}^\beta$ half as long. Generally speaking, we require the two generating integers $\tilde{n}^1, \tilde{n}^2$ to have no common denominator:

$$\gcd(\tilde{n}^1, \tilde{n}^2) \;=\; 1. \tag{5.94}$$

If on the other hand $(\tilde{n}^1)^2+(\tilde{n}^2)^2$ is odd (one even, one odd), still no problem, we can pick

$$n \;=\; (\tilde{n}^1)^2+(\tilde{n}^2)^2, \quad l \;=\; 2\tilde{n}^1. \tag{5.95}$$

Now let us see what this special alignment (5.85) will bring to us. If

$$\mathbf{g}^{\mathrm{M}} \;=\; \mathbf{g}^\beta - \mathbf{g}^\alpha \;=\; \frac{l}{n}\tilde{\mathbf{g}}^\beta \tag{5.96}$$

then

$$n\mathbf{g}^\beta - l\tilde{\mathbf{g}}^\beta \;=\; n\mathbf{g}^\alpha \tag{5.97}$$

so the two sets of reciprocal lattices are **in resonance** for some special subset of wavevectors (clearly not all of them usually, e.g. in cubic lattices unless $\theta = m\frac{\pi}{2}$ - the group symmetry rotation angles). This means there is some Coincidence Site Lattice (CSL) **in reciprocal lattice**. This special condition is called **commensurate**. I believe this concept aroses ealiest in civilization in measurement and trading (e.g. five cat's length is three dog's length, and when values are commensurate, one can make easy barter, e.g. three sacks of grain to trade ten bottles of wine, without either side of the trade having to make sacrifice due to roundoff).

When some reciprocal lattice vectors are in resonance, some real lattice vectors might also be **in resonance**. Consider taking arbitrary Burgers vector $\mathbf{b}^\beta$ and multiplying on both sides:

$$(n\mathbf{g}^\beta - l\tilde{\mathbf{g}}^\beta)\cdot\mathbf{b}^\beta \;=\; n\mathbf{g}^\alpha\cdot\mathbf{b}^\beta \;=\; 2m\pi \tag{5.98}$$

This means *arbitrary* Bravais translation in $\beta$ would be **fractionally reciprocal** to this particular reciprocal vector of $\alpha$, $\mathbf{g}^\alpha$! One could indeed say that every $n\mathbf{b}^\beta$ hits some $m$-tuple planes of $\alpha$. The $m$-tuple planes of $\alpha$ forms a grid, and $1/n$th division of this form

a **sub-grid**, like a Lined Paper with real and dash lines. So (5.97) is saying that **every equivalent atom of $\beta$ is sitting on some sub-grid of $\alpha$, if one atom of $\beta$ is aligned with one equivalent atom of $\alpha$ at $\mathbf{x} = 0$.** Isn't this cool? Next we will try to make more explicit the structure of this sub-grid.

(5.97) in the above is getting lucky once (**rational**, **commensurate** or **resonant** in some special direction). If we get lucky three times, then we will get a bicrystallographic **super-lattice**. In real space this will give us **Coincidence Site Lattice** (CSL), as well as the O-lattice (which CSL is a sublattice of). We would require

$$n_1\mathbf{g}_1^\beta - l_1\tilde{\mathbf{g}}_1^\beta = n_1\mathbf{g}_1^\alpha, \;\; n_2\mathbf{g}_2^\beta - l_2\tilde{\mathbf{g}}_2^\beta = n_2\mathbf{g}_2^\alpha, \;\; n_3\mathbf{g}_3^\beta - l_3\tilde{\mathbf{g}}_3^\beta = n_3\mathbf{g}_3^\alpha \tag{5.99}$$

where $\mathbf{g}_1^\alpha$, $\mathbf{g}_2^\alpha$, $\mathbf{g}_3^\alpha$ are linearly independent. Even though it does not have to be, without losing generality we can actually require the generators $\mathbf{g}_1^\beta$, $\mathbf{g}_1^\alpha$, $\mathbf{g}_2^\beta$, $\mathbf{g}_2^\alpha$, $\mathbf{g}_3^\beta$, $\mathbf{g}_3^\alpha$ to be primitive reciprocal vectors of each lattice. Then, *arbitrary* $\mathbf{b}^\beta$ can be resolved fractionally:

$$n_1\mathbf{g}_1^\alpha \cdot \mathbf{b}^\beta = 2\pi m_1, \;\; n_2\mathbf{g}_2^\alpha \cdot \mathbf{b}^\beta = 2\pi m_2, \;\; n_3\mathbf{g}_3^\alpha \cdot \mathbf{b}^\beta = 2\pi m_3. \tag{5.100}$$

So every atom of $\beta$ falls onto a **3D sub-grid** of $\alpha$ if they are atomically aligned at some point, and vice versa. The above still applies to generic phase boundaries - one could make certain phase boundaries (like between Si and Ge) commensurate by applying epitaxial elastic strain.

Also, we would have

$$\mathbf{g}_1^{\mathrm{M}} = \frac{l_1}{n_1}\tilde{\mathbf{g}}_1^\beta, \;\; \mathbf{g}_2^{\mathrm{M}} = \frac{l_2}{n_2}\tilde{\mathbf{g}}_2^\beta, \;\; \mathbf{g}_3^{\mathrm{M}} = \frac{l_3}{n_3}\tilde{\mathbf{g}}_3^\beta \tag{5.101}$$

Consider the real-space lattice formed by lattice vectors $\mathbf{c}_1, \mathbf{c}_2, \mathbf{c}_3$:

$$\mathbf{g}_i^{\mathrm{M}} \cdot \mathbf{c}_j \;=\; 2\pi\delta_{ij} \tag{5.102}$$

$\mathbf{c}_1, \mathbf{c}_2, \mathbf{c}_3$ can be obtained by matrix inversion, where $\mathbf{g}_i^{\mathrm{M}}$'s form the rows of a $\mathbf{G}$ matrix, and $\mathbf{c}_j$'s form the column of an $\mathbf{A}$ matrix. So we get

$$\frac{l_i}{n_i}\tilde{\mathbf{g}}_i^\beta \cdot \mathbf{c}_j \;=\; (\mathbf{g}_i^\beta - \mathbf{g}_i^\alpha) \cdot \mathbf{c}_j \;=\; 2\pi\delta_{ij}. \tag{5.103}$$

**The above can still apply to generic phase boundaries.**

Suppose $\alpha$ and $\beta$ lattice are **affinely related**, for example by elastic strain and/or rotation:

$$\mathbf{x}^\beta = \mathbf{A}\mathbf{x}^\alpha, \quad \mathbf{g}_i^\beta \;=\; \mathbf{g}_i^\alpha \mathbf{A}^{-1}, \;\; i = 1..3 \tag{5.104}$$

and suppose $i = 1..3$ are chosen to be the primitive reciprocal vectors (reciprocal to the primitive lattice vectors), so (5.104) defines a **lattice correspondence** relation. Then the definition (5.103) $\{\mathbf{c}_j\}$ has an interesting interpretation. Let us align an atom of $\alpha$ with an atom of $\beta$ and call that point $\mathbf{x} = 0$, and the bicrystal **atomically aligned**. (But it does not have to atom-onto-atom, but could be an equivalent interior position onto an equivalent interior position). The dimensionless internal coordinate with respect to the orgin is defined by

$$\mathbf{s}^\alpha \;\equiv\; \begin{bmatrix} \mathbf{g}_1^\alpha \cdot \mathbf{x} \\ \mathbf{g}_2^\alpha \cdot \mathbf{x} \\ \mathbf{g}_3^\alpha \cdot \mathbf{x} \end{bmatrix}, \tag{5.105}$$

But obviously if we add a $2\pi$ or subtract a $2\pi$ from one of the entries, the internal coordinate is identical. So (5.103) means $\mathbf{x} = \mathbf{c}_j$ represent a **identical interior position** to **both** $\alpha$ and $\beta$. Thus, the lattice formed by

$$\mathbf{x} \;=\; i_1\mathbf{c}_1 + i_2\mathbf{c}_2 + i_3\mathbf{c}_3 \tag{5.106}$$

are locations of **good alignment**, where either (a) identical atom lies on top of identical atom, or (b) no atoms, but identical charge density / wavefunction value on top of identical charge density / wavefunction value. Indeed, these points can all be chosen to be the **origin of alignment**, thus the name **O-lattice**, which stands for "**lattice of origins**" by Bollmann [65]. The key feature when sampling alignment on O-lattice is all-or-nothingness: if $\alpha$ and $\beta$ are atomically aligned, then all the equivalent positions are also aligned (and this should be low-energy configuration in construction grain boundary). But if one is misaligned, then all others are misaligned. It is as if $\alpha$ carries its O-lattice subgrid paper (the subgrid we mentioned before) that is partially atomically occupied by $\alpha$'s atoms, and $\beta$ carries its O-lattice subgrid paper (the subgrid we mentioned before) that is partially atomically occupied by $\beta$'s atoms, and when atomically aligned, the two subgrid papers overlap at some grid points both atomically occupied.

We see the above grid paper provides a good basis to talk about relative shifts between $\alpha$ and $\beta$. So far we have focussed heavily on reciprocal space structure of the bi-crystallography, and in real space, focusing on atomically aligned situation which is supposed to be low-

energy, high-symmetry configuration for the interface. However, when this interface absorbs a lattice dislocation, then there will be relative translations between the $\alpha$ block and the $\beta$ block. For example, since

$$(\mathbf{g}_i^\beta - \mathbf{g}_i^\alpha) \cdot \mathbf{c}_j \;=\; \mathbf{g}_i^\alpha \mathbf{a}_j^\alpha \tag{5.107}$$

from (5.103), we have

$$\mathbf{g}_i^\beta \cdot \mathbf{c}_j \;=\; \mathbf{g}_i^\alpha \cdot (\mathbf{c}_j + \mathbf{a}_j^\alpha). \tag{5.108}$$

and thus

$$\mathbf{g}_i^\beta \cdot \lambda \mathbf{c}_j \;=\; \mathbf{g}_i^\alpha \cdot \lambda(\mathbf{c}_j + \mathbf{a}_j^\alpha), \quad \forall \lambda = 0..1 \tag{5.109}$$

This corresponds to a special situation where, when the $\alpha$ block is shifting along $\lambda(\mathbf{c}_j + \mathbf{a}_j^\alpha)$ while the $\beta$ block is shifting along $\lambda \mathbf{c}_j$ (thus the relative shift is $\lambda \mathbf{a}_j^\alpha$), they would be each individually moving in their own equivalent (but diverging) trajectories, and so there will be an energy cost $Q(\lambda)$. When $\lambda = 1$, the grain boundary has absorbed a lattice dislocation and has also shifted the location of atomic alignment to $\mathbf{x} = \mathbf{c}_j$, so $Q(\lambda = 0) = Q(\lambda = 1) = 0$. We can use the above set-up to calculate the GB shear generalized stacking fault energy $Q(\lambda)$, where both crystals shift in the calculation. Aside from certain symmetry beauty (each moving in their own equivalent (but diverging) trajectories), there does not seem to be more general meaning to this exercise. It is like a couple doing what each believes is the "right" thing, but forming a "dislocation".

Plugging in

$$(\mathbf{g}_i^\alpha \mathbf{A}^{-1} - \mathbf{g}_i^\alpha) \cdot \mathbf{c}_j \;=\; 2\pi\delta_{ij} \;=\; \mathbf{g}_i^\alpha (\mathbf{A}^{-1} - \mathbf{I}) \mathbf{c}_j \tag{5.110}$$

we see there needs to be

$$(\mathbf{A}^{-1} - \mathbf{I}) \mathbf{c}_j \;=\; \mathbf{a}_j^\alpha \tag{5.111}$$

or

$$\mathbf{c}_j \;=\; (\mathbf{A}^{-1} - \mathbf{I})^{-1} \mathbf{a}_j^\alpha. \tag{5.112}$$

Since we can map

$$\mathbf{a}_j^\alpha \;=\; \mathbf{A}^{-1} \mathbf{a}_j^\beta \tag{5.113}$$

we can also write it as

$$\mathbf{c}_j \;=\; (\mathbf{I} - \mathbf{A}^{-1})^{-1} \mathbf{a}_j^\beta \tag{5.114}$$

which is the same as p.28 of 2.1.3. of Balluffi notes.

The concept of **phase matching and constructive interference** is well appreciated in the time domain. Suppose we have two sources of sound: $\cos(\phi_1(t))$ and $\cos(\phi_2(t))$ with different

frequencies, at time points of $\phi_1(t) = \phi_2(t) + 2n\pi$ we say they constructively interfere. At time points of $\phi_1(t) = \phi_2(t)+(2n+1)\pi$ we say they destructively interfere. Suppose $t = 0$ is a special point: $\phi_1(t = 0) = \phi_2(t = 0) = 0$, say $\phi_1(t) = \omega_1 t$ and $\phi_2(t) = \omega_2 t$. If the frequencies of $\phi_1(t)$ and $\phi_2(t)$ are irrationally related, i.e. $\omega_1/\omega_2$ is not integer fraction, then these points of phase matching will appear periodically, but these points are usually **not** special points (e.g. $\phi_1(t) = 2l\pi$) of $\phi_1(t)$ or $\phi_2(t)$. However, if the two frequencies are fractionally related, then some kind of resonance condition is satisfied, and the phase-matching points can be special points (like the minimum valley points) for both $\cos(\phi_1(t))$ and $\cos(\phi_2(t))$.

We are dealing with essentially the same thing now, but in the spatial domain. The bicrystallography (aka dichromatic pattern, e.g. black and white circles) can have phase-matching at many points, which are the O-points. If furthermore the spatial frequencies, e.g. the wavevectors are fractionally related, i.e. **commensurate** for special rotations, then it is further possible for these points to be special points of $\alpha$ and $\beta$, like the atom-to-atom matching of the CSL lattice (phase 0-or-integer to phase 0-or-integer matching). The O-lattice are all locations of phase matching $\mathbf{g}_i^\beta \cdot \mathbf{c}_j = \mathbf{g}_i^\alpha \cdot \mathbf{c}_j + 2\pi n$, which can include fractional phase to fractional phase matching.

It is clear that **CSL must be part of the O-lattice**. Consider (5.103), which can be rewritten as

$$\tilde{\mathbf{g}}_i^\beta \cdot (l_j \mathbf{c}_j) \;=\; 2\pi n_j \delta_{ij}. \tag{5.115}$$

(since if $i \neq j$, the RHS is zero, so we can multiply $l_j/l_i$). This means the lattice $\{l_j\mathbf{c}_j\}$ has **a good chance** of being on $\beta$'s atoms. And if they are, they must also be on $\alpha$'s atoms.

Note however that the above is not a proof that $\{l_j\mathbf{c}_j\}$ must be on $\beta$'s atoms. It could also be $\{2l_j\mathbf{c}_j\}$, for instance.

If we are dealing with simple cubic lattice **grain boundary**, then with the particular generation scheme ([001] twist), getting lucky once means getting lucky three times automatically. Since we do [001] twist generation,

$$\mathbf{g}_3^\beta \;=\; \mathbf{g}_3^\alpha \tag{5.116}$$

for arbitrary $\theta$. Then, since 90-degree rotation is symmetry operation of both lattices, if

$$n_1\mathbf{g}_1^\beta - l_1\tilde{\mathbf{g}}_1^\beta = n_1\mathbf{g}_1^\alpha \tag{5.117}$$

then

$$n_1\mathbf{g}_1^\beta\mathbf{R}_{90}^{-1} - l_1\tilde{\mathbf{g}}_1^\beta\mathbf{R}_{90}^{-1} = n_1\mathbf{g}_1^\alpha\mathbf{R}_{90}^{-1} \tag{5.118}$$

is automatically true. So the superlattice would also have 90-degree in-plane symmetry. According to previous calculations

$$\mathbf{g}_1^{\mathrm{M}} = \frac{l}{n}\tilde{\mathbf{g}}_1^{\beta} = \frac{l}{n}g\begin{bmatrix} \tilde{n}^1\cos\frac{\theta}{2} - \tilde{n}^2\sin\frac{\theta}{2} \\ \tilde{n}^1\sin\frac{\theta}{2} + \tilde{n}^2\cos\frac{\theta}{2} \\ 0 \end{bmatrix} = g\begin{bmatrix} 0 \\ 2\sin\frac{\theta}{2} \\ 0 \end{bmatrix} = 2g\begin{bmatrix} 0 \\ \sin\arctan\frac{\tilde{n}^1}{\tilde{n}^2} \\ 0 \end{bmatrix} = 2g\begin{bmatrix} 0 \\ \frac{\tilde{n}^1}{\sqrt{(\tilde{n}^1)^2+(\tilde{n}^2)^2}} \\ 0 \end{bmatrix} \tag{5.119}$$

$$\mathbf{g}_2^{\mathrm{M}} \;=\; 2g\begin{bmatrix} -\frac{\tilde{n}^1}{\sqrt{(\tilde{n}^1)^2+(\tilde{n}^2)^2}} \\ 0 \\ 0 \end{bmatrix}, \quad \mathbf{g}_3^{\mathrm{M}} \;=\; g\begin{bmatrix} 0 \\ 0 \\ 1 \end{bmatrix} \tag{5.120}$$

And therefore we specify the O-lattice to be

$$\mathbf{c}_1 \;=\; a\begin{bmatrix} 0 \\ \frac{\sqrt{(\tilde{n}^1)^2+(\tilde{n}^2)^2}}{2\tilde{n}^1} \\ 0 \end{bmatrix}, \quad \mathbf{c}_2 \;=\; a\begin{bmatrix} -\frac{\sqrt{(\tilde{n}^1)^2+(\tilde{n}^2)^2}}{2\tilde{n}^1} \\ 0 \\ 0 \end{bmatrix}, \quad \mathbf{c}_3 \;=\; a\begin{bmatrix} 0 \\ 0 \\ 1 \end{bmatrix} \tag{5.121}$$

and with

$$\mathbf{g}_1^{\beta} \;=\; g\begin{bmatrix} \cos\frac{\theta}{2} \\ \sin\frac{\theta}{2} \\ 0 \end{bmatrix}, \quad \mathbf{g}_2^{\beta} \;=\; g\begin{bmatrix} -\sin\frac{\theta}{2} \\ \cos\frac{\theta}{2} \\ 0 \end{bmatrix} \tag{5.122}$$

We therefore have

$$(\mathbf{g}_1^{\beta}\cdot\mathbf{c}_1,\;\; \mathbf{g}_1^{\beta}\cdot\mathbf{c}_2) \;=\; 2\pi\left(\frac{1}{2},\;\; -\frac{\tilde{n}^2}{2\tilde{n}^1}\right), \tag{5.123}$$

$$(\mathbf{g}_2^{\beta}\cdot\mathbf{c}_1,\;\; \mathbf{g}_2^{\beta}\cdot\mathbf{c}_2) \;=\; 2\pi\left(\frac{\tilde{n}^2}{2\tilde{n}^1},\;\; \frac{1}{2}\right), \tag{5.124}$$

If $(\tilde{n}^1)^2 + (\tilde{n}^2)^2$ is even (both odd, like 1,3), then we identify

$$n \;=\; \frac{(\tilde{n}^1)^2 + (\tilde{n}^2)^2}{2}, \quad l \;=\; \tilde{n}^1 \tag{5.125}$$

and $\{l_j\mathbf{c}_j\}$ for $j = 1, 2$ gives

$$(\mathbf{g}_1^{\beta}\cdot\tilde{n}^1\mathbf{c}_1,\;\; \mathbf{g}_1^{\beta}\cdot\tilde{n}^1\mathbf{c}_2) \;=\; 2\pi\left(\frac{\tilde{n}^1}{2},\;\; -\frac{\tilde{n}^2}{2}\right), \tag{5.126}$$

$$(\mathbf{g}_2^\beta \cdot \tilde{n}^1\mathbf{c}_1,\ \ \mathbf{g}_2^\beta \cdot \tilde{n}^1\mathbf{c}_2) \ = \ 2\pi\left(\frac{\tilde{n}^2}{2},\ \ \frac{\tilde{n}^1}{2}\right). \tag{5.127}$$

Plugging in odd-odd gives a lattice pattern that is one-quarter of a BCC pattern (see Fig.1 of Balluffi for 1,3 pattern, where there is a 45° twin plane) and half occupied by atoms, so we identify the square CSL pattern to be half as the size of the BCC CSL pattern:

$$\Sigma \ = \ 2 \times \frac{(\tilde{n}^1)^2 + (\tilde{n}^2)^2}{4} \ = \ \frac{(\tilde{n}^1)^2 + (\tilde{n}^2)^2}{2} \ = \ n \tag{5.128}$$

On the other hand, if $(\tilde{n}^1)^2 + (\tilde{n}^2)^2$ is odd (one even, one odd like 1,2), then

$$n \ = \ (\tilde{n}^1)^2 + (\tilde{n}^2)^2, \quad l \ = \ 2\tilde{n}^1. \tag{5.129}$$

$\{l_j\mathbf{c}_j\}$ for $j = 1, 2$ gives

$$(\mathbf{g}_1^\beta \cdot 2\tilde{n}^1\mathbf{c}_1,\ \ \mathbf{g}_1^\beta \cdot 2\tilde{n}^1\mathbf{c}_2) \ = \ 2\pi\left(\tilde{n}^1,\ \ -\tilde{n}^2\right), \tag{5.130}$$

$$(\mathbf{g}_2^\beta \cdot 2\tilde{n}^1\mathbf{c}_1,\ \ \mathbf{g}_2^\beta \cdot 2\tilde{n}^1\mathbf{c}_2) \ = \ 2\pi\left(\tilde{n}^2,\ \ \tilde{n}^1\right). \tag{5.131}$$

the pattern that forms is a square pattern (fully occupied CSL, with 90° twin plane), so

$$\Sigma \ = \ (\tilde{n}^1)^2 + (\tilde{n}^2)^2 \ = \ n. \tag{5.132}$$

As generators, the $(\tilde{n}^1)^2 + (\tilde{n}^2)^2$ odd generator ($\tilde{n}^1 = 2$, $\tilde{n}^2 = 1$, with 90° twin plane) and the $(\tilde{n}^1)^2 + (\tilde{n}^2)^2$ even generators ($\tilde{n}^1 = 3$, $\tilde{n}^2 = 1$, with 45° twin plane) can generate the dichromatic pattern, with the same CSL and same $\Sigma = 5$.

We also note that the CSL should have the same point group as the original lattice. The space group situation is more complicated.[65]

What is the utility of O-lattice? The O-points are where fractional good matching occurs, and therefore when the interface reconstructs, it is likely that the dislocations will avoid the O-points. This is shown for the case of twist boundary, where the dislocation laying in the GB avoid the O-points in Balluffi Fig.9, and the tilt boundary, where the dislocation core avoid thes O-points in Balluffi Fig.10.

The O-lattice is what the eye picks out, and its spacing is not really changing when there is arbitrary (even irrational) translation between $\beta$ and $\alpha$ (for example, when there is no atom-to-atom matching). This is because of the reciprocal space formulation does not really

care about translations.

Because its existence depends on it, the CSL lattice obviously depends on translation (for example, in the simplest case of misorientation $\theta = 0$, with slight translation there will be no CSL). When there is CSL, the O-lattice then is a superset of CSL. But the relationship between CSL and O-lattice is not too simple, and involves space group and integer gcd.[65] The O-lattice gives strong hints as to what the CSL might be (like our $\{l_j \mathbf{c}_j\}$ for simple cubic, but which could be half filled), but the final integers needs to be worked out explicitly depending on the detailed structure of $\{\mathbf{g}_i^\alpha, \mathbf{a}_i^\alpha\}$, $\{\mathbf{g}_i^\beta, \mathbf{a}_i^\beta\}$.

### 5.2.1 DSC lattice

The DSC lattice is formed when there is a CSL pattern, e.g. commensurability in real- and reciprocal space lattices. It is defined by all possible translation vectors, that would take a black atom ($\beta$) onto a white atom ($\alpha$) in the dichromatic pattern:

$$\mathbf{t} \equiv \mathbf{x}_m^\alpha - \mathbf{x}_n^\beta. \tag{5.133}$$

When we already have a CSL arrangement, $\mathbf{t}$ can be zero, small or large (comparable to $\mathbf{a}_j^\beta$ or even the the CSL spacing, which are all legitimate DSC translations). Clearly, when we drag $\beta$ by $\mathbf{t}$ above while fixing $\alpha$, the atom that was originally sitting on $\mathbf{x}_n^\beta$ will now move to

$$\mathbf{x}_n^\beta + (\mathbf{x}_m^\alpha - \mathbf{x}_n^\beta) = \mathbf{x}_m^\alpha \tag{5.134}$$

In other words, $\mathbf{x}_m^\alpha$, which originally may not be a location of atom-to-atom matching ("loner"), now is ("paired up"). The boundary energy would be the same as before, except the dichromatic pattern shifted by

$$\mathbf{T} \equiv \mathbf{x}_m^\alpha - \mathbf{x}_{m'}^\alpha \tag{5.135}$$

where $\mathbf{x}_{m'}^\alpha$ was a nearest atom-to-atom matching point

$$\mathbf{x}_{m'}^\alpha \equiv \mathbf{x}_{n'}^\beta \tag{5.136}$$

before the shift. Generally speaking

$$\mathbf{T} \neq \mathbf{t}, \tag{5.137}$$

that is to say, how much $\beta$ is physically shifted is **different from** how much the dichromatic pattern appears to have shifted ("pattern is mental").

We may insert (5.136) into (5.133), and get

$$\mathbf{t} \;=\; \mathbf{x}_m^\alpha - \mathbf{x}_{m'}^\alpha + \mathbf{x}_{n'}^\beta - \mathbf{x}_n^\beta \;=\; \mathbf{b}_m^\alpha - \mathbf{b}_n^\beta \tag{5.138}$$

The $\mathbf{b}_m^\alpha, \mathbf{b}_n^\alpha$ pair can therefore be thought as the generator of the DSC lattice. An obvious property of $\mathbf{t}$ is that when the interface absorbs a full lattice dislocation from $\beta$ ($\mathbf{t} \to \mathbf{t} + \mathbf{b}^\beta$), or a full dislocation from $\alpha$ ($\mathbf{t} \to \mathbf{t} - \mathbf{b}^\alpha$), it still belongs to the group, for obvious reason and as a sanity check. However, we can achieve

$$|\mathbf{t}| \;\ll\; |\mathbf{a}_i^\alpha| \tag{5.139}$$

under appropriate conditions.

To see this, consider the fact that there must be

$$\mathbf{b}_n^\beta \;=\; \mathbf{A}\mathbf{b}_n^\alpha \tag{5.140}$$

$$\mathbf{t} \;=\; \mathbf{b}_m^\alpha - \mathbf{A}\mathbf{b}_n^\alpha \tag{5.141}$$

If $\mathbf{A}$ corresponds to a small rotation

$$\mathbf{A} \;=\; \mathbf{R}(\mathbf{a}, \theta) \;\approx\; \mathbf{I} + \theta\mathbf{J}(\mathbf{a}) \tag{5.142}$$

where $\mathbf{J}(\mathbf{a})$ is an anti-symmetric matrix, then by making $\mathbf{b}_m^\alpha = \mathbf{b}_n^\alpha$, we can make $\mathbf{t}$ as small as we want. Indeed we have previously solved this problem for simple cubic lattice in **reciprocal space**. By using the generator $\tilde{n}^1, \tilde{n}^2$ to produce the rotation, we get the same kind of condition for commensurability, and we will get

$$\mathbf{t} \;=\; \mathbf{b}^\alpha - \mathbf{b}^\beta = \frac{l}{n}\tilde{\mathbf{b}}^\alpha, \quad l < n. \tag{5.143}$$

where the only difference with (5.85) is a label switch. This can work for all axis:

$$\mathbf{t}_i \;=\; \mathbf{a}_i^\alpha - \mathbf{a}_i^\beta = \frac{l_i}{n_i}\tilde{\mathbf{b}}_i^\alpha, \quad l < n. \tag{5.144}$$

We've shown before that for simple cubic, $\Sigma = n$. Also, recall that

$$\frac{l_i}{n_i}\tilde{\mathbf{g}}_i^\beta \cdot \mathbf{c}_j \;=\; (\mathbf{g}_i^\beta - \mathbf{g}_i^\alpha)\cdot \mathbf{c}_j \;=\; 2\pi\delta_{ij}. \tag{5.145}$$

from (5.103). $\{l_j\mathbf{c}_j\}$ for $j = 1, 2$ is actually the CSL lattice as we have explicitly shown before. So $\frac{1}{n_i}\tilde{\mathbf{g}}_i^\beta = \frac{1}{\Sigma}\tilde{\mathbf{g}}_i^\beta$ is reciprocal to CSL. On the other hand, we have

$$\mathbf{a}_i^\alpha - \mathbf{a}_i^\beta \;=\; \frac{a^2}{2\pi}\left(\mathbf{g}_i^\beta - \mathbf{g}_i^\alpha\right), \quad \mathbf{t}_i \;=\; \frac{a^2}{2\pi}\tilde{\mathbf{g}}_i^\beta \tag{5.146}$$

So we get $\frac{2\pi}{a^2\Sigma}\mathbf{t}_i = \frac{2\pi}{a^2\Sigma^2}\Sigma\mathbf{t}_i$ to be reciprocal to CSL. This means $\{\Sigma\mathbf{t}_i\}$ is actually the CSL, and so the DSC lattice $\{\mathbf{t}_i\}$ is $\Sigma$ times smaller than the CSL lattice in linear dimension. Since the CSL lattice is area-wise $\Sigma$ times the original lattice area, this means the DSC lattice is area-wise $\Sigma^{-1}$ times the original lattice area, for simple cubic.

### 5.2.2 Grain Boundary As Source/Sink of Incompatibility

In bicrystallography of GB, we talked about misorientation generated by rotation $\mathbf{A} = \mathbf{R}(\mathbf{r}, \theta)$ (3 rotational DOF), and translation in reference to the lattice frame of the DSC $\{\mathbf{t}_i\}$ (3 translational DOF). The last thing to choose is an inclination plane, which has 2 rotational DOF symbolized by $\mathbf{n}$, and 1 translational intercept:

$$\mathbf{n}\cdot\mathbf{x} \;=\; d. \tag{5.147}$$

There are also Gibbs excess $\{N_i^\gamma(T)/A\}$ to describe the chemistry, and excess grand potential $\gamma(T)$ per area to describe the energy penalty of creating the GB. And the above describes only an infinite, flat GB!

If $\mathbf{r}$ lies in the GB plane:

$$\mathbf{n}\cdot\mathbf{a} \;=\; 0 \tag{5.148}$$

this is called a **tilt boundary**. If $\mathbf{r}$ is perpendicular to the inclination plane, this is called a **twist boundary**. Otherwise, the GB is called **mixed**.

In reality the GB can be curvy, and can also interact with lattice dislocation flux, and they can have even more internal state variables.

We have seen previously that if a GB slides by a direction shift complete (DSC) lattice vector

$\mathbf{t}$, then the GB energy stays unchanged (or the pre-relaxation geometry stays unchanged, therefore after relaxation the energy is still the same). Since $\{\mathbf{t}_i\}$ is $\Sigma^{-\frac{1}{2}}$ times the length of the lattice vector, from the elastic energy expression $\propto b^2$, we see that **grain boundary** could be really easy to shear. Indeed, a full Burgers vector lattice dislocation, once it is absorbed into GB, may decompose into many small DSC dislocations, and have a very wide core. Concurrently, the dislocation core drops in energy, so the grain boundary becomes a trap for lattice incompatibility.

Recall that we used no crystallography at all in the definition of the Burger vector

$$\oint_C dl \left(\frac{\partial \mathbf{u}}{\partial l}\right)_{\text{elastic}} = \mathbf{b} \tag{5.149}$$

So even if this dislocation transformed to many smaller dislocations with reduced energy, the **incompatibility content** is still there, localized in the GB. It is like in fair trading involving multiple currencies, the same amount of "value" is always there regardless of how we trade (euro to dollar to pound). This dislocation content in GB is called the **Frank-Bilby content**, which trades with the dislocation content inside the lattice. Even in the situation where we cannot clearly see sharp dislocation cores (smeared cores), the incompatibility content is still there.

There are low-angle ($\theta < 10-15^\circ$) GBs, special high-angle GBs such as twin boundaries, and high-angle "random" GBs (see Fig. 3 of [66]). Near $\theta = 0$ as well as the special high-angle GBs, the grain boundary energy varies with $\Delta\theta$ as:

$$\Delta\gamma = A|\Delta\theta|(B - \ln|\Delta\theta|) \tag{5.150}$$

which represents the cusps (vicinal boundaries are those that are few degrees off from special high-angle GBs). This Read-Shockley formula is explained by so-called dislocation representation of crystal-crystal interfaces. Because dislocations have $1/r$ like stress field, the strain energy density is $\propto 1/r^2$, and so the energy stored near one such dislocation is $\int_{R_0}^{l} 2\pi r dr/r^2 \propto \ln(l/R_0)$, where $R_0$ is some cutoff distance. The dislocation density on the interface (unit 1/m) can be shown to be $\rho_{\text{int}} \equiv 1/l \propto |\Delta\theta| > 0$, thus the energy goes like $-|\Delta\theta|\ln(|\Delta\theta|R_0)$. Similar kind of argument can be made for $\phi$-dependence: it is "cuspy", because crystallographically the vicinal boundaries must exist as long stretches of coherent GBs, plus misfit steps. The energy landscape $\gamma(\theta, \phi)$ contain fractal features like the surface roughness [67], since any irrational $\theta$ can be made infinitely close to a rational special boundary. This mathematical problem can be resolved though by considering thermal fluctuations

and gradient energies.

## 5.3 Wulff stability analysis

Wulff plot: $\gamma(\mathbf{n})\mathbf{n}$, and inverse Wulff plot: $\gamma^{-1}(\mathbf{n})\mathbf{n}$.

Kossel crystal show that surface energy naturally have $\sin|\phi|$ type singularities, with cusps (locally minimal surface energy) occurring at certain special $\phi$'s that have especially well packed surface structure ($\{111\}$, $\{110\}$, $\{100\}$ surfaces in FCC crystals). When $\phi$ deviates just a little bit (either $+$ or $-$) from these special angles, there will be crystallographic *ledges* whose density is $\propto \sin|\Delta\phi|$, causing a singular cusp in the energy vs $\phi$ plot. Such singularity is due to crystallography, and ultimately, the discreteness of atoms.

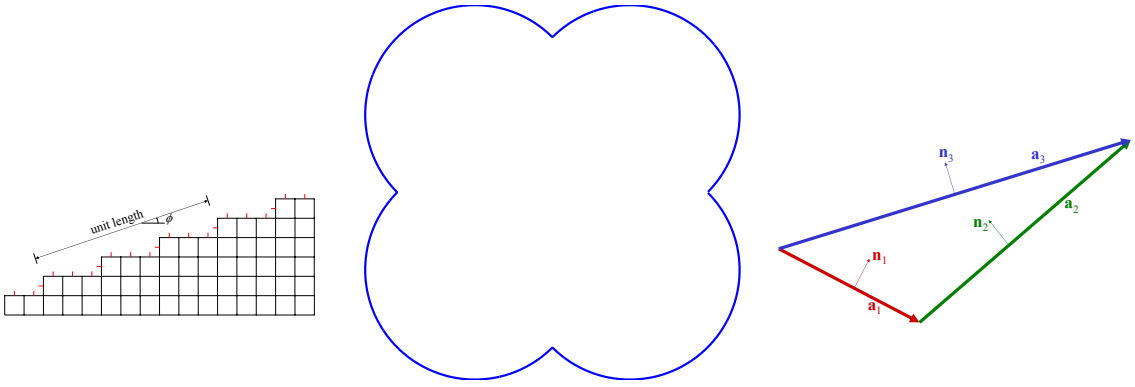


(a) (b) (c)

Figure 5.3:

Stability of a certain thin film surface (constrained on substrate) against decomposition. Consider $\mathbf{a}_1 + \mathbf{a}_2 = \mathbf{a}_3$. First we would like to show

$$a_1\mathbf{n}_1 + a_2\mathbf{n}_2 \;=\; a_3\mathbf{n}_3 \tag{5.151}$$

where $|\mathbf{a}_1| = a_1$, $|\mathbf{a}_2| = a_2$, $|\mathbf{a}_3| = a_3$. Since $a_1\hat{\mathbf{a}}_1 + a_2\hat{\mathbf{a}}_2 = a_3\hat{\mathbf{a}}_3$, we only need to apply $90^\circ$ rotation matrix $\mathbf{R}$ to both left and right-hand side to prove (5.151). There is a more general proof (applicable to tetrahedron in 3D) using Gauss theorem. Define all $\mathbf{n}_i$ of a polyhedra

to be pointing outward. The claim is that

$$\sum_i A_i \mathbf{n}_i \;=\; 0. \tag{5.152}$$

The proof is to consider

$$\mathbf{b}\cdot\sum_i A_i\mathbf{n}_i \;=\; \int_{\text{surface}} dA\mathbf{b}\cdot\mathbf{n} = \int_{\text{body}} d^3\mathbf{x}(\nabla\cdot\mathbf{b}) \;=\; 0. \tag{5.153}$$

for arbitrary $\mathbf{b}$. So (5.152) must be true, and (5.151) is a 2D special case, with normal of 1,2 defined inward as shown in Fig. 5.3(c).

Now the energy of 1+2 combination is $\gamma_1 a_1 + \gamma_2 a_2$. Define

$$\gamma_3^* \;\equiv\; \frac{\gamma_1 a_1 + \gamma_2 a_2}{a_3} \tag{5.154}$$

If the actual $\gamma_3 > \gamma_3^*$, the $\mathbf{n}_3$ facet would be unstable against decomposition into 1+2. However, the geometric equality (5.151) could be rewritten as

$$a_1\gamma_1\gamma_1^{-1}\mathbf{n}_1 + a_2\gamma_2\gamma_2^{-1}\mathbf{n}_2 \;=\; a_3\gamma_3^*\gamma_3^{*-1}\mathbf{n}_3 = \gamma_1 a_1\gamma_3^{*-1}\mathbf{n}_3 + \gamma_2 a_2\gamma_3^{*-1}\mathbf{n}_3 \tag{5.155}$$

So:

$$a_1\gamma_1(\gamma_1^{-1}\mathbf{n}_1 - \gamma_3^{*-1}\mathbf{n}_3) \;=\; a_2\gamma_2(\gamma_3^{*-1}\mathbf{n}_3 - \gamma_2^{-1}\mathbf{n}_2) \tag{5.156}$$

which means $\gamma_3^{*-1}\mathbf{n}_3$ must be on the straightline connecting $\gamma_1^{-1}\mathbf{n}_1$ and $\gamma_2^{-1}\mathbf{n}_2$. If the actual $\gamma_3^{-1}$ lies *inside* of this $\gamma_3^{*-1}$ line segment, then $\gamma_3$ will be unstable against decomposition.

So when we plot the inverse Wulff plot, $\gamma^{-1}(\mathbf{n})\mathbf{n}$. Any facet that is inside the common tangent construction of $\gamma^{-1}(\mathbf{n})\mathbf{n}$ will be unstable against decomposition (read p. 346-349, 608-615 of [68], ignore the discussion about the capillary vector $\xi(\mathbf{n})$). Note that it is possible to adjust the relative position of 1+2 to 3, such that beneath 3 contains exactly the same number of atoms.

Define the angle between $\mathbf{n}_3$ and $\mathbf{n}_1$ to be $\phi$. From the law of sine in inverse Wulff plot, we get

$$\frac{\sin(\pi-\alpha-\phi)}{\gamma_1^{-1}} \;=\; \frac{\sin\alpha}{\gamma_3^{*-1}}. \tag{5.157}$$

In above $\phi$ is variable as $\mathbf{n}_3$ scans between $\mathbf{n}_1$ and $\mathbf{n}_2$, but $\alpha$ is constant, set by $\gamma_1^{-1}\mathbf{n}_1$ and

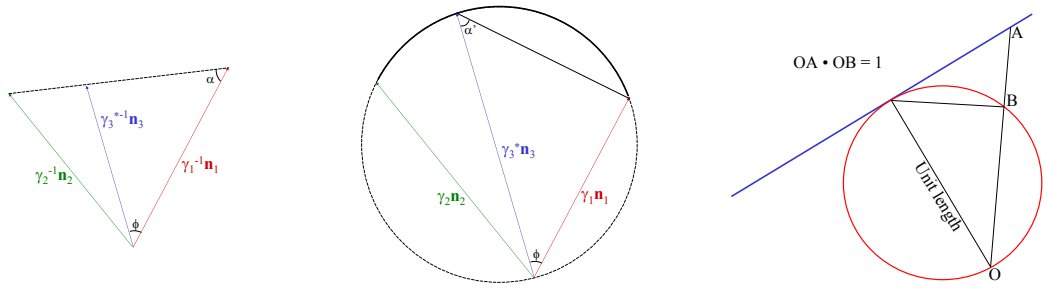


(a) (b) (c)

Figure 5.4: .

$\gamma_2^{-1}\mathbf{n}_2$. We may rewrite the equation then as

$$\gamma_3^*(\phi) \;=\; \gamma_1 \frac{\sin(\pi-\alpha-\phi)}{\sin\alpha}. \tag{5.158}$$

It turns out that $\gamma_3^*(\phi)$ must be part of a circle which goes through three points: the origin, $\gamma_1\mathbf{n}_1$ and $\gamma_2\mathbf{n}_2$. This can proven by the following, consider Fig. 5.4(b). Let us call the angle shown in Fig. 5.4(b) as $\alpha'$. By the law of sine, we have

$$\frac{\sin(\pi-\alpha'-\phi)}{\gamma_3^*(\phi)} \;=\; \frac{\sin\alpha'}{\gamma_1} \quad\rightarrow\quad \gamma_3^*(\phi) = \gamma_1\frac{\sin(\pi-\alpha'-\phi)}{\sin\alpha'}. \tag{5.159}$$

Comparing with (5.158), the only way this can be true is $\alpha' = \alpha$, which is constant. The set of points with such property forms a perfect circle (inscribed angle inside a circle facing a constant chord is constant). An alternative and simpler proof is that a straight line with unity distance to the origin maps to a circle after $r^{-1}$ transformation.

Define $\gamma^*(\mathbf{n})\mathbf{n}$ as the *stable* Wulff plot. Given $\gamma(\mathbf{n})\mathbf{n}$ (from say, a first-principles total energy calculation), one plots $\gamma^{-1}(\mathbf{n})\mathbf{n}$ and eliminate segments of $\gamma^{-1}(\mathbf{n})\mathbf{n}$ that lies *inside* the common tangent construction. The montage of straight-line common tangent segments plus uneliminated $\gamma^{-1}(\mathbf{n})\mathbf{n}$ segments form $\gamma^{*-1}(\mathbf{n})\mathbf{n}$. We then invert $\gamma^{*-1}(\mathbf{n})$ to get $\gamma^*(\mathbf{n})\mathbf{n}$.

Alternatively, the above can be formulated in Wulff space directly. **Tangent circle theorem**: Given $\gamma(\mathbf{n})\mathbf{n}$, both the necessary and sufficient condition that $\gamma^*(\mathbf{n}') = \gamma(\mathbf{n}')$ for a particular $\mathbf{n}'$ is that if one draws a circle through the origin and tangent to $\gamma(\mathbf{n})\mathbf{n}$ at $\mathbf{n}'$, such tangent circle lies completely *within* $\gamma(\mathbf{n})\mathbf{n}$ and do not hit any other points on $\gamma(\mathbf{n})\mathbf{n}$. This is because a tangent line of $\gamma^{-1}(\mathbf{n})\mathbf{n}$ that does not hit $\gamma^{-1}(\mathbf{n})\mathbf{n}$ at any other point maps to

a tangent circle inside $\gamma(\mathbf{n})\mathbf{n}$.

The tangent circle theorem and decomposition test is useful for thin-film surface on substrate. For free-standing crystallite such as formed in deposition, where surface energy dominates the shape, we need **Wulff construction**: consider a crystal with $f$ possible surface orientations $\mathbf{n}_i$. Denote their distance to the center as $h_i$. Then the exposed length is $a_i$. Clearly,

$$a_i \;=\; a_i(h_{i-1}, h_i, h_{i+1}). \tag{5.160}$$

We also have the following reciprocal relation:

$$\frac{\partial a_i}{\partial h_{i-1}} \;=\; \frac{\partial a_{i-1}}{\partial h_i} \;=\; \frac{1}{\sin\theta_{i,i-1}}, \tag{5.161}$$

which can be proven from inspecting the geometry, where $\theta_{i,i-1}$ is the angle between $\mathbf{n}_i$ and $\mathbf{n}_{i-1}$.

Now consider a free-standing particle of fixed volume $V$. We seek the shape that minimizes its surface energy:

$$F_{\text{surface}} \;=\; \sum_i \gamma_i a_i, \tag{5.162}$$

with the shape completely determined by the $\{h_i\}$. Change in volume must be constrained to zero:

$$0 \;=\; \sum_i a_i dh_i, \tag{5.163}$$

and

$$dF_{\text{surface}} \;=\; \sum_i \left(\gamma_{i-1}\frac{\partial a_{i-1}}{\partial h_i} + \gamma_i \frac{\partial a_i}{\partial h_i} + \gamma_{i+1}\frac{\partial a_{i+1}}{\partial h_i}\right) dh_i, \tag{5.164}$$

so there must be

$$\gamma_{i-1}\frac{\partial a_{i-1}}{\partial h_i} + \gamma_i \frac{\partial a_i}{\partial h_i} + \gamma_{i+1}\frac{\partial a_{i+1}}{\partial h_i} \;=\; \beta a_i, \tag{5.165}$$

where $a_i$ is the Lagrange multiplier. Using the reciprocal relation:

$$\gamma_{i-1}\frac{\partial a_i}{\partial h_{i-1}} + \gamma_i \frac{\partial a_i}{\partial h_i} + \gamma_{i+1}\frac{\partial a_i}{\partial h_{i+1}} \;=\; \beta a_i. \tag{5.166}$$

On the other hand, $a_i(h_{i-1}, h_i, h_{i+1})$ is a homogeneous function of degree 1 (in 2D):

$$a_i(lh_{i-1}, lh_i, lh_{i+1}) \;=\; la_i(h_{i-1}, h_i, h_{i+1}) \tag{5.167}$$

So by taking derivative against $l$ on both sides, and then setting $l = 1$, there is

$$h_{i-1}\frac{\partial a_i}{\partial h_{i-1}} + h_i\frac{\partial a_i}{\partial h_i} + h_{i+1}\frac{\partial a_i}{\partial h_{i+1}} \;=\; a_i. \tag{5.168}$$

In 3D, there is $a_i(lh_{i-1}, lh_i, lh_{i+1}) = l^2 a_i(h_{i-1}, h_i, h_{i+1})$ and $h_{i-1}\frac{\partial a_i}{\partial h_{i-1}} + h_i\frac{\partial a_i}{\partial h_i} + h_{i+1}\frac{\partial a_i}{\partial h_{i+1}} = 2a_i$.

Comparing the two equations, we see that

$$... = \frac{\gamma_{i-1}}{h_{i-1}} = \frac{\gamma_i}{h_i} = \frac{\gamma_{i+1}}{h_{i+1}} = ... = \beta \tag{5.169}$$

for all $i$, will be a variational extremum. In fact, $dF_{\text{surface}} = dF_{\text{bulk}} = (P_{\text{int}} - P_{\text{ext}})dV$ is the original Young-Laplace pressure argument (Fig. **??**(a)), and the facet-independent Lagrange multiplier $\beta$ can be identified to be simply the Young-Laplace pressure difference $\Delta P = P_{\text{int}} - P_{\text{ext}}$. So in 2D, we have $\Delta P = \frac{\gamma_i}{h_i}$.

The above means that the inner envelope formed by all Wulff planes (a Wulff plane lies perpendicular to $\gamma(\mathbf{n})\mathbf{n}$ at $\gamma(\mathbf{n})\mathbf{n}$) gives the equilibrium shape of a free-standing nanocrystal. This is called **Wulff construction**, which minimizes the total surface energy of a free-standing nanoparticle. Note that the Wulff construction serves a different purpose from the tangent circle theorem. The tangent circle theorem deals with the stability of *one* surface constrained to have overall inclination $\mathbf{n}'$ because it must conform to the substrate, whereas the Wulff construction needs to optimize all facets of the nanocrystal simultaneously.

In 3D, there is an extra factor of $\frac{1}{2}$ on RHS, and we get

$$... = \frac{\gamma_{i-1}}{h_{i-1}} = \frac{\gamma_i}{h_i} = \frac{\gamma_{i+1}}{h_{i+1}} = ... = \frac{\beta}{2} = \frac{\Delta P}{2} \tag{5.170}$$

or $\Delta P = \frac{2\gamma_i}{h_i}$ to be the pressure increase inside the solid particle. We see that for isotropic surface energy and spherical particle, this reduces to the familiar expression $\Delta P = \frac{2\gamma}{R}$.

## 5.4 Gradient Thermodynamics Description of the Interface

First-order phase transition is characterized by *finite jump* in the order parameter $\eta^\alpha \to \eta^\beta$ as soon as $T = T_e^{\pm}$ (the nucleation rate may be very small, but theoretically suppose one

waits long enough one can witness this finite jump at $T_e^{\pm}$). For example, melting of ice at $P = 1$atm is a first-order transition because as soon as $T$ rises up to 0.0001°C and melting can occur, there is a finite density change from ice to liquid water, and there is an *obvious* change in the viscosity as well. Also spatially, the transition from $\eta(\mathbf{x}) = \eta^{\alpha}$ to $\eta(\mathbf{x}') = \eta^{\beta}$ typically occurs over a *very narrow region*: the shortest distance between $\mathbf{x}$ and $\mathbf{x}'$ (interfacial thickness $w$) is *typically* less than 1nm. Previously, we assigned a capillary energy $\gamma$ to this interfacial region without discussing this region's detailed *structure*. Such "sharp interface" view, where one ignores the detailed interfacial structure and represent it as a geometric dividing surface, is sufficient for most first-order phase transition problems. If one is really interested in the physical thickness of this interfacial region however, one must use so-called gradient thermodynamics formulation [69] to be introduced below, where the capillary energy $\int \gamma dA$ in the sharp-interface representation is replaced by a 3D integral involving a gradient squared term $\int K|\nabla\eta(\mathbf{x})|^2 d^3\mathbf{x}$ with $K > 0$. The above replacement makes sense intuitively, since the interfacial region is characterized by large gradients in $\eta(\mathbf{x})$, absent in the homogeneous bulk regions of $\alpha$ or $\beta$. Nucleation and growth is a must for all first-order phase transitions, where *large change* ($\eta^{\alpha} \to \eta^{\beta}$) occurs in a *narrow region* (the interface) even during nucleation.

In contrast, second-order phase transition is characterized by *initially infinitesimal changes* over a *wide region*. These initially infinitesimal changes appear spontaneously in the system and grow with time, without going through a nucleation (large change in a small region) stage. For example, in the paramagnetic ($\alpha$)→ferromagnetic ($\alpha 1$,$\alpha 2$) transition of pure iron as $T$ is cooled below $T_c = 1043$K (the Curie temperature, also called the critical point), both the spin-down $\alpha 1$ and the spin-up $\alpha 2$ phase have very small magnetic moments: $\eta^{\alpha 1} = -m$, $\eta^{\alpha 2} = m$, with $m \propto (T_c - T)^{1/2}$. Microscopically, going from $\alpha 1$ to $\alpha 2$ near $T_c$ would involve the flipping of a very small number of spins. So the high-temperature paramagnetic phase, and the two low-temperature ferromagnetic phases are very similar to each other near $T_c$: $|\eta^{\alpha} - \eta^{\alpha 1}|, |\eta^{\alpha} - \eta^{\alpha 2}| \propto (T_c - T)^{1/2}$, where $\eta$ is the magnetic moment. The breakup of a uniform paramagnetic domain into multiple ferromagnetic domains upon a drop in temperature below $T_c$ is spontaneous and instantaneous and *does not require* a nucleation stage: it is growth, off the bat. In other words, no under-cooling is required for observing *the start* of second-order phase transition within a given observation period. The growth happens essentially instantaneously at $T = T_c^{\pm}$. Although, to see the growth and coarsening to a certain amplitude would require time.

The way a system can accomplish second-order transition vis-à-vis first-order transition is

best illustrated using the binary solution example: $g_{\text{soln}}(X_2, T) \equiv G_{\text{soln}}(N_1, N_2, T)/(N_1+N_2)$. Suppose $\Omega_1 = \Omega_2 = \Omega$, we may define specific volume free energy as

$$g_v(c_2) \equiv \Omega^{-1} g_{\text{soln}}(X_2 = c_2\Omega) \tag{5.171}$$

so the bulk solution free energy for a homogeneous system is just

$$G_{\text{soln}} = \left(\int d^3\mathbf{x}\right) g_v(c_2). \tag{5.172}$$

$g_v(c_2)$ is the same function as $g_{\text{soln}}(X_2)$ after horizontal and vertical scaling. So the tangent extrapolation of $g_v(c_2)$ to $c_2 = 0$ (corresponding to $\mathbf{X} = \mathbf{p}_1$) would give $\Omega^{-1}\mu_1$, and tangent extrapolation of $g_v(c_2)$ to $c_2 = \Omega^{-1}$ (corresponding to $\mathbf{X} = \mathbf{p}_2$) would give $\Omega^{-1}\mu_2$. $c_2(\mathbf{x})$ is our order parameter field $\eta(\mathbf{x})$ here. For an inhomogeneous system, the solution free energy should intuitively be written as

$$G_{\text{soln}} = \int d^3\mathbf{x} g_v(c_2(\mathbf{x})). \tag{5.173}$$

Using the above as reference, the total free energy then looks like:

$$G = \int d^3\mathbf{x}(g_v(c_2(\mathbf{x})) + K|\nabla c_2(\mathbf{x})|^2) + G_{\text{elastic}} \tag{5.174}$$

where the gradient squared term replaces the capillary energy $\int \gamma dA$. $G_{\text{elastic}} = 0$ if $\Omega_1 = \Omega_2 = \Omega$. (5.174) is a unified model that can be used to investigate both finite interfacial thickness in first-order transitions [69], as well as second-order transitions [70]. Since $K > 0$, the model (5.174) punishes sharp spatial gradients, the origin of interfacial energy. On the other hand if all changes occur smoothly over a large wavelength with small spatial gradients, then $G$ approaches $G_{\text{soln}}$. Since $G_{\text{soln}}$ is the driver of phase transformation (gradient/capillary and elastic energies are typically positive), let us consider what $G_{\text{soln}}$ wants to do first.

For a closed system, $c_2$ is *conserved*:

$$\int d^3\mathbf{x} c_2(\mathbf{x}) = \text{const} \tag{5.175}$$

which means it is possible to *partition* the solutes, but it is not possible to change the total amount of solutes in the entire system. For instance, if one starts out with a uniform concentration $c_2(\mathbf{x}) = c_2^\alpha$, a partition may roughly speaking occur as:

$$c_2^\alpha = f^{\alpha 1} c_2^{\alpha 1} + f^{\alpha 2} c_2^{\alpha 2}, \tag{5.176}$$

where volume fraction

$$f^{\alpha 1} \;=\; \frac{c_2^{\alpha 2} - c_2^{\alpha}}{c_2^{\alpha 2} - c_2^{\alpha 1}}, \quad f^{\alpha 2} \;=\; 1 - f^{\alpha 1} = \frac{c_2^{\alpha} - c_2^{\alpha 1}}{c_2^{\alpha 2} - c_2^{\alpha 1}} \tag{5.177}$$

of the region has $c_2(\mathbf{x}) = c_2^{\alpha 1}$ and $c_2(\mathbf{x}) = c_2^{\alpha 2}$, respectively, separated by sharp interfaces. The solution free energy of the *partitioned* system is then

$$G_{\text{soln}} \;=\; \left(\int d^3\mathbf{x}\right) \left(f^{\alpha 1} g_v(c_2^{\alpha 1}) + f^{\alpha 2} g_v(c_2^{\alpha 2})\right) \tag{5.178}$$

compared to the unpartitioned and uniform original system $\left(\int d^3\mathbf{x}\right) g_v(c_2^{\alpha})$.

*Local stability* means $G_{\text{soln}}$ is stable against small perturbations in $c_2(\mathbf{x})$. The necessary and sufficient condition for local stability is that

$$\frac{\partial^2 g_v}{\partial c_2^2} \;>\; 0. \tag{5.179}$$

If $\frac{\partial^2 g_v}{\partial c_2^2} < 0$, a small partition with $c_2^{\alpha 1} \approx c_2^{\alpha} \approx c_2^{\alpha 2}$ would be able to decrease $G_{\text{soln}}$. For example, with $c_2^{\alpha 2} = c_2^{\alpha} + \Delta c$, $c_2^{\alpha 1} = c_2^{\alpha} - \Delta c$, $f^{\alpha 1} = f^{\alpha 2} = 1/2$, one has

$$\frac{G_{\text{soln}}}{\int d^3\mathbf{x}} \;=\; \frac{1}{2} g_v(c_2^{\alpha} - \Delta c) + \frac{1}{2} g_v(c_2^{\alpha} + \Delta c) \;=\; g_v(c_2^{\alpha}) + \frac{1}{2}\frac{\partial^2 g_v}{\partial c_2^2}(c_2^{\alpha})(\Delta c)^2 + ... \tag{5.180}$$

which would be lower than uniform $g_v(c_2^{\alpha})$ if $\frac{\partial^2 g_v}{\partial c_2^2} < 0$. A sinusoidal perturbation

$$c_2(\mathbf{x}) \;=\; c_2^{\alpha} + a(t)\sin(\mathbf{k}\cdot\mathbf{x}) \tag{5.181}$$

would also have equal amount of "ups and downs", and would thus also reduce $G_{\text{soln}}$. The reason sinusoidal perturbation is preferred (at least initially) compared to the step function between $c_2^{\alpha} - \Delta c$ and $c_2^{\alpha} + \Delta c$ is that it minimizes the gradient energy by spreading the gradients around. Therefore if $\frac{\partial^2 g_v}{\partial c_2^2} < 0$, its amplitude $a(t)$ will increase with time. This is the trick behind spinodal decomposition, or more generally second-order phase transitions, which can reduce the system free energy without nucleation. *Nucleation is not needed here because the system's initial state does not have local stability.* The loss of local stability is induced by temperature, i.e.

$$\frac{\partial^2 g_v}{\partial c_2^2}(c_2^{\alpha}, T_{\text{C}}^{+}) \;>\; 0, \quad \frac{\partial^2 g_v}{\partial c_2^2}(c_2^{\alpha}, T_{\text{C}}^{-}) \;<\; 0 \tag{5.182}$$

thus

$$\frac{\partial^2 g_v}{\partial c_2^2}(c_2^\alpha, T_{\rm C}) \;=\; 0. \tag{5.183}$$

During initial growth of the sinusoidal profile in the unstable composition range, the solutes appears to diffuse *up* the concentration gradient (Fig. 5.39 of [71]). According to the phenomenological Fick's 1st law $\mathbf{J}_2 = -\tilde{D}\nabla c_2$, this would mean a negative interdiffusivity $\tilde{D}(c_2) < 0$. This is in fact not surprising, because $\tilde{D}$ (from $D_1, D_2$) contains thermodynamic factor $1 + \frac{d\ln\gamma_2}{d\ln c_2}$, which can be shown to be $\frac{X_2(1-X_2)}{k_{\rm B}T}\frac{\partial^2 g}{\partial X_2^2}$ and thus have the same sign as $\frac{\partial^2 g}{\partial X_2^2}$. When $\frac{\partial^2 g}{\partial X_2^2}$ is negative, $\tilde{D}$ is negative. This means that at the most fundamental level, diffusion is driven by the desire to reduce free energy or chemical potential, and *not* by the desire to smear out the concentration gradient.

Mathematically, while a positive diffusivity tends to smear out the profile (the shorter the wavelength, the faster the decay of the Fourier component amplitude), a negative diffusivity would tend to increase the roughness of the profile. The growth of very-small wavelength fluctuations in spinodal decomposition will be punished by the gradient energy, though. Thus an optimal wavelength will be selected initially, which can be tens of nms. Later, after the compositions have deviated largely from $c_2^\alpha$, the microstructural lengthscale may further coarsen, although the interfacial lengthscale will sharpen. Because $\alpha 1$ and $\alpha 2$ do not come out of a nucleation and growth process, but amplification of sinusoidal waves of certain optimal wavelength, they lead to unique-looking interpenetrating microstructures.

In contrast to spinodal instability, *in a first-order phase transition the system's initial state has never lost its local stability.* At $T = T_e^+$, one is in a *globally stable* uniform composition, which means

$$g_v(c_2^\alpha, T_e^+) \;<\; f^{\alpha 1} g_v(c_2^{\alpha 1}, T_e^+) + f^{\alpha 2} g_v(c_2^{\alpha 2}, T_e^+) \tag{5.184}$$

for small and large deviations $|c_2^{\alpha 2} - c_2^\alpha|$ alike (thus a globally stable system must be locally stable, but not vice versa). Then at $T = T_e^-$, $c_2(\mathbf{x}) = c_2^\alpha$ becomes locally stable *only*, which means small deviations would still induce the system energy to go up, but large deviations may induce the system energy to go down. *Thus, small perturbations like (5.181) would decay and die, but large enough perturbations may survive.* The chance survival of large enough perturbations/fluctuations in the order-parameter field is just nucleation.

(5.174) can be used to estimate interfacial thickness $w$ in the following manner. Since $\nabla c_2 \propto (c_2^\beta - c_2^\alpha)/w$ inside the interface, the gradient energy integral scales as $K(c_2^\beta - c_2^\alpha)^2/w$, so the wider the interface the better for the gradient energy. On the other hand, right at $T = T_e$,

$g_v(c_2)$ of the first term connects two energy-degenerate states $g_v(c_2 = c_2^\beta) = g_v(c_2 = c_2^\alpha)$, with a bump $g_v^* - g_v(c_2^\alpha)$ in between. The solution free energy first term thus gives an excess $\propto (g_v^* - g_v(c_2^\alpha))w$, that punishes wide interfaces. The best compromised is thus reached at $w \propto K^{1/2}|c_2^\beta - c_2^\alpha|(g_v^* - g_v(c_2^\alpha))^{-1/2}$, with interfacial energy $\gamma \propto K^{1/2}|c_2^\beta - c_2^\alpha|(g_v^* - g_v(c_2^\alpha))^{1/2}$. It turns out that for $T_e$ near $T_c$, $|c_2^\beta - c_2^\alpha| \propto (\Delta T)^{1/2}$, where $\Delta T = T_c - T_e$, and $g_v^* - g_v(c_2^\alpha) \propto (\Delta T)^2$, so the interfacial width near the critical temperature would diverge as $(\Delta T)^{-1/2}$, and the interfacial energy would vanish as $(\Delta T)^{3/2}$ [69].

Science advances greatly when two seemingly different concepts are connected, for instance the Einstein relation $M = D/k_{\mathrm{B}}T$. Cahn and Hilliard made a similar contribution when they connected interfacial energy to critical temperature and second-order phase transformation. Based on the insight that gradient term should be added to thermodynamic field theories (fundamentally this is because of atomic discreteness), they developed gradient thermodynamics formalism for chemical solution systems that predict finite interfacial width, interfacial energy, as well as wavelength selection in spinodal decomposition [70], under one unified framework. The development can in fact be traced back to the work of van der Waals for single-component systems, using density as order parameter[72]. Another offshoot of this approach was provided by Ginzburg and Landau in the theory of superconductivity.

Finally, if $\Omega_1 \neq \Omega_2$ the 1-rich $\alpha 1$ phase and 2-rich $\alpha 2$ will have different stress-free volumes, and to accommodate this mismatch coherently would involve finite elastic energy $G_{\mathrm{elastic}} > 0$. Growth of the sinusoidal concentration wave would require growth of the associated transformation strain wave. This would delay the onset of the spinodal instability.

# Appendix A

# Notes on Transformation Elasticity

## A.1 Inhomogeneous Elasticity Solver in Supercell under Periodic Boundary Condition

Given an original supercell [73] $\mathbf{H}_0$, with $\mathbf{x} = \mathbf{s}\mathbf{H}_0$, $\mathbf{s} \in [0, 1)$, we would like to solve the following problem:

$$F^{\text{el}}[\mathbf{H}, \boldsymbol{\epsilon}^0(\mathbf{x})] \equiv \min_{\mathbf{u}(\mathbf{x})} F^{\text{el}}[\mathbf{u}(\mathbf{x})|\mathbf{H}, \boldsymbol{\epsilon}^0(\mathbf{x})] \tag{A.1}$$

$$F^{\text{el}}[\mathbf{u}(\mathbf{x})|\mathbf{H}, \boldsymbol{\epsilon}^0(\mathbf{x})] \equiv \frac{1}{2}\int d^3\mathbf{x} c_{ijpq}(\mathbf{x})(\epsilon_{ij}(\mathbf{x}) - \epsilon^0_{ij}(\mathbf{x}))(\epsilon_{pq}(\mathbf{x}) - \epsilon^0_{pq}(\mathbf{x})) \tag{A.2}$$

where $\mathbf{u}(\mathbf{x}) \equiv \mathbf{x}' - \mathbf{x}$, the difference between the new position $\mathbf{x}'$ and the old position $\mathbf{x}$, and

$$\epsilon_{ij}(\mathbf{x}) \equiv \frac{u_{i,j} + u_{j,i}}{2}. \tag{A.3}$$

$\mathbf{H}$ is the new supercell: $\mathbf{H} = \mathbf{H}_0(\mathbf{I} + \bar{\boldsymbol{\epsilon}})$. Global rotation of $\mathbf{H}$ does not matter anyhow to (A.2) to first order in the global rotation angle, and is therefore ignored in this leading-order theory. Note that the untransformed material in $\mathbf{H}_0$ does not have to be stress free. The entire role of $\mathbf{H}_0$ in the above is to provide a reference grid.

(A.2) is motivated by the following idea experiment. One first cuts up the *untransformed supercell* $\mathbf{H}_0$ into many blocks $d^3\mathbf{x}$. Then imagine for instance the temperature is raised, and phase transformation / plasticity may induce some blocks to transform to a new state. Each block, if left alone (stress free), would like to transform to a new strain state $\boldsymbol{\epsilon}^0(\mathbf{x})$.

Additional local rotation $\mathbf{R}(\mathbf{x})$ of the block does not matter to the internal Helmholtz free energy of *this* block [74, 75], but needs to be globally optimized since $\mathbf{R}(\mathbf{x})$ must be globally consistent with $\mathbf{u}(\mathbf{x})$.

Because of the periodic boundary condition, there must be

$$\mathbf{u}(\mathbf{x}+\mathbf{h}_0)-\mathbf{u}(\mathbf{x}) \;=\; \mathbf{h}_0\bar{\boldsymbol{\epsilon}} \tag{A.4}$$

where $\mathbf{h}_0$ is one of the $\mathbf{H}_0$ edge vectors. So

$$\int_0^{\mathbf{h}_0} d\mathbf{x}'\cdot\frac{d\mathbf{u}(\mathbf{x}+\mathbf{x}')}{d\mathbf{x}'} \;=\; \mathbf{h}_0\bar{\boldsymbol{\epsilon}} \;\;\rightarrow\;\; \int d^3\mathbf{x}\frac{d\mathbf{u}}{d\mathbf{x}} = \det|\mathbf{H}_0|\bar{\boldsymbol{\epsilon}}. \tag{A.5}$$

Note that $\{\epsilon_{ij}(\mathbf{x})\}$, because of (A.3), need to satisfy three compatibility constraints

$$\epsilon_{ii,jj}+\epsilon_{jj,ii} \;=\; 2\epsilon_{ij,ij}, \quad \forall i\neq j \tag{A.6}$$

which means the $\{\epsilon_{ij}(\mathbf{x})\}$ fields are not independent fields in the variational functional (the $\{u_i(\mathbf{x})\}$ fields are). On the other hand, there is no compatibility constraint [76] on the stress-free strain fields $\{\epsilon^0_{ij}(\mathbf{x})\}$, which are "given" in the elastic constant minimization problem.

The functional to be minimized in (A.2) represents a quadratic expansion approximation of the Helmholtz free energy [75] around the *freely transformed* block. As such, there should be a conversion factor $\det|d^3\mathbf{x}'|/\det|d^3\mathbf{x}|$ as well as tensor rotation using $\mathbf{R}(\mathbf{x})$ to convert the isothermal elastic constant of the transformed material to $c_{ijpq}(\mathbf{x})$, which is based on the original volume and observation coordinates. However, this effect is higher order, same as the higher-order terms ignored in (A.3).

Unlike the more general nonlinear formulation of [76], the merit of the quadratic expansion is that (A.2) is quadratic in $\mathbf{u}(\mathbf{x})$, whose minimization (in principle at least) entertains a close-formed solution in the form of a matrix inverse, after real-space discretization of $\mathbf{u}(\mathbf{x})$ and representation of $\nabla^2$-like operators. We have the stress equilibrium equation in structurally inhomogeneous and elastically inhomogeneous material:

$$\left(c_{ijpq}(\mathbf{x})(u_{p,q}(\mathbf{x})-\epsilon^0_{pq}(\mathbf{x}))\right)_{,j} \;=\; 0, \quad \forall i=1..3 \tag{A.7}$$

### A.1.1 Homogeneous Special Case

If the system is elastically homogeneous [77], $c_{ijpq}(\mathbf{x}) = c^0_{ijpq}$, there is translational symmetry in the problem:

$$c^0_{ijpq}(u_{p,q}(\mathbf{x}) - \epsilon^0_{pq}(\mathbf{x}))_{,j} \;=\; 0, \quad \forall i = 1..3 \tag{A.8}$$

and the inverse can be done in the Fourier space on a $\mathbf{k}$-by-$\mathbf{k}$ basis. We first note that $u_p(\mathbf{x})$ can be decomposed into a secularly growing component in $\mathbf{x}$, plus a periodic component:

$$u_p(\mathbf{x}) \;\equiv\; \mathbf{x}\bar{\boldsymbol{\epsilon}} + \tilde{u}_p(\mathbf{x}) \tag{A.9}$$

Then stress equilibrium requires that in $\mathbf{k}$-space:

$$-c^0_{ijpq}k_q k_j \tilde{u}_p(\mathbf{k}) \;=\; ic^0_{ijpq}\epsilon^0_{pq}(\mathbf{k})k_j \tag{A.10}$$

where

$$\tilde{u}_p(\mathbf{k}) \;\equiv\; \int d^3\mathbf{x}\tilde{u}_p(\mathbf{x})e^{-i\mathbf{k}\cdot\mathbf{x}}, \quad \tilde{u}_p(\mathbf{x}) \;=\; \frac{1}{\det|\mathbf{H}_0|}\sum_{\mathbf{k}}\tilde{u}_p(\mathbf{k})e^{i\mathbf{k}\cdot\mathbf{x}}, \tag{A.11}$$

and similarly $\epsilon^0_{pq}(\mathbf{k}) \leftrightarrow \epsilon^0_{pq}(\mathbf{x})$. If we define symmetric matrix $\mathbf{C}(\hat{\mathbf{k}})$ [77]

$$C_{ip}(\hat{\mathbf{k}}) \;\equiv\; c^0_{ijpq}\hat{k}_q\hat{k}_j, \quad \hat{\mathbf{k}} \equiv \frac{\mathbf{k}}{|\mathbf{k}|}, \tag{A.12}$$

the inverse matrix is also real and symmetric: $\boldsymbol{\Omega}(\hat{\mathbf{k}}) \equiv \mathbf{C}^{-1}(\hat{\mathbf{k}})$. Let us also define strain-free stress:

$$\sigma^0_{ij}(\mathbf{x}) \;\equiv\; c^0_{ijpq}\epsilon^0_{pq}(\mathbf{x}), \quad \sigma^0_{ij}(\mathbf{k}) \;\equiv\; c^0_{ijpq}\epsilon^0_{pq}(\mathbf{k}), \tag{A.13}$$

then

$$-|\mathbf{k}|^2 C_{ip}(\hat{\mathbf{k}})\tilde{u}_p(\mathbf{k}) \;=\; i\sigma^0_{ij}(\mathbf{k})k_j \tag{A.14}$$

and $\tilde{u}_p(\mathbf{k})$ is obtained explicitly as

$$\tilde{u}_p(\mathbf{k}) \;=\; \frac{\Omega_{pi'}(\hat{\mathbf{k}})\sigma^0_{i'j'}(\mathbf{k})k_{j'}}{i|\mathbf{k}|^2}. \tag{A.15}$$

Since $i\sigma^0_{ij}(\mathbf{k})k_j$ represents the divergence of stress, or net force, $-\frac{\Omega_{pi}(\hat{\mathbf{k}})}{|\mathbf{k}|^2}$ is just the infinite-space Green's function relating force to displacement in this translationally invariant system. This Green's function is short-ranged in reciprocal space (in fact $\mathbf{k}$-by-$\mathbf{k}$ local), but long-ranged in real space. Thus it is advantageous to solve homogeneous-material problems in

reciprocal space, which is more generally called the spectral method.

The strain field that corresponds to the (A.15) displacement field is

$$\tilde{\epsilon}_{pq}(\mathbf{k}) \;=\; \frac{ik_q\tilde{u}_p(\mathbf{k}) + ik_p\tilde{u}_q(\mathbf{k})}{2} \;=\; \frac{\Omega_{pi'}(\hat{\mathbf{k}})\sigma^0_{i'j'}(\mathbf{k})\hat{k}_{j'}\hat{k}_q + \Omega_{qi'}(\hat{\mathbf{k}})\sigma^0_{i'j'}(\mathbf{k})\hat{k}_{j'}\hat{k}_p}{2}, \tag{A.16}$$

$$\epsilon_{pq}(\mathbf{x}) \;=\; \bar{\epsilon}_{pq} + \tilde{\epsilon}_{pq}(\mathbf{x}), \quad \int d^3\mathbf{x}\tilde{\epsilon}_{pq}(\mathbf{x}) = 0. \tag{A.17}$$

The rotation field $\mathbf{R}(\mathbf{x}) = \mathbf{I} + \mathbf{W}(\mathbf{x})$ that corresponds to (A.15) displacement field is

$$W_{pq}(\mathbf{k}) \;=\; \frac{\Omega_{pi'}(\hat{\mathbf{k}})\sigma^0_{i'j'}(\mathbf{k})\hat{k}_{j'}\hat{k}_q - \Omega_{qi'}(\hat{\mathbf{k}})\sigma^0_{i'j'}(\mathbf{k})\hat{k}_{j'}\hat{k}_p}{2}. \tag{A.18}$$

The stress field is

$$\sigma_{ij}(\mathbf{x}) = \quad c^0_{ijpq}\bar{\epsilon}_{pq} + c^0_{ijpq}\tilde{\epsilon}_{pq}(\mathbf{x}) - \sigma^0_{ij}(\mathbf{x}) \tag{A.19}$$

$$\begin{aligned}
\sigma_{ij}(\mathbf{k}) = \quad & \det|\mathbf{H}_0|c^0_{ijpq}\bar{\epsilon}_{pq}\delta_{\mathbf{k}} + c^0_{ijpq}\tilde{\epsilon}_{pq}(\mathbf{k}) - \sigma^0_{ij}(\mathbf{k}) \qquad (A.20)\\
= \quad & \det|\mathbf{H}_0|c^0_{ijpq}\bar{\epsilon}_{pq}\delta_{\mathbf{k}} + \frac{c^0_{ijpq}\Omega_{pi'}(\hat{\mathbf{k}})\sigma^0_{i'j'}(\mathbf{k})\hat{k}_{j'}\hat{k}_q + c^0_{ijpq}\Omega_{qi'}(\hat{\mathbf{k}})\sigma^0_{i'j'}(\mathbf{k})\hat{k}_{j'}\hat{k}_p}{2} - \sigma^0_{ij}(\mathbf{k})
\end{aligned}$$

We see that the $\sigma_{ij}(\mathbf{k})$ solution above satisfy stress equilibrium:

$$\begin{aligned}
\sigma_{ij}(\mathbf{k})k_j = \quad & |\mathbf{k}|\frac{c^0_{ijpq}\Omega_{pi'}(\hat{\mathbf{k}})\sigma^0_{i'j'}(\mathbf{k})\hat{k}_{j'}\hat{k}_q\hat{k}_j + c^0_{ijpq}\Omega_{qi'}(\hat{\mathbf{k}})\sigma^0_{i'j'}(\mathbf{k})\hat{k}_{j'}\hat{k}_p\hat{k}_j}{2} - |\mathbf{k}|\sigma^0_{ij}(\mathbf{k})\hat{k}_j\\
= \quad & |\mathbf{k}|\frac{C_{ip}(\hat{\mathbf{k}})\Omega_{pi'}(\hat{\mathbf{k}})\sigma^0_{i'j'}(\mathbf{k})\hat{k}_{j'} + C_{iq}(\hat{\mathbf{k}})\Omega_{qi'}(\hat{\mathbf{k}})\sigma^0_{i'j'}(\mathbf{k})\hat{k}_{j'}}{2} - |\mathbf{k}|\sigma^0_{ij}(\mathbf{k})\hat{k}_j\\
= \quad & |\mathbf{k}|\frac{\delta_{ii'}\sigma^0_{i'j'}(\mathbf{k})\hat{k}_{j'} + \delta_{ii'}\sigma^0_{i'j'}(\mathbf{k})\hat{k}_{j'}}{2} - |\mathbf{k}|\sigma^0_{ij}(\mathbf{k})\hat{k}_j\\
= \quad & 0. \qquad (A.21)
\end{aligned}$$

(A.2) is then relaxed to be:

$$\begin{aligned}
F^{\mathrm{el}}[\mathbf{H}, \boldsymbol{\epsilon}^0(\mathbf{x})] = \quad & \int \frac{d^3\mathbf{x}}{2}c^0_{ijpq}\epsilon^0_{ij}(\mathbf{x})\epsilon^0_{pq}(\mathbf{x}) - \int d^3\mathbf{x}c^0_{ijpq}\epsilon^0_{ij}(\mathbf{x})\epsilon_{pq}(\mathbf{x}) + \int \frac{d^3\mathbf{x}}{2}c^0_{ijpq}\epsilon_{ij}(\mathbf{x})\epsilon_{pq}(\mathbf{x})\\
= \quad & \int \frac{d^3\mathbf{x}}{2}c^0_{ijpq}\epsilon^0_{ij}(\mathbf{x})\epsilon^0_{pq}(\mathbf{x}) - \int d^3\mathbf{x}c^0_{ijpq}\epsilon^0_{ij}(\mathbf{x})\bar{\epsilon}_{pq} + \int \frac{d^3\mathbf{x}}{2}c^0_{ijpq}\bar{\epsilon}_{ij}\bar{\epsilon}_{pq}
\end{aligned}$$

$$
\begin{aligned}
- \quad & \int d^3\mathbf{x} c^0_{ijpq}\epsilon^0_{ij}(\mathbf{x})\tilde{\epsilon}_{pq}(\mathbf{x}) + \int \frac{d^3\mathbf{x}}{2} c^0_{p'q'pq}\tilde{\epsilon}_{p'q'}(\mathbf{x})\tilde{\epsilon}_{pq}(\mathbf{x}) \\
= \quad & \int \frac{d^3\mathbf{x}}{2} c^0_{ijpq}\epsilon^0_{ij}(\mathbf{x})\epsilon^0_{pq}(\mathbf{x}) - \bar{\epsilon}_{pq}\int d^3\mathbf{x} c^0_{ijpq}\epsilon^0_{ij}(\mathbf{x}) + \frac{\det|\mathbf{H}_0|}{2} c^0_{ijpq}\bar{\epsilon}_{ij}\bar{\epsilon}_{pq} \\
- \quad & \frac{1}{\det|\mathbf{H}_0|}\sum_{\mathbf{k}} \sigma^0_{pq}(\mathbf{k})\Omega_{pi}(\hat{\mathbf{k}})\sigma^{0*}_{ij}(\mathbf{k})\hat{k}_j\hat{k}_q \\
+ \quad & \frac{1}{2\det|\mathbf{H}_0|}\sum_{\mathbf{k}} c^0_{p'q'pq}\Omega_{p'i'}(\hat{\mathbf{k}})\sigma^0_{i'j'}(\mathbf{k})\hat{k}_{j'}\hat{k}_{q'}\Omega_{pi}(\hat{\mathbf{k}})\sigma^{0*}_{ij}(\mathbf{k})\hat{k}_j\hat{k}_q
\end{aligned} \tag{A.22}
$$

where we have used the property: $\sigma_{pq}(-\mathbf{k}) = \sigma^*_{pq}(\mathbf{k})$ for real $\sigma_{pq}(\mathbf{x})$ field.

But

$$
\begin{aligned}
c^0_{p'q'pq}\Omega_{p'i'}(\hat{\mathbf{k}})\sigma^0_{i'j'}(\mathbf{k})\hat{k}_{j'}\hat{k}_{q'}\Omega_{pi}(\hat{\mathbf{k}})\sigma^{0*}_{ij}(\mathbf{k})\hat{k}_j\hat{k}_q = \quad & C_{p'p}(\hat{\mathbf{k}})\Omega_{p'i'}(\hat{\mathbf{k}})\sigma^0_{i'j'}(\mathbf{k})\hat{k}_{j'}\Omega_{pi}(\hat{\mathbf{k}})\sigma^{0*}_{ij}(\mathbf{k})\hat{k}_j \\
= \quad & \delta_{i'p}\sigma^0_{i'j'}(\mathbf{k})\hat{k}_{j'}\Omega_{pi}(\hat{\mathbf{k}})\sigma^{0*}_{ij}(\mathbf{k})\hat{k}_j \\
= \quad & \sigma^0_{pj'}(\mathbf{k})\hat{k}_{j'}\Omega_{pi}(\hat{\mathbf{k}})\sigma^{0*}_{ij}(\mathbf{k})\hat{k}_j \\
= \quad & \hat{k}_{j'}\sigma^0_{j'p}(\mathbf{k})\Omega_{pi}(\hat{\mathbf{k}})\sigma^{0*}_{ij}(\mathbf{k})\hat{k}_j.
\end{aligned} \tag{A.23}
$$

So the final relaxed elastic energy [77] is

$$
\begin{aligned}
F^{\mathrm{el}}[\bar{\boldsymbol{\epsilon}}, \boldsymbol{\epsilon}^0(\mathbf{x})] = \quad & \int \frac{d^3\mathbf{x}}{2} c^0_{ijpq}\epsilon^0_{ij}(\mathbf{x})\epsilon^0_{pq}(\mathbf{x}) - \bar{\epsilon}_{pq}\int d^3\mathbf{x} c^0_{ijpq}\epsilon^0_{ij}(\mathbf{x}) + \frac{\det|\mathbf{H}_0|}{2} c^0_{ijpq}\bar{\epsilon}_{ij}\bar{\epsilon}_{pq} \\
- \quad & \frac{1}{2\det|\mathbf{H}_0|}\sum_{\mathbf{k}} \hat{k}_q\sigma^0_{qp}(\mathbf{k})\Omega_{pi}(\hat{\mathbf{k}})\sigma^{0*}_{ij}(\mathbf{k})\hat{k}_j,
\end{aligned} \tag{A.24}
$$

the last term being the non-affine relaxation energy.

The supercell stress $\bar{\boldsymbol{\sigma}}$ is

$$
\begin{aligned}
\bar{\sigma}_{ij} \equiv \quad & \frac{1}{\det|\mathbf{H}_0|}\left.\frac{\partial F^{\mathrm{el}}[\bar{\boldsymbol{\epsilon}}, \boldsymbol{\epsilon}^0(\mathbf{x})]}{\partial \bar{\epsilon}_{ij}}\right|_{\boldsymbol{\epsilon}^0(\mathbf{x})} \\
= \quad & c^0_{ijpq}\bar{\epsilon}_{pq} - \frac{1}{\det|\mathbf{H}_0|}\int d^3\mathbf{x} c^0_{ijpq}\epsilon^0_{pq}(\mathbf{x}) \\
= \quad & \frac{1}{\det|\mathbf{H}_0|}\int d^3\mathbf{x} c^0_{ijpq}\epsilon_{pq}(\mathbf{x}) - \frac{1}{\det|\mathbf{H}_0|}\int d^3\mathbf{x} c^0_{ijpq}\epsilon^0_{pq}(\mathbf{x}) \\
= \quad & \frac{1}{\det|\mathbf{H}_0|}\int d^3\mathbf{x}\sigma_{ij}(\mathbf{x}),
\end{aligned} \tag{A.25}
$$

which is physically intuitive.

### A.1.2 General Solver

Wang, Jin and Khachaturyan (WJK) proposed an iterative solver to (A.7) based on an operator splitting technique. The idea is one wants to avoid direct handling of $\mathbf{u}(\mathbf{x})$, and real-space representations of $\nabla^2$-like operators, as in the usual finite-difference scheme. The finite-difference or finite-element schemes are philosophically similar to atomistic simulations. It is known that solving elasticity problems in real space often have slow convergence. In the WJK treatment, the section A.1.1 solver is used as a "pre-conditioner". If the system is close to an elastically homogeneous state, the inhomogeneity can be regarded as a perturbation and convergence should be fast.

The key idea in [77] is the introduction of a reference homogeneous system $c^\circ_{ijpq}$, which has the same displacement field $\mathbf{u}(\mathbf{x})$, strain field $\boldsymbol{\epsilon}(\mathbf{x})$ and stress field $\boldsymbol{\sigma}(\mathbf{x})$ as the real inhomogeneous system. This can always be done by tuning the virtual stress-free strain field $\epsilon^\circ_{pq}(\mathbf{x})$:

$$c_{ijpq}(\mathbf{x})(u_{p,q}(\mathbf{x}) - \epsilon^0_{pq}(\mathbf{x})) \;=\; c^\circ_{ijpq}(u_{p,q}(\mathbf{x}) - \epsilon^\circ_{pq}(\mathbf{x})) \tag{A.26}$$

where there are as many equations (stress components) as unknowns (stress-free strain components, which do not need to satisfy compatibility [76]), and have unique solution for positive definite $c^\circ_{ijpq}$. So there is one-to-one mapping between a given inhomogeneous system to a virtual homogeneous system, and vice versa, similar to the mapping from interacting-electrons system to fictitious non-interacting-electrons system in density functional theory (DFT) [78]. In hindsight, the success of the Kohn-Sham treatment of DFT and associated planewave solvers (in contrast to older Thomas-Fermi treatment, which forced to be completely local) largely originated from the splitting of the kinetic energy $\nabla^2$ operator which has nonlocal effects, such as boundary sensitivity, from the total energy, Eq. (2) in [78]. The remainder part, defined as exchange-correlation energy, is more local. The WJK treatment which takes advantage of planewave solver for virtual homogeneous system is philosophically quite similar to the Kohn-Sham treatment.

Suppose *we know* what $\boldsymbol{\epsilon}^\circ(\mathbf{x})$ should be used, it is easy to obtain $\mathbf{u}(\mathbf{x})$, $\boldsymbol{\epsilon}(\mathbf{x})$ and $\boldsymbol{\sigma}(\mathbf{x})$ based on section A.1.1 nonlocal planewave solver:

$$\boldsymbol{\epsilon}^\circ(\mathbf{x}) \;\rightarrow\; \mathbf{u}(\mathbf{x}), \boldsymbol{\epsilon}(\mathbf{x}), \boldsymbol{\sigma}(\mathbf{x}). \tag{A.27}$$

This set of $\boldsymbol{\epsilon}(\mathbf{x}), \boldsymbol{\sigma}(\mathbf{x})$ is supposed to be identical as that of the inhomogeneous system. But,

is is true? We can plug into (A.26) *locally* and check:

$$c^{\circ}_{ijpq}\epsilon^{\circ}_{pq}(\mathbf{x}) \;=\; c_{ijpq}(\mathbf{x})\epsilon^{0}_{pq}(\mathbf{x}) + (c^{\circ}_{ijpq} - c_{ijpq}(\mathbf{x}))\epsilon_{pq}(\mathbf{x}). \tag{A.28}$$

The above should be satisfied exactly if we have an exact guess for $\boldsymbol{\epsilon}^{\circ}(\mathbf{x})$. But if our guess of $\boldsymbol{\epsilon}^{\circ}(\mathbf{x})$ contains some error, the LHS will not be exactly the same as the RHS. But then we can invert the RHS to update the guess $\epsilon^{\circ}_{pq}(\mathbf{x})$, and repeat the process until convergence is reached.

When convergence is reached, we have from (A.2)

$$\begin{aligned} F^{\mathrm{el}}[\bar{\boldsymbol{\epsilon}}, \boldsymbol{\epsilon}^{0}(\mathbf{x})] = \quad & \frac{1}{2}\int d^3\mathbf{x}\sigma_{pq}(\mathbf{x})(\epsilon_{pq}(\mathbf{x}) - \epsilon^{\circ}_{pq}(\mathbf{x}) + \epsilon^{\circ}_{pq}(\mathbf{x}) - \epsilon^{0}_{pq}(\mathbf{x})) \\ = \quad & F^{\mathrm{el}\circ}[\bar{\boldsymbol{\epsilon}}, \boldsymbol{\epsilon}^{\circ}(\mathbf{x})] + \int \frac{d^3\mathbf{x}}{2}\sigma_{pq}(\mathbf{x})(\epsilon^{\circ}_{pq}(\mathbf{x}) - \epsilon^{0}_{pq}(\mathbf{x})). \end{aligned} \tag{A.29}$$

So the mapping of energy needs a correction.

The supercell stress $\bar{\boldsymbol{\sigma}}$ is

$$\begin{aligned} \bar{\sigma}_{ij} \;\equiv \quad & \frac{1}{\det|\mathbf{H}_0|}\left.\frac{\partial F^{\mathrm{el}}[\bar{\boldsymbol{\epsilon}}, \boldsymbol{\epsilon}^{0}(\mathbf{x})]}{\partial \bar{\epsilon}_{ij}}\right|_{\boldsymbol{\epsilon}^{0}(\mathbf{x})} \\ = \quad & \frac{1}{\det|\mathbf{H}_0|}\left.\frac{\partial F^{\mathrm{el}\circ}[\bar{\boldsymbol{\epsilon}}, \boldsymbol{\epsilon}^{0}(\mathbf{x})]}{\partial \bar{\epsilon}_{ij}}\right|_{\boldsymbol{\epsilon}^{0}(\mathbf{x})}. \end{aligned} \tag{A.30}$$

The reason is that in (A.29), the value of $F^{\mathrm{el}}$ obviously depends parametrically on $\boldsymbol{\epsilon}^{\circ}(\mathbf{x})$, and with change in $\bar{\boldsymbol{\epsilon}}$ there will be associated $\delta\boldsymbol{\epsilon}^{\circ}(\mathbf{x})$. However,

$$\frac{\delta F^{\mathrm{el}}[\boldsymbol{\epsilon}^{\circ}(\mathbf{x})|\bar{\boldsymbol{\epsilon}}, \boldsymbol{\epsilon}^{0}(\mathbf{x})]}{\delta\boldsymbol{\epsilon}^{\circ}(\mathbf{x})} \;=\; 0 \tag{A.31}$$

so (A.25) can still be used, which is physically intuitive.

### A.1.3 3D Isotropic Media

A 3D isotropic medium has

$$c_{ijpq} \;=\; \lambda\delta_{ij}\delta_{pq} + \mu(\delta_{ip}\delta_{jq} + \delta_{iq}\delta_{jp}). \tag{A.32}$$

The relationship between the Lamé parameters $\lambda, \mu$ and $E, \nu$ are:

$$\lambda = \frac{2\nu\mu}{1-2\nu} = \frac{E\nu}{(1+\nu)(1-2\nu)}, \quad \mu = \frac{E}{2(1+\nu)}, \tag{A.33}$$

and the relationship between stress and strain is:

$$\sigma^0_{ij}(\mathbf{k}) = (\lambda\epsilon^0_{pp}(\mathbf{k}))\delta_{ij} + 2\mu\epsilon^0_{ij}(\mathbf{k}), \quad \sigma^0_{ij}(\mathbf{x}) = (\lambda\epsilon^0_{pp}(\mathbf{x}))\delta_{ij} + 2\mu\epsilon^0_{ij}(\mathbf{x}). \tag{A.34}$$

Then (A.12) becomes:

$$C_{ip}(\hat{\mathbf{k}}) = c_{ijpq}\hat{k}_j\hat{k}_q = \lambda\hat{k}_i\hat{k}_p + \mu\delta_{ip} + \mu\hat{k}_p\hat{k}_i = \mu\delta_{ip} + (\lambda+\mu)\hat{k}_i\hat{k}_p \tag{A.35}$$

or

$$\mathbf{C}(\hat{\mathbf{k}}) \;=\; \mu\mathbf{I} + (\lambda+\mu)\hat{\mathbf{K}} \tag{A.36}$$

with $K_{ip} \equiv \hat{k}_i\hat{k}_p$. The $\hat{\mathbf{K}}$ matrix is real and symmetric. It is also idempotent: $\hat{\mathbf{K}}^n = \hat{\mathbf{K}}$.

The inversion of $\mathbf{C}(\hat{\mathbf{k}})$ can be done by matrix series expansion:

$$\mathbf{\Omega}(\hat{\mathbf{k}}) \;=\; \frac{1}{\mu}\sum_{n=0}^{\infty}(-\frac{\lambda+\mu}{\mu})^n\hat{\mathbf{K}}^n = \frac{1}{\mu}(\mathbf{I} - \frac{\lambda+\mu}{\mu}\frac{\hat{\mathbf{K}}}{1+\frac{\lambda+\mu}{\mu}}) = \frac{1}{\mu}(\mathbf{I} - \frac{\lambda+\mu}{\lambda+2\mu}\hat{\mathbf{K}}). \tag{A.37}$$

Define dimensionless quantity

$$\alpha \;\equiv\; \frac{\lambda+\mu}{\lambda+2\mu} = \frac{1}{2(1-\nu)}, \tag{A.38}$$

we then have $\mathbf{\Omega}(\hat{\mathbf{k}}) = (\mathbf{I} - \alpha\hat{\mathbf{K}})/\mu$.

So (A.15) would become

$$\tilde{u}_p(\mathbf{k}) \;=\; \frac{(\delta_{pi'} - \alpha\hat{k}_p\hat{k}_{i'})\sigma^0_{i'j'}(\mathbf{k})\hat{k}_{j'}}{\mu i|\mathbf{k}|} = \frac{\sigma^0_{pj'}(\mathbf{k})\hat{k}_{j'} - \alpha\hat{k}_p\sigma^0_{i'j'}(\mathbf{k})\hat{k}_{i'}\hat{k}_{j'}}{\mu i|\mathbf{k}|}. \tag{A.39}$$

Define vector and scalar

$$\mathbf{f}(\mathbf{k}) \;\equiv\; \boldsymbol{\sigma}^0(\mathbf{k})\cdot\hat{\mathbf{k}}, \quad g(\mathbf{k}) \;\equiv\; \hat{\mathbf{k}}\cdot\mathbf{f}(\mathbf{k}), \tag{A.40}$$

which can be pre-computed, we then have

$$\tilde{\mathbf{u}}(\mathbf{k}) \;=\; \frac{\mathbf{f}(\mathbf{k}) - \alpha g(\mathbf{k})\hat{\mathbf{k}}}{\mu i|\mathbf{k}|}. \tag{A.41}$$

The periodic part of the strain field is then

$$\tilde{\boldsymbol{\epsilon}}(\mathbf{k}) \;=\; \frac{i\tilde{\mathbf{u}}(\mathbf{k})\mathbf{k} + i\mathbf{k}\tilde{\mathbf{u}}(\mathbf{k})}{2} \;=\; \frac{\mathbf{f}(\mathbf{k})\hat{\mathbf{k}} + \hat{\mathbf{k}}\mathbf{f}(\mathbf{k}) - 2\alpha g(\mathbf{k})\hat{\mathbf{K}}}{2\mu}, \tag{A.42}$$

with $\mathrm{tr}(\mathbf{f}(\mathbf{k})\hat{\mathbf{k}}) = \mathrm{tr}(\hat{\mathbf{k}}\mathbf{f}(\mathbf{k})) = \hat{\mathbf{k}} \cdot \mathbf{f}(\mathbf{k}) = g(\mathbf{k})$, $\mathrm{tr}(\tilde{\boldsymbol{\epsilon}}(\mathbf{k})) = (1-\alpha)g(\mathbf{k})/\mu$, and

$$\boldsymbol{\epsilon}(\mathbf{x}) \;=\; \bar{\boldsymbol{\epsilon}} + \tilde{\boldsymbol{\epsilon}}(\mathbf{x}), \quad \int d^3\mathbf{x}\tilde{\boldsymbol{\epsilon}}(\mathbf{x}) = 0. \tag{A.43}$$

The rotation field $\mathbf{R}(\mathbf{x}) = \mathbf{I} + \mathbf{W}(\mathbf{x})$ field is

$$\mathbf{W}(\mathbf{k}) \;=\; \frac{\mathbf{f}(\mathbf{k})\hat{\mathbf{k}} - \hat{\mathbf{k}}\mathbf{f}(\mathbf{k})}{2\mu}. \tag{A.44}$$

The $c^0_{ijpq}\tilde{\epsilon}_{pq}(\mathbf{k})$ stress component in (A.20) is simplified to be

$$\begin{aligned} \lambda\mathrm{tr}(\tilde{\boldsymbol{\epsilon}}(\mathbf{k}))\mathbf{I} + 2\mu\tilde{\boldsymbol{\epsilon}}(\mathbf{k}) = &\quad \frac{\lambda(1-\alpha)g(\mathbf{k})}{\mu}\mathbf{I} + \mathbf{f}(\mathbf{k})\hat{\mathbf{k}} + \hat{\mathbf{k}}\mathbf{f}(\mathbf{k}) - 2\alpha g(\mathbf{k})\hat{\mathbf{K}} \\ = &\quad \beta g(\mathbf{k})\mathbf{I} + \mathbf{f}(\mathbf{k})\hat{\mathbf{k}} + \hat{\mathbf{k}}\mathbf{f}(\mathbf{k}) - 2\alpha g(\mathbf{k})\hat{\mathbf{K}} \end{aligned} \tag{A.45}$$

where

$$\beta \;\equiv\; \frac{\lambda(1-\alpha)}{\mu} = \frac{\nu}{1-\nu} \tag{A.46}$$

so

$$\boldsymbol{\sigma}(\mathbf{k}) = \quad \det|\mathbf{H}_0| c^0_{ijpq}\bar{\epsilon}_{pq}\delta_{\mathbf{k}} + \mathbf{f}(\mathbf{k})\hat{\mathbf{k}} + \hat{\mathbf{k}}\mathbf{f}(\mathbf{k}) + \frac{\nu\mathbf{I} - \hat{\mathbf{K}}}{1-\nu}g(\mathbf{k}) - \sigma^0_{ij}(\mathbf{k}). \tag{A.47}$$

In the real-space inversion of (A.28):

$$c^\circ_{ijpq}\epsilon^\circ_{pq}(\mathbf{x}) \;=\; \tau_{ij}(\mathbf{x}), \quad \lambda\mathrm{tr}(\boldsymbol{\epsilon}^\circ)\mathbf{I} + 2\mu\boldsymbol{\epsilon}^\circ \;=\; \boldsymbol{\tau}, \tag{A.48}$$

we note that

$$3\lambda\mathrm{tr}(\boldsymbol{\epsilon}^\circ) + 2\mu\mathrm{tr}(\boldsymbol{\epsilon}^\circ) \;=\; \mathrm{tr}(\boldsymbol{\tau}), \quad \mathrm{tr}(\boldsymbol{\epsilon}^\circ) \;=\; \frac{\mathrm{tr}(\boldsymbol{\tau})}{3\lambda + 2\mu}, \tag{A.49}$$

so

$$\boldsymbol{\epsilon}^{\circ} \;=\; \frac{\boldsymbol{\tau}}{2\mu} - \frac{\lambda}{2\mu}\frac{\mathrm{tr}(\boldsymbol{\tau})}{3\lambda+2\mu}\mathbf{I}. \tag{A.50}$$

**Sanity Check 1**

To perform a sanity check, consider:

$$\nu^{\circ} = 0, \;\; \lambda^{\circ} = 0, \;\; \alpha^{\circ} = \frac{1}{2}, \;\; \beta^{\circ} = 0 \tag{A.51}$$

In this case

$$\boldsymbol{\sigma}^{\circ}(\mathbf{x}) \;=\; 2\mu\tilde{\boldsymbol{\epsilon}}^{\circ}(\mathbf{x}). \tag{A.52}$$

One requires:

$$\nabla\cdot\tilde{\boldsymbol{\sigma}}(\mathbf{x}) \;=\; \nabla\cdot\boldsymbol{\sigma}^{\circ}(\mathbf{x}) \tag{A.53}$$

or

$$i\mathbf{k}\cdot\tilde{\boldsymbol{\sigma}}(\mathbf{k}) \;=\; i\mathbf{k}\cdot\boldsymbol{\sigma}^{\circ}(\mathbf{k}) = i|\mathbf{k}|(\hat{\mathbf{k}}\cdot\boldsymbol{\sigma}^{\circ}(\mathbf{k})) \equiv i|\mathbf{k}|\mathbf{f}(\mathbf{k}) \tag{A.54}$$

But

$$i\mathbf{k}\cdot\tilde{\boldsymbol{\sigma}}(\mathbf{k}) = i|\mathbf{k}|2\mu\hat{\mathbf{k}}\cdot\tilde{\boldsymbol{\epsilon}}(\mathbf{k}) = i|\mathbf{k}|\mu\hat{\mathbf{k}}\cdot(i\mathbf{k}\tilde{\mathbf{u}}(\mathbf{k}) + i\tilde{\mathbf{u}}(\mathbf{k})\mathbf{k}), \tag{A.55}$$

so

$$\tilde{\mathbf{u}}(\mathbf{k}) + (\hat{\mathbf{k}}\cdot\tilde{\mathbf{u}}(\mathbf{k}))\hat{\mathbf{k}} \;=\; \frac{\mathbf{f}(\mathbf{k})}{i|\mathbf{k}|\mu} \tag{A.56}$$

$$2\hat{\mathbf{k}}\cdot\tilde{\mathbf{u}}(\mathbf{k}) \;=\; \frac{\hat{\mathbf{k}}\cdot\mathbf{f}(\mathbf{k})}{i|\mathbf{k}|\mu} \tag{A.57}$$

$$\tilde{\mathbf{u}}(\mathbf{k}) \;=\; \frac{\mathbf{f}(\mathbf{k})}{i|\mathbf{k}|\mu} - \frac{(\hat{\mathbf{k}}\cdot\mathbf{f}(\mathbf{k}))\hat{\mathbf{k}}}{2i|\mathbf{k}|\mu} \tag{A.58}$$

$$\tilde{\boldsymbol{\epsilon}}(\mathbf{k}) \;=\; \frac{1}{2}\left(\frac{\hat{\mathbf{k}}\mathbf{f}(\mathbf{k})}{\mu} - \frac{\hat{\mathbf{k}}(\hat{\mathbf{k}}\cdot\mathbf{f}(\mathbf{k}))\hat{\mathbf{k}}}{2\mu} + \frac{\mathbf{f}(\mathbf{k})\hat{\mathbf{k}}}{\mu} - \frac{\hat{\mathbf{k}}(\hat{\mathbf{k}}\cdot\mathbf{f}(\mathbf{k}))\hat{\mathbf{k}}}{2\mu}\right) \;=\; \frac{\hat{\mathbf{k}}\mathbf{f}(\mathbf{k}) + \mathbf{f}(\mathbf{k})\hat{\mathbf{k}} - (\hat{\mathbf{k}}\cdot\mathbf{f}(\mathbf{k}))\hat{\mathbf{k}}\hat{\mathbf{k}}}{2\mu} \tag{A.59}$$

so

$$\tilde{\boldsymbol{\sigma}}(\mathbf{k}) \;=\; \hat{\mathbf{k}}\mathbf{f}(\mathbf{k}) + \mathbf{f}(\mathbf{k})\hat{\mathbf{k}} - (\hat{\mathbf{k}}\cdot\mathbf{f}(\mathbf{k}))\hat{\mathbf{k}}\hat{\mathbf{k}} \tag{A.60}$$

It's clear that

$$\hat{\mathbf{k}}\cdot\tilde{\boldsymbol{\sigma}}(\mathbf{k}) \;=\; \mathbf{f}(\mathbf{k}) + (\hat{\mathbf{k}}\cdot\mathbf{f}(\mathbf{k}))\hat{\mathbf{k}} - (\hat{\mathbf{k}}\cdot\mathbf{f}(\mathbf{k}))(\hat{\mathbf{k}}\cdot\hat{\mathbf{k}})\hat{\mathbf{k}} \;=\; \mathbf{f}(\mathbf{k}) \tag{A.61}$$

which satisfies the stress equilibrium condition.

**Sanity Check 2: Green's function**

Imagine a point force $\mathbf{F}$ at $\mathbf{x} = 0$, compensated by a uniform $-\mathbf{F}$ (jellium) spread over the entire supercell. When one performs Fourier transform on this external force field $\mathbf{F}\delta(\mathbf{x}) - \mathbf{F}/\det|\mathbf{H}_0|$, all finite-$\mathbf{k}$ Fourier component are $\mathbf{F}$, while the $\mathbf{k} = 0$ component is 0. We can identify $-i|\mathbf{k}|\mathbf{f}(\mathbf{k})$ in (A.54) with $\mathbf{F}$, in which case

$$\mathbf{f}(\mathbf{k}) \;=\; \frac{i\mathbf{F}}{|\mathbf{k}|}, \quad g(\mathbf{k}) = \hat{\mathbf{k}}\cdot\mathbf{f}(\mathbf{k}) = \frac{i\hat{\mathbf{k}}\cdot\mathbf{F}}{|\mathbf{k}|}. \tag{A.62}$$

The displacement, according to (A.41), should be

$$\tilde{\mathbf{u}}(\mathbf{k}) \;=\; \frac{\mathbf{F} - \alpha(\hat{\mathbf{k}}\cdot\mathbf{F})\hat{\mathbf{k}}}{\mu|\mathbf{k}|^2}. \tag{A.63}$$

Consider a problem

$$\nabla^2\phi_{\rm G}(\mathbf{x}) \;=\; \frac{4\pi}{\det|\mathbf{H}_0|} - 4\pi\delta(\mathbf{x}), \tag{A.64}$$

from electrostatics point-charge solution we know that near $\mathbf{x} = 0$, $\phi_{\rm G}(\mathbf{x})$ should behave as $\frac{1}{|\mathbf{x}|}$. On the other hand, if we do Fourier transform in the supercell, we will have

$$-|\mathbf{k}|^2\phi_{\rm G}(\mathbf{k}) \;=\; -4\pi, \quad \forall\mathbf{k}\neq 0. \tag{A.65}$$

Thus $4\pi|\mathbf{k}|^{-2}$ is the Fourier transform of $\phi_{\rm G}(\mathbf{x}) \approx \frac{1}{|\mathbf{x}|}$. Furthermore, suppose

$$\nabla^2\psi_{\rm G}(\mathbf{x}) \;\equiv\; 2\phi_{\rm G}(\mathbf{x}) \tag{A.66}$$

from real space we see that $\psi_{\rm G}(\mathbf{x}) \approx |\mathbf{x}|$ would work well near $\mathbf{x} = 0$. Thus,

$$\psi_{\rm G}(\mathbf{k}) \;=\; -\frac{2\phi_{\rm G}(\mathbf{k})}{|\mathbf{k}|^2} = -\frac{8\pi}{|\mathbf{k}|^4}, \tag{A.67}$$

and so the real-space correspondent to $-\frac{k_ik_j}{|\mathbf{k}|^4}$ would be $\partial_i\partial_j(-\psi_{\rm G}(\mathbf{x})/8\pi) = -\partial_i\partial_j\frac{|\mathbf{x}|}{8\pi}$. Thus,

the real-space displacement near the origin (or anywhere, with $\mathbf{H}_0 \to \infty$) is

$$\mathbf{u}_{\mathrm{G}}(\mathbf{x}) \;=\; \frac{\mathbf{F}\phi_{\mathrm{G}}(\mathbf{x})/4\pi - \alpha\nabla(\mathbf{F}\cdot\nabla\psi_{\mathrm{G}}(\mathbf{x}))/8\pi}{\mu} \;\approx\; \frac{\mathbf{F}}{4\pi\mu|\mathbf{x}|} - \frac{\alpha}{8\pi\mu}\nabla(\mathbf{F}\cdot\nabla|\mathbf{x}|) \qquad \text{(A.68)}$$

which agrees with Eqn (2.5) of [18].

### Sanity Check 3: Cylindrical Inclusion

Imagine a cylindrical inclusion of radius $R$ which would like to undergo spontaneous transformation strain $\epsilon^0_{12}$, with equal modulus before and after the transformation. According to Eqn (2.8) of [18]:

$$u_i \;=\; \frac{\epsilon^0_{12}}{4\pi(1-\nu)}\psi_{,i12} - \frac{\epsilon^0_{12}}{2\pi}\phi_{,1}\delta_{i2} - \frac{\epsilon^0_{12}}{2\pi}\phi_{,2}\delta_{i1} \qquad \text{(A.69)}$$

$$\phi(\mathbf{x}) \;=\; \int_{\text{cylinder}} \frac{d^3\mathbf{x}'}{|\mathbf{x}-\mathbf{x}'|} = \int_R^r \frac{-4\pi\cdot\pi R^2}{2\pi r}dr = -2\pi R^2\ln r \qquad \text{(A.70)}$$

Also from Eqn (2.9) of [18],

$$\nabla^2\psi(\mathbf{x}) \;=\; 2\phi(\mathbf{x}) \quad\to\quad r^{-1}\partial_r(r\partial_r\psi(r)) = -4\pi R^2\ln r \qquad \text{(A.71)}$$

so $\psi(r) = \pi R^2(r^2 - r^2\ln r)$.

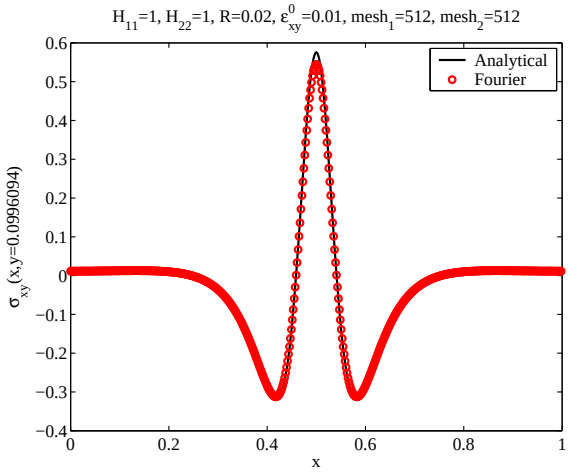


Figure A.1:

Using Mathematica[79] to do the differentiations, we obtain:

$$\sigma_{xy}(x,y) \;=\; \frac{\mu\epsilon_{12}^0 R^2(x^4-6x^2y^2+y^4)}{(x^2+y^2)^3(1-\nu)}, \quad x^2+y^2>R^2 \tag{A.72}$$

The comparison with numerical solution is shown in Fig. A.1.

**Sanity Check 4: Cylindrical Void**

Imagine a cylindrical hole of radius $R$ under a far field stress $\sigma_{ij}^{\infty}=0$ except $\sigma_{22}^{\infty}>0$. This is a plane-strain condition, where $\sigma_{33}(x,y)$ is tuned to make $\epsilon_{33}(x,y)=0$. We have non-zero $\epsilon_{11}(x,y)$, $\epsilon_{22}(x,y)$, $\epsilon_{12}(x,y)$ that must satisfy the compatibility constraint:

$$\epsilon_{11,22}+\epsilon_{22,11} \;=\; 2\epsilon_{12,12}. \tag{A.73}$$

There are two stress equilibrium equations:

$$\sigma_{11,1}+\sigma_{12,2} \;=\; 0, \quad \sigma_{21,1}+\sigma_{22,2} \;=\; 0 \tag{A.74}$$

the finite $\sigma_{33}(x,y)$ is canceled for finite-thickness samples near the hole exit by 3D indentation like local stress field. Define Airy stress function:

$$\varphi_{,22}\equiv\sigma_{11}, \;\; \varphi_{,12}\equiv-\sigma_{12}, \;\; \varphi_{,11}\equiv\sigma_{22} \tag{A.75}$$

Stress equilibrium is satisfied. We also have $\sigma_{33}=\lambda(\epsilon_{11}+\epsilon_{22})$, $\sigma_{22}=\lambda(\epsilon_{11}+\epsilon_{22})+2\mu\epsilon_{22}$, $\sigma_{11}=\lambda(\epsilon_{11}+\epsilon_{22})+2\mu\epsilon_{11}$, so $\mathrm{tr}(\boldsymbol{\sigma})=(3\lambda+2\mu)(\epsilon_{11}+\epsilon_{22})$, and based on (A.50):

$$\boldsymbol{\epsilon} \;=\; \frac{\boldsymbol{\sigma}}{2\mu}-\frac{\lambda}{2\mu}\frac{\mathrm{tr}(\boldsymbol{\sigma})}{3\lambda+2\mu}\mathbf{I}. \tag{A.76}$$

Plugging above back into (A.73), we get

$$\nabla^4\varphi \;=\; (\partial_{11}+\partial_{22})(\partial_{11}+\partial_{22})\varphi \;=\; (r^{-1}\partial_r(r\partial_r)+r^{-2}\partial_\theta^2)^2\varphi \;=\; 0. \tag{A.77}$$

Converting to cylindrical coordinate, we also have

$$\sigma_{rr}=r^{-1}\partial_r\varphi+r^{-2}\partial_\theta^2\varphi, \quad \sigma_{\theta\theta}=\partial_r^2\varphi, \quad \sigma_{r\theta}=-\partial_r(r^{-1}\partial_\theta\varphi) \tag{A.78}$$

Since $\sigma_{22}^{\infty} = \sigma_{22}(x, y \to \infty) = \varphi_{,11}(x, y \to \infty)$, we see that $\varphi(x, y)$ must contain $\sigma_{22}^{\infty} x^2/2 = \sigma_{22}^{\infty} r^2 \cos^2(\theta)/2 = \sigma_{22}^{\infty} r^2(\cos(2\theta) + 1)/4$ as the leading-order term. Presume $\varphi = r^m g(\theta)$, a $\cos(n\theta)$ angular term excites in (A.77):

$$0 \;=\; (r^{-1}\partial_r(r\partial_r) - n^2 r^{-2})^2 f(r) \;=\; r^{m-4}((m-2)^2 - n^2)(m^2 - n^2), \tag{A.79}$$

which means $m = \pm n, 2 \pm n$. For $n = 0$, the solution can be $r^2$, $r^2 \ln r$, 1, $\ln r$. So we know the general solution should look like

$$\varphi \;=\; \frac{\sigma_{22}^{\infty}}{4}\left[(r^2 + ar^{-2} + b + 0r^4)\cos(2\theta) + (c\ln r + r^2)\cos(0\theta)\right] \tag{A.80}$$

$0r^4$ because we know it does not satisfy the far-field asymptote. Thus,

$$\begin{aligned}
\sigma_{rr} = \quad & r^{-1}\partial_r\varphi + r^{-2}\partial_\theta^2\varphi \\
= \quad & \frac{\sigma_{22}^{\infty}}{4}\left[\cos(2\theta)(r^{-1}(2r - 2ar^{-3}) - 4r^{-2}(r^2 + ar^{-2} + b)) + r^{-1}(2r + cr^{-1})\right] \\
= \quad & \frac{\sigma_{22}^{\infty}}{4}\left[\cos(2\theta)(-2 - 6ar^{-4} - 4br^{-2}) + 2 + cr^{-2}\right]
\end{aligned} \tag{A.81}$$

$$\begin{aligned}
\sigma_{r\theta} = \quad & -\partial_r(r^{-1}\partial_\theta\varphi) \\
= \quad & \frac{\sigma_{22}^{\infty}}{4}\left[2\sin(2\theta)(\partial_r(r + ar^{-3} + br^{-1}))\right] \\
= \quad & \frac{\sigma_{22}^{\infty}}{4}\left[2\sin(2\theta)(1 - 3ar^{-4} - br^{-2}\right]
\end{aligned} \tag{A.82}$$

To satisfy the traction-free boundary condition: $0 = \sigma_{rr}(r = R, \theta)$, $0 = \sigma_{r\theta}(r = R, \theta)$, we should have: $c = -2R^2$, $1 + 3aR^{-4} + 2bR^{-2} = 0$. Also,

$$1 - 3aR^{-4} - bR^{-2} \;=\; 0 \tag{A.83}$$

then $b = -2R^2$, $a = R^4$. So

$$\varphi \;=\; \frac{\sigma_{22}^{\infty}}{4}\left[\cos(2\theta)(r^2 + R^4 r^{-2} - 2R^2) + r^2 - 2R^2\ln r\right] \tag{A.84}$$

$$\sigma_{\theta\theta} \;=\; \frac{\sigma_{22}^{\infty}}{2}\left[\cos(2\theta)(1 + 3R^4 r^{-4}) + 1 + R^2 r^{-2}\right]. \tag{A.85}$$

$$\sigma_{rr} = \frac{\sigma_{22}^{\infty}}{2}\left[\cos(2\theta)(-1 - 3R^4 r^{-4} + 4R^2 r^{-2}) + 1 - R^2 r^{-2}\right]. \tag{A.86}$$

$$\sigma_{r\theta} = \frac{\sigma_{22}^{\infty}}{2}\left[\sin(2\theta)(1 - 3R^4 r^{-4} + 2R^2 r^{-2})\right]. \tag{A.87}$$

And

$$\sigma_{yy}(x,y) = \sigma_{22}^{\infty}\frac{2(x^2+y^2)^4 + 3R^4(x^4 - 6x^2y^2 + y^4) + R^2(x^6 + 13x^4y^2 + 7x^2y^4 - 5y^6)}{2(x^2+y^2)^4} \tag{A.88}$$

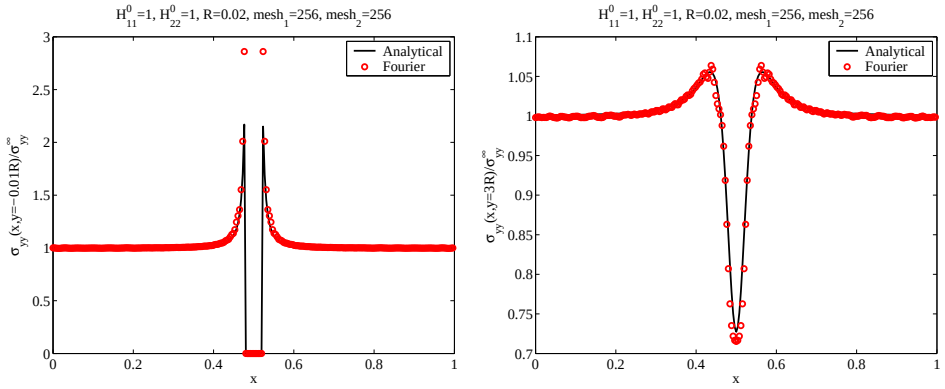


(a) (b)

Figure A.2:

The above solution is independent of $\nu$ and plane strain vs plane stress condition. The only difference between those lies in the displacement field, not in the stress field.

### A.1.4 2D Isotropic Media

A 2D isotropic medium has

$$c_{ijpq} \;=\; \lambda\delta_{ij}\delta_{pq} + \mu(\delta_{ip}\delta_{jq} + \delta_{iq}\delta_{jp}). \tag{A.89}$$

The relationship between the Lamé parameters $\lambda, \mu$ and $E, \nu$ are:

$$\lambda = \frac{E\nu}{1-\nu^2} = \frac{2\nu\mu}{1-\nu}, \quad \mu = \frac{E}{2(1+\nu)}, \tag{A.90}$$

and the relationship between stress and strain is:

$$\sigma_{ij}^0(\mathbf{k}) = (\lambda\epsilon_{pp}^0(\mathbf{k}))\delta_{ij} + 2\mu\epsilon_{ij}^0(\mathbf{k}), \quad \sigma_{ij}^0(\mathbf{x}) = (\lambda\epsilon_{pp}^0(\mathbf{x}))\delta_{ij} + 2\mu\epsilon_{ij}^0(\mathbf{x}). \tag{A.91}$$

Then (A.12) becomes:

$$C_{ip}(\hat{\mathbf{k}}) = c_{ijpq}\hat{k}_j\hat{k}_q = \lambda\hat{k}_i\hat{k}_p + \mu\delta_{ip} + \mu\hat{k}_p\hat{k}_i = \mu\delta_{ip} + (\lambda+\mu)\hat{k}_i\hat{k}_p \tag{A.92}$$

or

$$\mathbf{C}(\hat{\mathbf{k}}) \;=\; \mu\mathbf{I} + (\lambda+\mu)\hat{\mathbf{K}} \tag{A.93}$$

with $K_{ip} \equiv \hat{k}_i\hat{k}_p$. The $\hat{\mathbf{K}}$ matrix is real and symmetric. It is also idempotent: $\hat{\mathbf{K}}^n = \hat{\mathbf{K}}$.

The inversion of $\mathbf{C}(\hat{\mathbf{k}})$ can be done by matrix series expansion:

$$\mathbf{\Omega}(\hat{\mathbf{k}}) \;=\; \frac{1}{\mu}\sum_{n=0}^{\infty}(-\frac{\lambda+\mu}{\mu})^n\hat{\mathbf{K}}^n = \frac{1}{\mu}(\mathbf{I} - \frac{\lambda+\mu}{\mu}\frac{\hat{\mathbf{K}}}{1+\frac{\lambda+\mu}{\mu}}) = \frac{1}{\mu}(\mathbf{I} - \frac{\lambda+\mu}{\lambda+2\mu}\hat{\mathbf{K}}). \tag{A.94}$$

Define dimensionless quantity

$$\alpha \;\equiv\; \frac{\lambda+\mu}{\lambda+2\mu} = \frac{1+\nu}{2}, \tag{A.95}$$

we then have $\mathbf{\Omega}(\hat{\mathbf{k}}) = (\mathbf{I} - \alpha\hat{\mathbf{K}})/\mu$.

So (A.15) would become

$$\tilde{u}_p(\mathbf{k}) \;=\; \frac{(\delta_{pi'} - \alpha\hat{k}_p\hat{k}_{i'})\sigma^0_{i'j'}(\mathbf{k})\hat{k}_{j'}}{\mu i|\mathbf{k}|} = \frac{\sigma^0_{pj'}(\mathbf{k})\hat{k}_{j'} - \alpha\hat{k}_p\sigma^0_{i'j'}(\mathbf{k})\hat{k}_{i'}\hat{k}_{j'}}{\mu i|\mathbf{k}|}. \tag{A.96}$$

Define vector and scalar

$$\mathbf{f}(\mathbf{k}) \;\equiv\; \boldsymbol{\sigma}^0(\mathbf{k})\cdot\hat{\mathbf{k}}, \quad g(\mathbf{k}) \;\equiv\; \hat{\mathbf{k}}\cdot\mathbf{f}(\mathbf{k}), \tag{A.97}$$

which can be pre-computed, we then have

$$\tilde{\mathbf{u}}(\mathbf{k}) \;=\; \frac{\mathbf{f}(\mathbf{k}) - \alpha g(\mathbf{k})\hat{\mathbf{k}}}{\mu i|\mathbf{k}|}. \tag{A.98}$$

The periodic part of the strain field is then

$$\tilde{\boldsymbol{\epsilon}}(\mathbf{k}) \;=\; \frac{i\tilde{\mathbf{u}}(\mathbf{k})\mathbf{k} + i\mathbf{k}\tilde{\mathbf{u}}(\mathbf{k})}{2} \;=\; \frac{\mathbf{f}(\mathbf{k})\hat{\mathbf{k}} + \hat{\mathbf{k}}\mathbf{f}(\mathbf{k}) - 2\alpha g(\mathbf{k})\hat{\mathbf{K}}}{2\mu}, \tag{A.99}$$

with $\mathrm{tr}(\mathbf{f}(\mathbf{k})\hat{\mathbf{k}}) = \mathrm{tr}(\hat{\mathbf{k}}\mathbf{f}(\mathbf{k})) = \hat{\mathbf{k}}\cdot\mathbf{f}(\mathbf{k}) = g(\mathbf{k})$, $\mathrm{tr}(\tilde{\boldsymbol{\epsilon}}(\mathbf{k})) = (1-\alpha)g(\mathbf{k})/\mu$, and

$$\boldsymbol{\epsilon}(\mathbf{x}) \;=\; \bar{\boldsymbol{\epsilon}} + \tilde{\boldsymbol{\epsilon}}(\mathbf{x}), \quad \int d^3\mathbf{x}\tilde{\boldsymbol{\epsilon}}(\mathbf{x}) = 0. \tag{A.100}$$

The rotation field $\mathbf{R}(\mathbf{x}) = \mathbf{I} + \mathbf{W}(\mathbf{x})$ field is

$$\mathbf{W}(\mathbf{k}) \;=\; \frac{\mathbf{f}(\mathbf{k})\hat{\mathbf{k}} - \hat{\mathbf{k}}\mathbf{f}(\mathbf{k})}{2\mu}. \tag{A.101}$$

The $c^0_{ijpq}\tilde{\epsilon}_{pq}(\mathbf{k})$ stress component in (A.20) is simplified to be

$$\begin{aligned}\lambda\mathrm{tr}(\tilde{\boldsymbol{\epsilon}}(\mathbf{k}))\mathbf{I} + 2\mu\tilde{\boldsymbol{\epsilon}}(\mathbf{k}) = &\quad \frac{\lambda(1-\alpha)g(\mathbf{k})}{\mu}\mathbf{I} + \mathbf{f}(\mathbf{k})\hat{\mathbf{k}} + \hat{\mathbf{k}}\mathbf{f}(\mathbf{k}) - 2\alpha g(\mathbf{k})\hat{\mathbf{K}} \\ = &\quad \beta g(\mathbf{k})\mathbf{I} + \mathbf{f}(\mathbf{k})\hat{\mathbf{k}} + \hat{\mathbf{k}}\mathbf{f}(\mathbf{k}) - 2\alpha g(\mathbf{k})\hat{\mathbf{K}}\end{aligned} \tag{A.102}$$

where

$$\beta \;\equiv\; \frac{\lambda(1-\alpha)}{\mu} = \nu \tag{A.103}$$

so

$$\boldsymbol{\sigma}(\mathbf{k}) = \quad \det|\mathbf{H}_0| c^0_{ijpq}\bar{\epsilon}_{pq}\delta_{\mathbf{k}} + \mathbf{f}(\mathbf{k})\hat{\mathbf{k}} + \hat{\mathbf{k}}\mathbf{f}(\mathbf{k}) + (\nu\mathbf{I} - (1+\nu)\hat{\mathbf{K}})g(\mathbf{k}) - \sigma^0_{ij}(\mathbf{k}). \tag{A.104}$$

In the real-space inversion of (A.28):

$$c^\circ_{ijpq}\epsilon^\circ_{pq}(\mathbf{x}) \;=\; \tau_{ij}(\mathbf{x}), \quad \lambda\mathrm{tr}(\boldsymbol{\epsilon}^\circ)\mathbf{I} + 2\mu\boldsymbol{\epsilon}^\circ \;=\; \boldsymbol{\tau}, \tag{A.105}$$

we note that

$$2\lambda\mathrm{tr}(\boldsymbol{\epsilon}^\circ) + 2\mu\mathrm{tr}(\boldsymbol{\epsilon}^\circ) \;=\; \mathrm{tr}(\boldsymbol{\tau}), \quad \mathrm{tr}(\boldsymbol{\epsilon}^\circ) \;=\; \frac{\mathrm{tr}(\boldsymbol{\tau})}{2\lambda + 2\mu}, \tag{A.106}$$

so

$$\boldsymbol{\epsilon}^\circ \;=\; \frac{\boldsymbol{\tau}}{2\mu} - \frac{\lambda}{2\mu}\frac{\mathrm{tr}(\boldsymbol{\tau})}{2\lambda + 2\mu}\mathbf{I}. \tag{A.107}$$

## A.2 Isotropically Random Strain Matrix

### A.2.1 2D

Consider stress-free transformation strain $\boldsymbol{\epsilon}^0$ of volume elements in an isotropically random material like bulk glass:

$$\boldsymbol{\epsilon}^0 = \begin{pmatrix} \epsilon^0_{11} & \epsilon^0_{12} \\ \epsilon^0_{12} & \epsilon^0_{22} \end{pmatrix} \equiv \boldsymbol{\epsilon}^0_{\mathbf{I}} + \boldsymbol{\eta} \equiv \frac{\mathrm{Tr}\boldsymbol{\epsilon}^0}{2}\mathbf{I} + \begin{pmatrix} \eta_1 & \eta_3 \\ \eta_3 & -\eta_1 \end{pmatrix} \tag{A.108}$$

where we have decomposed $\boldsymbol{\epsilon}^0$ into a hydrostatic part $\boldsymbol{\epsilon}^0_{\mathbf{I}}$ and a deviatoric part $\boldsymbol{\eta}$. Assuming the hydrostatic part is decoupled from the deviatoric part, one wonders how to sample $\eta_1$, $\eta_3$, so the *distribution* of $\boldsymbol{\eta}$ is indistinguishable from that viewed in a rotated frame

$$\tilde{\boldsymbol{\eta}} = \mathbf{R}^T\boldsymbol{\eta}\mathbf{R}, \;\; \tilde{\eta}_{ij} = \eta_{i'j'}R_{i'i}R_{j'j} \tag{A.109}$$

where the rotation matrix is

$$\mathbf{R} \;=\; \begin{pmatrix} \cos\theta & -\sin\theta \\ \sin\theta & \cos\theta \end{pmatrix}. \tag{A.110}$$

$\mathbf{R}\mathbf{R}^T = \mathbf{I}$, connecting $d\mathbf{x} = \mathbf{R}d\tilde{\mathbf{x}}$, and $(dl)^2 = d\mathbf{x}^T(\mathbf{I} + 2\boldsymbol{\eta})d\mathbf{x} = d\tilde{\mathbf{x}}^T(\mathbf{I} + 2\tilde{\boldsymbol{\eta}})d\tilde{\mathbf{x}}$.

We have

$$\tilde{\eta}_1 \;=\; \begin{bmatrix} \cos\theta & \sin\theta \end{bmatrix} \begin{pmatrix} \eta_1 & \eta_3 \\ \eta_3 & -\eta_1 \end{pmatrix} \begin{bmatrix} \cos\theta \\ \sin\theta \end{bmatrix} = \eta_1\cos 2\theta + \eta_3 \sin 2\theta. \tag{A.111}$$

$$\tilde{\eta}_3 \;=\; \begin{bmatrix} \cos\theta & \sin\theta \end{bmatrix} \begin{pmatrix} \eta_1 & \eta_3 \\ \eta_3 & -\eta_1 \end{pmatrix} \begin{bmatrix} -\sin\theta \\ \cos\theta \end{bmatrix} = -\eta_1\sin 2\theta + \eta_3 \cos 2\theta. \tag{A.112}$$

The above is basically Mohr's circle.

Because

$$\begin{bmatrix} \tilde{\eta}_1 \\ \tilde{\eta}_3 \end{bmatrix} \;=\; \begin{pmatrix} \cos 2\theta & \sin 2\theta \\ -\sin 2\theta & \cos 2\theta \end{pmatrix} \begin{bmatrix} \eta_1 \\ \eta_3 \end{bmatrix}, \;\; \mathbf{W} \;=\; \begin{pmatrix} \cos 2\theta & \sin 2\theta \\ -\sin 2\theta & \cos 2\theta \end{pmatrix} \tag{A.113}$$

is a rotational matrix, we get the feeling that $\eta_1$ and $\eta_3$ are "equivalent" like $x$- and $y$-axis.

Therefore, the proposal is to sample $\eta_1$ and $\eta_3$ as independent Gaussians.

The $J_2$ invariant is

$$J_2 \equiv -\det(\boldsymbol{\eta}) = \eta_1^2 + \eta_3^2 \tag{A.114}$$

confirming the view that $\eta_1$ and $\eta_3$ are "equivalent" dimensions in strain space.

### A.2.2 3D

Consider

$$\boldsymbol{\eta} = \begin{pmatrix} \eta_1 & \eta_6 & \eta_5 \\ \eta_6 & \eta_2 & \eta_4 \\ \eta_5 & \eta_4 & -\eta_1 - \eta_2 \end{pmatrix} \tag{A.115}$$

This is more complicated because clearly $\eta_1$ and $\eta_2$ cannot be drawn independently, because if drawn independently, the first and second diagonals will be uncorrelated, but the first with third diagonals will be negatively correlated, making the third dimension "special".

Because $\boldsymbol{\eta}$ is a symmetric real matrix, which can always be diagonalized into

$$\boldsymbol{\eta} = \hat{\mathbf{R}}^T \begin{pmatrix} k_1 & 0 & 0 \\ 0 & k_2 & 0 \\ 0 & 0 & k_3 \end{pmatrix} \hat{\mathbf{R}} \tag{A.116}$$

i.e. principal-axes representation, we come up with the following algorithm:

1. Draw $h_1, h_2, h_3$ as three independent Gaussian random variables with equal variance $\sigma^2$:
$$dP(h_i, h_i + dh_i) = \frac{dh_i}{\sqrt{2\pi\sigma^2}} \exp(-\frac{h_i^2}{2\sigma^2}) \tag{A.117}$$
This creates a spherically symmetric cloud.

2. Compute $\bar{h} = (h_1 + h_2 + h_3)/3$

3. Compute $k_1 = h_1 - \bar{h}$, $k_2 = h_2 - \bar{h}$, $k_3 = h_3 - \bar{h}$. The $[k_1, k_2, k_3]$ cloud falls onto the (111) plane that passes through the origin, which is the requirement, but otherwise has no preference among 1-2-3 permutations.

4. Create a "spherically isotropic" random rotation matrix $\hat{\mathbf{R}}$ (see below).

5. Plug into (A.116), do the matrix multiplications, to get $\boldsymbol{\eta}$.

To obtain "spherically isotropic" random rotation matrix $\hat{\mathbf{R}}$, one must first know how to draw "spherically isotropic" vector $\mathbf{v}$. This can be done by looking at the $4\pi$ solid angle in 3D:

$$4\pi \;=\; -\int_{\theta=0}^{\pi} d\cos\theta \int_{\phi=0}^{2\pi} d\phi. \tag{A.118}$$

The algorithm is

1. Draw a uniformly random number $\alpha$ from -1 to 1.
2. Obtain $\theta = \cos^{-1}(\alpha) \in (0, \pi)$
3. Draw a uniformly random number $\phi \in (0, 2\pi)$
4. Compute $\mathbf{v} = [\sin\theta\cos\phi, \sin\theta\sin\phi, \cos\theta]$.

With normalized "spherically isotropic" vector generator, "spherically isotropic" random rotation matrix can be easily generated by:

1. Draw two independent "spherically isotropic" vectors $\mathbf{v}_1$, $\mathbf{v}_2$,
2. Obtain $\mathbf{u}_2 = \mathbf{v}_2 - (\mathbf{v}_2 \cdot \mathbf{v}_1)\mathbf{v}_1$
3. Obtain normalized $\hat{\mathbf{u}}_2 = \mathbf{u}_2/|\mathbf{u}_2|$
4. Obtain cross product $\mathbf{v}_3 = \mathbf{v}_1 \times \hat{\mathbf{u}}_2$
5. $\hat{\mathbf{R}} = [\mathbf{v}_1, \hat{\mathbf{u}}_2, \mathbf{v}_3]$.

Matlab code of the above generator is at http://li.mit.edu/S/e/Matlab/RandomStrain3D/. One can verify, via histograms, that any component of $\boldsymbol{\eta}$ and $\tilde{\boldsymbol{\eta}} = \mathbf{R}^T\boldsymbol{\eta}\mathbf{R}$ indeed have the same distribution. For example, $\eta_5$ would have the same histogram as $\tilde{\eta}_5$.

# Appendix B

# Review of Bulk Thermodynamics

Equilibrium: given the constraints, the condition of the system that will eventually be approached if one waits long enough.

Example: gas-in-box. Box is the constraint (**volume**, heat: isothermal/**adiabatic**, permeable/**non-permeable**). One initialize the atoms any way one likes, for example all to the left half side, and suddenly remove the partition: BANG! one gets a non-equilibrium state. But after a while, everything settles down.

Atoms in solids, liquids or gases at equilibrium satisfy **Maxwellian velocity distribution**:

$$dP \;\propto\; \exp\left(-\frac{m(v_x-\bar{v}_x)^2}{2k_{\rm B}T}\right)dv_x, \quad \langle v_x^2\rangle \;=\; \frac{k_{\rm B}T}{m}. \tag{B.1}$$

$k_{\rm B} = 1.38\times10^{-23}$ J/K is the Boltzmann constant, it is the gas constant divided by $6.022\times10^{23}$. If I give you a material at equilibrium without telling you the temperature, you could use the above relation to measure the temperature.

But in high-energy Tokamak plasma, or dilute interstellar gas, the velocity distribution could be non-Gaussian, bimodal for example. Then $T$ is ill-defined. Since entropy is conjugate variable to $T$, entropy is also ill-defined for such far-from-equilibrium states.

Equilibrium is however yet a bit more subtle: it is possible to reach equilibrium among a subset of the degrees of freedom (all atoms in a shot) or subsystem, while this subsystem is not in equilibrium with the rest of the system.

This is why engineering and material thermodynamics is useful for cars and airplanes. Imagine a car going 80 mph on highway: the car is not in equilibrium with the road, the axel is not in equilibrium with the body, the piston is not in equilibrium with the engine block. Yet, most often, we can define temperature (local temperature) for rubber in the tire, steel in the piston, hydrogen in the fuel tank, and apply equilibrium materials thermodynamics to analyze these components individually.

This is because of **separation of timescales**. The atoms in condensed phases collide much more frequently ($10^{12}$/second) than car components collide with each other. Thus, it is possible for atoms to reach equilibrium with adjacent atoms, before components reach equilibrium with each other.

Define "Type A non-equilibrium", or "local equilibrium": atoms reach equilibrium with each other within each **representative volume element (RVE)**; the RVE may not be in equilibrium with other RVEs.

For "Type A non-equilibrium", we can define local temperature: $T(\mathbf{x})$, and local entropy.

In this course, we will be mainly investigating "Type A non-equilibrium", and study how the RVEs reach equilibrium with each other across large distances compared to RVE size. Type B non-equilibrium, such as in Tokamak plasma, or radiation knockout in radiation damage, can be of interest, but is not the main focus of this course.

Consider a binary solid solution composed of two types of atoms, $N_1, N_2$ in absolute numbers (we prefer to use absolute number of atoms instead of moles in this class). **Helmholtz free energy** $F \equiv E - TS = F(T, V, N_1, N_2)$: $dF = dE - TdS - SdT$ is a complete differential. For closed system $dN_1 = dN_2 = 0$, the first law says $dE = \delta Q - PdV$, where $PdV$ is work (coherent energy transfer) and $\delta Q$ is heat (incoherent energy transfer via random noise).

For open system, $dE = \delta Q - PdV$ needs to be modified as

$$dE \;=\; \delta Q - PdV + \mu_1 dN_1 + \mu_2 dN_2 \tag{B.2}$$

$\mu_1, \mu_2$ are the **chemical potentials** of type-1 and type-2 atoms, respectively. To motivate the additional terms $\mu_1 dN_1 + \mu_2 dN_2$ for open systems, consider a process of atom attachment at $P = 0$, $T = 0$. And for simplicity assume for a moment $N_2 = 0$ (just type-1 atoms). In this case, before and after attaching an additional atom, kinetic energies $K$ are zero. $E = U + K = U(\mathbf{x}_1, \mathbf{x}_2, ..., \mathbf{x}_{3N_1})$. $U(\mathbf{x}_1, \mathbf{x}_2, ..., \mathbf{x}_{3N_1})$ is called the **interatomic potential**

**function**, a function of $3N_1$ arguments. For some materials, such as rare-gas solids, it is a good approximation to expand $U(\mathbf{x}_1, \mathbf{x}_2, ..., \mathbf{x}_{3N_1}) \approx \sum_{i<j} u_{ij}(|\mathbf{x}_j - \mathbf{x}_i|)$, where $i, j$ label the atoms and run from $1..N_1$, and $u_{ij}(r)$ is called the pair potential (energy=0 reference state is an isolated atom infinitely far away). Clearly then, $E$ will change, since there is one more atom in the sum, within interaction range from the previous set of atoms. Since $P = 0$, $PdV = 0$. In order to maintain $T = 0$, $\delta Q = 0$. To do this there must be an "intelligent magic hand" to drag on the atom to have a "soft landing". The energy input by the "intelligent magic hand" is coherent energy transfer, $\delta Q = 0$ (if not convinced, consider a layer of atoms adding on top of solid by a "forklift" - the added layer will move like a piston - no heat is needed). Also, the "intelligent magic hand" or "forklift" accomplishes so-called "mass action" (addition or removal of atoms), and is different from traditional $PdV$ work, which describes a process of changing volume *without* changing the number of atoms. And thus $\mu_1$ is motivated. In fact, from this microscopic idea experiment we have derived $\mu_1(T = 0, P = 0) = \sum_j u_{ij}(|\mathbf{x}_j - \mathbf{x}_i|)/2$ when $\mathbf{x}_j$ runs over lattice sites.

A well-known pair potential is the Lennard-Jones potential:

$$u_{ij}(r) \;=\; 4\epsilon_{ij}\left[\left(\frac{\sigma_{ij}}{r}\right)^{12} - \left(\frac{\sigma_{ij}}{r}\right)^{6}\right], \tag{B.3}$$

which achieves minimum potential energy $-\epsilon_{ij}$ when $r = 2^{1/6}\sigma_{ij} = 1.122\sigma_{ij}$. For an atom inside a perfect crystal lattice, its number of nearest neighbors (aka coordination number) is denoted by $Z$. For instance, in BCC lattice $Z = 8$, in FCC lattice $Z = 12$. To further simplify the discussion, we can assume the pair interaction occurs only between nearest-neighbor atoms, and the Lennard-Jones potential is approximated by expansion $u_{ij}(r) = -\epsilon_{ij} + k_{ij}(r - 2^{1/6}\sigma_{ij})^2/2$ (perform a Taylor expansion on Lennard-Jones potential and truncate at $u = 0$).

The simplest model for a crystal is a simple cubic crystal with nearest neighbor springs $u_{ij}(r) = -\epsilon_{ij} + k_{ij}(r - a_0)^2/2$ (Kossel crystal), where $a_0$ is the lattice constant of this simple cubic crystal. With $Z$ nearest neighbors ($Z = 4$ in 2D and 6 in 3D), $\mu(T = 0, P = 0) = -Z\epsilon/2$.

From dimensional argument, we see $\mu$ is some kind of energy per atom, thus on the order of minus a few eV (eV=$1.602 \times 10^{-19}$J), in reference to isolated atom. To compare, at room temperature, thermal fluctuation on average gives $k_{\mathrm{B}}T_{\mathrm{room}} = 4.14 \times 10^{-21}\mathrm{J} \approx 0.0259$ eV $=$ eV/40 per degree of freedom.

Second law says $TdS = \delta Q$ when comparing two adjacent equilibrium states (integral form is $S_2 - S_1 = \int_{\text{any quasi-static path connecting 1-2}} \delta Q/T$). Thus

$$dF(T, V, N_1, N_2) \;=\; -PdV - SdT + \mu_1 dN_1 + \mu_2 dN_2 \tag{B.4}$$

We thus have:

$$P \;=\; -\left.\frac{\partial F}{\partial V}\right|_{T,N_1,N_2}, \;\; S \;=\; -\left.\frac{\partial F}{\partial T}\right|_{V,N_1,N_2}, \;\; \mu_1 \;=\; \left.\frac{\partial F}{\partial N_1}\right|_{T,V,N_2}, \;\; \mu_2 \;=\; \left.\frac{\partial F}{\partial N_2}\right|_{T,V,N_1}. \tag{B.5}$$

$(T, V, N_1, N_2)$ describes the outer characteristics of (or outer constraints on) the system, and (B.4) describes how $F$ would change when these outer constraints are changed, and could go up or down. But there are also inner degrees of freedom inside the system (for example, precipitate/matrix microstructure, which you cannot see or fix from the outside, and can only observe when you open up the material and take to a TEM). When the inner degrees of freedom change under fixed $(T, V, N_1, N_2)$, the 2nd law states that $F$ must decrease with time.

From theory of statistical mechanics it is convenient to start from $F$, since there is a direct microscopic expression for $F$, $F = -k_{\text{B}}T \ln Z$, where $Z$ is so-called **partition function** [80, 81]. Plugging into (B.5), one then obtains direct microscopic expressions for $P$, the so-called internal pressure (or its generalization in 6-dimensional strain space, the stress tensor $\boldsymbol{\sigma}$, in so-called Virial formula), as well as $S$, $\mu_1$, $\mu_2$. This then allows atomistic simulation people to calculate so-called equation-of-state $P(T, V, N_1, N_2)$ and thermochemistry $\mu_i(T, V, N_1, N_2)$, if only the correct interatomic potential $U(\mathbf{x}^{3(N_1+N_2)})$ is provided. The so-called first-principles CALPHAD (CALculation of PHAse Diagrams) [82] is based on this approach, and is now a major source of phase diagram and thermochemistry information for alloy designers (metal hydrides for hydrogen storage, battery electrodes where you need to put in and pull out lithium ions, and catalysts). Since atomistic simulation can access metastable states and even saddle-points, there is also first-principles calculations of *mobilities*, such as diffusivities, interfacial mobilities, chemical reaction activation energies, etc. So $F$ is important quantity computationally.

For experimentalist, however, most experiments are done under constant external pressure instead of constant volume (imagine melting of ice cube on the table, there is a natural tendency for volume change, illustrating the concept of *transformation volume*). For discussing phase change under constant external pressure, we define Gibbs free energy

$G \equiv F + PV = E - TS + PV$. The full differential of $G$ is

$$dG \;=\; VdP - SdT + \mu_1 dN_1 + \mu_2 dN_2 \tag{B.6}$$

so

$$V \;=\; \left.\frac{\partial G}{\partial P}\right|_{T,N_1,N_2}, \;\; S \;=\; -\left.\frac{\partial G}{\partial T}\right|_{P,N_1,N_2}, \;\; \mu_1 \;=\; \left.\frac{\partial G}{\partial N_1}\right|_{T,P,N_2}, \;\; \mu_2 \;=\; \left.\frac{\partial G}{\partial N_2}\right|_{T,P,N_1}. \tag{B.7}$$

The above describes how a homogeneous material's $G$ would change when its $T, P, N_1, N_2$ are changed, which could go up or down. If the system has internal inhomogeneities that are evolving under constant $T, P, N_1, N_2$, however, then $G$ must decrease with time. Internal microstructural changes under constant $T, P, N_1, N_2$ that *increase* $G$ are *forbidden*.

Also,

$$d(E + PV) \;=\; \delta Q + VdP + \mu_1 dN_1 + \mu_2 dN_1 \tag{B.8}$$

so if a closed system is under constant pressure, the heat it absorbs is the change in the enthalpy $H \equiv E + PV = G + TS$. $H$ is also related to $G$ through the so-called **Gibbs-Helmholtz relation**:

$$H \;=\; \left.\frac{\partial (G/T)}{\partial (1/T)}\right|_{N_1,N_2,P}. \tag{B.9}$$

Putting $\Delta$ before both sides of (B.9), the *heat of transformation* $\Delta H$ is related to the free-energy *driving force of transformation* as

$$\Delta H \;=\; \left.\frac{\partial (\Delta G/T)}{\partial (1/T)}\right|_{N_1,N_2,P}. \tag{B.10}$$

Now we formally introduce the concept of *thermodynamic driving force* for phase transformation. Consider two possible phases $\phi = \alpha, \beta$ that the system could be in. Both phases have the same numbers of atoms $N_1, N_2$, the same $T$ and $P$. Consider pressure-driven phase transformation, $dG^\alpha = V^\alpha dP$, $dG^\beta = V^\beta dP$. Suppose $V^\alpha > V^\beta$, when we plot $G^\alpha$ and $G^\beta$ graphically on the same plot, we see that at low pressure, the high-volume phase $\alpha$ may win; but at high pressure, the low-volume (denser phase) $\beta$ will win. As a general rule, when $P$ is increased keeping $T$ fixed, the denser phase will win. So liquid phase will win over gas, and typically solid phase will win over liquid. Consider for example Fig. B.1(a). Density ranking: $\epsilon > \gamma > \alpha$. For fixed $T, N_1, N_2$, there exists an equilibrium pressure $P_{\text{eq}}$ where the

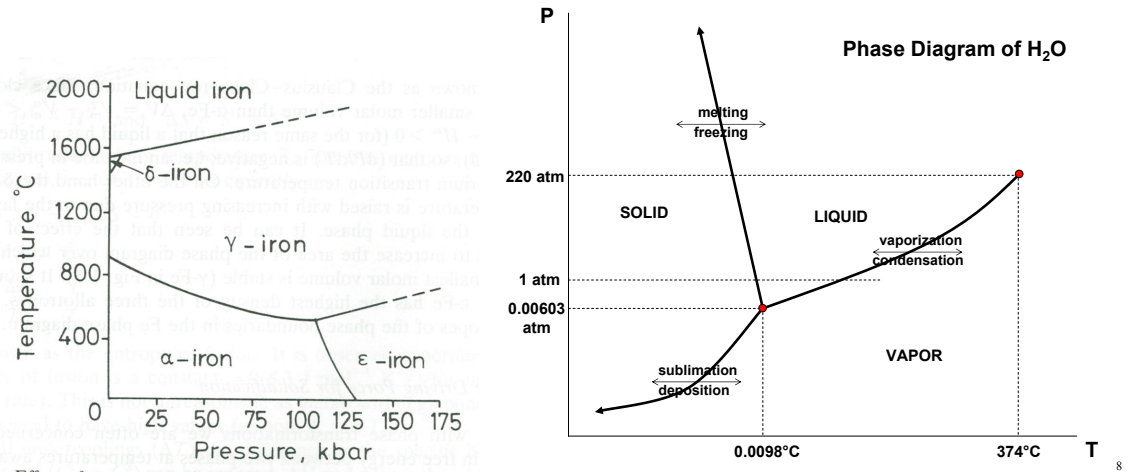


Figure B.1: (a) Figure 1.5 of Porter & Easterling [71]. (b) Phase diagram of pure $H_2O$: the solid-liquid boundary has negative $dP/dT$, which is an anomaly, because ice has larger volume than liquid water.

Gibbs free energy curves cross, at which

$$G^\alpha(P_{\rm eq}, T, N_1, N_2) \;=\; G^\beta(P_{\rm eq}, T, N_1, N_2). \tag{B.11}$$

At $P > P_{\rm eq}$, the driving force for $\alpha \to \beta$ is $\Delta G \approx (V^\alpha - V^\beta)(P - P_{\rm eq})$. Vice versa, at $P < P_{\rm eq}$, the driving force for $\beta \to \alpha$ is $\Delta G \approx (V^\alpha - V^\beta)(P_{\rm eq} - P)$ (by convention, we make the driving force positive). $P - P_{\rm eq}$ ($P_{\rm eq} - P$) may be called the overpressure (underpressure), respectively.

We could also have temperature-driven transformation, keeping pressure fixed: $dG^\alpha = -S^\alpha dT$, $dG^\beta = -S^\beta dT$. So $G$ vs $T$ is a downward curve. The question is which phase is going down faster, $G^\alpha$ or $G^\beta$. The answer is that the state that is more disordered (larger $S$) will go down faster with $T \uparrow$. So at some high enough $T$ there will be a crossing. Liquid is going down faster than solid, gas is going down faster than liquid, with $T \uparrow$ holding $P$ constant. For a fixed pressure, there exists an equilibrium temperature $T_{\rm eq}$ where the Gibbs free energy curves cross, at which

$$G^\alpha(P, T_{\rm eq}, N_1, N_2) \;=\; G^\beta(P, T_{\rm eq}, N_1, N_2). \tag{B.12}$$

Consider for example solid↔liquid transformation. In this case, $T_{\rm eq} = T_{\rm M}(P)$, the equilibrium bulk melting point. $\alpha$=liquid, $\beta$=solid, $S^\alpha > S^\beta$. At $T > T_{\rm eq}$, the more disordered

phase is favored, and the driving force for $\beta \to \alpha$ transformation, which is melting, is $\Delta G \approx (S^\alpha - S^\beta)(T - T_{\rm M})$. Vice versa at $T < T_{\rm eq}$, the more ordered phase is favored, which is solidification, and the driving force for $\alpha \to \beta$ is $\Delta G \approx (S^\alpha - S^\beta)(T_{\rm M} - T)$. Because we are doing first-order expansion, it is OK to take $S^\alpha - S^\beta$ to be the value at $T_{\rm M}$. However, at $T_{\rm M}$ we have $E^\alpha + PV^\alpha - T_{\rm M}S^\alpha = H^\alpha - T_{\rm M}S^\alpha = H^\beta - T_{\rm M}S^\beta = E^\beta + PV^\beta - T_{\rm M}S^\beta$, we have $S^\alpha - S^\beta = (H^\alpha - H^\beta)/T_{\rm M}$. $H^\alpha - H^\beta$ is in fact the heat released during phase change under constant pressure, and is called the **latent heat** $L$. So we have

$$\Delta G \;\approx\; \frac{L}{T_{\rm M}}|T_{\rm M} - T|. \tag{B.13}$$

$|T_{\rm M} - T|$ is called undercooling / superheating for solidification / melting. We see that the thermodynamic driving force for phase change is proportional to the amount of undercooling / superheating (in Kelvin), with proportionality factor $\frac{L}{T_{\rm M}} = \Delta S$. Later we will see later why a finite thermodynamic driving force is needed, in order to observe phase change within a *finite amount of time*. (If you are extremely leisurely and have infinite amount of time, you can observe phase change right at $T_{\rm eq}$).

solid/liquid: melting, freezing or solidification. liquid/vapor: vaporization, condensation. solid/vapor: sublimation, deposition. At low enough pressure, the gas phase is going to come down in free energy significantly, that the solid goes directly to gas, without going through the liquid phase.

Thus, typically, high pressure / low temperature stabilizes solid phase, low pressure / high temperature stabilizes gas phase. The tradeoff relation can be described by the **Clausius-Clapeyron relation** for polymorphic phase transformation (single-component) in $T - P$ plane. The question we ask is that suppose you are already sitting on a particular $(T, P)$ point that reaches perfect equilibrium between $\alpha, \beta$,

$$G^\alpha(N_1, N_2, T, P) \;=\; G^\beta(N_1, N_2, T, P) \tag{B.14}$$

in which direction on the $(T, P)$ plane should one go, $(T, P) \to (T+dT, P+dP)$, to *maintain* that equilibrium, i.e.:

$$G^\alpha(N_1, N_2, T + dT, P + dP) \;=\; G^\beta(N_1, N_2, T + dT, P + dP) \tag{B.15}$$

$$G^\alpha(N_1, N_2, T, P) - S^\alpha dT + V^\alpha dP \;=\; G^\beta(N_1, N_2, T, P) - S^\beta dT + V^\beta dP. \tag{B.16}$$

So:

$$-S^\alpha dT + V^\alpha dP \;=\; -S^\beta dT + V^\beta dP. \tag{B.17}$$

and the direction is given by

$$\frac{dP}{dT} \;=\; \frac{S^\alpha - S^\beta}{V^\alpha - V^\beta} \;=\; \frac{L}{T(V^\alpha - V^\beta)}. \tag{B.18}$$

The above equation keeps one "on track" on the $T-P$ phase diagram. It's like in pitch darkness, if you happen to stumble upon a rail, you can *follow* the rail to map out the whole US railroad system. The Clausius-Clapeyron relation tells you how to follow that rail. $L$ is called "latent heat". $V^\alpha - V^\beta$ is the volume of melting/vaporization/sublimation, you may call it the "latent volume".

In above we have only considered the scenario of so-called congruent transformation $\alpha \leftrightarrow \beta$, where $\alpha$ and $\beta$ are single phases with the same composition. We have not considered the possibility of for example $\alpha \leftrightarrow \beta + \gamma$, where $\gamma$ has different composition or even structure from $\beta$. To understand the driving force for such transformations which are indeed possible in binary solutions, we need to further develop the **language of chemical potential**.

The total number of particles is $N \equiv N_1 + N_2$. Define mole fractions $X_1 \equiv N_1/N$, $X_2 \equiv N_2/N$. Since there is always $X_1 + X_2 = 1$, we cannot regard $X_1$ and $X_2$ as independent variables. Usually by convention one takes $X_2$ to be the independent variable, so-called *composition*. Composition is dimensionless, but it could be a multi-dimensional vector if the number of species $C > 2$. For instance, in a ternary solution, $C = 3$, and composition is a 2-dimensional vector $\mathbf{X} \equiv [X_2, X_3]$. Composition can spatially vary in inhomogeneous systems, for instance in an inhomogeneous binary solution, $X_2 = X_2(\mathbf{x}, t)$. In order for $\alpha \leftrightarrow \beta + \gamma$ to happen kinetically, for instance changing from $X_2(\mathbf{x}) = 0.3$ uniformly (initially $\alpha$ phase) to some region with $X_2(\mathbf{x}) = 0.5$ (in $\beta$ phase, "solute sink") and some region with $X_2(\mathbf{x}) = 0.1$ (in $\gamma$ phase, 'solute source"). This requires would require long-range diffusion of type-2 solutes over distances on the order of the sizescale of the inhomogeneities, which is called **solute partitioning**.

We can define the *particle average Gibbs free energy* to be $g \equiv G/N = G(T, P, N_1, N_2)/(N_1 + N_2)$. Like the chemical potentials, $g$ will be minus a few eV in reference to isolated atoms ensemble. It can be rigorously proven, but is indeed quite intuitively obvious, that $g = g(X_2, T, P)$, which is to say the particle average Gibbs free energy depends on chemistry but not quantity (think of $(N_1, N_2) \leftrightarrow (N, X_2)$ as a variable transform that decomposes

dependent variables into *quantity* and *chemistry*). It is customary to plot $g$ versus $X_2$ at constant $T, P$. It can be mathematically proven that $\mu_1$, $\mu_2$ are the *tangent extrapolations* of $g(X_2)$ to $X_2 = 0$ and $X_2 = 1$, respectively. Algebraically this means

$$\begin{aligned} \mu_1(X_2, T, P) &= g(X_2, T, P) + \left.\frac{\partial g}{\partial X_2}\right|_{T,P} (0 - X_2) \\ \mu_2(X_2, T, P) &= g(X_2, T, P) + \left.\frac{\partial g}{\partial X_2}\right|_{T,P} (1 - X_2). \end{aligned} \tag{B.19}$$

It is also clear from the above that $g(X_2, T, P) = X_1\mu_1 + X_2\mu_2$, so

$$G(T, P, N_1, N_2) = N_1\mu_1 + N_1\mu_2 = N_1 \left.\frac{\partial G}{\partial N_1}\right|_{T,P,N_2} + N_2 \left.\frac{\partial G}{\partial N_2}\right|_{T,P,N_1} \tag{B.20}$$

On first look, the above seems to imply that particle 1 and particle 2 do not interact. But this is very far from true! In fact, $\mu_1 = \mu_1(X_2, T, P)$, $\mu_2 = \mu_2(X_2, T, P)$.

For pure systems: $X_2 = 0$, $g(X_2 = 0, T, P) = \mu_1(X_2 = 0, T, P) \equiv \tilde{\mu}_1(T, P)$; or $X_2 = 1$, $g(X_2 = 1, T, P) = \mu_2(X_2 = 1, T, P) \equiv \tilde{\mu}_2(T, P)$. $\tilde{\mu}_1(T, P)$, $\tilde{\mu}_2(T, P)$ are called Raoultian reference-state chemical potentials (they are not the isolated-atoms-in-vaccuum reference states, but already as interacting-atoms). In this class we take the $\tilde{\mu}_1$, $\tilde{\mu}_2$ reference states to the same structure as the solution, but in pure compositions (so-called Raoultian reference states).

When plotted graphically, it is seen that $g(X_2)$ is typically convex up with $\mu_1(X_2, T, P) < \tilde{\mu}_1(T, P)$ and $\mu_2(X_2, T, P) < \tilde{\mu}_2(T, P)$ (if not, what would happen?) This negative difference is defined as the *mixing chemical potential*

$$\mu_i^{\text{mix}} \equiv \mu_i(X_2, T, P) - \tilde{\mu}_i(T, P), \quad i = 1, 2 \tag{B.21}$$

and *mixing free energy*

$$g^{\text{mix}} \equiv X_1\mu_1^{\text{mix}} + X_2\mu_2^{\text{mix}} = g - X_1\tilde{\mu}_1(T, P) - X_2\tilde{\mu}_2(T, P), \quad G^{\text{mix}} = Ng^{\text{mix}} \tag{B.22}$$

respectively. Clearly, by definition, $G^{\text{mix}} = 0$ at pure competitions. $g^{\text{mix}}(X_2, T, P)$ can be interpreted as the driving force to react pure 1 and pure 2 of the same structure as the solution to obtain a solution of non-pure composition, per particle in the mixed solution. $\Delta G = -Ng^{\text{mix}}(X_2, T, P)$ is in fact the *chemical driving force* to make a solution by mixing

pure constituents.

It turns out there exists "partial" version of the full differential (B.6):

$$dg(X_2, T, P) \;=\; vdP - sdT + \left.\frac{\partial g}{\partial X_2}\right|_{T,P} dX_2 \tag{B.23}$$

$$d\mu_i(X_2, T, P) \;=\; v_i dP - s_i dT + \left.\frac{\partial \mu_i}{\partial X_2}\right|_{T,P} dX_2 \tag{B.24}$$

where

$$\begin{aligned} v_1 \;&\equiv\; \left.\frac{\partial V}{\partial N_1}\right|_{T,P,N_2}, \;\; v_2 \;\equiv\; \left.\frac{\partial V}{\partial N_2}\right|_{T,P,N_1}, \;\; s_1 \;\equiv\; \left.\frac{\partial S}{\partial N_1}\right|_{T,P,N_2}, \;\; s_2 \;\equiv\; \left.\frac{\partial S}{\partial N_2}\right|_{T,P,N_1}, \\ e_1 \;&\equiv\; \left.\frac{\partial E}{\partial N_1}\right|_{T,P,N_2}, \;\; e_2 \;\equiv\; \left.\frac{\partial E}{\partial N_2}\right|_{T,P,N_1}, \;\; h_1 \;\equiv\; \left.\frac{\partial H}{\partial N_1}\right|_{T,P,N_2}, \;\; h_2 \;\equiv\; \left.\frac{\partial H}{\partial N_2}\right|_{T,P,N_1}, \;\; ... \end{aligned} \tag{B.25}$$

Generally speaking, for arbitrary extensive quantity $A$ (volume, energy, entropy, enthalpy, Helmholtz free energy, Gibbs free energy), "particle partial $A$" is defined as:

$$a_i \;\equiv\; \left.\frac{\partial A}{\partial N_i}\right|_{N_{j\neq i},T,P}. \tag{B.26}$$

The meaning of $a_i$ is the increase in energy, enthalpy, volume, entropy, etc. when an additional type-$i$ atom is added into the system, keeping the temperature and pressure fixed. The *particle-average* $a$ is simply

$$a \;\equiv\; \frac{A}{N} \;=\; \sum_{i=1}^{C} X_i a_i. \tag{B.27}$$

For instance, the particle average volume and particle average entropy

$$v \;\equiv\; \frac{V}{N} = X_1 v_1 + X_2 v_2, \;\; s \;\equiv\; \frac{S}{N} = X_1 s_1 + X_2 s_2, \tag{B.28}$$

is simply the composition-weighted sum of particle partial volumes and partial entropies of different-species atoms, respectively. While (B.27) relates all $a_i(X_2, ..., X_C, T, P)$s to $a(X_2, ..., X_C, T, P)$, it is also possible to obtain individual $a_i(X_2, ..., X_C, T, P)$ from $a(X_2, ..., X_C, T, P)$

by the tangent extrapolation formula:

$$a_i(X_2, ..., X_C, T, P) \;=\; a(X_2, ..., X_C, T, P) + \sum_{k=2}^{C} (\delta_{ik} - X_k) \frac{\partial a(X_2, ..., X_C, T, P)}{\partial X_k}, \qquad \text{(B.29)}$$

where $\delta_{ik}$ is the Kronecker delta: $\delta_{ik} = 1$ if $i = k$, and $\delta_{ik} = 0$ if $i \neq k$. Note in (B.29), although the $k$-sum runs from 2 to $C$, $i$ can take values 1 to $C$. (B.19) is a special case of (B.29): for historical reason the particle partial Gibbs free energy is denoted by $\mu_i$ instead of $g_i$.

The so-called Gibbs-Duhem relation imposes constraint on the partial quantities when composition is varied while holding $T, P$ fixed:

$$0 \;=\; \sum_{i=1}^{C} X_i da_i|_{T,P}, \qquad \text{(B.30)}$$

For binary solution, this means

$$0 = X_1 d\mu_1|_{T,P} + X_2 d\mu_2|_{T,P} = X_1 dv_1|_{T,P} + X_2 dv_2|_{T,P} = X_1 ds_1|_{T,P} + X_2 ds_2|_{T,P} = ... \qquad \text{(B.31)}$$

The above can be proven, but we will not do it here.

The above is the general solution thermodynamics framework. To proceed further, we need some detailed models of how $g$ depends on $X_2$. In so-called ideal solution:

$$\mu_1^{\text{ideal}-\text{mix}}(X_2, T, P) \;=\; k_{\text{B}} T \ln X_1, \;\; \mu_2^{\text{ideal}-\text{mix}}(X_2, T, P) \;=\; k_{\text{B}} T \ln X_2. \qquad \text{(B.32)}$$

And so

$$g^{\text{ideal}-\text{mix}}(X_2, T, P) \;\equiv\; k_{\text{B}} T (X_1 \ln X_1 + X_2 \ln X_2), \qquad \text{(B.33)}$$

which is a symmetric function that is always negative (that is to say it always prefer mixing), with $-\infty$ slope on both sides. Ideal solution is realized nearly exactly in isotopic solutions such as $^{235}$U - $^{238}$U. In such case, there is no chemical difference between the two species ($\epsilon_{\text{AA}} = \epsilon_{\text{BB}} = \epsilon_{\text{AB}}$), so the enthalpy of mixing is zero. The driving force for mixing is entirely entropic in origin, because there would be many ways to arrange $^{235}$U and $^{238}$U atoms on a lattice, whereas there is just one in pure $^{235}$U or pure $^{238}$U crystal ($^{235}$U atoms are indistinguishable among themselves, and so are $^{238}$U atoms). This can be verified from the formula $s^{\text{mix}} = -\partial g^{\text{mix}}/\partial T$, $h^{\text{mix}} = \partial(g^{\text{mix}}/T)/\partial(1/T)$.

We define excess as difference between the actual mix and the ideal-mix functions:

$$g^{\text{excess}} \equiv g^{\text{mix}}(X_2, T, P) - g^{\text{ideal-mix}}(X_2, T, P), \quad \mu_i^{\text{excess}} \equiv \mu_i^{\text{mix}} - k_{\text{B}} T \ln X_i. \tag{B.34}$$

Clearly, excess quantities for ideal solution is zero.

In so-called regular solution model,

$$g^{\text{excess}}(X_2, T, P) = \omega X_1 X_2, \tag{B.35}$$

where $\omega$ is $X_2$,$T$,$P$ independent constant. Using (B.19), we get

$$\mu_1^{\text{excess}} = \omega X_2^2, \quad \mu_2^{\text{excess}} = \omega X_1^2. \tag{B.36}$$

And so

$$\mu_1(X_2) = \tilde{\mu}_1 + k_{\text{B}} T \ln X_1 + \omega X_2^2, \quad \mu_2(X_2) = \tilde{\mu}_2 + k_{\text{B}} T \ln X_2 + \omega X_1^2. \tag{B.37}$$

It is also customary to define *activity coefficient* $\gamma_i$, so that

$$\mu_i(X_2, T) \equiv \tilde{\mu}_i(T) + k_{\text{B}} T \ln \gamma_i X_i. \tag{B.38}$$

Contrasting with (B.37), we see that in the regular solution model, the activity coefficients are $\gamma_2(X_2, T) = e^{\omega X_1^2 / k_{\text{B}} T}$, $\gamma_1(X_2, T) = e^{\omega X_2^2 / k_{\text{B}} T}$.

When $\omega < 0$, the driving force for mixing is *greater* than in ideal solution. When one uses the formula $s = -\partial g / \partial T$, $h = \partial (g/T) / \partial (1/T)$, we can see that the ideal-mixing contribution is entirely *entropic*, whereas the excess contribution is entirely *enthalpic* if $\omega$ is independent of temperature. In fact, it can be shown from statistical mechanics that

$$\omega = Z \left( (\epsilon_{\text{AA}} + \epsilon_{\text{BB}})/2 - \epsilon_{\text{AB}} \right), \tag{B.39}$$

where $\epsilon_{\text{AB}}$ is the Kossel spring binding energy between A-B ("heteropolar bond"), and $\epsilon_{\text{AA}}$ and $\epsilon_{\text{BB}}$ are the Kossel spring binding energy between A-A and B-B (homopolar bonds).

Derivation of the **regular solution model** (this has been shown in MSE530 Thermodynamics of Materials): arrange $X_{\text{A}} N$ A atoms and $X_{\text{B}} N$ B atoms on a lattice. The number

of choices:

$$\Omega \;=\; \frac{N!}{(X_{\rm A}N)!(X_{\rm B}N!)} \tag{B.40}$$

*Assume* all these choices (microstates) have the same enthalpy:

$$\begin{aligned} H &= -Z(X_{\rm A}N(X_{\rm B}\epsilon_{\rm AB}+X_{\rm A}\epsilon_{\rm AA})+X_{\rm B}N(X_{\rm B}\epsilon_{\rm BB}+X_{\rm A}\epsilon_{\rm AB}))/2 \\ &= -NZ(2X_{\rm A}X_{\rm B}\epsilon_{\rm AB}+X_{\rm A}^2\epsilon_{\rm AA}+X_{\rm B}^2\epsilon_{\rm BB})/2 \end{aligned} \tag{B.41}$$

in contrast to reference state of pure A and pure B

$$H^{\rm ref} \;=\; -NZ(X_{\rm A}\epsilon_{\rm AA}+X_{\rm B}\epsilon_{\rm BB})/2 \tag{B.42}$$

so the excess is:

$$\begin{aligned} H^{\rm excess} &= -NZ(2X_{\rm A}X_{\rm B}\epsilon_{\rm AB}+X_{\rm A}^2\epsilon_{\rm AA}-X_{\rm A}\epsilon_{\rm AA}+X_{\rm B}^2\epsilon_{\rm BB}-X_{\rm B}\epsilon_{\rm BB})/2 \\ &= -NZ(2X_{\rm A}X_{\rm B}\epsilon_{\rm AB}-X_{\rm A}X_{\rm B}\epsilon_{\rm AA}-X_{\rm B}X_{\rm A}\epsilon_{\rm BB})/2 \\ &= NZX_{\rm A}X_{\rm B}\left((\epsilon_{\rm AA}+\epsilon_{\rm BB})/2-\epsilon_{\rm AB}\right) \;=\; N\omega X_{\rm A}X_{\rm B}. \end{aligned} \tag{B.43}$$

According to the Boltzmann formula $S = k_{\rm B}\ln\Omega$, the entropy is

$$\begin{aligned} S &= k_{\rm B}\ln\frac{N!}{(X_{\rm A}N)!(X_{\rm B}N!)} \approx k_{\rm B}(N\ln N - X_{\rm A}N\ln X_{\rm A}N - X_{\rm B}N\ln X_{\rm B}N) \\ &= -Nk_{\rm B}(X_{\rm A}\ln X_{\rm A}+X_{\rm B}\ln X_{\rm B}), \end{aligned} \tag{B.44}$$

using the Stirling formula: $\ln N! \approx N\ln N - N$ for large $N$. $S$ is the same as that in ideal solution, because the regular solution model takes the "mean-field" view that all possible configurations are iso-energetic. The regular solution model in the form of (B.35) is a well-posed *model* with algebraic simplicity, but it may not reflect reality very well.

For positive $\omega$, spinodal decomposition will happen below a critical temperature $T_{\rm C}$: a random 50%-50% A-B solution $\alpha$ would separate into A-rich solution $\alpha_1$ and B-rich solution $\alpha_2$ - see plots of $g(X_2, T)$ at different $T$. We have studied this model in detail in MSE530.

For negative $\omega$, although nothing will happen as seen from the regular solution model, in reality **order-disorder transition** will happen below a critical temperature $T_{\rm C}$, where the A-B solution starts to posses **chemical long-range order** (CLRO). A good example is $\beta$-brass, a Cu-Zn alloy in BCC structure ($Z = 8$). See Chap. 17 of [68]. Cu and Zn atoms like each other energetically, more than Cu-Cu, and Zn-Zn. Suppose $X_{\rm Zn} = 0.5$, at $T = 0$, what

would be the optimal microscopic configuration? Since $F = E - TS$, at $T = 0$ minimization of $F$ is the same as minimization of $E = U$, the system will try to maximize the number of Cu-Zn bonds. Indeed, so-called long-range chemical order, that is, Cu occupying one sub-lattice (') and Zn occupying another sub-lattice ("), or Cu occupying sub-lattice " and Zn occupying sub-lattice ' would give the maximum number of Cu-Zn bonds. The regular solution model did not distinguish between the two sub-lattices, statistically speaking. In order to be able to distinguish, let us define sub-lattice compositions $X'_{\rm A} + X'_{\rm B} = 1$, $X''_{\rm A} + X''_{\rm B} = 1$. Clearly the overall composition

$$X_{\rm A} \;=\; \frac{1}{2}(X'_{\rm A} + X''_{\rm A}), \;\; X_{\rm B} \;=\; \frac{1}{2}(X'_{\rm B} + X''_{\rm B}). \tag{B.45}$$

By defining sub-lattice compositions, we have effectively added one more "coarse" degree of freedom to describe our alloy, the so-called $\eta$ order parameter:

$$\eta \;\equiv\; \frac{1}{2}(X''_{\rm B} - X'_{\rm B}). \tag{B.46}$$

$Cu_{50}Zn_{50}$ taking the CsCl structure at $T = 0$ would have $\eta = 0.5$ or $\eta = -0.5$. Previously, the regular solution model constrains $\eta = 0$ (because it does not entertain an $\eta$ order parameter). Now, with $\eta$, we would have

$$X''_{\rm B} = X_{\rm B} + \eta, \;\; X'_{\rm B} = X_{\rm B} - \eta, \;\; X''_{\rm A} = 1 - X_{\rm B} - \eta, \;\; X'_{\rm A} = 1 - X_{\rm B} + \eta. \tag{B.47}$$

Still under the mean-field approximation (so called **Bragg-Williams** approach [83, 84] in alloy thermochemistry), as the regular solution model, we can estimate the proportion of A(')-A(") bonds:

$$p_{\rm AA} \;=\; X''_{\rm A}X'_{\rm A} = (1 - X_{\rm B} - \eta)(1 - X_{\rm B} + \eta), \tag{B.48}$$

the proportion of B(')-B(") bonds:

$$p_{\rm BB} \;=\; X''_{\rm B}X'_{\rm B} = (X_{\rm B} + \eta)(X_{\rm B} - \eta), \tag{B.49}$$

the proportion of A(')-B(") bonds:

$$p_{\rm AB} \;=\; X'_{\rm A}X''_{\rm B} = (1 - X_{\rm B} + \eta)(X_{\rm B} + \eta), \tag{B.50}$$

the proportion of A(")-B(') bonds:

$$p_{\mathrm{BA}} \;=\; X'_{\mathrm{B}} X''_{\mathrm{A}} = (X_{\mathrm{B}} - \eta)(1 - X_{\mathrm{B}} - \eta) \tag{B.51}$$

among all the nearest-neighbor bonds in the alloy. Clearly, the above Bragg-Williams estimation satisfies the sum rule constraint:

$$p_{\mathrm{AA}} + p_{\mathrm{BB}} + p_{\mathrm{AB}} + p_{\mathrm{BA}} \;=\; 1. \tag{B.52}$$

The particle-average energy is thus just

$$h \;=\; -\frac{Z}{2}(p_{\mathrm{AA}}\epsilon_{\mathrm{AA}} + p_{\mathrm{BB}}\epsilon_{\mathrm{BB}} + (p_{\mathrm{AB}} + p_{\mathrm{BA}})\epsilon_{\mathrm{AB}}) \tag{B.53}$$

From derivations of the regular solution model and discussions in the last semester, we see that if we chose our reference state appropriately, then we can say $\epsilon_{\mathrm{AA}} = 0$, $\epsilon_{\mathrm{BB}} = 0$, $\epsilon_{\mathrm{AB}} = -\omega/Z$, to simplify the algebra:

$$h(X_{\mathrm{B}}, \eta) \;=\; \omega(X_{\mathrm{A}} X_{\mathrm{B}} + \eta^2). \tag{B.54}$$

which we see is the same as the regular solution model if $\eta = 0$. The physics of the above expression is that, if with CLRO and solute partitioning onto the two sub-lattices, one can increase the number of A-B bonds from $X_{\mathrm{A}} X_{\mathrm{B}}$ to $X_{\mathrm{A}} X_{\mathrm{B}} + \eta^2$.

The entropy is just the sum of the entropies of the two sub-lattices (in other words, the total number of possible microstates is the product of the numbers of microstates on ' sublattice and that on " sublattice). Therefore:

$$s(X_{\mathrm{B}}, \eta) \;=\; -\frac{k_{\mathrm{B}}}{2}(X'_{\mathrm{A}} \ln X'_{\mathrm{A}} + X'_{\mathrm{B}} \ln X'_{\mathrm{B}} + X''_{\mathrm{A}} \ln X''_{\mathrm{A}} + X''_{\mathrm{B}} \ln X''_{\mathrm{B}}). \tag{B.55}$$

The free energy (of mixing) per particle is thus

$$g(X_{\mathrm{B}}, \eta) \;=\; \omega(X_{\mathrm{A}} X_{\mathrm{B}} + \eta^2) + \frac{k_{\mathrm{B}} T}{2}(X'_{\mathrm{A}} \ln X'_{\mathrm{A}} + X'_{\mathrm{B}} \ln X'_{\mathrm{B}} + X''_{\mathrm{A}} \ln X''_{\mathrm{A}} + X''_{\mathrm{B}} \ln X''_{\mathrm{B}}) \tag{B.56}$$

with

$$\frac{\partial g}{\partial \eta} \;=\; 2\omega\eta + \frac{k_{\mathrm{B}} T}{2}\left(-\ln \frac{X'_{\mathrm{B}}}{X'_{\mathrm{A}}} + \ln \frac{X''_{\mathrm{B}}}{X''_{\mathrm{A}}}\right), \tag{B.57}$$

$$\frac{\partial^2 g}{\partial \eta^2} \;=\; 2\omega + \frac{k_{\mathrm{B}}T}{2}\left(\frac{1}{X'_{\mathrm{B}}X'_{\mathrm{A}}} + \frac{1}{X''_{\mathrm{B}}X''_{\mathrm{A}}}\right). \tag{B.58}$$

In a real material, both $X_{\mathrm{B}}$ and $\eta$ are fields: $g(X_{\mathrm{B}}(\mathbf{x},t),\eta(\mathbf{x},t))$. However, we note there is a fundamental difference between $X_{\mathrm{B}}$ and $\eta$. $X_{\mathrm{B}}(\mathbf{x},t)$ is conserved:

$$\int d\mathbf{x} X_{\mathrm{B}}(\mathbf{x},t) \;=\; \text{const} \tag{B.59}$$

if integration is carried out in the entire space. Thus, when optimizing

$$G \;=\; \frac{1}{\Omega}\int d\mathbf{x} g(X_{\mathrm{B}}(\mathbf{x}),\eta(\mathbf{x})) \tag{B.60}$$

we can not do an unconstrained optimization on $g(X_{\mathrm{B}})$: there has to be a Lagrange multiplier (the chemical potential) on the total free energy minimization. On the other hand, there is no such constraint on $\eta$: we can do an unconstrained optimization with respect to $\eta$ (and indeed that is what Nature does). More involved discussions [68] show that $X_{\mathrm{B}}$ is so-called **conserved order parameter**, and evolve according to the so-called **Cahn-Hilliard** evolution equation [69] (basically diffusion equation), whereas **non-conserved order parameter** like the CLRO evolve according to the so-called **Allen-Cahn** equation [85], in the linear response regime.

For a given $T, X_{\mathrm{B}}$, we thus have

$$g(X_{\mathrm{B}}) \;=\; \min_{\eta} g(X_{\mathrm{B}},\eta) \tag{B.61}$$

at thermodynamic equilibrium. So:

$$\ln\frac{(X_{\mathrm{B}}-\eta)(1-X_{\mathrm{B}}-\eta)}{(X_{\mathrm{B}}+\eta)(1-X_{\mathrm{B}}+\eta)} \;=\; \frac{4\omega\eta}{k_{\mathrm{B}}T} \tag{B.62}$$

We note that $\eta = 0$ is always a solution to above, i.e. it is always a stationary point in the variational problem. But is $\eta = 0$ a minimum or a maximum? From (B.58) we note that at high enough $T$, $\eta = 0$ would always be a free energy minimum. But as $T$ cools down, at

$$T_{\mathrm{C}}(X_{\mathrm{B}}) \;=\; \frac{-2\omega X_{\mathrm{B}}(1-X_{\mathrm{B}})}{k_{\mathrm{B}}} \tag{B.63}$$

$g(X_{\mathrm{B}},\eta)$ would lose stability with respect to $\eta$ at $\eta = 0$, in a manner of 2nd order phase transformation (for example, magnetization at Curie temperature). This is called order-disorder

transformation, where chemical long-range order emerges at a low enough temperature. In particular, the highest temperature where chemical order may emerge is at $X_\mathrm{B} = 0.5$, where the enthalpic driving force for two sub-lattice partition is especially strong:

$$T_\mathrm{C}^* \;=\; -\frac{\omega}{2k_\mathrm{B}}. \tag{B.64}$$

We also note that $T_\mathrm{C}^*$ exists only for $\omega < 0$. If $\omega > 0$, $\frac{\partial^2 g}{\partial \eta^2} > 0$ always and $\eta = 0$ stays stable global minimum. Thus the Bragg-Williams model is the same as the regular solution model for $\omega > 0$. The Bragg-Williams model gives only different results from the regular solution model for $\omega < 0$, and in that case for

$$T \;<\; T_\mathrm{C}(X_\mathrm{B}) = 4T_\mathrm{C}^* X_\mathrm{B}(1 - X_\mathrm{B}) \tag{B.65}$$

only. At $T < T_\mathrm{C}(X_\mathrm{B})$, we have the CLRO at equilibrium:

$$\ln \frac{(X_\mathrm{B} + \eta)(1 - X_\mathrm{B} + \eta)}{(X_\mathrm{B} - \eta)(1 - X_\mathrm{B} - \eta)} \;=\; \frac{8\eta T_\mathrm{C}^*}{T}, \tag{B.66}$$

from which we can solve for $\eta$.

The above is called the Bragg-Williams approach, which is at the same level of theory (mean-field approximation) as the regular solution model, and only gives different results ($\eta \neq 0$) if $\omega < 0$ and $T < T_\mathrm{C}$. There are certain solid-state chemistries where $\omega$ is very negative, in which case CLRO is close to the maximum possible value for a large temperature range. These are so-called *line compounds* (because off-stoichiometry solubility range is so low, these phases appear as lines in $T - X_2$ phase diagrams) or *ordered phases*, with formulas like $\mathrm{A}_m\mathrm{B}_n$ where $m$ and $n$ are integers. Many crystalline ceramics (oxides, nitrides, carbides etc.) are line *compounds*, as the solubility range is typically very narrow besides the ideal stoichiometry. In metallic alloys, these would be called *intermetallics compound* phases. These phases are typically very strong mechanically (stability due to very negative $\omega$), and are used as strengthening phases (precipitates) to impede dislocation motion. There are special symbols to denote these phases with long-range chemical order, such as $\mathrm{L2}_0$ (bcc based), $\mathrm{L1}_2$ (fcc based), $\mathrm{L1}_0$ (fcc based), $\mathrm{D0}_3$, $\mathrm{D0}_{19}$, Laves phases, etc.

There is still a higher-level of theory called the **quasi-chemical approximation** [62, 86], originating from a series of approximations by Edward A. Guggenheim [80]. It proposes the concept of **chemical short-range order** (CSRO): even in so-called random solid solution ($\omega > 0$, or $\omega < 0$ but $T > T_\mathrm{C}$) which has no long-range chemical order, $\eta = 0$, the atomic

arrangements may not be random as in the mean-field sense, and manifest "correlations". For example, a pair "correlation" means the probability of finding a particular kind of A-B bond is larger than the product of average probabilities of finding A in a particular sublattice and B in another sublattice. Beyond pair correlations, there are also triplet correlations, quartet correlations, ..., in a so-called **cluster expansion** approach [82], each addressing an excess probability beyond the last level of theory. Specifically, in the quasi-chemical approximation one uses the pair probabilities $p_{\mathrm{AA}}$, $p_{\mathrm{BB}}$, $p_{\mathrm{AB}}$, $p_{\mathrm{BA}}$ as coarse degrees of freedom. These are valid order parameters, because at least in principle one could count the fraction of A(')-A("), B(')-B("), A(')-B("), A(")-B(') bonds in a given RVE. These coarse-grained statistical descriptors will take certain values, and one can formulate a variational problem based on them.

$p_{\mathrm{AA}}$, $p_{\mathrm{BB}}$, $p_{\mathrm{AB}}$, $p_{\mathrm{BA}}$ must satisfy sum rule (B.52). Therefore, in addition to $X_{\mathrm{B}}$, $\eta$, the quasi-chemical approximation introduces three more degrees of freedom. In systems where CLRO vanish, there is no statistical distinction between the two sub-lattices, so $p_{\mathrm{AB}} = p_{\mathrm{BA}}$, in which case only two additional degrees of freedom from the quasi-chemical approach. The quasi-chemical free energy reads:

$$\begin{aligned} g(X_{\mathrm{B}}, \eta, p_{\mathrm{AB}}, p_{\mathrm{BA}}, p_{\mathrm{BB}}) \;=\; & \frac{\omega(p_{\mathrm{AB}} + p_{\mathrm{BA}})}{2} + \\ & \frac{k_{\mathrm{B}}T}{2}(X'_{\mathrm{A}} \ln X'_{\mathrm{A}} + X'_{\mathrm{B}} \ln X'_{\mathrm{B}} + X''_{\mathrm{A}} \ln X''_{\mathrm{A}} + X''_{\mathrm{B}} \ln X''_{\mathrm{B}}) + \\ & \frac{Zk_{\mathrm{B}}T}{2}(p_{\mathrm{BB}} \ln \frac{p_{\mathrm{BB}}}{X'_{\mathrm{B}}X''_{\mathrm{B}}} + p_{\mathrm{AB}} \ln \frac{p_{\mathrm{AB}}}{X'_{\mathrm{A}}X''_{\mathrm{B}}} + p_{\mathrm{BA}} \ln \frac{p_{\mathrm{BA}}}{X'_{\mathrm{B}}X''_{\mathrm{A}}} + \\ & (1 - p_{\mathrm{BB}} - p_{\mathrm{AB}} - p_{\mathrm{BA}}) \ln \frac{1 - p_{\mathrm{BB}} - p_{\mathrm{AB}} - p_{\mathrm{BA}}}{X'_{\mathrm{A}}X''_{\mathrm{A}}}) \end{aligned} \tag{B.67}$$

with sub-lattice compositions $X'_{\mathrm{A}}$, $X''_{\mathrm{A}}$, $X'_{\mathrm{B}}$, $X''_{\mathrm{B}}$ taken from (B.47) The actual chemical free energy at local equilibrium is

$$g(X_{\mathrm{B}}) \;=\; \min_{\eta, p_{\mathrm{AB}}, p_{\mathrm{BA}}, p_{\mathrm{BB}}} g(X_{\mathrm{B}}, \eta, p_{\mathrm{AB}}, p_{\mathrm{BA}}, p_{\mathrm{BB}}) \tag{B.68}$$

As a general remark, a compound phase would tend to manifest as sharp "needle" in $g(X_{\mathrm{B}})$, which means small deviation from the ideal stoichiometry $\mathrm{A}_m\mathrm{B}_n$ would cause large "pain" or increase in $g(X_{\mathrm{B}})$, since A-A and B-B bonds must be formed (due to the host lattice structure) which are much more energetically costly than A-B bonds.

Both spinodal decomposition and order-disorder transformation are *2nd-order phase trans-*

*formations*, defined by a vanishingly small jump in the *order parameter*, as one crosses the transition temperature $T_{\rm C}$. In contrast, 1st-order phase transition are characterized by a *finite jump* in order parameter. For instance, in melting, we can use the local density as order parameter to distinguish between liquid and solid, or some feature of the selected area electron diffraction (SAED) pattern. In either case, before and after melting, there is a finite jump in this order parameter field ($\rho(\mathbf{x}, T^-_{\rm melt}) = \rho^s$ but $\rho(\mathbf{x}, T^+_{\rm melt}) = \rho^l$ for some $\mathbf{x}$). Thus, melting is a 1st-order phase transitions. Also, consider an eutectic decomposition reaction: $l \rightarrow \alpha + \beta$, defined by $(T^{\rm E}, X_2^{l{\rm E}}, X_2^{\alpha{\rm E}}, X_2^{\beta{\rm E}})$. If one uses the local composition as the order parameter: then there is also a finite change ($X_2(\mathbf{x}, T^{{\rm E}+}) = X_2^{l{\rm E}}$ but $X_2(\mathbf{x}, T^{{\rm E}-}) = X_2^{\alpha{\rm E}}$ or $X_2^{\beta{\rm E}}$, for some $\mathbf{x}$). In contrast, in the case of $\omega > 0$ and spinodal decomposition $\alpha \rightarrow \alpha_1 + \alpha_2$ which is 2nd-order phase transformations, $X_2^{\alpha_2} - X_2^{\alpha_1} \propto \sqrt{T_{\rm C} - T}$. Whereas $X_2(\mathbf{x}, T^-_{\rm C}) = X_2^{\alpha}$ uniformly $T^+_{\rm C}$, one sees only *infinitesimal* compositional modulations at $T^-_{\rm C}$: $X_2(\mathbf{x}, T^-_{\rm C}) = X_2^{\alpha_1}$ or $X_2^{\alpha_2}$. The *amplitude* of the concentration wave (concentration is our order parameter here) is infinitesimal.

Common tangent construction: $\mu_2^{\alpha}(X_2^{\alpha}, T) = \mu_2^{\beta}(X_2^{\beta}, T)$, $\mu_1^{\alpha}(X_2^{\alpha}, T) = \mu_1^{\beta}(X_2^{\beta}, T)$ manifest as common tangent between $g^{\alpha}(X_2)$ and $g^{\beta}(X_2)$ curves. This equation has two unknowns, $X_2^{\alpha}$ and $X_2^{\beta}$, and we need to solve two joint equations which are generally nonlinear (thus numerical solution by computer may be needed). Show graphically how this may be established for two phases $\alpha$, $\beta$, rich in A and B, respectively, by diffusion. Since

$$dG \;=\; VdP - SdT + \sum_{i=1}^{C} \mu_i dN_i, \tag{B.69}$$

atoms/molecules will always migrate from high chemical potential phase/condition to low chemical potential phase/condition.

Let us now investigate situations where a large-solubility phase ($\alpha$) is in contact with a line compound phase ($\beta$). The common tangent construction can be simplified in these situations. Let us consider two limiting cases (**a**) and (**b**), where the $g^{\beta}(X_2, T)$ needle is "around" (**a**) $X_2 \approx 0$ and (**b**) $X_2 \approx 1$, respectively. (**a**) corresponds to an example of adding antifreeze to water, where the liquid solution delays freezing due to addition of solutes. (**b**) corresponds to an unknown solubility problem, which is to say how much can be dissolved in $\alpha$ for a given temperature when it is interfaced with a precipitate $\beta$ phase that is nearly pure 2.

(**a**): people add antifreeze to say liquid water, to suppress the freezing temperature. How

does that work?

In this case, $g^\beta(X_2, T)$ is a needle "around" $X_2 \approx 0$ (the ice phase), whereas $\alpha$ is the liquid phase. The first thing to realize is the solubility of B is typically lower in solids than in liquids. Energetic interaction between atoms is more important in solids than liquids, since atoms in solids are bit closer in distance, and also put a premium on periodic packing. "Misfit" molecules B would feel much more comfortable living in a chaotic environment like liquid, than in a crystal (think about societal analogies). To first approximation, we can assume the ice crystals that first precipitates out as temperature is cooled is pure ice: $\mu^{\rm ice}_{\rm H_2O}(X^{\rm ice}_{\rm B}, T, P) \approx \tilde{\mu}^{\rm ice}_{\rm H_2O}(T, P)$.

The second thing to realize is that

$$\mu^{\rm liquid}_{\rm H_2O} \;\approx\; \tilde{\mu}^{\rm liquid}_{\rm H_2O}(T, P) + k_{\rm B}T \ln X^{\rm liquid}_{\rm H_2O} \tag{B.70}$$

If the $\approx$ in above is $=$, then it is an ideal solution. Raoult's law says that no matter what kind of solution (solid,liquid,gas), as long as the solutes become *dilute enough*, the *solvent* molecule's chemical potential approaches that in an ideal solution. This is in fact also true for the ice crystals, but $X^{\rm ice}_{\rm B}$ is so small that it's not going to have any effect on $H_2O$ in ice. For the liquid, we have

$$\ln X^{\rm liquid}_{\rm H_2O} \;=\; \ln(1 - X^{\rm liquid}_{\rm B}) \;\approx\; -X^{\rm liquid}_{\rm B}. \tag{B.71}$$

So the chemical potential of water in liquid solution is lowered by $X^{\rm liquid}_{\rm B} k_{\rm B}T$ due to the presence of B in liquid. How much does that lower the melting point? (compared to what?)

$$\tilde{\mu}^{\rm liquid}_{\rm H_2O}(T, P) - k_{\rm B}T X^{\rm liquid}_{\rm B} \;=\; \tilde{\mu}^{\rm ice}_{\rm H_2O}(T, P) \tag{B.72}$$

Remember that $T^{\rm pure}_{\rm melt}$ is *defined* by

$$\tilde{\mu}^{\rm liquid}_{\rm H_2O}(T^{\rm pure}_{\rm melt}, P) \;=\; \tilde{\mu}^{\rm ice}_{\rm H_2O}(T^{\rm pure}_{\rm melt}, P). \tag{B.73}$$

Perform Taylor expansion with respect to $T$:

$$-\Delta s^{\rm pure}_{\rm melt}(T - T^{\rm pure}_{\rm melt}) \;=\; k_{\rm B}T X^{\rm liquid}_{\rm B}, \tag{B.74}$$

we get

$$T^{\rm pure}_{\rm melt} - T \;\approx\; \frac{k_{\rm B}T^{\rm pure}_{\rm melt}}{\Delta s^{\rm pure}_{\rm melt}} X^{\rm liquid}_{\rm B}. \tag{B.75}$$

The pure liquid with larger entropy of melting will have less relative melting point suppression (essentially steeper $\mu_i(T)$ will be less sensitive). What is interesting about (B.75) is that the potency of an antifreeze is independent of the chemical type of the antifreeze, at least when only a tiny amount of antifreeze is added. When the solution is very dilute, the stabilization of the *solvent* is entirely entropic.

Richard's rule: simple metals have $\Delta s^{\text{pure}}_{\text{melt}} \approx 1 - 2k_{\text{B}}$. Water has $\Delta s^{\text{pure}}_{\text{melt}} \approx 2.65 k_{\text{B}}$.

Trouton's rule: $\Delta s^{\text{pure}}_{\text{evap}} \approx 10.5 k_{\text{B}}$, for various kinds of liquids. Water has $\Delta s^{\text{pure}}_{\text{evap}} \approx 13.1 k_{\text{B}}$.

Now consider the opposite limit (**b**): in this case, $g^\beta(X_2, T)$ is a needle around $X_2 \approx 1$. Then for a given $T$, $g^\beta(X_2^\beta, T) \approx \mu_2^\beta(X_2^\beta, T) \approx \tilde{\mu}_2^\beta(T)$, and we just need to solve

$$\mu_2^\alpha(X_2^\alpha, T) \;=\; \tilde{\mu}_2^\beta(T) \tag{B.76}$$

It can be shown mathematically, but is quite obvious visually, that the second equation $\mu_1^\alpha(X_2^\alpha, T) = \mu_1^\beta(X_2^\beta, T)$ for the solvent atoms becomes "unimportant" (still rigorously true, just that whether we solve it or not has little bearing on what we care about - one can draw a bunch of tangent extrapolations on $g^\beta(X_2^\beta)$ with slight differences in $X_2^\beta$, we can see huge changes in $\mu_1^\beta$ but little changes in $\mu_2^\beta$, due to the vast difference in extrapolation distances - such equations are called "stiff" - stiff equations can make analytical approaches easier, but general numerical approaches more difficult). So we have effectively reduced to 1 unknown and 1 equation (or rather, we have decoupled a previously 2-unknowns-and-2-equations into two nearly indepedent 1-unknown-and-1-equations).

Suppose $\alpha$=simple cubic, $\beta$=BCC. Suppose $\alpha$ phase can be described by regular solution with $\omega > 0$ (see Fig. 1.36 of [71], there is an eutectic phase diagram and $g^\alpha(X_2^\beta)$ bulges out in the middle):

$$\tilde{\mu}_2^\alpha(T) + k_{\text{B}}T \ln X_2^\alpha + \omega(1 - X_2^\alpha)^2 \;=\; \tilde{\mu}_2^\beta(T) \tag{B.77}$$

Rearranging the terms we get

$$X_2^\alpha \;=\; \exp\left(-\frac{\tilde{\mu}_2^\alpha(T) - \tilde{\mu}_2^\beta(T) + \omega(1 - X_2^\alpha)^2}{k_{\text{B}}T}\right) \tag{B.78}$$

The above can be solved iteratively. We first plug in $X_2^\alpha = 0$ on RHS, get a finite $X_2^\alpha$ on the LHS, then plug this new $X_2^\alpha$ to RHS and iterate. From the very first iteration, however, we

get

$$X_2^\alpha \;=\; \exp\left(-\frac{\tilde{\mu}_2^\alpha(T) - \tilde{\mu}_2^\beta(T) + \omega}{k_\mathrm{B}T}\right) \tag{B.79}$$

and if $Q(T) \equiv \tilde{\mu}_2^\alpha(T) - \tilde{\mu}_2^\beta(T) + \omega \gg k_\mathrm{B}T$, $X_2^\alpha$ would be small and then the first iteration would be close enough to convergence. $\tilde{\mu}_2^\alpha(T) - \tilde{\mu}_2^\beta(T)$ is how much more uncomfortable it is for a type-2 atom to be living in pure-2 $\alpha$ structure compared to pure-2 $\beta$ structure. $\omega$ is still how much more uncomfortable it is for type-2 atom to be living among a vast sea of type-1 atoms rather than among its own kind (at 0K, $\tilde{\mu}_2^\alpha = -Z^\alpha\epsilon_{22}/2$, $\omega = Z^\alpha(-\epsilon_{12} + (\epsilon_{11}+\epsilon_{22})/2)$, so $\tilde{\mu}_2^\alpha + \omega = Z^\alpha(-\epsilon_{12}) - (-Z^\alpha\epsilon_{11}/2)$, which corresponds to the process of squeezing out a type-1 atom and placing it on a ridge, then inserting a type-2 atom into this sea of 1). Thus $Q(T)$ is an energy that can be interpreted as how much more uncomfortable it is to transfer a B atom from pure $\beta$ phase to dilute $\alpha$ phase, excluding the configurational entropy of B in $\alpha$ phase. Exponential forms of the kind $e^{-Q/k_\mathrm{B}T}$ are called Boltzmann distribution in thermodynamics, and Arrhenius expression when one talks about rates in kinetics. It says that even though some places are (very) uncomfortable to be at or somethings are (very) difficult to do, there will always be some fraction of the population who will do those, because thermal fluctuations reward disorder and risk-taking. A prominent feature of these Boltzmann/Arrhenius forms, especially at low temperatures, is that $k_\mathrm{B}T$ in the denominator is a very violent term. A change in $T$ by 100°C can conceivably cause many orders of magnitude change in the solubility.

The above train of thought can be extended to vacancies. A monatomic crystal made of type-A atoms, but with the possibility of "porosity" inside (non-occupancy of lattice sites), can be regarded as a fully dense A-B crystal with B identified as "Vacadium". In this case, $\epsilon_{\mathrm{BB}} = \epsilon_{\mathrm{AB}} = 0$, so $\omega = Z\epsilon_{\mathrm{AA}}/2$, i.e. it is enthalpically costly to mix Vacadium with A, and they would prefer to segregate if based entirely from enthalpy standpoint or at $T = 0$ K. However, entropically A and Vacadium would prefer to mix. When you mix a block of pure Vacadium (in $\beta$ phase) with pure A in $\alpha$ (fully dense), the solubility of Vacadium in $\alpha$ would be $X_\mathrm{V} = e^{-Q/k_\mathrm{B}T}$. Also, when you are 100% Vacadium it does not matter what structure the Vacadium atoms are arranged, so $\tilde{\mu}_2^\alpha(T) - \tilde{\mu}_2^\beta(T) = 0$ thus $Q = \omega = Z\epsilon_{\mathrm{AA}}/2$. $Q$ is called the *vacancy formation energy* in this context. Physically, $Q$ is identified as the energy cost to extract an atom from lattice (break $Z$ bonds) and attach it to an ledge on surface (form $Z/2$ bonds), in a Kossel crystal. In this class the above process is called the *canonical vacancy creation process*. The canonical vacancy creation process creates porosity inside the solid, making the solid appear *larger* than the fully dense state (social analogy would be "hype"). Note that the canonical vacancy creation process is not an *atomization* process, where one

extracts an atom and put it away to infinity.

An abstract view of phase transformation. Define order parameter $\eta$, which could be density, structure factor, magnetic moment, electric polarization, etc. $\eta$ is a scalar of your choice that best reflects the nature of the problem (phase transition). The Gibbs free energy is defined as $G(N_1, N_2, ..., N_C, T, P; \eta)$. There are global minimum, metastable minima, and saddle point. For example, at low temperature, for pure iron, both $G(\eta_{\text{FCC}})$ and $G(\eta_{\text{BCC}})$ are local minima of $G(\eta)$, but $G(\eta_{\text{FCC}}) > G(\eta_{\text{BCC}})$. To go from $\eta_1 = \eta_{\text{FCC}}$ to $\eta_2 = \eta_{\text{BCC}}$, $G(\eta)$ must first go even higher than $G(\eta_1)$. This energy penalty is called the activation energy, and $\eta \in (\eta_1, \eta_2)$ is called the reaction coordinate. Define $\eta^*$ to be the position of saddle point, we have

$$Q_{1\to 2} \;=\; G(\eta^*) - G(\eta_1), \quad Q_{2\to 1} \;=\; G(\eta^*) - G(\eta_2). \tag{B.80}$$

According to statistical mechanics, all possible states of $\eta$ can exist, just with different probability. The rate of transition, if one is at $\eta_1$, to $\eta_2$, is given by:

$$R_{1\to 2} \;=\; \nu_0 \exp(-\frac{Q_{1\to 2}}{k_{\text{B}}T}), \tag{B.81}$$

where $\nu_0$ is some attempt frequency (unit 1/s), corresponding to the oscillation frequency around $\eta_1$ (imagine a harmonic oscillator coupled to heat bath). The rate of transition, if one is already at $\eta_2$, to $\eta_1$, is given by:

$$R_{2\to 1} \;=\; \nu_0 \exp\left(-\frac{Q_{2\to 1}}{k_{\text{B}}T}\right). \tag{B.82}$$

If $G(\eta_1) > G(\eta_2)$, then $Q_{1\to 2} < Q_{2\to 1}$, and $R_{1\to 2} \gg R_{2\to 1}$ since $Q$'s are in the exponential, and $Q_{2\to 1} - Q_{1\to 2} = G(\eta_1) - G(\eta_2)$ is proportional to the sample size.

One can also express $\eta$ as function of position, $\eta(\mathbf{x})$, to represent an interface. Consider the condition when FCC is in equilibrium with BCC: $G(\eta_{\text{FCC}}) = G(\eta_{\text{BCC}})$, and there is an interface that separates them. $\eta(x)$ is then a sigmoid-like curve, with characteristic width defined as interfacial width. The interfacial energy arises because atoms in the interface are neither FCC or BCC, and have energy density higher than either of them. This would lead to a positive interfacial energy (Chap. 3)

The common tangent construction gives unique solution in composition when $T, P$ is fixed. If $T, P$ come into play, however, then the game is richer. The single-component Clausius-Clapeyron relation (B.18) can be generalized to $C$-component solutions. If we consider $i$ in

$\alpha$ of composition $\mathbf{X}^\alpha \equiv [X_2^\alpha, ..., X_C^\alpha]$, or in $\beta$ of composition $\mathbf{X}^\beta \equiv [X_2^\beta, ..., X_C^\beta]$, there needs to be

$$\mu_i^\alpha(\mathbf{X}^\alpha, T, P) \;=\; \mu_i^\beta(\mathbf{X}^\beta, T, P) \tag{B.83}$$

to maintain mass action equilibrium (chemical equilibrium), to make sure atom $i$ is "equally happy" in $\alpha$ as in $\beta$. Let us investigate what $dP/dT$ needs to be in order to maintain that way, if $\mathbf{X}^\alpha$ and $\mathbf{X}^\beta$ are fixed (for instance two "compound" phases, or one compound phase in contact with a large constant-composition reservoir): because we have

$$d\mu_i^\alpha \;=\; v_i^\alpha dP - s_i^\alpha dT, \quad d\mu_i^\beta \;=\; v_i^\beta dP - s_i^\beta dT. \tag{B.84}$$

To maintain (B.83), we need

$$\frac{dP}{dT} \;=\; \frac{s_i^\alpha - s_i^\beta}{v_i^\alpha - v_i^\beta} \;=\; \frac{h_i^\alpha - h_i^\beta}{T(v_i^\alpha - v_i^\beta)}, \tag{B.85}$$

the latter equality is because if $\alpha, \beta$ are already at chemical equilibrium for $i$ at a certain $(T, P)$, there is:

$$\mu_i^\alpha = h_i^\alpha - Ts_i^\alpha \;=\; \mu_i^\beta = h_i^\beta - Ts_i^\beta. \tag{B.86}$$

Consider for example, the equilibria between pure liquid water ($\beta$) and air ($\alpha$): air is a solution. Then one has:

$$\frac{dP}{dT} \;\approx\; \frac{h_i^\alpha - h_i^\beta}{T(v_i^\alpha)} \tag{B.87}$$

since $v_i^\alpha$ is larger than $v_i^\beta$ by a factor of $10^3$. For the air solution $\mathbf{N} = (N_1, N_2, N_3, ...N_c)$, we have

$$V \;\approx\; \frac{Nk_\mathrm{B}T}{P} \quad \rightarrow \quad v_i \equiv \left.\frac{\partial V}{\partial N_i}\right|_{N_{j\neq i}, T, P} = \frac{k_\mathrm{B}T}{P}. \tag{B.88}$$

Thus

$$\frac{dP}{dT} \;\approx\; \frac{h_i^\alpha - h_i^\beta}{T(k_\mathrm{B}T/P)}, \quad \frac{d\ln P}{d(1/T^2)} \;\approx\; -\frac{\Delta h_i}{k_\mathrm{B}}. \tag{B.89}$$

So:

$$\ln\frac{P^\mathrm{eq}}{P_\mathrm{ref}^\mathrm{eq}} \;\approx\; \frac{\Delta h_i}{k_\mathrm{B}}\left(\frac{1}{T_\mathrm{ref}} - \frac{1}{T}\right), \tag{B.90}$$

when temperature is raised, the equilibrium vapor pressure goes up.

Notice that the gas phase always beats *all* condensed phases at low enough (but still positive) pressure. One can thus draw a $\ln P$-$T$ diagram, and down under it is always the gas phase.

This is because chemical potential in the gas phase goes as

$$\mu_i^{\rm gas}(\mathbf{X}^{\rm gas}, T, P) \;\approx\; k_{\rm B}T \ln X_i P + \tilde{\mu}_i^{\rm gas}(T, 1{\rm atm}), \tag{B.91}$$

which goes to $-\infty$ as $P \to 0$, whereas chemical potentials in condensed phases are bounded. (The physical reason for going to $-\infty$ as $P \to 0$ is that the entropy of gas blows up as $k_{\rm B} \ln v$). Thus, all condensed phases (liquid,solid) become metastable at low enough pressure (see water phase diagram, Fig. B.1 (b)). Another way of saying it is that there always exists an equilibrium vapor pressure for any temperature and composition, which may be small but always positive, below which components in the liquid or solid solution would rather prefer to come out into the gas phase (volatility).

However, they are two manners by which vapor can come out. When you heat up a pot of water, at say 80°C, you can already feel vapor coming out if you stand over the pot, and maybe see some steam, but it's very peaceful *evaporation* process. However, when the temperature reaches 100°C, there is a very sharp transition. Suddenly there is a lot of commotion, and there is *boiling*. What *defines* the boiling transition?

The commotion is caused by the presence of *gas bubbles*, not present before $T$ reaches $T_{\rm boil}$. The boiling transition is defined by $P^{\rm eq} = 1$ atm, the atmospheric pressure. Before $T < T_{\rm boil}$, there may be $P^{\rm eq} > P^{\rm ambient}_{\rm H_2O}$, so the water molecules would like to come out. But they can only come out from the gas-liquid interface, not inside the liquid, so the evaporation action is limited only to the water molecules in the narrow interfacial region $<$ 1nm. This is because any pure $H_2O$ gas bubbles formed inside would be *crushed* by the hydrostatic pressure AND surface tension. But when $P^{\rm eq} > 1$ atm, pure $H_2O$ gas bubbles can now nucleate **inside** the liquid. These bubbles nucleate, grow, and eventually rise up and break. At $T > T_{\rm boil}$ the whole body of liquid can join the action of phase transformation, not just the lucky few near the gas-liquid interface. Thermodynamically, there is nothing very special about the boiling transition, but if you look at the rate of water vapor coming out, there is a drastic upturn at $T = T_{\rm boil}$. So the boiling transition is a *transition in kinetics*. The availability of nucleation sites is important for such kinetic transitions. In the case of boiling, the nucleation sites are likely to be the container wall (watch a bottle of coke). Without the heterogeneous nucleation sites, it is possible to significantly superheat the liquid past its boiling point, without seeing the bubbles.

One can have superheating/supercooling because of the barriers to transformation. The

amount of thermodynamic driving force in a temperature-driven phase transformation is:

$$\Delta G \equiv \mu_i^{\alpha} - \mu_i^{\beta} \equiv \Delta\mu_i \approx \Delta s_i^{\mathrm{eq}} \Delta T = \frac{\Delta h_i^{\mathrm{eq}}}{T^{\mathrm{eq}}} \Delta T \tag{B.92}$$

if the reaction coordinate is identified as mass transfer from one phase to another ($\eta_1$ state: $N_i^{\alpha} + 1$ in $\alpha$, $N_i^{\beta}$ in $\beta$; $\eta_2$ state: $N_i^{\alpha}$ in $\alpha$, $N_i^{\beta} + 1$ in $\beta$). To drive kinetics at a finite speed, the driving force (thermodynamic potential loss or dissipation) must be finite.

# Bibliography


[1] T Neeraj, R Srinivasan, and J Li. Hydrogen embrittlement of ferritic steels: Observations on deformation microstructure, nanoscale dimples and failure by nanovoiding. *Acta Mater.*, 60:5160–5171, 2012.

[2] PY Zhao, J Li, and YZ Wang. Heterogeneously randomized stz model of metallic glasses: Softening and extreme value statistics during deformation. *Int. J. Plast.*, 40:1–22, 2013.

[3] PY Zhao, J Li, and YZ Wang. Extended defects, ideal strength and actual strengths of finite-sized metallic glasses. *Acta Mater.*, 73:149–166, 2014.

[4] SZ Li, YG Li, YC Lo, T Neeraj, R Srinivasan, XD Ding, J Sun, L Qi, P Gumbsch, and J Li. The interaction of dislocations and hydrogen-vacancy complexes and its importance for deformation-induced proto nano-voids formation in alpha-fe. *Int. J. Plast.*, 74:175–191, 2015.

[5] DG Xie, ZJ Wang, J Sun, J Li, E Ma, and ZW Shan. In situ study of the initiation of hydrogen bubbles at the aluminium metal/oxide interface. *Nat. Mater.*, 14:899–+, 2015.

[6] MS Ding, JP Du, L Wan, S Ogata, L Tian, E Ma, WZ Han, J Li, and ZW Shan. Radiation-induced helium nanobubbles enhance ductility in submicron-sized single-crystalline copper. *Nano Lett.*, 16:4118–4124, 2016.

[7] KP So, A Kushima, JG Park, X Liu, DH Keum, HY Jeong, F Yao, SH Joo, HS Kim, H Kim, J Li, and YH Lee. Intragranular dispersion of carbon nanotubes comprehensively improves aluminum alloys. *Adv. Sci.*, 5:1800115, 2018.

[8] XH Liu, JF Gu, Y Shen, and J Li. Crystal metamorphosis at stress extremes: how soft phonons turn into lattice defects. *NPG Asia Mater.*, 8:e320, 2016.

[9] A Manthiram. An outlook on lithium ion battery technology. *ACS Cent. Sci.*, 3:1063–1069, 2017.

[10] M. S. Daw and M. I. Baskes. Embedded-atom method - derivation and application to impurities, surfaces, and other defects in metals. *Phys. Rev. B*, 29:6443–6453, 1984.

[11] M. W. Finnis and J. E. Sinclair. A simple empirical n-body potential for transition-metals. *Philos. Mag. A-Phys. Condens. Matter Struct. Defect Mech. Prop.*, 50:45–55, 1984.

[12] J. Li, K. J. Van Vliet, T. Zhu, S. Yip, and S. Suresh. Atomistic mechanisms governing elastic limit and incipient plasticity in crystals. *Nature*, 418:307–310, 2002.

[13] S. Ogata, J. Li, and S. Yip. Ideal pure shear strength of aluminum and copper. *Science*, 298:807–811, 2002.

[14] unknown Mandelbr.B. How long is coast of britain - statistical self-similarity and fractional dimension. *Science*, 156:636–&, 1967.

[15] VK de Souza and DJ Wales. The potential energy landscape for crystallisation of a lennard-jones fluid. *J. Stat. Mech.-Theory Exp.*, page 074001, 2016.

[16] Y. Mishin, M. J. Mehl, D. A. Papaconstantopoulos, A. F. Voter, and J. D. Kress. Structural stability and lattice defects in copper: Ab initio, tight-binding, and embedded-atom calculations. *Phys. Rev. B*, 6322:224106, 2001.

[17] R. O. Simmons and R. W. Balluffi. Measurements of equilibrium vacancy concentrations in aluminum. *Phys Rev*, 117:52–61, 1960.

[18] J. D. Eshelby. The determination of the elastic field of an ellipsoidal inclusion, and related problems. *Proc R Soc London Ser A-Math*, 241:376–396, 1957.

[19] Ju Li. Atomistic calculation of mechanical behavior. In S. Yip, editor, *Handbook of Materials Modeling*, pages 773–792, Dordrecht, 2005. Springer. Mistake free version at http://alum.mit.edu/www/liju99/Papers/05/Li05-2.19.pdf.

[20] D. J. Srolovitz. On the stability of surfaces of stressed solids. *Acta Met*, 37:621–625, 1989.

[21] R. J. Asaro and W. A. Tiller. Interface morphology development during stress-corrosion cracking .1. via surface diffusion. *Met Trans*, 3:1789–&, 1972.

[22] C. Herring. Diffusional viscosity of a polycrystalline solid. *J. Appl. Phys.*, 21:437–445, 1950.

[23] Gary S. Was. *Fundamentals of Radiation Materials Science: Metals and Alloys*. Springer, 2017.

[24] W Schilling. Self-interstitial atoms in metals. *J. Nucl. Mater.*, 69-7:465–489, 1978.

[25] T. S. Ke. Experimental evidence of the viscous behavior of grain boundaries in metals. *Phys Rev*, 71:533–546, 1947.

[26] F. A. Kroger and H. J. Vink. Relations between the concentrations of imperfections in crystalline solids. *Solid State Phys-Adv Res Appl*, 3:307–435, 1956.

[27] Donald Morgan Smyth. *The defect chemistry of metal oxides*. Oxford University Press, New York, 2000.

[28] M Youssef and B Yildiz. Intrinsic point-defect equilibria in tetragonal zro2: Density functional theory analysis with finite-temperature effects. *Phys. Rev. B*, 86:144109, 2012.

[29] C. Barry Carter and M. Grant Norton. *Ceramic Materials: Science and Engineering*. Springer, New York, 2013.

[30] Michel W. Barsoum. *Fundamentals of Ceramics*. IOP, Bristol, 2003.

[31] C. Wagner. The theory of the warm-up process. *Z. Phys. Chem. B-Chem. Elem. Aufbau. Mater.* (*http://alum.mit.edu/www/liju99/Reference/Modeling/Papers/Oxidation/CarlWagner/Wagner33a.pdf*), 21:25–41, 1933.

[32] American Society for Metals. *Atom Movements*. ASM, Cleveland, 1951.

[33] C. Wagner. The theory of the warm-up process. ii. *Z. Phys. Chem. B-Chem. Elem. Aufbau. Mater.* (*http://alum.mit.edu/www/liju99/Reference/Modeling/Papers/Oxidation/CarlWagner/Wagner36a.pdf*), 32:447–462, 1936.

[34] PE Blochl and JH Stathis. Hydrogen electrochemistry and stress-induced leakage current in silica. *Phys. Rev. Lett.*, 83:372–375, 1999.

[35] J.P. Hirth and J. Lothe. *Theory of dislocations*. Wiley, New York, second edition, 1982.

[36] S. Ogata and J. Li. Toughness scale from first principles. *J. Appl. Phys.*, 106:113534, 2009.

[37] J. Frenkel. The theory of the elastic limit and the solidity of crystal bodies. *Z. Phys.*, 37:572–609, 1926.

[38] A. J. Foreman, M. A. Jaswon, and J. K. Wood. Factors controlling dislocation widths. *Proc Phys Soc Lond A*, 64:156–163, 1951.

[39] S. Ogata, J. Li, N. Hirosaki, Y. Shibutani, and S. Yip. Ideal shear strain of metals and ceramics. *Phys. Rev. B*, 70:104104, 2004.

[40] G. I. Taylor. The mechanism of plastic deformation of crystals. part i.-theoretical; part ii.-comparison with observations. *Proc. R. Soc. Lond. A*, 145:362–404, 1934.

[41] E. Orowan. Zur kristallplastizitat. i. tieftemperaturplastizität und beckersche formel; ii. die dynamische auffassung der kristallplastizitat; iii. uber den mechanismus des gleitvorganges. *Z. Phys.*, 89:605–659, 1934.

[42] M. Polanyi. Uber eine art gitterstorung, die einen kristall plastisch machen konnte. *Z. Phys.*, 89:660–664, 1934.

[43] J. P. Hirth. A brief history of dislocation theory. *Met Trans A-Phys Met Mater Sc*, 16:2085–2090, 1985.

[44] A. Timpe. *Diss. Gottingen (Leipzig, 1905); Z. Math. Phys.*, 52:348, 1905.

[45] Vito Volterra. Sur l'équilibre des corps élastiques multiplement connexes. *Annales scientifiques de l'École Normale Supérieure*, 24:401–517, 1907.

[46] A. R. Bausch, M. J. Bowick, A. Cacciuto, A. D. Dinsmore, M. F. Hsu, D. R. Nelson, M. G. Nikolaides, A. Travesset, and D. A. Weitz. Grain boundary scars and spherical crystallography. *Science*, 299:1716–1718, 2003.

[47] W. T. M. Irvine, V. Vitelli, and P. M. Chaikin. Pleats in crystals on curved surfaces. *Nature*, 468:947–951, 2010.

[48] P. E. Cladis and M. Kleman. Non-singular disclinations of strength s = + 1 in nematics. *J Phys-Paris*, 33:591–&, 1972.

[49] P.M. Chaikin and T.C. Lubensky. *Principles of condensed matter physics*. Cambridge University Press, Cambridge, 1994.

[50] P. B. Hirsch, R. W. Horne, and M. J. Whelan. Direct observations of the arrangement and motion of dislocations in aluminum. *Philos Mag*, 1:677–&, 1956.

[51] R. Peierls. The size of a dislocation. *Proc. Phys. Soc*, 52:34–37, 1940.

[52] F. R. N. Nabarro. Dislocations in a simple cubic lattice. *Proc Phys Soc Lond*, 59:256–272, 1947.

[53] J. Li, C. Z. Wang, J. P. Chang, W. Cai, V. V. Bulatov, K. M. Ho, and S. Yip. Core energy and peierls stress of a screw dislocation in bcc molybdenum: A periodic-cell tight-binding study. *Phys. Rev. B*, 70:104113, 2004.

[54] M. J. Bierman, Y. K. A. Lau, A. V. Kvit, A. L. Schmitt, and S. Jin. Dislocation-driven nanowire growth and eshelby twist. *Science*, 320:1060–1063, 2008.

[55] H. Mughrabi. Deformation-induced long-range internal stresses and lattice plane misorientations and the role of geometrically necessary dislocations. *Philos. Mag.*, 86:4037–4054, 2006.

[56] A.A. Griffith. The phenomena of rupture and flow in solids. *Philos. Trans. R. Soc. London A*, 221:163–198, 1920.

[57] J. H. Rose, J. Ferrante, and J. R. Smith. Universal binding-energy curves for metals and bimetallic interfaces. *Phys. Rev. Lett.*, 47:675–678, 1981.

[58] J. Li, Z-W. Shan, and E. Ma. Elastic strain engineering for unprecedented materials properties. *MRS Bulletin*, 39:108–114, 2014.

[59] T. Zhu and J. Li. Ultra-strength materials. *Prog. Mater. Sci.*, 55:710–757, 2010.

[60] Z. T. Trautt, M. Upmanyu, and A. Karma. Interface mobility from interface random walk. *Science*, 314:632–635, 2006.

[61] T Kadoyoshi, H Kaburaki, F Shimizu, H Kimizuka, S Jitsukawa, and J Li. Molecular dynamics study on the formation of stacking fault tetrahedra and unfaulting of frank loops in fcc metals. *Acta Mater.*, 55:3073–3080, 2007.

[62] Claude H.P. Lupis. *Chemical thermodynamics of materials*. North-Holland, New York, 1983.

[63] B. Franklin. Of the stilling of waves by means of oil. extracted from sundry letters between benjamin franklin, ll. d. f. r. s. william brownrigg, m. d. f. r. s. and the reverend mr. farish. *Philosophical Transactions*, 64:445–460, 1774.

[64] P Behroozi, K Cordray, W Griffin, and F Behroozi. The calming effect of oil on water. *Am. J. Phys.*, 75:407–414, 2007.

[65] A.P. Sutton and R.W. Balluffi. *Interfaces in crystalline materials*. Clarendon Press, Oxford, first edition, 1995.

[66] W. T. Read and W. Shockley. Dislocation models of crystal grain boundaries. *Phys. Rev.*, 78:275–289, 1950.

[67] VV Bulatov, BW Reed, and M Kumar. Grain boundary energy function for fcc metals. *Acta Mater.*, 65:161–175, 2014.

[68] Robert W. Balluffi, Samuel M. Allen, and W. Craig Carter. *Kinetics of Materials*. Wiley, New York, 2005.

[69] J. W. Cahn and J. E. Hilliard. Free energy of a nonuniform system .1. interfacial free energy. *J. Chem. Phys.*, 28:258–267, 1958.

[70] J. W. Cahn. On spinodal decomposition. *Acta. Met.*, 9:795–801, 1961.

[71] David A. Porter and Kenneth E. Easterling. *Phase transformations in metals and alloys*. Chapman & Hall, London, second edition, 1992.

[72] Johannes Diderik van der Waals. The thermodynamik theory of capillarity under the hypothesis of a continuous variation of density. *Konink. Akad. Weten. Amsterdam*, 1:56, 1893.

[73] Ju Li. Atomistic visualization. In S. Yip, editor, *Handbook of Materials Modeling*, pages 1051–1068, Dordrecht, 2005. Springer. Mistake free version at http://alum.mit.edu/www/liju99/Papers/05/Li05-2.31.pdf.

[74] J. H. Wang, J. Li, S. Yip, S. Phillpot, and D. Wolf. Mechanical instabilities of homogeneous crystals. *Phys. Rev. B*, 52:12627–12635, 1995.

[75] Ju Li. *Modeling Microstructural Effects on Deformation Resistance and Thermal Conductivity*. PhD thesis, Massachusetts Institute of Technology, August 2000. http://alum.mit.edu/www/liju99/Papers/00/Thesis/.

[76] E. A. Jagla. Strain localization driven by structural relaxation in sheared amorphous solids. *Phys. Rev. E*, 76:046119, 2007.

[77] Y. U. Wang, Y. M. M. Jin, and A. G. Khachaturyan. Phase field microelasticity theory and modeling of elastically and structurally inhomogeneous solid. *J. Appl. Phys.*, 92:1351–1360, 2002.

[78] W. Kohn and L. J. Sham. Self-consistent equations including exchange and correlation effects. *Phys Rev*, 140:1133, 1965.

[79] Ju Li. Mathematica manipulations, August 2008. http://mt.seas.upenn.edu/Stuff/e/Mathematica/.

[80] Terrell L. Hill. *An Introduction to Statistical Thermodynamics*. Dover, New York, 1987.

[81] Donald A. McQuarrie. *Statistical Mechanics*. Harper & Row, New York, 1976.

[82] A. van de Walle and G. Ceder. Automating first-principles phase diagram calculations. *J. Phase Equilib.*, 23:348–359, 2002.

[83] W. L. Bragg and E. J. Williams. The effect of thermal agitation on atomic arrangement in alloys. *Proc. R. Soc. Lond. A*, 145:699–730, 1934.

[84] W. L. Bragg and E. J. Williams. The effect of thermal agitation on atomic arrangement in alloys - ii. *Proc. R. Soc. Lond. A*, 151:0540–0566, 1935.

[85] S. M. Allen and J. W. Cahn. Microscopic theory for antiphase boundary motion and its application to antiphase domain coarsening. *Acta Met*, 27:1085–1095, 1979.

[86] Mats Hillert. *Phase Equilibria, Phase Diagrams and Phase Transformations: Their Thermodynamic Basis*. Cambridge University Press, New York, 1998.